Modelization of Generation Cost and Demand Uncertainties in Power System Optimization Problems and in Nodal Marginal Price Calculations

Bruno André Pereira Santos Gomes

Mestre em Engenharia Electrotécnica e de Computadores
pela Faculdade de Engenharia da Universidade do Porto

Dissertação submetida para a satisfação parcial dos requisitos do Programa Doutoral em Engenharia Electrotécnica e de Computadores

Porto, Janeiro de 2010

Dissertação realizada por

Bruno André Pereira Santos Gomes

Sob a Orientação de

Doutor João Paulo Tomé Saraiva
Professor Associado Agregado da Faculdade de Engenharia da Universidade do Porto

e Co-Orientação de

Doutor Luís Miguel Pires Neves
Professor Adjunto da Escola Superior de Tecnologia e Gestão de Leiria
Instituto Politécnico de Leiria

Departamento de Engenharia Electrotécnica e de Computadores da Faculdade de Engenharia da Universidade do Porto

“ … Whatever your contribution, there is a great future ahead. I encourage you to actively engage, seek, accept no bounds, nor any limits to your creativity. It is indeed a wonderful time to be what you are …”

(Phillip G. Harris, President of the PJM Interconnection, L.L.C.)

“ … Organizational wealth will be created around skills and talents that are unique and that create value for customers … ”

(Phillip G. Harris, President of the PJM Interconnection, L.L.C.)

Resumo

O processo de reestruturação do sector eléctrico iniciado nos Estados Unidos da América e no Chile nos finais dos anos 70 e intensificado na década de 90, deu origem ao desenvolvimento de mercados de electricidade um pouco por todo o mundo motivados, essencialmente, pelos potenciais benefícios resultantes da separação das actividades de rede - estritamente monopolistas - das de produção e comercialização que podem ser realizadas em regime de mercado. Neste contexto, o livre acesso às redes de transmissão e distribuição apresenta-se como uma característica essencial a ser garantida de forma a permitir que o desenvolvimento desses mesmos mercados se processe de forma adequada. Neste sentido, no decorrer desta Tese serão apresentadas e analisadas algumas das metodologias de alocação de custos de transmissão disponíveis na literatura e mais comummente utilizadas em aplicações reais. Neste trabalho será ainda dado especial ênfase às metodologias do tipo marginal dada a boa aceitação técnica, económica e científica que nos dias de hoje sobre elas recaem.

Tendo em conta a volatilidade do mundo em que hoje vivemos, no decorrer deste trabalho serão também analisadas as incertezas que hoje afectam a operação e o planeamento dos sistemas eléctricos de energia. Como teremos oportunidade de verificar, estas incertezas encontram-se associadas, nomeadamente, a uma crescente consciencialização relativa às questões de ordem ambiental, à conjuntura económica mundial cujas repercussões se fazem sentir, por exemplo, nas incertezas associadas aos preços das energias primárias ou mesmo no previsível crescimento de carga, à crescente integração de energias renováveis, algumas delas de carácter intermitente e, por último, à incerteza inerente à fiabilidade dos componentes dos sistemas eléctricos de energia. Neste contexto, neste trabalho serão apresentadas diversas metodologias disponíveis na literatura relativas à modelização de incertezas nos problemas de operação e planeamento dos sistemas eléctricos de energia, nomeadamente, as metodologias Probabilística, *Interval Arithmetic*, *Boundary Load Flow* e *Fuzzy*. Esta última merecerá especial atenção uma vez que, conceptualmente, é aquela que melhor permitirá modelizar fenómenos não completamente caracterizados ou cujo carácter repetitivo seja reduzido.

Neste contexto, a principal contribuição deste trabalho de investigação poderá ser entendida como o desenvolvimento de uma metodologia que permite integrar incertezas relativas às potências activas de carga e/ou aos custos de produção nos estudos habituais realizados em sistemas eléctricos de energia. Para o efeito o autor, partindo de uma metodologia adequadamente documentada na literatura, *Fuzzy Optimal Power Flow*, apresenta um modelo matemático de optimização linear paramétrica e/ou multiparamétrica para a resolução de problemas integrando as referidas incertezas modelizadas por intermédio de números difusos. A adopção deste tipo de metodologias matemáticas revela-se da maior importância, na medida em que as mesmas permitirão aumentar a precisão dos resultados obtidos o que, por si só, representará uma característica inovadora face às metodologias actualmente disponíveis na literatura. Por último, serão também apresentados os algoritmos desenvolvidos de forma a integrar o efeito das perdas de transmissão nos resultados obtidos, bem como, os algoritmos

desenvolvidos para o cálculo das funções de pertença dos preços marginais nodais de curto-prazo nos nós do sistema.

Em linha com os modelos anteriormente referidos, neste trabalho será também apresentada uma nova metodologia híbrida (difusa/probabilística) que permite modelizar o efeito das incertezas de carga e/ou dos custos de produção (representadas por intermédio de números difusos), em simultâneo, com os modelos de fiabilidade dos componentes dos sistemas eléctricos de energia (representados de forma probabilística). Utilizando este algoritmo será possível obter o valor esperado das funções de pertença das potências produzidas e dos preços marginais nodais, bem como alguns índices de risco, como sejam, os índices de robustez e de exposição do sistema face às incertezas modelizadas.

Por último e com o objectivo de testar as metodologias desenvolvidas, serão apresentados resultados baseados em sistemas eléctricos de 3 nós/3 ramos, 6 nós/8 ramos e de 24 nós/38 ramos.

Abstract

The restructuring process of the electric sector, started in the United States of America and in Chile in the 70's and intensified in the 90's, origined the development of numerous electricity markets all over of the world, essentially, motivated by the potential benefits that could result from the separation of the wiring activities – typically monopolistic – from those of generation and retailing, that can be operated in liberalized markets. In this context, the open access to the transmission and distribution networks becomes an essential issue that must be guaranteed in order to create the conditions for the adequate development of these interconnected electricity markets. In this scope, this Thesis includes a description of several allocation cost methodologies currently available in the literature and commonly used in real systems. Among them, marginal methodologies will deserve special attention given their technical, economic and scientific well acceptance.

Taking into account the volatility of our world, along this work they will also be analysed the uncertainties that nowadays affect the operation and planning of power systems. As it will be seen, they are related namely with the growing consciousness regarding environmental concerns, the macro world economic situation whose repercussions are felt, for instance, on the uncertainties of the primary energy prices, or even, on the predicted load growth, with the increasing penetration of renewables energy resources, some of them of intermittent nature and, finally, with the uncertainties inherent to the reliability of the power system components. In this context, in this work we will present several methodologies available on the literature regarding the uncertainty modelling problem in the planning and operation of power systems, namely, the Probabilistic, the Interval Arithmetic, the Boundary Load Flow and Fuzzy approaches. This last one will deserve special attention since, from a conceptual point of view, it corresponds to the one that better matches with the modelization of phenomena not completely characterized or displaying low frequency of occurrence.

In this context, the main contribution of this research work corresponds to the development of a methodology that allows the integration of generation cost and/or load uncertainties in the traditional power system studies. To accomplish this objective the author, departing from a well known methodology, Fuzzy Optimal Power Flow, presents a linear parametric and/or multiparametric optimization model to the solution of the problems integrating the referred uncertainties modelled by fuzzy numbers. The adoption of this kind of methodologies is of extreme importance, since it will allow to improve the accuracy of the results which, by itself, represents an innovate characteristic with respect to the methodologies currently available in the literature. At least, using the results of the referred model, they will be also presented the algorithms developed to evaluate the impact of those uncertainties in the membership functions of the nodal marginal prices.

In line with the models previously referred, in this work it will be also presented a new hybrid methodology (fuzzy/probabilistic) that allows modelling the effect of the generation costs and/or load (represented by fuzzy numbers) together with the reliability data of the power system components (represented by probabilistic models). This algorithm enables us to compute the expected values of the membership functions of

generations and nodal marginal prices, as well as, some risk indices as, for instance, the robustness and exposure indices that derive from the modelled uncertainties.

Finally, in order to test the efficiency and to demonstrate the interest of the developed algorithms they are also presented results based on a 3 bus/3 branch power system, on a 6 bus/8 branch power system and on a 24 bus/38 IEEE test power system.

Résumé

Le processus de restructuration du secteur électrique surgi aux États-Unis et au Chili à la fin des années 70 et il est intensifié pendant les années 90. Celui-ci est à l`origine du développement des marchés d'électricité au monde entier motivés, essentiellement, par les bénéfices potentiels résultants de la séparation des activités du réseau – strictement monopoliste – de celles de production et de commercialisation, qui peuvent être réalisées en régime de concurrence. Actuellement, dû à des questions d'ordre technique et économique, ce processus de restructuration se caractérise surtout par le développement des marchés internationaux, desquels sont mis en évidence, par exemple, le *Nord Pool* et le projet du marché Européen de l'électricité. Dans ce contexte, l'approche ouverte à la transmission et aux réseaux de distribution se présente comme une question essentielle qui doit être garantie pour créer les conditions pour l`adéquat développement de ces marchés d'électricité raccordés. Dans ce sens, dans cette Thèse, ce seront présentées et analysées plusieurs méthodologies de coûts d'allocation.

Ce travail, ayant conscience de la volatilité de notre planète, présentera une description, de toutes sortes d'incertitudes qui affectent l'opération et la planification des systèmes électriques d`énergie. Nous aurons l`opportunité d`éprouver que ces incertitudes se trouvent particulièrement associées à une croissante conscience en ce qui concerne les inquiétudes sur l'environnement, à la conjoncture macro économique mondiale dont les répercussions sont estimées, par exemple, sur les incertitudes des prix de l'énergie primaires, ou même à la conjecture croissante de charge électrique, à l´intégration des énergies renouvelles, quelques unes de caractère intermittent et, finalement, les incertitudes inhérentes à l'intégrité des composantes du système de pouvoir. Dans ce contexte, dans ce travail, on va présenter plusieurs méthodologies disponibles sur la littérature en ce qui concerne l'incertitude en modelant le problème de la planification et de l'opération de systèmes de pouvoir, à savoir, le *Probabilistic*, *Interval Arithmetic*, *Boundary Load Flow* et *Fuzzy*. Celui-ci, aura une attention spéciale et, conceptuellement, il correspond à celui qui s'accord mieux avec la modélisation de phénomènes pas complètement caractérisés ou avec une réduite d'occurrence.

Dans ce contexte, la contribution principale de ce travail de recherche pourrait être interprétée comme le développement d'une méthodologie qui permet d'intégrer la charge et/ou les incertitudes de coûts de génération dans les études du système de pouvoir traditionnel. Pour le faire, l'auteur, en partant d'une méthodologie bien connue, *Fuzzy Optimal Power Flow*, présente un modèle d'optimisation linéaire paramétrique et/ou multiparamétrique à la solution des problèmes intégrant les incertitudes renvoyées modelées par les nombres *Fuzzy*. Au moins, en utilisant les résultats du modèle renvoyé, on va aussi présenter les algorithmes développés pour évaluer l'effet de ces incertitudes dans les fonctions d'adhésion des prix marginaux nodaux.

Conformément aux modèles auparavant renvoyés, dans ce travail on va aussi présenter une méthodologie hybride (*Fuzzy/Probabilistic*) qui permet de modeler l'effet de la charge et/ou les coûts de génération (représentés par les nombres *Fuzzy*) en même temps que les données d'intégrité des composantes du système de pouvoir (représenté par les

moyens de *Probabilistic*). Comme attendu, avec ce dernier algorithme, on pourra calculer les valeurs attendues des fonctions d'adhésion de générations et de prix marginaux nodaux, aussi bien que, quelques signes de risque, par exemple, la robustesse et l`exposition des indices par rapport aux incertitudes modelées.

Finalement, avec le but d'évaluer l'efficacité des algorithmes développés, on va aussi présenter quelques résultats basés sur un système de pouvoir de 3 nodaux/3 branches, sur un 6 système de pouvoir de 6 nodaux/8 branches et sur un système de pouvoir de 24 nodaux/38 branches du IEEE 24.

À minha esposa Emília,
ao meu filho Bruno Tiago e aos
meus pais os meus sinceros agradecimentos pelo conforto e
equilíbrio afectivo e emocional que sempre me transmitiram ao longo
deste percurso

Ao Professor João Paulo Tomé Saraiva e ao
Doutor Luís Miguel Pereira Neves o meus sinceros
agradecimentos pela forma como orientaram este trabalho, pelo rigor
e clareza cientifica sempre transmitida e por me terem elegido
merecedor de tão nobre e enriquecedora experiência

Ao INESC Porto, à FCT e a todos os restantes colegas,
familiares, Professores da FEUP, colegas do INESC Porto, da ENP e
ex-colegas da ESTG – Leiria pelos seus importantes e decisivos apoios
na realização deste trabalho

Index

List of Figures

List of Tables

Abbreviations list

AGC - Automatic Generation Control

ANEEL - Agência Nacional de Energia Eléctrica

BLF - Boundary Load Flow

CoS/RoR - Cost of Service/Rate of Return

ETS - Emissions Trading System

EU - European Union

FCOPD - Fuzzy Constrained Optimal Power Dispatch

FOR - Forced Outage Rate

GGDF - Generalized Generation Distribution Factor

GLDF - Generalized Load Distribution Factors

ISO - Independent System Operator

LTMC - Long Term Marginal Cost

MCS - Monte Carlo Simulation

NGC - National Grid Company

OPF - Optimal Power Flow

PNS - Power Not Supplied

RER - Renewable Energy Resources

REN - Redes Energéticas Nacionais

STMC - Short Term Marginal Cost

TSO - Transmission System Operator

TUoS - Time Use of System

WhC - White Certificate

CHAPTER I Introduction

1. Introduction

1.1. General aspects

The development of electricity markets and the consequent unbundling process that, as we know, creates a clear separation between the transmission/distribution activities (regulated activities typically operated by monopolies) and the generation and retailing activities became in recent years a common practice in several countries all over the world. In this context, the open assess to the transmission and distribution networks becomes an essential issue in this process. As a result, the definition of the allocation cost methodologies as well as the system planning activities in this new uncertain and volatile world becomes a central element of the regulation activity.

In this context, several authors mention that the main challenge of any tariff structure relies on the identification or the development of methods that could promote the short-term efficient use of the system and, at the same time, that guaranties their long-term stability. In this sense, several allocation cost methodologies have been proposed like embedded, incremental, composite and marginal ones.

The embedded methodologies although their weak economic characteristics were the methodologies traditionally adopted given their simplicity and their capacity in guaranteeing an adequate remuneration of the transmission systems. Nowadays, however, marginal methodologies are better accepted since they can give better economic signals to the system users. Nevertheless, some limitations have also been pointed, such as the incapacity to adequately remunerate the transmission activity, the temporal and spatial volatility of nodal marginal prices, the fact that they are more based on generation costs than on transmission costs and, at last, the fact that they could create or even exacerbate some social asymmetries.

The planning and operation of power systems are nowadays performed within a reality characterized by several uncertainties with different natures. In fact, uncertainties are related with the energy primary resource prices, with the increasing integration of renewable resources some of them having intermittent nature, with a growing environmental consciousness and, at last, with several factors (such as the load growth) depending on the economic growth that, as we know, is currently extremely volatile. Together, all these uncertainties are putting extreme emphases on the development or improvement of methodologies that allow their integration on power system planning and operation studies. In this context, we can then state that the problem associated with the treatment of uncertainties gained a renewed interest visible in the number of papers that, in recent years, were published related with this topic. Generally, these contributions only consider load uncertainties represented by probabilistic distributions or possibility distributions, as it is the case of the fuzzy models. Common to all of them is, however, the integration of system reliability data like, for instance, failure and repair rates.

Among all the available methods, the *Fuzzy Optimal Power Flow* approach represents a model that, departing from a deterministic DC Optimal Power Flow model, allows to evaluate in a systematic and structured way the impact of load uncertainties, modelled by

fuzzy numbers, on the power system behaviour (generation, branch flows and voltage phase angles) and on the nodal marginal prices computed in all buses of the system.

In this context and tacking as a reference the previous mentioned approach, the present research work aims at presenting the mathematical models as well as their corresponding solution algorithms in order to integrate not only load uncertainties or generation cost uncertainties, but both of them, simultaneously, in the traditional power system studies. To accomplish this objective and to increase the accuracy of the obtained results, in this research work we used linear multiparametric optimization techniques. Using these models and algorithms it will be also presented an algorithm to integrate an estimation of the transmission losses on the mentioned results and also an algorithm to compute the possibility distributions of the nodal marginal prices in the presence of such uncertainties. Finally, departing from the concepts of the Fuzzy Monte Carlo algorithm and of the mentioned mathematical models, it will be also presented an improved version of the Fuzzy Monte Carlo algorithm that will allow us to consider not only generation cost and/or load uncertainties represented by fuzzy numbers, but also the probabilistic reliability data of the system components in order to obtain the membership functions of the expected value of the Power Not Supply and of the nodal marginal prices in all buses of the system.

In this context, among other advantages these algorithms will allow us to analyse the effect of several kind of uncertainties on the planning and operation of power systems, and also on the behaviour of nodal marginal prices regarding the specified uncertainties. The impact on nodal marginal prices performs an important role, since it will help the decision making process in the planning environment, it will contribute to create better tariff schemes and, finally, it will also contribute to help the generation companies in adjusting their corresponding positions in accordance with different possible situations. It is then clear that this kind of methodologies could perform an important role and will be useful for regulatory boards, for transmission and distributors operators, and also, for generation companies that want to improve their profits.

1.2. Thesis structure

This Thesis is organized in nine different Chapters. Along them they will be developed topics related with the allocation of transmission cost methodologies currently available on the literature, as well as some implementation practical experiences all over the world, with the uncertainties nowadays present on power systems as well as the currently available methodologies developed in order to integrate them on the traditional power systems studies and, finally, a full description of the theoretical bases of the developed models and their corresponding solution algorithms.

Chapter 1 comprises the general aspects, the motivation, the main goals and the structure of the Thesis.

Chapter 2 includes a description of some of the transmission cost allocation methodologies currently available on the literature, as well as some implementation practical experiences all over the world.

Chapter 3 comprises a description of the uncertainties nowadays present on power systems and the currently available methodologies developed in order to integrate them on the traditional power system studies.

Chapter 4 presents the theoretical concepts of the developed linear parametric or multiparametric optimization models used to integrate generation cost and/or loads uncertainties on the power system studies.

Chapter 5 details the mathematical formulation of the New Fuzzy DC Optimal Power Flow model that corresponds to a linear parametric or multiparametric optimization problem allowing us to integrate generation cost and/or load uncertainties on the power system studies.

Chapter 6 presents the mathematical concepts to integrate transmission losses on the algorithms presented on Chapter V and also the mathematical models that allow us to compute the fuzzy membership functions of the nodal marginal prices reflecting the mentioned uncertainties.

Chapter 7 presents some theoretical concepts regarding the reliability evaluation of composite transmission / generation systems as well as the Monte Carlo algorithm. In this Chapter they are also presented some techniques to speed up the convergence of the Monte Carlo simulation. This Chapter also comprises the theoretical concepts of the Fuzzy Monte Carlo algorithm in order to clarify how the developed algorithm will determine the expected fuzzy membership functions of the Power Not Supply and of the nodal marginal prices, as well as, some risk indices, like the exposure and the robustness indices.

Chapter 8 includes results based on a full didactic three bus/three branch power system, on a small six bus/eight branch power system and on the IEEE 24 bus/38 branch power system.

Finally, Chapter 9 details the main conclusions and contributions of this research work. It will mention a number of topics that, in the author's opinion, could in the future enlarge and improve the currently presented work.

CHAPTER II Transmission Pricing

2. Transmission pricing

2.1. Introduction

In recent years, power systems went through a restructuring process that determined the unbundling of the traditional vertically integrated companies in different agents and providers that can be gathered in several activities as generation, transmission, distribution and retailing, as well as several coordination activities including the market operator, the system operator and the regulatory boards. The extreme activities of this value chain, generation and retailing, are typically provided through competitive mechanisms, while wiring transmission and distribution activities are framed in terms of monopoly regulated basis. In this context and according to Pérez-Arriaga *et al.* (1995), the transmission and distribution activities tend to develop by means of geographical monopolies since in these activities apparently there are not signals to obtain economies of scale. In this sense, the open access to the transmission and distribution networks becomes one of the most important issues in all this process and, as a consequence, the planning and operation of electric system becomes a central element of the regulation activity (Lima, 1996).

In this scenario, one of the most important challenges falls into the development of rules that allow the open access to the transmission and distribution networks, since only in this way it will be possible to avoid situations like those that took place in Europe on the period subsequent to the 96/92/EC Directive approval, concerning common rules for the internal electricity market. In fact, since each Member-State solves by its own national system the question of the transmission pricing of electricity transactions between countries, they were created several distortions on competition and, in several cases, the addition of transmission tariffs, which means the application of tariffs by all Member-States between generator and consumer. In this context, it is easy to understand why the 2003/54/EC Directive (that revoked the 96/92/EC Directive) and the Regulation 1228/2003, regarding the conditions for access to the network for cross border exchanges of electricity put an end to the so called network negotiated access allowed by the 1996 Directive and, as an alternative, put in practice the open access to the transmission networks (including interconnections) to all agents by means of regulated transmission tariffs. Additionally this regulation imposed, when applicable, that the tariffs applied to generators and/or consumers must provide geographical signals at an European level and must take into account losses and the congestions imposed to the system, as well the infrastructure investment costs.

In this context, apart from the technical quality of the transmission service, the rules that guarantee the open access to networks must also satisfy several criteria such as:

- Avoid cross subsidiation;
- Transparency on the allocation of costs;
- Be of easy regulation;
- Guarantee present and future efficiency remuneration to all investment costs;
- Provide proper short and long-term economical signals;
- Guarantee the stability of the tariff scheme.

Since transmission and distribution wiring companies are usually in different technical and economical situations, their corresponding regulatory methodologies are also usually different. Taking into account their economic characteristics, its regulatory scheme may take a form of Cost of Service/Rate of Return Regulation - CoS/RoR and Incentive Regulation or Performance Based Regulation. The Cost of Service/Rate of Return Regulation determines the regulated value that a regulated company can annually receive, reducing in this way its exposition to more volatile situations. This kind of methodologies was adopted to the transmission companies in several countries like, for instance, in Portugal and Spain, since these companies are usually very efficient and typically have smaller investment requirements.

Differently, Incentive Regulation intends to create signals to the efficiency increasing by establishing limits in benefits (Revenue Caps Regulation) or in prices (Price Caps Regulation) or even by comparison (Yardstick or Benchmark Regulation) (Braga *et al.*, 2004a). This type of approaches is usually adopted for distribution companies because they typically have worse performances. Their smaller level of automation requires high levels of investments and, as a consequence, the share of distribution costs in the final costs is also larger. Any of these regulatory methodologies must be accompanied by a quality of service regulatory methodology that imposes minimum technical requirements and penalties if those requirements are not respected (Leão *et al.*, 2003).

The quality of service can be increased by means of the specification of reference values for different reliability and quality of service indices of the wiring companies. Acting in this way, the regulatory board induces wiring companies to make reinforcements and expand the networks contributing to the long-term improvement of transmission and distribution activities.

As it can be seen, the development and implementation of a regulatory methodology is a complex task. In fact it must guarantee the proper economical viability of the regulated companies while inducing their efficient behavior. It must also guarantee the equality and justice principle of the tariff scheme as well its stability and the universality of service (Munasinghe, 1981). In this sense, Shirmohammadi *et al.* (1996) mentions that the evaluation of the transmission services is a hard task and requires complex analytical tools for handling data. The problem becomes even more complex and subjective when the goal is to evaluate the cost of those transmission services.

In this context, Krauser (2003) refers that the main objective of any tariff scheme and congestion solution methodology consists of adopting methods that improve the short-term use of the system and, at the same time, guarantees its long-term stability. This author also mentions that there are not methods applied in a generalized way and so its individual application in each case must be always carefully analyzed. As a result, several methodologies were proposed and classified as average, incremental and marginal cost methods. The short-term marginal cost methodology is very popular, since it gives proper economical signals to the system efficient operation. On the opposite side, the average cost methods guarantee, in a generalized way, the proper remuneration of the transmission systems and are of easy implementation. For these reasons and although their weak economical foundations, they still represent the mostly used methods, for

instance the Postage Stamp approach (Lima, J. M., 1996; Pan, *et al.*, 2000; UNIPEDE, 1997). Composite methods were also suggested as a solution for the problem identified, since they explore the properties of different approaches. However, the use of average methods is frequently criticized because they distort the economical signals created by the marginal methodologies (Lima, J. M., 1996).

2.2. Cost identification

The implementation of a regulatory scheme is always preceded by the identification of all costs related with the regulated activities. As expected the classification of all these costs as well their corresponding values could origin a high level of disagreement between the regulatory board and the regulated companies (Saraiva *et al.*, 2002).

In this context, Shirmohammadi *et al.* (1991) divides the costs related to the transmission services in four categories:

- Operational costs, that correspond to the fuel costs that the wire companies face in order to carry out the transactions. In this sense, they correspond to the costs resultant from the re-scheduling and re-dispatch of generators;
- Opportunity costs, corresponding to the loss felt by system users because when accepting a transaction, some others, eventually more advantages to the system will not be accepted (Saraiva *et al*., 2002);
- Reinforcement and expansion costs, corresponding to the capital costs related with the acquisition and building of new equipments (lines, substations and all the accessory equipment) necessary to carry out new energy transactions. These costs can be difficult to determine because they involve solving minimization cost expansion planning problems in response to any given transaction;
- System costs, that correspond to the capital costs related with the construction, operation and maintenance of the system and its corresponding capital rates and equipments depreciation.

In UNIPEDE (1997), transmission cost are, however, organized in a distinct way. In this context, it was chosen the following structure:

- Capital costs related with capital rates and equipment depreciation;
- Operational costs related with transmission losses;
- Operational costs related with the operation, maintenance and monitoring of the network;
- Administrative and human resource costs;
- Costs related with the ancillary services corresponding to:
    - Active power reserve supply (hot and cold reserve) necessary to maintain a proper security margin of operation (activity also related with the frequency control);
    - Active power supply to face active energy losses;
    - Supplied services related with voltage and reactive power control;
    - Services related with metering and settlement;
    - Services related with the re-dispatch as consequence of grid congestions;

- Costs related with power not supplied that eventually cause some kind of penalty to the companies acting in this area;
- Costs of indirect nature corresponding to:
    - Costs that should be faced by all community by means of taxes but that, for simplicity, are distributed by the system users and so could, eventually, create inefficiencies in system operation;
    - Costs resulting from regulatory or tariff scheme revision or, eventually, resultant from some tariff scheme parameters revision;
    - Costs resultant from the universal service obligations when these are not clearly defined;
    - Stranded costs resulting from investments carried out in the past monopoly based structure of the electricity sector, eventually not justified in present given the re-restructuring process.

Regarding the ancillary services, Saraiva *et al.* (2002) adverts to the fact that in several regulatory and organized schemes, some of these services are bought by system operators in a direct manner or in the scope of some specific markets like it happens in England and Wales or in other cases like, for instance, in the Iberian Electricity Market, MIBEL. In this market, some of the ancillary services are supplied by several agents in a mandatory scheme as a condition to be a market agent (Gomes, B., 2005). As a consequence, this kind of costs is not always directly remunerated by the transmission and distribution tariffs.

Regarding the costs of indirect nature the same authors mention that these costs are not always directly included in the regulatory scheme. The most evident example of this kind of situations corresponds, in several countries, to stranded costs given that for these costs there are specific schemes. In those situations, however, it becomes clear the idea and necessity to completely identify all costs as a way to avoid situations of double remuneration or cross subsidiation.

The costs of the transmission activity can also be grouped in short or long-term costs of constant or variable nature. In this sense, Shirmohammadi *et al.* (1991), defines short-term incremental costs as the operation and opportunity costs and long-term incremental costs as the operation, opportunity, reinforcement and expansion costs. In UNIPEDE (1997), the short-term transmission costs are still divided in two main categories:

- Constant costs, independent of the grid level of use, must be recovered from a independent way regarding the transmitted energy. These costs are constituted essentially by two components:
    - One component strongly dependent on the interconnection point (voltage level, consumer characteristics, available power and distance to other interconnection points);
    - One component that takes into account the maintenance and capital costs required to maintain the system security operation within certain levels. Since all users benefit from this security level, it could be argued that this kind of costs should not depend on the geographical location of the interconnection point;

- Variable costs that are a function of the system level of use. These costs are essentially dependent on losses and re-dispatch situations caused by network congestions. In accordance with several regulatory schemes in force in several countries, this kind of costs can be explained by the use of variables associated to the energy or power, eventually discriminated by hourly, daily or seasonal periods.

2.3. Allocation cost methodologies

2.3.1. General considerations

Once identified all costs related with the use of the transmission or distribution networks and adopted a regulatory scheme, it becomes necessary to allocate all these costs to the system users. Nowadays there are several methodologies to perform this allocation. All these methodologies display several advantages and disadvantages from the point of view of their technical robustness, fairness, easiness of implementation, transparency, ability to create short and long-term economical signals and also their ability to be applied to the existent open markets.

These differences make them very attractive in some situations and less appropriated in some others. In particular and in what respects to their easiness of implementation, it happens that the more complex ones are also, in general, those that reveal more fairness and transparency reflecting in a proper manner the system operation conditions. In many situations, however, their simplicity and easiness of implementation is pointed as the main reason to explain their use in practice (Saraiva *et al.*, 2002).

Independently of the motivations behind a given choice, it is important to note that it will definitively influence the tariff characteristics, namely, in what respects to its temporal and spatial differentiation, to its interconnection voltage level differentiation (increasing the cost allocation fairness, since the costs can be imputed in a more direct manner to the companies that use each individual voltage level, at the same time that reduces the undesirable effect of cross subsidization) and to its geographical uniformity. In fact, several methods allow obtaining geographic uniform tariffs - at least for each voltage level - while others consider an operation model of the system - DC or AC - and obtain nodal tariffs considering the energy or power consumption or injection. The adoption (or not) of these models is inserted in a more extended discussion regarding the requirements of tariff geographic dispersion, the adoption of inter-regional solidarity mechanisms or, in the opposite side, the adoption of purely economic mechanisms in which the tariff geographic dispersion corresponds, by election, to the mechanism used to transmit economical signals to induce more efficient behaviors from the point of view of operation, reinforcement and expansion investments on the network.

In this context, it is also important to mention that the competition level of the market is dependent on the adopted tariff model, since that as the dependence regarding the distance between injection and consumption nodes gets reduced on the adopted tariff model the competition will be larger. It must be noted that in the absence of this

dependence all agents would have equal conditions to operate in the market (UNIPEDE, 1997).

2.3.2. Cost allocation using average models

Several of these models had their origin in the United States of America with the advent of the wheeling transactions, which means, transactions in which two companies, usually vertically integrated, establish between them an acquisition/selling electricity contract whose effectiveness required the use of the facilities of a third wiring company. The allocation of the costs incurred by this third company to the two initial ones was typically performed using some kind of measurement of the network use imposed by those transactions. In this context, the average type methodologies of cost allocation differ between them in the definition and in the measurement of the network use. This kind of models can be classified in Rolled In methods in the sense they do not require the execution of power flow studies, such as Postage Stamp and Contract Path methods and those that require this kind of studies, such as MW.mile, Module or Use, *ZeroCounterflow* and Dominant Flow (Lima, J. M., 1996). For this reason, several of these methods are more adapted to the situations in which the electrical system is organized in terms of transactions and not in terms of centralized day-ahead markets. Saraiva *et al.* (2002), present also other methods of average type, such as, General Agreement on Parallel Paths and also the Rated System Path that, given their lower level of application, will not be detailed in this section.

2.3.2.1. Rolled In type methods

Postage Stamp

Given its extreme simplicity, the Postage Stamp method was frequently applied to the wheeling transactions in the U.S.A and it was adopted in several European countries in the liberalized markets context that resulted from the 96/92/CE Directive.

Considering that all transmission system is used in any transaction independently from the geographical location of its injection and consumption nodes, this method does not take into account the effective use that each agent or transaction makes of the system, the physical laws that govern the system operation, not even can it produce some kind of economical signals regarding the costs associated to transactions with different distances between injection and demand. The absence of economic rationality together with the potential occurrence of cross subsidization situations between different agents or transactions, conducted to the integration of mechanisms such as tariff differentiation by voltage level and coefficient market mechanisms for loss adjustments in an attempt to mitigate its disadvantages (Happ, 1994; Saraiva *et al.*, 2002).

In expression (2.1), CT_j, represents the value that a given agent or transaction j will pay by the use of the transmission network when it is adopted the Postage Stamp method.

$$CT_j = P_j.TF = CT.\frac{P_j}{P_{total}} \tag{2.1}$$

In this expression:

- CT - represents the total regulated transmission cost of the company, in €;
- P_j - represents a variable that measures the use that each agent or transaction j makes of the network, in MW or MWh. This measure of the network use can, eventually, correspond to the consumption or effective power or energy generation of that agent or transaction. In any case, it must be specified in what moment or period of time this variable should be evaluated, which, typically corresponds to the peak period (Shirmohammadi *et al.*, 1996; Saraiva *et al.*, 2002);
- P_{total} - represents the total value of the variable P adopted as a measure of the network use evaluated in a given moment or period of time, in MW or MWh;
- TF - represents the tariff to be paid by any agent or transaction, in €/MW or €/MWh.

According to Saraiva *et al.* (2002), the application of this method can be justified by its simplicity whenever the economical signals to transmit are not very geographically discriminated as a consequence of the good design of the system and the reduced cost of transmission losses and investments to be made.

Contract Path Method

Also denominated as Red-Line Allocation, this method is based on the assumption that the energy transactions take place within a given electric continuous and perfectly identified path that interconnects the energy injection and consumption nodes in the transmission system (Happ, 1994), which once defined can not be modified by any change in the power flow or injections (Saraiva *et al.*, 2002).

Once selected the electric path and its corresponding components, the transaction costs are determined by a variable that measures the network use like in the Postage Stamp method in accordance with expression (2.2).

$$CT_j = \sum_{k=1}^{n} C_k.\frac{P_{jk}}{P_{totalk}} \tag{2.2}$$

In this expression:

- CT_j - represents the cost that the transaction j will pay, in €;
- C_k - represents the cost of the component k, in €;

n - represents the number of components in the electric path "used" by the transaction j;

P_{jk} - represents the value of the variable adopted to measure the network use, which in this case corresponds to the use that a given transaction makes of the component k, in MW or MWh;

P_{totalk} - represents the total value of the variable adopted to measure the use of the component k, in a given moment or period of time, in MW or MWh.

According to several authors, this method is far more irrational an unjustified than the Postage Stamp method, since the selection of the mentioned electric path is not based on any kind of technical study that takes into account the physical laws that govern power system operation. Additionally, it is also indicated that the existence of transactions originating changes in the pre-existent power flows, such as, loop flows should not be ignored.

This method can not produce any kind of economically signals and it also can originate high tariff levels to transactions performed between two distant nodes independently of the new operation point of the power system. Additionally, it is also verified that the CT_j sum can, eventually, not correspond to the total regulated transmission cost, CT , of the company.

MW.mille based on distance

The MW.mille method represents the first methodology of cost allocation that proposes a transmission cost allocation based on the effective use that each user makes of the network (Pan, *et al*, 2000). In opposition to the previous methods, the MW.mille based on distance considers not only power flows, but also the physical distance between the energy injection and consumption nodes. In this way, this method aims at producing economical signals that benefit the installation of generators more closely to loads and vice-versa. In this context, the cost that a given transaction j will pay is given by expression (2.3) (Shirmohammadi *et al.*, 1989):

$$CT_j = CT.\frac{P_j.X_j}{\sum_t P_t.X_t} \qquad (2.3)$$

In this expression:

$P_j.X_j$ - represents the product of power by the distance associated to the transaction j. In a general way, this element corresponds to the sum of the products of the contributions of the transaction j to the power flow in each branch by the length of the corresponding branches. Therefore, this sum represents the number of MW.mile allocated to transaction j;

$\sum_t P_t.X_t$ - represents the total number of MW.mile to distribute by all agents or transactions in the transmission system.

2.3.2.2. Average methods based on power flow studies

To overcome some of the disadvantages of the methods previously described it was developed a new class of methods based, precisely, on the results of power flow studies or of optimal power flow studies. Among them, we must point out the MW.mile, the Dominant Flow, the General Agreement on Parallel Paths – GAPP, the Rated System Path methods and the Generalized Distribution Factors related to generation or loads – GGDF and GLDF, respectively.

Generally, these methods adopt the DC model of the network to represent the operation conditions of the transmission system and also to obtain the coefficient values that translate the way each transaction or each generation or demand contributes to the power flow in each branch. This option can be justified, for one side, by the simplicity required by these methods and, for another, because the use of AC models of the network could eventually means that some variables inherent to the power system operation would be twice considered in the tariff scheme as it could be the case of losses.

MW.mille based on power flow studies (MWM)

In this method the first step corresponds to the execution of a power flow study for a base or reference situation of the network, which must correspond to a significant situation from the point of view of the system operation and must include all the transactions. The computation of the individual contribution of each transaction j to the power flow in each equipment can be performed running a power flow study considering only these injections and consumptions associated to the transaction under analysis. In this context, the cost that a given transaction j will pay is given by expression (2.4):

$$CT_j = \sum_{k=1}^{n} \frac{c_k.l_k}{\overline{fc_k}}.\left|fc_k(j)\right| = \sum_{k=1}^{n} \frac{C_k}{\overline{fc_k}}.\left|fc_k(j)\right| \qquad (2.4)$$

In this expression:

- c_k and l_k - represent, respectively, the cost of the equipment k by unit length and its length. $C_k = c_k.l_k$, corresponds to the cost of the equipment k;
- $fc_k(j)$ - represents the contribution of the transaction j to the power flow on the k equipment;
- $\overline{fc_k}$ - represents the maximum transmission capacity of the branch k;
- n - represents the total number of equipments whose cost, C_k, will be distributed by all agents or transactions.

The use of expression (2.4) can, eventually, not allow the total remuneration of the wiring companies since, in general, branch power flows are smaller than their corresponding maximum capacity. To solve this problem, the exact remuneration of the transmission costs can be achieved by means of the expression (2.5), where, $CTF_{j,}$ corresponds to the final cost allocated to the j transaction.

$$CTF_j = CT.\frac{CT_j}{\sum_j CT_j} \tag{2.5}$$

In this expression, $\sum_j CT_j$ represents the sum of the costs to be paid by all j transactions computed according with (2.4).

This is in fact a matter of great importance, since not using expression (2.5) could mean the postponement of some important decisions like, for instance, network expansion plans as a way to bring the flows closer to its capacity decreasing, in this way, the difference between the collected remuneration and the transmission cost of the company. It must be also noted that the existence of energy transactions that originate power flows in the opposite direction could originate situations in which the company remuneration becomes larger than its total cost, CT. In fact, this can happen if there are flows in opposite directions in the same branch, given the contributions of different transactions.

According to Shirmohammadi *et al.* (1989) this method presents the following advantages:

- It is insensible to the sequence by which the energy transactions are considered, since all transactions are treated in a separated manner considering only its corresponding load and generation;
- It creates proper economical signals to consumers located at short and long distances;

Taking into account that the wire thermal limits are specified in MVA and that generators and wiring companies have reactive power requirements, it can be referred that the concept of network use is more easily quantified by monitoring the active and reactive powers. In this context, Pan *et al.* (2000) presents the MVA.mile methodology (an extension of the MW.mile) that performs AC power flow studies and determines the network use from the reactive power flow by means of sensibility analysis and Power Flow Decomposition.

Module or Use method

In this method the cost to allocate to a given transaction j is given by expression (2.6) (Kovacs *et al.*, 1994).

$$CT_j = \sum_{k=1}^{n} C_k . \frac{\left| fc_k(j) \right|}{\sum_s \left| fc_k(s) \right|} \qquad (2.6)$$

In this expression, $\sum_s \left| fc_k(s) \right|$ corresponds to the sum of the modules of the individual contributions of all transactions or agents connected to the system to the power flow in equipment k.

In this method the evaluation of the individual contributions of each transaction is determined removing the transaction under analysis from the reference situation. In this context, the contribution of the transaction under analysis corresponds to the difference between the power flow computed for the reference scenario and for this new situation.

Considering the absolute value of the contribution of all transactions or agents on the system instead of the maximum transmission capacities, when compared with the MW.mile this method presents the advantage of leading to a remuneration that closely matches the total cost even in the periods of network pos-expansion where they are generally less stressed. Nevertheless, in accordance with some authors (Lima *et al.*, 1995; Pan *et al*., 2000) this method presents the following disadvantages:

- It will not give any kind of incentive to the participants that effectively benefit all system reducing the global power flow;
- It will not induce the efficient use of the system, since independently of the used capacity it always allows a remuneration close to the total regulated cost;
- It does eventually be considered unfair for some users, since they can share the expansion cost of a given equipment they are using in a reduced way;
- It did not consider some reserve of transmission capacity necessary to guarantee the proper reliability of the system.

In this sense, the total regulated cost remuneration resultant, for instance, by the existence of reserve capacity or economies of scale associated costs, can be obtained by means of the expression (2.5), considering, in this case that the CT_j values are determined by (2.6). The final cost of each transaction is then proportional to the ratio of the network use associated to that transaction and the network use associated to the transactions under analysis.

Zero Counter Flow method

The Zero Counter Flow method can be considered as an improved version of the Module or Use method, since it gives clear economical signs to the agents in relation to the larger or smaller convenience of being connected to a given node. In fact, in this method the transactions or agents that benefit the system, which means producing power flows in the opposite direction regarding the dominant power flow, are not cost allocated. In this context, the cost to allocate to a given transaction j is given by expression (2.7).

$$\begin{cases} CT_j = \sum_{k=1}^{n} C_k \cdot \dfrac{fc_k(j)}{\sum_{s} fc_k(s+)} & for\ fc_k(j) > 0 \\ CT_j = 0 & for\ fc_k(j) \le 0 \end{cases} \qquad (2.7)$$

In this expression, s+ represents the set of transactions that contribute with power flows in the same direction of the power flow effectively existent in branch k.

Some of the most common critics to this method are related to the fact that in all those less stressed systems or in those with a small number of transactions, the application of the method could eventually originate situations of tariff discontinuity or volatility. Lima *et al.* (1995) also refers that in some specific situations associated, for instance, with an excessive transmission capacity as a consequence of an incorrect load forecasting, the application of the method could be inadequate. Nevertheless, its use can also improve the general operation system conditions or even postpone investment decisions.

Dominant Flow method

Originally developed by Lima *et al.* (1995), in this method the tariff corresponds to the addition of two different components:

- $CT1_j$, related with the effective use of the transmission system branches, called base-capacity;
- $CT2_j$, related with the system available branch capacities or with the reserve capacity for system security and reliability purposes, called additional capacity.

The base-capacity tariff is obtained by the Zero Counter Flow method considering, in this case, that the cost related with the electric circuit does not correspond to the total cost, but to the cost of each branch effectively used. In this sense, the cost associated with the base capacity is given by expression (2.8):

$$\begin{cases} CT1_j = \sum_{k} C_k \cdot \dfrac{fc_k}{\overline{fc_k}} \cdot \dfrac{fc_k(j)}{\sum_{s+} fc_k(s+)} & for \quad fc_k(j) > 0 \\ CT1_j = 0 & for \quad fc_k(j) \le 0 \end{cases} \qquad (2.8)$$

The additional capacity or reserve capacity, viewed as the difference between the capacity effectively used and the total branch capacity, is allocated using the Module or Use method considering in this case that the difference between the capacity effectively used and the total branch capacity is given by (2.9).

$$CT2 = \sum_{k} C_k \cdot \frac{\left(\overline{fc_k} - fc_k\right)}{\overline{fc_k}} \cdot \frac{|fc_k(j)|}{\sum_{s} |fc_k(s)|} \qquad (2.9)$$

In both expressions, fc_k represents the power flow in branch k obtained by adding the contributions of all individual transactions.

Comparing this approach with the Zero Counter Flow method, in this method the agents or transactions that contribute to power flows in the opposite direction of the dominant power flow benefit from an incentive not in a zero tariff form, but in a more reduced way corresponding to the additional capacity tariff. This characteristic allows differentiations between transactions and agents in a proportional form to the benefit effectively given to the system. It also eliminates the problem related with utilities that would not receive any kind of remuneration by its transmission services if some allocation methods were used (Lima *et al.*, 1995).

2.3.2.3. Mean Participation Factors

The Mean Participation Factors method determines, by means of power flow studies, the percentage of cost that must be allocated to system users. This approach has not physical basis since once known the power flow on branches and the injected powers, the method considers a simplified approach by relating in a proportional way the use of a branch and the injected power. In this way, the networks are treated as any other transmission infrastructure.

This method has been used in countries as New Zeeland, South Africa, Poland and in the state of New South Wales in Australia for the computation of a supplementary tariff in an attempt to remove the so called revenue reconciliation problem that results from the application of marginal methodologies (Odériz *et al.*, 2000).

2.3.2.4. Generalized Distribution Factors and sensibility coefficients

In models that use AC power flow studies, the sensibility analysis of branch power flows in relation to the injected power (Jacobean matrix) allows obtaining, with some simplifications, information similar to the obtained by the Generalized Distribution Factors in DC power flow studies. Nevertheless, in the situations where it is required information with increased accuracy, the referred sensibility analysis must be replaced by the comparison of AC power flow studies with and without the transaction under analysis. The problem becomes more complex when the objective is to analyse the effect of several transactions given the non-linearity of the power flow model and the interaction between the different transactions. In this context, Baran *et al.* (1999) proposed a methodology in which this comparison is replaced by one of the following actions:

- Two simulations of the power flow study to determine the global effect of all transactions in the system, one for the reference case (without the transaction) and another one to the operational situation (considering all transactions). These effects must include the power flow in branches, the generation output and the active transmission losses;

- Analysis of different scenarios for each transaction. In the first scenario only the transaction t is considered while in the other one all except the referred transaction are considered. The results of the comparison of these two simulations with the results obtained for the simulation of the reference situation allows the determination of the incremental effects of each transaction on the system;
- The resource allocation is subsequently determined distributing the active and reactive power flows, the active generation and the active transmission losses to each transaction. As an example, expressions (2.10) and (2.11) show the allocation of the reactive generation of each generator to each transaction minimizing the square of the sum of the difference between the current allocation and its incremental values.

$$\min \quad \sum_{t \in T} \left[\left(\Delta Q_{i,t} - \Delta Q_{i,t}^{M} \right)^2 + \left(\Delta Q_{i,t}^{I} - \Delta Q_{i,t} \right)^2 \right] \tag{2.10}$$

subj.

$$\sum_{t \in T} \Delta Q_{i,t} = \Delta Q_i \tag{2.11}$$

In this problem:

$\Delta Q_{i,t}$ - represents the current allocation;

$\Delta Q_{i,t}^{M}$ - represents the marginal reactive power support for transaction t;

$\Delta Q_{i,t}^{I}$ - represents the incremental reactive power support for transaction t;

ΔQ_i - represents the reactive power output of generators.

This method reveals particularly useful when the market structure comprises more than one pool and the objective is to determine the impact of a given transaction in the base operational conditions (Pan *et al*., 2000).

Like it was previously mentioned, the sensibility coefficient, $A_{i-k,b}$, represents the effect of the modification of the injected power in a given node, ΔP_b, in the power flow in a given branch i-k, ΔF_{i-k}. The original definition considers that the injected power modification is absorbed by a corresponding modification in the reference node injected power, ΔP_R. In this context, generations, losses and system load remain constant. Mathematically, these considerations can be described by expressions (2.12) and (2.13).

$$\Delta F_{i-k} = \sum_{b \neq R} A_{i-k,b} . \Delta P_b \tag{2.12}$$

$$\sum_{b \neq R} \Delta P_b + \Delta P_R = 0 \tag{2.13}$$

These sensitivity coefficients can also be obtained by means of DC power flow studies using the reactances X_{ik}. In this way, they correspond to linear approximations of the power flow modifications regarding the injected power in a given node, and so, they are dependent on the network configuration and on the reference node. However, they are independent of the system operation point.

$$A_{i-k,b} = \left(Z'_{ib} - Z'_{kb}\right) / X_{ik} \tag{2.14}$$

In this expression:

- Z'_{ib} - represents the element on the ith row and bth column of the inverse of the nodal susceptance matrix, B^{-1};
- Z'_{kb} - represents the element on the kth row and bth column of the inverse of the nodal susceptance matrix, B^{-1};

In opposition to the sensibility coefficients that represent the impact of one unity injected power modification in a given node (except in the reference node) in the branch power flows, the GGDFs (Generalized Generation Distribution Factors) represent the impact in the branch power flows originated by generation modifications in all system generation nodes. In a similarly way, the GLDFs (Generalized Load Distribution Factors) represent the load variation impact of all load system nodes in the branch power flows. In this way, they offer three distinct possibilities of cost allocation between users: only to generators, only to loads or to both. These Distribution Factors were widely used in the power systems security analysis domain in establishing relations between branch power flows and generation/loads. The application of these Distribution Factors to cost allocation problems gives a different way to allocate transmission costs between users (generators or loads) taking their injected power as reference (Pan *et al*., 2000).

On the other side, the Generalized Distribution Factors are formulated independently from the reference node. The Generalized Distribution Factors for the generation relate the generation in a given node g, G_g, with the active power flow in a $i-k$ branch, F_{i-k}, in accordance with expression (2.15).

$$F_{i-k} = \sum_{g} GGDF_{i-k,g} . G_g \tag{2.15}$$

These factors are not incremental, once they relate the total generation with the power flow. They are dependent on the system operation point and can be computed using the power flow studies results. To a given node g, the Distribution Factor can be computed using (2.16) where $A_{i-k,b}$ represents the corresponding DC sensitivity coefficient.

$$GGDF_{i-k,g} = A_{i-k,g} + GGDF_{i-k,ref} \tag{2.16}$$

In this expression:

$$GGDF_{i-k,ref} = \frac{F_{i-k} - \sum_{p \neq \text{Re}\, f} A_{i-k,g}.G_p}{\sum_g G_g} \tag{2.17}$$

The Generalized Distribution Factors regarding the loads can be described similarly to the GGDF. They relate the load in a node j, L_j, with the power flow in a branch $i-k$, F_{i-k}, in accordance with expression (2.18).

$$F_{i-k} = \sum_g GLDF_{i-k,j}.L_j \tag{2.18}$$

These factors present properties analogous to those referred to the generation and can also be computed by means of the DC sensitivity coefficients and from the power flow study results using expressions (2.19) and (2.20).

$$GLDF_{i-k,j} = GLDF_{i-k,ref} - A_{i-k,j} \tag{2.19}$$

In this expression:

$$GLDF_{i-k,ref} = \frac{F_{i-k} + \sum_{j \neq \text{Re}\, f} A_{i-k,j}.L_j}{\sum_j L_j} \tag{2.20}$$

From an economical point of view, Rudnick *et al.* (1995) indicates that the sensitivity coefficients and the Distribution Factors have a distinct meaning. The sensitivity coefficients reflect the incremental use of the resources, while the Distribution Factors reflect the total use of the resources (generation and load). On the other hand, the sensitivity coefficients are strongly dependent on the reference node, and so, their use can be more complex in systems in which the marginal node is not unique.

2.3.3. Cost allocation using incremental methods

An incremental cost can be defined as the necessary remuneration to pay a new equipment whose use is assigned to a given agent or transaction. If the use of this equipment is associated to more than one agent or transaction, the incremental cost should be allocated to each of these transactions or agents in accordance to their respective use levels (Saraiva *et al.*, 2002; Shirmohammadi *et al.*, 1996).

The incremental cost of a given transaction or agent corresponds, in this way, to the difference between the transmission costs on a base or reference situation and the cost associated with another situation that includes the respective transaction or agent.

Despite the contribution to a more efficient and economical system use that the incremental nature gives, to this kind of methodologies are frequently pointed some disadvantages related with their complexity, namely, in the presence of a larger number of transactions and with the discriminatory evaluation of the cost allocation process. This discriminatory character can directly result from the fact that in this process it is not taken into account the non-linearity of the power systems due to the adoption of the DC power flow model. Another major reason is related to the fact that the cost allocation results are dependent on the order following which the transactions or agents are considered or removed from the computation process.

Taking into account the previously mentioned disadvantage, Saraiva *et al.* (2002) refers that in a scenario like the present one where the open access to the network is generalized and the power systems are structured in terms of anonymous centralized markets the application of this kind of methodologies becomes increasingly difficult.

The incremental methods are potentially fairer than the average methods once they translate with more accuracy the technical operation conditions of networks and, in several cases, transmit economical signals of greater quality. Nevertheless, several of these methods are too complex for practical application in real situations with large number of transactions. In these conditions and given the non-linearities related to system operation, it could be verified that the sequence following which the transactions are considered is not indifferent. In this sense, the practical application of these methods presents many problems, because there is a field for subjective evaluations related, for instance, with the transactions ordering in an environment that should be characterized by high levels of transparency, objectivity and technical previsibility.

2.3.3.1. Short-term incremental methods

The most important difference between the incremental methodologies and the marginal ones relies on the way followed to determine the costs, which means, in cost definition. The incremental cost of a transaction is determined by comparing the power system costs with and without one given transaction. On the other side, the marginal cost corresponds to the product of an additional transaction unity cost (usually determined by means of a lineraized model of the system) by the size of that transaction. For this reason it is possible to obtain large differences between marginal and incremental costs of a given transaction (Shirmohammadi *et al.*, 1996).

The implementation of incremental models presents several difficulties:

- The first one results from the fact that the market requires economical signals, and so, it is necessary to determine the operational, maintenance and opportunity costs to the time horizon of the study. Additionally, as the period under analysis is extended, the cost identification would be more complex and affected by uncertainty;

- The second is related with the existence of various transactions that can be responsible for that cost variation. In this case, it is necessary to select a method to distribute the total cost by the involved companies in each transaction;
- The third one is related with the fact that it is difficult to forecast and take economic decisions regarding long-term contracts, using only information related with short-term costs of transmission network use. Considering only short-term costs can originate more volatile results;
- The use of methodologies that only consider short-term costs, not including reinforcement and expansion network costs, will turn insufficient the transmission grid remuneration obtained by this approach, situation similar to the ones that result from the use of short-term marginal prices by opposition to the long-term marginal prices;
- Finally, this remuneration only pays the short-term costs resultant from a given transaction, and so, the companies could eventually not feel motivated to make investments to reinforce the available capacity or the service quality.

2.3.3.2. Long-term incremental methods

This kind of methodologies evaluates the expansion and reinforcement long term investment costs, as well operational, maintenance and opportunity costs required to accommodate a new transaction. The expansion and reinforcement components of costs will be evaluated at long-term taking into account the effects that each transaction will have in the system. This evaluation must include several scenarios and consider load forecasting in a more extended time horizon. On the other side, this evaluation must include the possibility of the long-term incremental costs being negative. This will mean that a given transaction will have a positive impact on the system operation conditions and so it will be possible to remove or postpone some planed investments (Saraiva *et al.*, 2002).

The expansion and reinforcement cost concept is easily understood but its evaluation is complex and requires the solution of planning problems more or less complete and complex to identify the most adequate actions to the expansion and reinforcement of the networks. If several transactions are identified as responsible for a new investment, it becomes difficult to allocate the cost to each of these transactions taking into account this optimization expansion and reinforcement problem. In this context, Happ (1994) presents the Long-Run Fully Incremental method that aims at eliminating this disadvantage. This approach doesn't allow that one given transaction exceeds the transmission capacity, but instead it induces the reinforcement of the network in the electric circuit used by it.

In this sense, if there is more than one transaction in that study it will be necessary to proceed to a network reinforcement for each considered transaction removing in this way the need to allocate the total cost of the grid reinforcement by several transactions. Another advantage of this method comes from the fact that it doesn't require the solution of optimization network expansion planning problems to determine the instant and the kind of reinforcements necessary for a given network.

2.3.3.3. Areas of influence

In this approach the network use is defined as the incremental modification in a given branch power flow as the result of a unity MW variation of the load or generation in a given node. Once obtained the power flow variation in each branch for each agent or transaction and for several annual scenarios, it becomes possible to determine the annual use index for each user. This index U_{kc} is determined using expression (2.21). As it can be seen, they are only considered incremental positive variations of power flows. However, it only considers the contributions of negative incremental variations (Odériz *et al.*, 2000).

$$U_{kc} = \sum_{\substack{c \\ |F_{ce}^k|-|F_{ce}|>0}} \left(|F_{ce}^k| - |F_{ce}|\right).P_{kc}.D_e \tag{2.21}$$

In this expression,

- U_{kc} - represents the annual use index of the branch c by the transaction or agent k;
- F_{ce} - represents the power flow on branch c on scenario e;
- F_{ce}^k - represents the power flow on branch c when the k agent consumption or generation in scenario e is increased by 1 MW;
- P_{ke} - represents the k agent power consumption or generation;
- D_e - represents the duration of the scenario e in branch c.

Once this incremental factor is computed, it is necessary to weight each factor U_{kc} by the consumed or generated energy. In this context, the participation factor of each agent k in the cost of branch c, $Part_{kc}$, is given by expression (2.22), where p represents an agent of the system.

$$Part_{kc} = \frac{U_{kc}}{\sum_p U_{pc}} \tag{2.22}$$

Regarding this method Saraiva *et al.* (2002) emphasize several important aspects, namely:

- In this method the set of equipments that each agent contributes to pay corresponds to what is usually called the area of influence which is sometimes much extended. As a consequence, these agents would contribute to the installation of equipments eventually located far away from its interconnection point;

- The method does not detect or originates some additional remuneration in situations where the power flows are close to the capacity limits of the corresponding branches. In fact, the power flow in each branch is obtained by the solution of optimal power flow studies that include operational constraints which means that all these situations are inherently addressed. The use of those studies explains the high computational effort of this approach.

This method was applied in Argentina and Chile with some modifications. For instance, it was defined one slack node to respond to load or generation variations. This simplification, however, is only accepted in real systems characterized by a central high level of load and, as a consequence, in more distributed systems this is not valid, as it happens, for instance, in Portugal or Spain.

2.3.3.4. Beneficiaries method or Benefit Factors method

Conceptually simple, this method is very demanding from the point of view of its computational requirements, once it implies the annual simulation of the system operation conditions considering, individually, the existence and inexistence of branches whose costs will be allocate. Once obtained the results of these simulations, it should be determined the value of the individual benefit factors (positive or negative) of each participant. It must also be emphasized that the computation of these benefit factors is performed in an undifferentiated way for consumers and generators. In fact, for consumers the benefit corresponds to the reduction of the global electricity tariff, while for generators the benefit corresponds to the global increase of profits, that is, the remuneration obtained by selling energy minus operation costs. In this context, the benefit factor of a given agent k associated to a branch c is defined by the expression (2.23), where p represents an agent of the system.

$$Part_{kc} = \frac{B_{kc}}{\sum_{\substack{p \\ B_{pc}>0}} B_{pc}} \tag{2.23}$$

In this expression, B_{kc} corresponds to the economical benefit that the use of a branch c represents to the k participant along of the period under analysis. Since the entities that present negative benefits generally have market power (as a consequence of network constraints, for example), the method considers only positive benefits, which means that no participant will receive any kind of credit if its benefit is negative (Odériz *et al.*, 2000).

Finally, it should be emphasized that this method is not used for global cost allocation, but instead to allocate the difference between these costs and the remuneration obtained using another approach.

2.3.4. Marginal methods

2.3.4.1. General aspects

In accordance with the basic principles of the economic theory, the optimal efficiency both at short and long-term is obtained when perfect competition conditions exist and consumers and generators pay and are paid to their consumption or generated energy, respectively, at marginal prices (Rivier *et al.*, 1993).

In a market environment the economical optimum is achieved when goods and services are paid at the marginal cost and the systems are economically adapted (a system is economically adapted when it produces a given quantity at a minimum price). The marginal cost methodology underlined principle has been used by the electrical sector companies, namely, in the scope of the economical centralized dispatch. The developments of Schweppe, Tabors, Caramanis and Bohn started the extension process of the marginal cost structures concept to the electricity tariffs applied to big consumers (Tabors, 1994). In this context, marginal methodologies perform an important function in the promotion of efficiency in electrical transmission systems, given that (Tabors, 1994):

- They transmit economical signals to the wiring companies favoring in this way the investment decision making that induces the increase of efficiency operation, maintenance, reinforcement and expansion of the system;
- They transmit economical signals to generators and consumers, favoring the decision making from the point of view of its geographical locating (Short-Term Marginal Costs - STMC and Long Term Marginal Costs - LTMC) and system operation;
- They allow the evaluation of the quality of the generation and consumption investments in the global operation system context;
- When computing future marginal prices, they make it easier the transition of the electricity system to a market environment, as well as the internal management of the wiring companies in these transitions periods.

Nevertheless, in activities that present clear economies of scale, the marginal prices don't allow the total remuneration of the operation, maintenance, reinforcement and expansion costs incurred by wiring companies, given that these marginal prices are more reduced than the corresponding average costs. According to Leão (1999) another disadvantage could, eventually, result from the social distortions that the application of these methodologies could originate.

In this context, the composed methods (average/marginal) constitute an interesting option because they produce economical incentives to the efficient system operation and also eliminate the revenue reconciliation problem (Arriaga *et al.*, 1995).

2.3.4.2. Short-term marginal methods

The nodal marginal price of electricity corresponds to the cost of supplying an additional load unity in a given node and in a given instant of time t for a given system topology and load level. This price is, in this way, defined as the derivate of the system operation cost in relation to the load in a given node at a given instant of time (Peréz-Arriaga *et al.*, 1995). According to Schweppe *et al.* (1988), the short-term marginal price must reflect the following components:

- Marginal cost of generation;
- Cost of losses;
- Costs related with the generators quality of service;
- Costs of the quality of service.

The application of the marginal price concept at a given system originates a nodal marginal price matrix, which represents the expected spatial dispersion of nodal prices in the time period for which the system was analyzed (Tabors, 1994).

The marginal price of transmitting energy between two nodes could then correspond to the difference of the marginal prices in these two nodes. The remuneration of the wiring companies corresponds in this way to the sum, extended to all nodes, of the value paid by consumers and to be paid to generators. Mathematically, this marginal remuneration could be described by expression (2.24) (Arriaga *et al.*, 1995).

$$MR = \sum \rho_k \left(d_k - g_k \right) \tag{2.24}$$

In this expression,

MR - represents the marginal remuneration of the wiring companies in €/h;
ρ_k - represents the nodal marginal price in node k in €/MWh;
d_k - represents the load in node k in MW;
g_k - represents the generation in node k in MW.

Regarding this expression, Peréz-Arriaga *et al.* (1995) presents some important considerations, namely:

- The principle related with expression (2.24) isn't directly related to the remuneration of the network, and so, its proper remuneration is not guaranteed;
- Expression (2.24) gives origin to perverse incentives, because if the performance of network gets worse the marginal remuneration is increased.

In this context, in an ideal system without losses or any other kind of limitations, at a given instant of time t the marginal prices will be equal in all system nodes. However, in any real system the grid losses and congestions originate nodal price differences and, as a consequence, the consumers and generators receive different prices dependent on their

respective geographical locations. In this way, it is possible to create proper incentives to decisions both in the generation and in the consumer side, in short and in the long-term. Due to this reason, this methodology received large attention in network tariff schemes not only in the academic environment, but also in practical application (Oren *et al.*, 1995). Several authors mention that the marginal remuneration should constitute the basis of any tariff scheme that aims at allocating the operation, congestion and transmission loss costs to system users.

Several models and computational tools have been presented for the computation of marginal prices. Between them we must emphasize the works developed by Caramanis *et al.* (1989) aiming at establishing wheeling rates based on marginal operation costs and on a revenue reconciliation adjustment to ensure capital recovery. This model uses the results of DC or AC power flow studies. Baughman *et al.* (1992) presents a model based on the Monte Carlo simulation method that allows determining the probabilistic distribution of the nodal marginal prices in any node of the system considering data related with several outages of generation or transmission components. In this method, the losses and power flow computations are performed by means of a DC optimization problem. The nodal marginal price probabilistic distribution determined in this way reflects the generation marginal costs and, when appropriated, the overcosts related with network congestions and/or power not supplied.

Saraiva *et al.* (1994a) presents a model that aims at systematically evaluating the impact of load uncertainties in nodal marginal price values in all system nodes. The method uses a Fuzzy DC Optimal Power Flow model to represent the operation conditions of the system and it also considers an estimate of the transmission active losses. In this model, active loads are represented by trapezoidal fuzzy numbers and so the nodal marginal prices in each system node are represented by fuzzy membership functions.

Farmer *et al.* (1995) presents a model to determine the short-term marginal prices that considers a security transmission factor that relates the power flows in outage situations of the network with the power flow in the same network in the absence of these outages. Gil *et al.* (2006) presents a model called Transmission Rent Economic Dispatch that introduces penalties into the traditional economic dispatch as a way to create different nodal marginal prices allowing in this way the complete recovery of the total regulated transmission costs. As a consequence these electricity prices reflect not only marginal generation costs subjected to network constraints, but also the capital costs of the transmission grids.

According with the results presented by Farmer *et al.* (1995), the adopted methodology to modify the nodal marginal prices is conducted in such a way that it penalizes in a more intensive way users that, by its geographical location, use more intensively the network resources and, in the opposite side, it benefits those that contribute to the reduction of the system use. Due to this reason, these authors concluded that the method presents the additional advantage of creating strong economic signals that will induce a more efficient long-term use of the system. Even directly applied to market structures that consider nodal marginal prices (like, for example, the PJM in the U.S.A.), the model could also be applied to structures with a unique system marginal price or, even, in mixed market

structures (pool and bilateral contracts). In this case, it is suggested that part of the regulated costs are allocated to bilateral contracts, whose tariff should correspond to the difference between the injection and consumption nodal prices.

As previously mentioned, in the literature we can find several short-term marginal price computation models. According to (Leão *et al.*, 2000) there are formulations that:

- Compute the active energy price in just one significantly load node, and then applies penalty factors to determine the spatial distribution of marginal prices to all system;
- Consider a representation of the whole system and include active transmission losses by means of successive linear approximations;
- Adopt an AC model to determine nodal marginal prices for active and reactive energy.

In this context, Chapter 6 of this Thesis presents more details related with the nodal marginal price computation, their temporal and spatial volatility, as well as, the currently available methods used to mitigate the Revenue Reconciliation problem.

2.3.4.3. Long-term marginal methods

The long-term marginal price of electricity is defined as the marginal price of an additional MW of load when the installed capacity, for instance of the transmission system, is allowed to optimally respond to that load variation. In this sense, it comprises capital and operation costs having to be computed along a temporal period that reflects the system expansion cost (Tabors, 1994).

The long-term marginal prices contribute to eliminate some disadvantages of the short-term marginal prices, once they reflect the long-term investment costs and the short-term operation costs. Given the small difference between regulated costs and the remuneration potentially obtained by this methodology, they also remove or even eliminate the revenue reconciliation problem. Nevertheless, the long-term marginal cost computation is not simple as a consequence of, for instance, the uncertainties related with network configuration, with the hydrological conditions, with load forecasting and with investment decisions in new generation and transmission capacity (Lima, 1998).

Even requiring a more complex computation, the long-term marginal prices are more transparent and fair, and so they are more adequate to be applied to the transmission tariff scheme. In this context, some authors (Leão *et al.*, 2000) mention that these prices must reflect operational costs, $\Delta C(O)$, reliability costs, $\Delta C(R)$ and investments costs, $\Delta C(I)$ when a unity variation of load, ΔD, occurs. Mathematically this idea can be represented by expression (2.25).

$$LMTP = \frac{\Delta C(O)}{\Delta D} + \frac{\Delta C(R)}{\Delta D} + \frac{\Delta C(I)}{\Delta D} \tag{2.25}$$

Among many other methods in the literature for the computation of long-term marginal prices, Leão *et al.* (2000) presents a multi-objective model to determine the distribution network expansion planning and its corresponding long-term marginal prices that considers investment and operation costs and also takes into account uncertainties in loads and on equipment reliability rates.

Braga *et al.* (2003) presents a method to determine the transmission network expansion planning and its corresponding long-term marginal prices computation. The method presented by these authors uses a DC optimization model for the operation costs computation that comprises active losses estimation. In this model the equipments to install are selected between the ones in a list of possible alternatives, being the corresponding investment plans obtained by temporal discrimination of the equipments installation. To obtain the referred transmission system expansion plan, the authors use the Simulated Annealing metaheuristic given that this technique preserves the discrete nature of the investment decisions and, at the same time, it admits a multiperiod dynamic formulation. The investment plans are evaluated using three criteria: investment costs, operation costs and a reliability index represented by the Power Not Supplied. In the solution of the multicriteria problem, the authors use the ε-constraint method in which all objectives except one are converted into constraints by the specification of expectation levels. After being obtained a first non-dominated solution of this problem, the decision agent has the opportunity to modify the expectation levels initially used to improve some specific criteria. The algorithm proceeds with subsequent modifications until the decision agent identifies a non-dominated satisfactory solution (Braga *et al.*, 2004a). Leão *et al.* (2003) also presents a method to compute long-term marginal prices very similar to that presented by the previously authors, but in this case load uncertainties are represented by fuzzy numbers.

Although transmission tariffs are essentially composed by constant terms, the evaluation of cost variations due to energy transactions imposes the determination of its impact on the expansion transmission system investments. It can also be observed that the process is cyclic, that is, the transmission tariff computation depends on the generation planning and the generation decisions depend on the transmission tariffs. In this context, it is important to know if the regulatory board responsible for the evaluation of the expansion plans is able to control the investments in the direction of the system social welfare maximization (Lima, 1998).

A possible strategy could be to define a reference plan based on cost minimization criteria that takes into account the generation and the transmission system. This plan could be prepared by the regulatory board or by the system operator and should be posted to all agents. Another strategy could, eventually, consider the evaluation that the generators make of the impact of new resources in the transmission system. However, in both cases, it does not exist the guaranty that the agents will follow the desired options (Lima, 1998). In this context, Lima *et al.* (1998), mentioned that the previous problem should be analysed in an integrated way as illustrated in Figure 2.1.

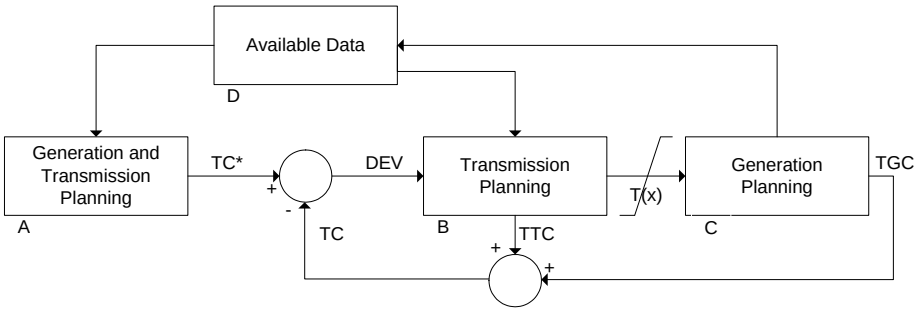

Figure 2.1: Structure of the system expansion-planning problem in partially decentralized systems (source: Lima, 1998).

Clearly, the proposed analysis resembles a closed loop control system. Block B corresponds to the control system that comprises the reinforcement and expansion transmission plan activity and the structure tariff definition, T(x). This tariff corresponds, in this case, to the nodal price vector for a given decision investment x and is the control variable. Block A gives the reference for the total system cost, TC*, which derives from the centralized generation and transmission system expansion planning. The sum of the total generation cost (TGC) with the total transmission cost (TTC) corresponds to the total cost (TC). The deviations of TC regarding TC*, ideally zero, could be controlled by means of a control variable T(x). Load forecasting, generation decisions, transmission rights, between others, represent some examples of the available information to perform transmission system planning studies as well as its corresponding tariff structure (Lima, 1998). At this respect, it must be noted that in Figure 2.1 the variable T(x) is subjected to some limits. From the practical point of view, one of the possible limits could correspond, for instance, the annual maximum investment value of the wiring companies.

According with this author, the use of T(x) vector to control the generation system expansion represents an option more attractive than the reference plan, once the system transmission tariff represents, in fact, the unique sensitivity factor for all generators that present selling offers in the market.

Taking as base a didactic example and the Brazilian power system, this author concludes that the control efficiency provided by the transmission tariffs in the system optimization strongly depends on the adopted cost allocation model and on the relation between generation and transmission costs. In this context, the author indicates that as the costs get larger, more reduced will be the control efficiency. He also concluded that the system planning control remains under the responsibility of the regulatory board and of the system operator and that regulatory structures of CoS/RoR type and the non-negative transmission tariffs, even widely spread, can cause undesirable effects in an attempt to achieve the social welfare optimum. Considering these studies this author also indicates that the tariffs based on long-term marginal price models are those that can be more properly adapted to this strategy implementation, even thought, given its computational inherent difficulty, they must be replaced by an approach easier to be computed. In this context, he proposes the use of a tariff based on Mean Incremental Costs when there is available an expansion reference plan.

2.3.4.4. Investment cost related pricing

Given the inadequacy of the short-term marginal cost methodology to the English and Welsh system (Saraiva *et al.*, 2002), the National Grid Company decided to substitute it by a long-term marginal price methodology to allow the integration of investment costs. In this sense and clearly in an attempt to simplify the long-term marginal price methodologies, it was developed the Investment Cost Related Pricing – ICRP methodology. In accordance with Bakirtzis *et al.* (2001), the introduced simplifications result from the following considerations:

- The optimal network is constructed using only the existent routes of the current network;
- The optimal network is constructed taking into account the maximum load conditions. Its allocation to generators is performed in proportion to their registered capacity with no regard to economic criterions;
- All branches of the ideal network are equal and their investment costs are proportional to their length;
- The transmission capacity of the ideal network is exactly equal to the energy quantity transferred from generators to load in maximum load conditions. The construction of that network does not take into account security conditions and ignores the temporal discrimination of its expansion;
- The power flows in the ideal network respect the generation/load balance equation, however, they ignore the Kirchhoff laws. Consequently, many electric circuits become useless and the configuration of this ideal network becomes radial. In this context, the electric circuits having more reduced length get more widely used, and so, only these circuits contribute to the construction costs.

Taking into account these considerations, the optimization problem can be formulated according to (2.26) and (2.27).

$$\min \sum_{ij} l_{ij} . \left| f_{ij} \right| \qquad [MW.km] \tag{2.26}$$

Subj.

$$\sum_{j} f_{ij} = P_i \quad \forall i \tag{2.27}$$

In this formulation,

l_{ij} - represents the length between nodes i and j;

f_{ij} - represents the power flow between nodes i and j;

P_i - represents the injected power in node i (in maximum load conditions).

The annual network construction cost is subsequently computed multiplying the total MW.km cost by the expansion constant of the grid $\overline{c}$ (annual transmission cost in €/MW.km.year)

Given that the optimal network is radial, there is only one electric path from one node to another, and so, the reference node can be arbitrarily chosen. In this context, the long-term marginal cost of the energy transmission of a given node i represents the total MW.km quantity of the optimal network reinforcement necessary to supply one MW increase of the load in node i. According to this model, this nodal load increase will be compensated by an equal generation increase in the reference node. The required reinforcement corresponds to the addition of one MW transmission capacity for all lines along the unique electric path from the reference node to the i node. In this sense, the nodal marginal cost is related with the distance, in kilometers, from the reference node to the node i along the optimal network. This distance concept is used to efficiently compute the long-term marginal costs.

The optimal network could then be obtained solving the following optimization problem (2.28) to (2.30):

$$\min \sum_i \sum_j l_{ij}.b_{ij}.\left(\theta_i - \theta_j\right) \qquad [MW.km] \tag{2.28}$$

Subj.:

$$\sum_j b_{ij}.\left(\theta_i - \theta_j\right) = P_i \tag{2.29}$$

$$-P_{ij}^{máx} \le b_{ij}.\left(\theta_i - \theta_j\right) \le P_{ij}^{máx} \tag{2.30}$$

In this expression:

- b_{ij} - represents the susceptance of the branch linking nodes i and j;
- $P_{ij}^{máx}$ - represents the maximum transmission capacity of the branch linking nodes i and j;
- θ_i - represents the voltage phase angles in node i;
- θ_j - represents the voltage phase angles in node j.

As it can be seen, in this model the generation and loads are fixed, and as a result the optimization problem has no degrees of freedom to adjust the generation to obtain the minimum global value. In this sense, the solution of this optimization problem corresponds to the solution of a DC power flow and the long-term marginal costs are determined as the difference between the MW.km of the initial load situation and the situation where the load in a given node is increased by 1 MW.

The computation of these long-term marginal costs presents the following characteristics:

- The LTMC in the reference node is zero;
- The modification of the reference node implies a modification of nodal costs that, however, preserve their geographical dispersion. Like other marginal methodologies, the remuneration obtained by this way will not allow the proper remuneration of the wiring companies. The additive term introduced by this reason represents the unique component independent of the reference node;

- The LTMC related to generation and load in each node are symmetric.

2.3.4.5. Marginal price of reactive power

The unbundling process and the consequent open access to transmission grids requires that the wiring companies provide a set of services, namely of energy transmission and voltage control within its control area to ensure proper system security levels. In this context it could be observed that the proper definition of the cost of this service as well as the establishment of proper price structures performs an important function from the operational and financial point of view of the system (Hao *et al.*, 1997).

Nevertheless, the proper price structure definition for the reactive power is very difficult given the numerous aspects that are involved. These include technical and economical considerations, such as system maintenance, simplification of the administrative requirements and tariff uniformity between different users. They comprise also considerations regarding the reactive power reserve (in interconnected system each control area is responsible for the corresponding satisfaction of the reactive energy requirements, including the interconnected circuits reserves guaranteed by means of generation units, synchronous capacitors and static var compensators – SVC), to the inductive and capacitor resources management, with the generation costs and with the cost allocation methodologies (Hao *et al.*, 1997).

Some authors (Chattopadhyay *et al.*, 1995) propose a reactive power price computation methodology based on the generation capacity of this resource given that, according to these authors, its marginal generation cost is neglectable and the reserve margins are quantified from the point of view of this capacity (Lamont *et al.*, 1999). In this context, in all the situations where the operation point of the generation unit is bellow its generation capacity limit, the price of reactive power will be zero. This approach will, obviously, imply that the generation units having larger capacity will never be able to receive any kind of remuneration for their contribution given their larger probability of operating within their capacity limits. This fact presents by itself a disincentive to reactive power generation, and so, it would not induce an efficient system operation (Ma *et al.*, 1998).

Due to this reason, some authors (Baughman *et al.*, 1991) indicate that only rigorous methodologies for price computation, such as the ones produced by marginal mechanisms could create proper signals that benefit the planning and investment decision making, as well the system social welfare, because they represent a sensitivity factor to reactive power generation cost regarding to load variation. Nevertheless, according to this method, the generation cost should only include generation variable costs and this would only represent a small fraction of the real cost incurred in providing this service. This problem, together with the enormous complexity and spatial volatility of the reactive power nodal marginal prices, represent the main difficulty in the application of nodal marginal methods to the development of reactive power tariff schemes (Hao *et al.*, 1997).

Li *et al.* (1994a) draws the attention to the fact that the potential error that could arise from not integrating reactive power marginal prices in tariff schemes would increase with

the transaction magnitudes and with the reduction of its associated power factors, because as it was previously mentioned, this power affects the active energy transaction costs since it interferes with active transmission losses, with generation costs and with transmission capacities. For this reason, these authors defend that in the energy transmission costs computation it should be considered not only reactive power flows, but also their effects on the active power flows. With the introduction of these costs, these authors believe that it would be possible to induce modifications into the system reactive power resource operation and planning, since the reactive power marginal generation costs are smaller, but their associated transmission costs could be very large.

Li *et al.* (1994a), using an IEEE test grid, show that the reactive power marginal costs are generally smaller than 1% of the corresponding active power prices. However, wheeling rate of the reactive power could vary from 14 to 72% of the active power corresponding prices. Additionally, Hao *et al.* (1997), show that in general the reactive power transmission losses are typically ten times larger than the active transmission losses and that in several situations they are even larger than the reactive system load.

From the point of view of the computation models, the main consequence of the reactive power consideration is the inadequacy of the DC power flow model, since it neglects the effect of reactive power flows. As a result, several other models were proposed as, for instance, the one detailed in Ma *et al.* (1998). It proposes a model based on a decoupled Optimal Power Flow to determine the active and reactive nodal marginal prices. In this approach, the objective function of the reactive power problem corresponds to minimize active transmission losses subjected to physical (generator nodal voltage levels and voltage ratio of transformers) and operational (reactive generation capacity limits and nodal voltage levels) limit constraints. The minimization of active transmission losses is equivalent to the minimization of generation costs in the reference node, and so, the mathematical formulation of the Q sub-problem of the decoupled OPF corresponds to (2.31) to (2.34).

$$\min\ C_l(P_{G1}) \tag{2.31}$$

Subj.:

$$V_i^{\min} \le V_i \le V_i^{máx} \tag{2.32}$$

$$Q_{Gi}^{\min} \le Q_{Gi} \le Q_{Gi}^{máx} \tag{2.33}$$

$$t_l^{\min} \le t_l \le t_l^{máx} \tag{2.34}$$

In this formulation:

- $C_l(P_{G1})$ - represents the generation cost function in the reference node, admitting to be node 1;
- V_i - represents the voltage magnitude in node i;
- Q_{Gi} - represents the reactive generation in node i;
- t_l - represents the voltage ratio of the transformer on branch l.

In this context, the reactive power marginal price can be determined using expression (2.35) (El-Keib *et al.*, 1997). As we can see, expression (2.35) indicates that the reactive power short-term marginal price in a given node includes three components. The first one corresponds to the short-term marginal price of the active losses, which is described by the marginal generation price in the reference node. The magnitude of this component is defined by the system marginal cost, λ, and by the sensitivity of the active power losses regarding the reactive power injection in a given node. This price component clearly shows that the reactive power transmission directly affects the system generation cost.

The second component is related with system security, namely with voltage levels. If the voltage in a given node is on its lower limit, the reactive generation resources must be used in a more intensive way originating a price increase.

The third component reflects the influence of the reactive generation capacity limits on prices, which could be used as a way to measure the need to increase the reactive power generation capacity. If reactive power generation equipment is on its capacity limit, then the prices will increase.

$$\rho_{Qi} = \frac{\partial L(V_G, t)}{\partial Q_i} = -\lambda \frac{\partial C_1(P_{G1})}{\partial Q_i} + \sum_{k=m+1}^{n} \left[-v_{VDi}^{\min} + v_{VDi}^{máx} \right] \frac{\partial V_k}{\partial Q_i} - v_{QGi}^{\min} + v_{QGi}^{máx}, \quad i = 1,2,...,n \qquad (2.35)$$

In this expression:

- ρ_{Qi} - represents the reactive power marginal price in node i;
- $v_{VDi}^{\min}$ - represents the Lagrangian multiplier associated with the minimum voltage level in constraint node i;
- $v_{VDi}^{máx}$ - represents the Lagrangian multiplier associated with the maximum voltage level in constraint node i;
- $v_{QGi}^{\min}$ - represents the Lagrangian multiplier associated with the minimum limit of the reactive generated power in node i;
- $v_{QGi}^{máx}$ - represents the Lagrangian multiplier associated with the maximum limit of the reactive generated power in node i.

El-Keib *et al.* (1997) indicates that, similarly to the active power marginal prices, the reactive power marginal prices can also be negative. A negative reactive power marginal price in a given node means that a load increase contributes to operate the system in better conditions, thus reducing its costs.

Taking the developed model, the authors (Ma *et al.*, 1998) conclude that:

- The economical signals associated to these prices can represent a way to effectively control the security level of power systems in a market environment;
- The unsuitable use of security limits could conduct to unfair tariffs to system users;

- The explicit identification of the active and reactive nodal marginal price components and, in particular, the active transmission losses component related with the reactive energy becomes an important aspect;
- The explicit identification of the several reactive price components contributes to a better understanding of the way following which the reactive power generation capacity investment should be performed in a open access environment (El-Keib *et al.*, 1997).

Apart from the advantages previously mentioned, these authors also indicate that the developed model allows the integration of new constraints, such as those related with the system spinning reserve, originating to a new cost component that should be distributed between users (El-Keib *et al.*, 1997).

Chattopadhyay *et al.* (1995) present a reactive generation power and capacitor bank distribution optimization problem that considers all the available resources, that is, generation capacity in generation nodes and capacitor banks in load nodes. Afterwards, it is minimized the system cost to determine the optimal combination of the available resources. The objective function includes two distinct terms related with the system marginal generation cost and with the cost of capacitor banks. In the proposed model these authors consider that the reactive price should provide the remuneration of the wiring companies by the reactive power generation costs and by the investment in capacitor banks and that these costs should be distributed fairly among all system users.

2.3.4.6. System services marginal price computation

Security always represents a crucial operational concern of the generation and wiring companies. In fact, in interconnected systems security constitutes a problem of particular importance, because it is not determined by the individual capacity of each generator, load or transmission line, but instead it represents a global system property (Kaye *et al.*, 1995).

Several market models were developed and adopted in an attempt to satisfy these system operation requirements. Between them we can refer the models in which the independent generators and the consumers subject its autonomy to the system operator. Others, like those referred by Kaye *et al.* (1995), adopted methods by which several participants determine, in each operation situation, the additional power quantity that could offer (in terms of load reduction or generation increase) in case of a contingency occurrence. In accordance with these authors, these models allow to attain the optimum social welfare minimizing the cost related with security control. Others, however, are characterized by the application of real time prices during the contingency period encouraging in this way the generation increase and/or the load reduction. During the normal system operation state, one should then use models that reflect the uncertainties on several variables in order to determine future prices and, consequently, obtain suitable levels of energy offers.

The ancillary services cost allocation represents a more complex task than the transmission services cost allocation since, for example, the operational reserve cost

could involve capacity, energy and opportunity costs. Additionally, some ancillary service costs present large temporal and geographical volatility being also function of the system load level (Pan, *et al*, 2000).

These costs are frequently allocated between system users regarding their respective loads and scheduled or effectively measured generation. However, the current trend corresponds to the development of specific mechanisms and in the creation of specific markets for this kind of services (Pan *et al*, 2000).

2.3.4.7. Transmission Congestion Contracts and Capacity Rights

In a condensed way we can say that a Transmission Congestion Contract constitutes an arrangement in which it is specified an active power transmission price between any two points of the system, independently of its state. They involve a node specification, a target price for the congestion component of the marginal price and the power to be injected or consumed in that node. In practice, the power is sold and bought at marginal prices (including the congestion marginal component) and, in this way, if the congestion marginal component is larger than the target price defined in the contract, the subscriber of that contract will receive an amount corresponding to the difference between these values. In the opposite case (target price larger than the congestion marginal component) the subscriber of the contract will pay to the company a value equal to the difference between these two values (Finney *et al.*, 1997).

If the contract involves two companies and a grid company, then the contract should specify two nodes and their respective target-prices, as well the value of power to inject in a node and to consume in the other. In this case, the companies involved in that contract will only receive a discount if the difference between the target-prices is smaller than the marginal active power transmission cost between these nodes.

According to Oren *et al.* (1995), establishing this kind of contracts has two main objectives. Firstly, they guarantee that the wiring companies will be remunerated by the use of their infrastructures. Secondly, they give the users a protection mechanism against eventual grid congestions. Since they correspond to long-term contracts, they represent a protection mechanism against future nodal marginal price volatility. However, these contracts are redundant and unnecessary if the systems are able to implement future nodal marginal price computation methodologies. In this context, these contracts represent a mechanism very similar to the well-known Contracts for Differences that can be established between producers and consumers.

The target price definition required by this kind of contracts imposes the computation of nodal marginal prices to a given future instant of time. In this context, the authors (Certo *et al.*, 2001) using a Monte Carlo simulation model presented a nodal marginal price computation model as well its expected values. In the developed model the unavailability of the equipments and load variations are considered using probabilistic concepts.

In this scope, Finney *et al.* (1997) presents a work that models the performance of an electricity energy market in the presence of network congestions and its corresponding nodal marginal prices. Taking this study as a reference, these authors also analyzed different technical and economical alternatives to the solution of that problem, namely the capacitor banks allocation, the grid expansion and the use of Transmission Congestion Contracts, in a clear attempt to illustrate the competition currently existing between technical and economical mechanisms in the solution of these problems. In this context, the authors conclude that these methodologies contribute to reduce the high transmission active power prices unleashed by the congestion occurrence. However, the alternatives having technical nature contribute to a better global system performance.

Several organization systems allow the existence of contracts not only of financial type, but also of physical type, called Capacity Rights. This kind of contracts gives the companies the possibility to have their power flows approved in a priority way by the wiring companies or system operators in case there is a congestion situation.

In this context, the simultaneous ownership of Transmission Congestion Contracts and Capacity Rights makes the owner companies more immune to congestion problems, reducing or even removing the risks that can emerge from the system operation and short-term marginal price volatility conditions. Nevertheless, they have been criticized because, to some extent, they represent a way back to the re-verticalization of the power sector (Saraiva *et al.*, 2002).

2.4. International experiences

2.4.1. General aspects

According to Krauser (2003), the allocation methodologies of the transmission energy costs must take into account the corresponding structure of the markets where they will be implemented. In this context, this author indicates that the marginal cost allocation methodology seems as one of the most adequate approach to be applied in centralized structures (based on pool markets), because in these cases, the nodal prices could be viewed like an integrated methodology of prices including several components (such as, generation, transmission, losses, capacity, between others), eventually interpreted as a result of the system social welfare optimization methodology.

Among marginal approaches, there is a trend to apply short-term marginal costs given that they are less complex and easier to compute when compared with the long-term ones. However, as it was previously mentioned, this kind of methodology does not allow to recover all the transmission costs. In this context, the tariff structures in use in countries that restructured their power systems include:

- Interconnection tariffs to remunerate the required reinforcement cost;
- Use of system tariffs (capacity tariff), that remunerate the wiring companies for the investments in the transmission system, together with its operation and maintenance cost;

- System operation tariff (energy tariff), to remunerate the wiring companies by the costs incurred in the electricity market as a consequence of the non-ideal nature of the system. The remuneration obtained can be used to compensate suppliers of services such as losses, system balancing, congestion management, among others. If based on short-term marginal prices, the revenues obtained by the TSO could be used to reduce the use of system tariffs or to compensate the capacity transmission rights owners.

In this context, in the next Sections we will present some details of the tariff structures in practice in several countries all over the world.

2.4.2. Chile and other South American countries

In the 80's a set of South American countries and, in particular Chile in 1982, became a pioneer country in the re-regulation of the electricity sector when introducing a law that established the necessary conditions to create an open electricity energy market including generators and large consumers that could chose their energy suppliers. In this process, they were also created the conditions to the open access to the electric networks paying an adequate tariff. In these countries, the regulation of this service established a tariff structure that typically includes two different components: a short-term marginal price component and an additional tariff term based on the area of influence of each generator in order to ensure the full cost recovery (Rudnick *et al.*, 1995).

In the Chilean system, the energy marginal price is computed by dispatching all generation units admitting they are connected to the same system node. In Argentina the short-term marginal prices are computed using the JUANAC software (Rivier *et al*., 1990). In Figure 2.2 it is displayed the percentage of the remuneration that is provided by the marginal tariff applied to the main branches of the Chilean transmission system.

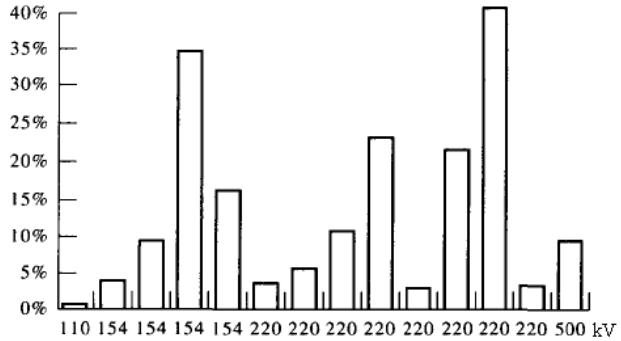

Figure 2.2: Percentage of transmission costs recovered by the marginal tariff term in Chile (source: Rudnick *et al*., 1997).

Given the transmission marginal pricing limitations, these countries implemented a supplementary tariff that combines the marginal and average cost concept. In Argentina, Bolivia and in Chile this component is determined by means of the concept of the area of influence of each user, which corresponds to the set of lines and substations directly influenced by the peak user injected energy and power. This area of influence aims at

representing the effective use that each user makes of the system, independently of the commercial contracts they had established. In Peru, however, this component is computed using the postage stamp method.

In any of these cases, the adopted tariff schemes also define that only those transactions that contribute with positive power flows must pay for the equipment capacity and those that contribute to relieve the system don't have to pay and are not remunerated by their contribution. In Chile, only generators pay this tariff component.

All these regulatory schemes consider marginal transmission losses as an economic signal to be transmitted to system users. However, in all of them, with exception of the Argentinean system, the economical signals related with congestions are not considered. The Argentinean model includes a factor that reflects the network reliability, the merit order of the dispatch and the Power Not Supplied (Rudnick, 1997).

Some of the critics that are usually made to the Chilean model are essentially related with the general and less transparent way used to define the supplementary tariff and with the fact that the marginal remuneration only contributes with a small fraction (approximately 14% in average) of the regulated remuneration, since it only considers losses and completely neglects network constraints. Since the Chilean system is basically radial, this approximation can, however, have a significant impact (Rudnick *et al.*, 1995).

Taking into account the tariff model adopted in Chile, namely in what respects to the ambiguous way by which it was evaluated the effective system use, in March 2004 it was approved the law 19.940, defining a new transmission tariff structure. According to this law, the transmission tariffs are determined in four distinct stages (Galetovic *et al.*, 2006):

- Each four years the networks are evaluated by external auditors in order to determine the annualized investment costs and the administrative, operation and maintenance costs that correspond to the regulated costs;
- The transmission tariff is allocated to producers and consumers according to the use that each one makes of the system. In this context, it is introduced the "common influence area" concept (defined as a set of components between two nodes for which at least 75% of the total power is injected in the area, at least 75% of the total load is in the area and the density factor is maximum). For this "common influence area" it is defined that 80% of the transmission cost is allocated to the generators and the remainder 20% to consumers. Out of that "common influence area", the grid use is determined by the direction of power flows: branches that inject energy in the "common influence area" are considered as used by the generation units and, in the opposite side, branches that consume energy from the "common influence area" are considered as used by loads;
- Once identified the users of each branch, the individual use of each generator is determined by means of the GGDF method. By analogy, the individual use of each consumer is determined using the GLDF method;
- Differently from the previously used approach, according to this new methodology the consumers pay directly to wiring companies by the use of their

network resources. The applied tariffs are equal for the majority of consumers (< 2 MW), since that for these it was introduced the postage stamp method.

In this context, the wiring companies receive an annual remuneration given by expression (2.36).

$$RM = AIC + AOMC \tag{2.36}$$

In this expression:

RM - represents the annual remuneration that the wiring company can receive;
AIC - represents the annualized investment network cost;
AOMC - represents the administrative, operation and maintenance costs.

Part of the amount required to cover these costs comes from the nodal marginal price differences of energy and power. Since the Chilean system adopts a centralized dispatch model based on the marginal costs merit order, the value to pay by a branch use corresponds to the difference between the marginal costs in the extreme nodes in the branch under analysis, as described by expression (2.37).

$$tc = \rho^N.P - \rho^S.(P + pl) \tag{2.37}$$

In this expression:

tc - represents the marginal transmission tariff;
ρ^N and ρ^S - represents the energy marginal prices in extreme nodes N and S, respectively;
P - represents the branch power flow;
pl - represents the losses in the branch under analysis.

The remaining tariff term corresponds to the price difference between the regulated transmission cost and the remuneration obtained by the marginal method. In this context, the tariffs paid by generators and consumers are given by the expressions (2.38) and (2.39), respectively (Galetovic *et al.*, 2006).

$$TG = \lambda_G \times T \times \frac{\alpha_g.I_g}{\sum_j (\alpha_j.I_j)} = \lambda_g \times T \times A_g \tag{2.38}$$

$$TL = \lambda_L \times T \times \frac{\beta_l.D_l}{\sum_k (\beta_k.D_k)} = \lambda_L \times T \times B_l \tag{2.39}$$

In these expressions:

TG and *TL* - represent the transmission tariffs paid by generators and consumers, respectively;

λ_G and λ_L - represent the cost fraction allocated to generators and loads, respectively. By definition, in the "common influence area" these fractions take the values of 0.8 and 0.2, respectively;

I_g - represents the energy injected by generator g;

D_l - represents the energy consumed by load l;

α_g - represents the utilization factor of generator g for a given branch determined using the GGDF ($\alpha_g \in [0;1]$);

β_l - represents the utilization factor of load l for a given branch determined using the GLDF ($\beta_l \in [0;1]$);

T - represents the difference between the regulated cost and the remuneration obtained by the marginal method.

Figure 2.3 presents, schematically, the new transmission cost allocation structure adopted in Chile (Galetovic *et al.*, 2006).

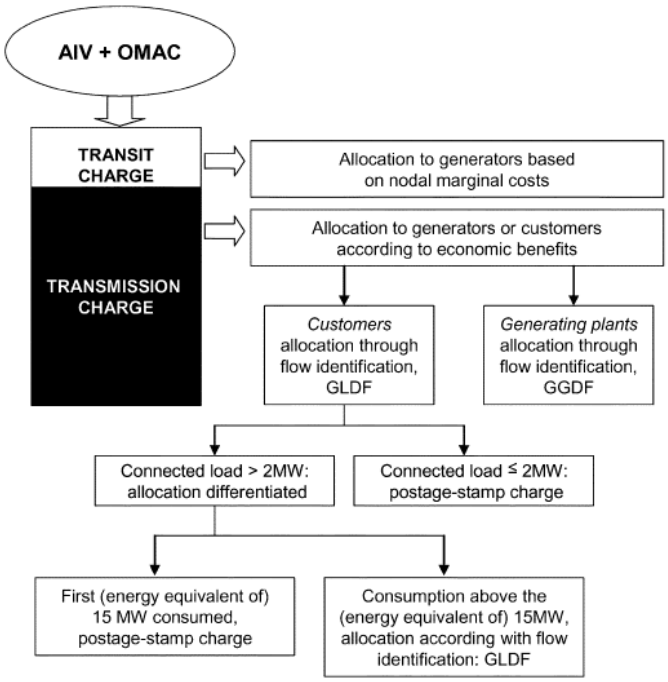

Figure 2.3: New energy cost allocation structure in Chile (source: Galetovic *et al.*, 2006).

Galetovic *et al.* (2006) indicates that this tariff model is able to create proper economical signals to the entrance of new generation in the system. However, he considers that the definition of the "common influence area" could, to some extend, weaken the economical signals transmitted to the users. At this respect, he also criticizes the way by which the "common influence area" was defined, because it is confined to the small system region that surrounds Santiago (main consumer region of the country). These authors also mention the fact that the introduction of the Postage Stamp method in the computation of

the tariffs applied to consumers turns the new structure tariff less able to produce proper price signals in relation to their geographical location.

2.4.3. Portugal

In Portugal the tariff system is of the *Entidade Reguladora dos Serviços Energéticos* - ERSE - responsibility, since this entity defines its main principles and tariffs for a given regulatory period. The current tariff scheme adopted the Postage Stamp methodology and comprises the following characteristics:

- The tariffs are differentiated by voltage levels, comprising tariffs for the use of the very high voltage networks and another for the high voltage networks;
- These tariffs comprise two power prices defined as the contracted power and the peak hour power, both in €/kW.month, two prices for the reactive energy (absorbed and supplied) defined in €/kvarh and prices for the active energy defined in €/kWh. Energy prices are also divided in hourly periods like (*ponta, cheias, vazio* and *super-vazio*) and tri-monthly periods in an attempt to model the different weather conditions as the wet and dry periods.

Since this tariff scheme is based on the transmission cost, for each regulatory period ERSE also publishes the expression by which it must be determined the amount of money that the wiring company could receive in each year of that regulatory period in order to guarantee all the costs of its activity.

Saraiva *et al.* (2001), in the sequence of the Portuguese tariff regulated revision work and, more specific, in a study regarding the estimation of the marginal remuneration that could be obtained by the Portuguese transmission network company concluded that, at least in 1998, the remuneration that could be obtained by means of that tariff corresponded only to about 10% of the transmission regulated costs approved by ERSE. In this context, the authors concluded that this reduced value clearly indicated that the Portuguese transmission network was well planned and also that the adoption of such tariff scheme clearly would create an enormous revenue reconciliation problem.

The same authors (Silva, *et al.*, 2001) also concluded that the remaining 90% of the regulated costs, even contradicting the uniformity principle in force since 1995, could be allocated using the Module or Use method because, in treating load contributions in a equality way they would allow reflecting in a more transparent way the system use. In this study, these authors also analyzed the use of the Zero Counterflow and MW.Mille methods. The first one has the disadvantage of creating tariff discontinuities and it would conduct to less predicable tariffs and, eventually, not so well understood by the users. The second would create some cost allocation unfair situations to the users.

Having in mind the evaluation of the investments performed in the transmission grid in the period between 1998 and 2001, in this latest year it was performed a new study analogous to the previously mentioned now regarding 2001. In this context, the authors (Saraiva *et al.*, 2004) concluded that in 2001 the remuneration that could potentially be

recovered using the short-term marginal approach more than duplicate regarding the values estimated for 1998, corresponding to about 21% of the transmission regulated costs. Such increase means that the transmission grid operation conditions were degraded in terms of losses and congestions conducting to increased nodal prices differences. Comparing these two studies it was possible to conclude that new grid investments should be made to avoid future operation problems.

2.4.4. Brazil

In Brazil the Regulatory board (ANEEL – *Agência Nacional de Energia Eléctrica*) established the tariff system for the use of the transmission networks using a methodology called *Precificação Relativa aos Custos de Investimento* – PRCI, analogous to the Investment Cost Relating Price methodology adopted in England and Wales. As mentioned, this approach constitutes an approximation to the long-term marginal cost method. In fact, the PRCI only differs from the ICRP in the fact that the first one, in opposition to the last one, considers that the grid power flows respect the balance equation and the Kirchhoff laws.

The tariff computation method considers a factor to reduce the temporal volatility of the tariffs. According to Machado *et al.* (2001), these tariffs are computed using expression (2.40).

$$\pi_B = \sum_{L=1}^{NL} \beta_{LB}.c_L.fp_L \tag{2.40}$$

In this expression:

$$fp_L = \begin{cases} 0 & if, \quad r_L < r_{\min} \\ \dfrac{r_L - r_{\min}}{r_{\max} - r_{\min}} & if, \ r_{\min} \le r_L \le r_{\max}, \\ 1 & if, \quad r_L > r_{\max} \end{cases} \qquad r_L = \frac{|f_L|}{capac_L} \tag{2.41}$$

- π_B - represents the nodal tariff of the generation (load) connected to node B;
- NL - represents the number of transmission elements;
- β_{LB} - represents the sensitivity factor that relates the power flow in circuit L with the injected power in node B;
- c_L - represents the unit transmission cost of the element L;
- fp_L - represents the factor associated to the transmission element L;
- r_L - represents the load of the transmission element L;
- $r_{\min}$ - represents the load value of the transmission element L, bellow which the factor is zero;
- $r_{\max}$ - represents the load value of the transmission element L, above which the factor is unitary;

f_L - represents the power flow in the transmission element L;
$capac_L$ - represents the capacity of the transmission element L.

In this system, the nodal tariffs obtained using this approach do not allow the complete remuneration of the transmission cost services. To solve this problem, it is used a supplementary tariff. In the Brazilian system this supplementary tariff is divided in two distinct components. One of them is applied to generators and the other is applied to loads. These terms are computed using expressions (2.42) and (2.43), respectively.

$$\Delta g = \frac{\left(RG - \sum_{B=1}^{NB} \pi_B . g_B \right)}{\sum_{B=1}^{NB} g_B} \tag{2.42}$$

$$\Delta c = \frac{\left(RC - \sum_{B=1}^{NB} \pi_B . d_B \right)}{\sum_{B=1}^{NB} d_B} \tag{2.43}$$

In these expressions:

Δg - represents the supplementary tariff term applied to generators, which is uniform for all generators;
Δc - represents the supplementary tariff term applied to consumers, which is uniform for all consumers;
RG - represents the fraction of the transmission service costs to be paid by generators (50% of the total transmission costs);
RG - represents the fraction of the transmission service costs to be paid by consumers (50% of the total transmission costs);
π_B - represents the nodal tariff of the generator connected to node B, computed by the expression (2.41);
NB - represents the number of buses in the system;
g_B - represents the installed capacity of generator B[1];
d_B - corresponds to the value of the contracted or registered load power (the largest one) to the considered hourly period (peak or out of peak).

Finally, it must be noted that the total amount paid by a generator connected to node B is given by its transmission tariff (marginal fraction plus the supplementary tariff) multiplied by the corresponding installed capacity.

[1] According to ANEEL (1999), when the tariff to be applicable to generators is negative, instead of the installed capacity it must be used monthly dispatched values. Using this criterion, the regulatory board wishes to avoid situations of over-remuneration of generators which, for being frequently off or dispatched at reduced values and although geographical close to loads, do not avoid grid expansion investments. At the same time, this criterion recognizes that, for being geographical close to loads, they could eventually be dispatched out of the merit order in all those situations where the transmission system is unavailable, postponing, in this way, transmission investments in an attempt to guarantee load supply in faulty network configurations.

2.4.5. Norway

In Norway, the transmission grid tariff comprises four distinct terms. Two of them result from short-term methodologies, and so they are dependent on grid use. The other two are defined on an annual basis. These variable components of tariffs remunerate of the costs incurred by losses and congestions.

The tariff element related with losses is based on the market marginal prices and constitute an approximation to marginal losses caused by generation and consumption on a given region. This element represents approximately 25% of the total cost and is computed as the product of the energy transactions registered on the system by a marginal loss factor computed for each time period for each location and by the electricity market price. For loss factors computation purposes, Norway is divided into five distinct regions for which the system operator determines the marginal losses that result from the generation and consumption in three typical load situations (Braten, 1997). Some of the critics pointed to this methodology are related to the fact that the model only determines a marginal losses approximation caused by each generator or consumer, once that:

- Generations in different nodes within the some region can contribute in a distinct way to the marginal loss value. However, they are treated in a equal way by the model;
- The model did not recognize that generations and consumptions in the same node are cancelled from the point of view of their effects in system losses;
- The model neglects eventual variations of load within the three typical scenarios.

In the Norwegian system, network congestions eventually predictable in the operational system scheduling stage are treated by establishing different price areas. In fact, this procedure represents part of the process used to obtain the daily prices in the Nordpool electricity market. Firstly, it is computed the system price without considering the possibility of occurrence of any kind of congestions. If the resulting schedule originates any congestion, different price areas are created. In this system congestion costs are internalized in the energy prices as the difference between the system price and the price in an area, and so, paid by the market participants. In this context, the prices induce the agents to adjust their system use in accordance with the available capacity.

When different price areas are established, the wiring companies are remunerated by a value that corresponds to the sum of the price differences between areas multiplied by the transacted energy. When the congestion occurs between the Norway and Sweden this quantity is shared by the two system operators. In 1997, however, as a consequence of the reduced number of congestion situations, this term corresponded to less than 1% of the total regulated costs.

The costs related to the Regulation Power Market activity in an attempt to guarantee the system balance in real time operation and to remove eventual congestions not predicted in

the scheduling stage are also included in the transmission tariff (Braten, 1997; Gomes, 2005).

The remaining tariff terms are justified with the necessity to guarantee the total remuneration of the transmission costs. In this system, these terms are called interconnection tariff and power tariff. The interconnection tariff is paid by generators and consumers and in 1996 it represented 19% of the total transmission regulated costs. The power tariff is based on the injected power on the system in each region along the peak hours.

According to Braten (1997), the main disadvantage of the Norwegian tariff system is related with the inexistence of economical signals that reflect long-term marginal costs. In the opinion of this author, other problems are related with the existence of differences between tariff structures of the main and regional networks that originated situations of investments in regional network interconnections that only benefit them. This author also refers that the power tariff conducted, in the past, to situations in which some generators reduced their installed generation capacity. The marginal losses computation by area is mentioned as another imperfection of the tariff system, and so this author suggests the use of nodal loss factors.

2.4.6. New Zeeland

Since 1996 the transmission tariff scheme of New Zeeland considers a DC optimization model that includes losses computed using a linear approximation. The implemented model computes the nodal prices in approximately 600 nodes, although they are published only, approximately, 150 different nodal prices. These prices take into account the thermal limits of lines, marginal energy losses and reserve conditions. There is also the possibility of incorporating additional security constraints if that becomes necessary.

According to Read (1997), the simplicity and transparency of the adopted model is the basis for its good acceptance. Nevertheless, some critics were pointed, especially from those consumers that become more exposed to price volatility and from remote consumers that experimented higher prices.

2.4.7. England and Wales

Till 2000 in the English and Welsh market, the NGC is the company concessionary of the transmission grid. This company rejected the tariff model based on long-term marginal costs by considering that they are unpredictable and difficult to compute. In this context, it was adopted the ICRP model, by considering that this method could produce more stable and transparent economical signals.

The ICRP method consists in a linear optimization programming model that minimizes the MW.km associated to a transaction, considering that the electricity flows along the least distant electric circuit between the generation and load nodes. In any node, the

generation cost is equal to the symmetrical of the load cost. By simplicity, the system was divided in several price areas of TUoS (Time of Use of System) given that nodes with similar prices were grouped into price areas. In each of these areas the price corresponds to the average nodal prices of the nodes in each area. As an example, in 1996/97 the system comprised eleven price areas, and afterwards it passed to fourteen price areas. After 1997/98, NGC started to consider distinct weighting factors for generation and load tariff computation effects (Bakirtzis *et al.*, 2001).

According to Green (1997a), the model adopted by NGC presented some drawbacks, namely in what respects to its capacity to recover all the company incurred costs. In 1992, this forced NGC to increase the tariffs. In fact, according to Bakirtzis *et al.* (2001), the model only allowed to recover approximately 20% of the total company incurred costs, essentiality because it does not consider the grid reliability in the computation of those prices. The linear optimization model used to compute the expansion system costs also presented some problems, once it assumed that the electricity flows by the shortest electric circuit between two nodes, what in fact this does not happen. For another side, the expansion cost – represented by the MW.km value – assumes that lines would be operated at full load, which does not have correspondence with reality. Finally, NGC tariffs did not include the cost of losses. Losses were considered as a pool matter similarly to other transmission operation costs (initially the pool started to conceive a tariff scheme to reflect the costs of losses, however, this model was substituted by another that considers a marginal cost factor) (Green, 1997a).

In the operational costs it is included the ancillary services of reactive energy and the secondary reserve that the NGC buys from generators. Subsequently, these costs were passed to the pool as an additional tariff called Uplift that did not have any kind of geographical distinction. Congestion costs were obtained by means of a tariff called Operational Out-Turn. In fact, when NGC determined the next day operational programme it ignored any kind of congestion constraints. Afterwards, any generator that faces congestion could not produce and would be considered Constraint-off. The bid price of this Constrained-off generator was below the Pool Purchase Price (PPP). As a result of constraining off a generator, another generation unit would be forced to operate (Constraint-on) selling in this way energy to pool at its offered price (which would be larger than the Pool Purchase Price). In this context, the cost of the congestion solution process corresponds to the total costs of this procedure that is the offer price of the Constraint-on generation unit minus the offer price of the Constraint-off generation unit.

Given the higher costs of this procedure, in 1994/95 it was approved an incentive model, Uplift Management Incentive Scheme, aimed at giving an incentive to NGC to reduce the system operation costs. This model was maintained and even improved until a more detailed model called Transmission Services Project were approved. This model identified in a more exhaustive way the congestion costs using a computer application requiring a larger system security level taking into account the eventual unavailability of the generation units. In this new model, the Uplift term was divided in Transport Uplift and Energy Uplift with different incentive schemes. The Transmission Services Project also gives an incentive to NGC to reduce losses forcing it to pay 20% of losses larger than a specified reference level (Green, 1997a).

Finally, it must be also emphasized that both distribution wiring companies and NGC were subjected to a price cap regulatory model. In Table 2.1, it is detailed the tariff value approved for each of the NGC price areas in 1997 (Tabors, 1994).

Table 2.1: Tariffs proposed by NGC [£/MW] (source: Tabors, 1994).

Area	Name	Load [£/MW]	Generation [£/MW]
1	North	0	8500
2	Yorkshire	5900	4700
3	North Wales & West Lancaster	6200	4300
4	East Lancaster	8100	2200
5	Nottinghamshire	6700	3600
6	West Midlands	10000	1700
7	Anglia	11500	-200
8	West & Wales	13000	-500
9	Estuary	10500	800
10	Outer London	13500	-1700
11	Inner London	18500	-7900
12	South Coast	14300	-3300
13	Wesses	18300	-4800
14	Peninsula	22100	-7900

As it can be seen in Table 2.1, there is a significant transmission price spatial dispersion. Some South and East regions have small generation capacity, and so, the transmission tariff applied to generators in these areas is negative. The North has a high generation capacity but reduced load, and so the consumers in these regions face a reduced transmission tariff. As a result, the tariff system in England and Wales gives strong economical price signals to the geographical location of generators in the system (Tabors, 1997).

CHAPTER III Uncertainties in Power System Studies

3. Uncertainties in power system studies

3.1. General aspects

Power systems were always affected by a huge number of uncertainties. They were traditionally related with load growth, consumer response to demand-side options, longevity and performance of life-extended or converted plants, potential supply of renewable resources, measurement error or forecast inaccuracy, unscheduled outages, technological developments, fuel prices (in the absence of long-term contracts with specific and known fuel prices, for example, facilities could be rendered uneconomic by price run-ups) or even regulatory definitions (Merrill *et al.*, 1990). In fact, these uncertainties are related with different variables, such as physical, technical, economic, regulatory and political.

Nowadays, power systems are facing a new set of uncertainties that derive from a growing consciousness about environmental concerns that are driving the future of the sector. In this context, and as an attempt to deal with this new kind of concerns, in 2005 the European Union (EU) launched the European Union Emissions Trading System (EU ETS) which is a market based instrument that allows the participants to trade CO_2 allowances aiming at creating incentives to reduce CO_2 emissions.

Since Renewable Energy Resources (RER) are carbon free, it is also being implemented in some European Countries a green certificate market as a way to create incentives to invest in this type of technologies. More recently and since energy efficiency is also an essential element of the EU energy policy, some member states also launched the White Certificates market (WhC) as a way to promote energy efficiency (Farinelli *et al.*, 2005).

In case these market instruments work properly, it is expected a net electricity demand reduction, essentially driven by the WhC market and the investments financed by the revenues of the EU ETS (Farinelli *et al.*, 2005; Ruth *et al.*, 2008).

It is also expected that the EU ETS alters the merit order of generators quite substantially decreasing the share of some still predominant fuel sources more carbon intense like, for instance, coal and gas. This decrease can be larger if the Green Certificate system works properly in promoting RER investments. Simultaneously, it is expected a reduction of the investments in new generation capacity given the expected demand reduction. It is also important to refer that the implementation of more ambitious quota for RER together with the Green Certificate system will contribute to reduce the price of the allowances within the EU ETS. As a result, market participants will face a net combined effect. In fact, they have to face uncertainties in fuel prices, cost of purchasing EU ETS allowances if the CO_2 emissions exceed the limited amount of allowances allocated in a administrative way, opportunity costs of selling allowances in case they are not fully used and, finally, uncertainties on demand and on RER generation levels (Rathmann, 2007; Soderholm, 2008).

As a conclusion, internalizing the environmental damages due to energy generation and consumption into prices is bringing to the power sector a more conscious and sustainable

way of planning and operating the system. On the other hand, it also brings to the sector a huge number of new uncertainties and challenges that can contribute to raise the cost of capital and alter investment decisions. Accordingly, market participants should be able to use and adopt methods that are able of addressing all these uncertainties and integrate them into the investment decision making processes. In fact, risk has to be adequately addressed if one wants to have a complete and consistent picture of the future power system operation while ensuring that profits are large enough to compensate the cost of capital (Blyth *et al.*, 2007).

3.2. Modeling uncertainties in power system planning and operation

When planning and operating a power system it is necessary to perform power flow studies in order to assess and monitor the steady state security of the system. These studies are one of the most frequently performed network calculations and there are several well developed techniques that allow these studies to be made very quickly and accurately. These methods have, however, a deterministic nature and so, during each power flow solution, the nodal loads, the generation and the topology of the network are assumed constant. However, these parameters can not be considered perfectly constant, since uncertainty could have multiple sources as it was indicated in the previous section. One possible way to overcome this problem is, obviously, by solving a set of deterministic power flow studies for combinations of the input parameters. This strategy becomes, however, unpractical given the prohibitive amount of calculations (for networks with N nodes and k different load values at each node, k^N power flows would be required) and also because it becomes difficult to analyse and synthesize the results of so many studies (Borkowska, 1974).

An attempt to solve this problem would correspond to select a limited number of scenarios (usually large) for which the problem should be solved. Apart from the high computational effort, this kind of approach wouldn't also give any kind of guarantee about the quality of the results since they are function of the selected scenarios that are generally chosen arbitrarily. In this context, in the next sections we will detail some of the most representative methods available in literature to address this kind of problems, namely the Probabilistic, Boundary, Fuzzy and Interval Arithmetic methods.

3.2.1. Probabilistic methods

As a consequence of the concerns just referred, during the 70's it emerged a new class of methodologies named Probabilistic Power Flow that, for the first time, allowed the incorporation of uncertainties in power flow studies. In fact, from the 70's till nowadays several Probabilistic Power Flow models were developed and proposed to address the power flow uncertainty problem. These models can correspond to simulation approaches, analytical methods, or to a combination of both (Lien, 2005).

3.2.1.1. Simulation methods

The simplest evaluation of the Probabilistic Power Flow problem is through Monte Carlo Simulation (MCS). This method involves a repeated selection of the value of the input variables using the respective probability distribution and then, for the selected values of these input variables (active and reactive power), obtaining the values of the state vector exactly in the same way as in deterministic analysis.

Theoretically, there is no limitation on the use of the MCS method. For instance, the exact nonlinear power flow equations can be used, statistical dependencies between loads and generations can be easily considered, probability of different network configurations can be taken into account, etc. On the other hand, the MCS approach requires a large number of trials to ensure obtaining accurate results. This means that a huge amount of storage and computing time is necessary, which makes the process less attractive. To reduce the computational effort, linearised power flow equations can be used when the input uncertainty in load is not very large and the degree of nonlinearity in the power flow functions is reasonably small (Leite da Silva, 1985). The final step consists of obtaining the probabilistic description of the state vector from the results of the repeated simulations.

3.2.1.2. Analytical methods

To reduce the computational effort in solving the Probabilistic Power Flow problem, several analytical approaches were proposed to estimate the power flow solution. Owing to the inherent complexity of the analytical solution, the following assumptions were considered by most Probabilistic Power Flow algorithms (Leite da Silva, 1985):

- Linearized power flow equations;
- Independency between input parameters;
- Constant network configuration.

Therefore, the accuracy of the analytical methods is also limited because of the assumptions used to overcome the inherent difficulties. In this context, the first contributions in this area were proposed by Borkowska (1974) and Allan *et al.* (1974) that developed Probabilistic DC Power Flow models considering nodal data uncertainty and convolution techniques to determine the power flow output variables. In these methods all input data are firstly converted to the expected values and their variances in such a way that it is possible to define the power flow in any branch of the system as a function of sensitivity coefficients and the expected values and variances of the input data (Allan *et al.*, 1974).

One of the main difficulties of these methods is the mathematical control of the power balance that, as we know, is a nonlinear function of the power inputs and outputs in particular nodes. For simplicity, these two approaches admitted that the balance of power is only a function of the sum of the power inputs and outputs. This means, it does not

depend on the power inputs and outputs in particular nodes and so, as a consequence, the dispatcher's activity is confined to the slack node (Borkowska, 1974).

The first contribution in terms of an AC model was given by Allan *et al.* (1976a). In fact, they presented a Probabilistic AC Power Flow algorithm that considers linearized versions of the power flow equations, an active and reactive power decoupled approach and uses convolution techniques to obtain the density functions of the output variables. In particular, in this Probabilistic AC Power Flow approach they were considered some of the assumptions that were also used in the DC formulations in what respects the active power. For the reactive power two formulations were developed. In the first one, the reactive power equations were linearized by considering that voltages are set at 1 p.u. in all nodes. The second one admits that nodal voltages are close to the unity. Nevertheless, since both of these formulations transform the nonlinear equations into linear equations consisting of the sum or difference of independent random variables, in both of them mathematical convolution techniques can be applied in a straightforward manner to obtain the density functions of the unknown quantities. Based on the results obtained with these two formulations, the authors concluded that even when the majority of input data are normally distributed, the output data are not and that the amount by which the density curves deviate from the normal distribution depends on the system and on the specified input nodal quantities. As an example, as the number of binominal and discrete powers are increased for a given system size, the computed density curves deviate more from a normal distribution.

Comparing the density curves obtained with these two formulations, it was observed that the computed density function was shifted slightly relative to each other. It was also observed that the errors in the expected values may be overcome by shifting the computed density curve, without changing its shape, until its expected value coincides with the value obtained with a conventional deterministic analysis. This newly positioned curve would then represent a reasonably precise distribution for the quantity being computed (Allan *et al.*, 1976a).

Recognizing that the demand is not always completely independent, but instead it could be correlated owing to common effects such as weather conditions and human behaviour patterns, Allan *et al.* (1976b) presents a Probabilistic Power Flow algorithm assuming that demands could be totally uncorrelated (independent), totally correlated (dependent) or partially correlated. In the case of correlated nodal demands, linearly functionally dependent and normally distributed random variables are considered and so the convolution process was modified so that a net arithmetic addition of the correlated variables is first identified for each circuit. This results in a new independent random variable that is then convoluted with all the remaining independent random variables. This work also discusses the impact of transmission equipment outages.

Since the previously Probabilistic AC Power Flow models produce some inaccuracies on the results, Allan *et al.* (1977) presents a new technique that uses the expected value obtained from a deterministic solution as the basis for computing the probability density curves that could also account for the coupling effect between active and reactive power In fact, these authors presented two distinct formulations: one of them assumes that

active and reactive power are decoupled while the other one does not make this assumption. In this context, in this new model the linearization process of the power flow equations is made around the solution point of a conventional deterministic power flow study that corresponds to the expected value of the probabilistic analysis. Comparing the results obtained with the first approach in Allan *et al.* (1976a) with the results obtained with this new technique, the authors concluded that angles and active power flows are quite close. However, in case of voltages, reactive power flows and injected reactive power, considerable differences can arise.

As an attempt to improve the accuracy of this kind of methods and in order to reduce the computation time, Allan *et al.* (1981a) presents a new Probabilistic AC Power Flow that uses a discrete frequency domain convolution technique - Fast Fourier Transform. Comparing the results of this new technique with the ones obtained from a Monte Carlo Simulation the authors showed that the performance of the linearized model is very good within a certain range of uncertainty of the input random variations. This reference also indicates that the convolution technique used in the Probabilistic Power Flow method to combine realistically an infinite range of solutions is a very powerful tool and that the Fast Fourier Transform method corresponds to a very significant improvement of the conventional method and gives faster and more precise results.

In the work under analysis, the Central Limit Theorem also received considerable attention. Based on the obtained results, the authors concluded that even if the input parameters are normally distributed, the output parameters will not be due to the nonlinearity of the power flow equations. The normal assumption is, at best, a rough approximation to the exact answer. In line with these concerns Allan *et al.* (1981b) developed a new Probabilistic Power Flow algorithm that uses linearized equations, but that can also take into account the nonlinear effects of the power flow equations. In fact, recognizing that the linearized models generally performed well near the region of the expected value (linearization point) and worse in regions far from it, as illustrated in Figure 3.1, the authors presented the Boundary Load Flow (BLF) iterative algorithm that tries, in a first stage, to determine the maximum and minimum values of the output random variables (values associated to a probability between 0.997 and 1.0 if the output follows a normal distribution and 1.0 if the output follows a discrete distribution) in an attempt to determine new points where the linearization concept could be applied. This iterative algorithm was also modified so that it can determine other different linearization points, either on the right hand side or on the left hand side of the expected value depending on the region of interest.

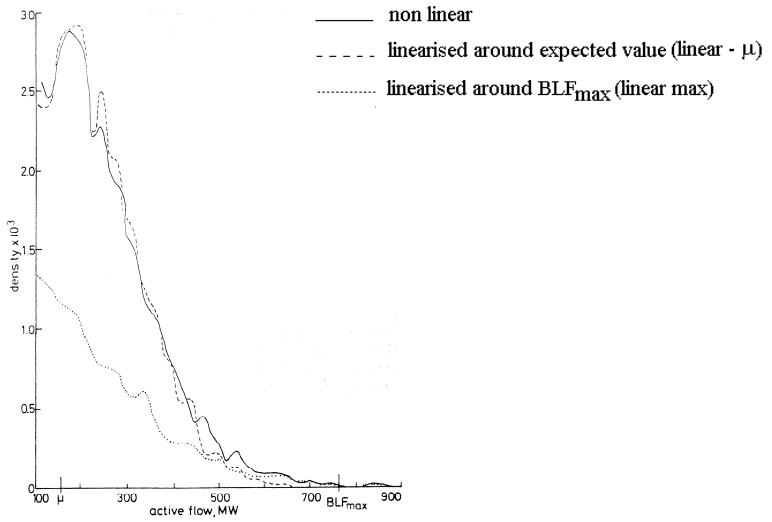

Figure 3.1: Effect of BLF algorithm on the probability density function of $P_{1\text{-}2}$ (source: Allan *et al.*, 1981b).

As a consequence, in the new Probabilistic Power Flow algorithm, the BLF is called to evaluate the sensitivity coefficients for different points of linearization. A convolution technique is then used to obtain the probability density function for each of these linearization points. Finally, these partial solutions are properly combined to give the final representation of the required output random variable.

Karakatsanis *et al.* (1994) presents a method for network constrained setting of control variables based on Probabilistic Power Flow analysis that allows decisions regarding the relaxation of some operating constraints to be based on information like probabilities of occurrence. This approach determines operating constraint violations (voltage magnitude of load buses, active and reactive powers injected at generator buses, power flows on branches, etc.) for a whole planning period together with the probability of each violation. An iterative algorithm is subsequently employed providing adjustments on the control variables based on sensitivity analysis of the constrained variables in order to select the ones which have the largest effect on the limit violation.

More recently, Zhang *et al.* (2004) presented a new method to compute the Probabilistic DC Power Flow that combines the concept of Cumulants and Gram-Charlier expansion theory to obtain the probabilistic distributions functions of transmission line flows. Taking as reference the obtained results and its comparison with the ones obtained with a Monte Carlo Simulation, the authors concluded that the developed method is able to accurately approximate the output distribution functions but, more important, it allows a significant improvement in reducing data storage requirements.

Hu *et al.* (2006) presented a methodology based on the previously mentioned method to deal with the random branch and generating unit outages and load uncertainties of nodal power injections using their moments and comulants. Finally, Schellenberg *et al.* (2005) described the use of a cumulant-based approach to compute the output probability

distributions while comparing these results with the ones obtained by Monte Carlo simulations as a way to evaluate their accuracy.

Lien (2005) also presented a new approach for this problem that considers uncertainties on bus data and line parameters and uses a point estimate based method to perform statistical inferences and obtain the probability distributions of a power flow solution through simple numerical computations. This approach uses the nonlinear power flow equations and can be applied with the currently available power flow codes. Using the results obtained with a Monte Carlo Simulation as basis, this author concluded that the proposed method could reach similar results with less numerical computation effort and has a better performance than the combined simulation and the analytical approaches. He also concluded that, to get better results, a larger number of estimate points could be used in the proposed method.

3.2.1.3. Combined methods

Aboytes (1977) and Allan *et al.* (1979) presented new methodologies to obtain a Probabilistic Power Flow solution when network outages are modelled as random variables following a discrete distribution. These calculations could be carried out using Monte Carlo Simulation techniques, analytical methods or by a combination of both. In these works the authors present two distinct formulations both of them using the DC model for the power flow equations. The main differences between the two approaches are on the adopted contingency simulation method. In the first formulation (Aboytes, 1977), the contingencies are simulated using a compensation method. This means that the addition or the removal of branches is simulated by means of suitable injections into the system without effectively adding or removing any line. Following Leite da Silva *et al.* (1985), the main disadvantage of this method relies on the probabilistic model used for the contingencies. In fact, only first-order contingencies are considered and the final active power flow in a given component is computed as a weighted summation of flows in this element for each analysed contingency. In fact, this corresponds to an approximation of the probabilities associated with the basic configuration and with the configurations considering the outage of each component.

In the second method (Allan *et al.*, 1979), the probabilistic contingency model considers all first and some selected second order outages and it also uses the exact probability value of each configuration, assuming independency between outages. However, following Leite da Silva *et al.* (1985) if only first and some selected second order outages are analysed, a number of possible configurations will be neglected, and so, the subspace of these configurations states summates to a probability less than the unit due to the truncation of the list of network states. To minimize this problem, the probabilistic model considering contingencies is structured in a way that compensates this truncation. Based on this work the authors concluded that the probabilistic behaviour of the network components is extremely relevant in the Probabilistic Power Flow solution. Moreover, the network uncertainties have more influence in the solution when the load uncertainty level is not very high, which usually occurs in operational planning. In the same line of research, Leite da Silva *et al.* (1985) proposed a new algorithm in which the distributions

of the power flow solution are conditionally evaluated based on each possible network configuration. The final solution is obtained as a weighted sum of density distributions by using the probability associated with each network configuration. In Leite da Silva *et al.* (1990a) it is detailed an application of the Probabilistic Power Flow techniques to the expansion planning of a power system that takes into account probabilistic data of the composite generation and transmission system (Hierarchical Level II) and uncertainty on load data.

Leite da Silva *et al.* (1990b) described a new approach termed as multilinear simulation algorithm to obtain the Probabilistic Power Flow solution that combines the Monte Carlo Simulation techniques and the linearized power flow equations for different system load levels. This approach uses a criterion based on the total active system load in order to determine different linearization points avoiding, in this way, the use of the Boundary Load Flow algorithm and, consequently, turning the Probabilistic Power Flow more accurate and its assessment more efficient. Taking into account the obtained results, the authors concluded that the accuracy of the proposed algorithm is larger when the level of uncertainty is high since it is on these situations that the Boundary Load Flow algorithm exhibits its maximum inaccuracy. This means that the error reduction was particularly significant in the tail regions of the probability density functions associated with network random variables. They also concluded that the addition of more linearization points, generally, improves significantly the accuracy of the results. The increasing number of linearization points can therefore be seen as a strategy to reduce the output errors.

3.2.1.4. Probabilistic Optimal Power Flow methods

Apart from Probabilistic Power Flow models, the literature also includes a few references addressing the integration of probabilistic data in Optimal Power Flow models. In this scope, El-Hawarry *et al.* (1989) admits that the demand has a normal distribution probability function and describes the computation of the expected values of the output variables. Madrigal *et al.* (1998) considers that the demand is represented by a vector of random correlated variables so that nodal dependencies can be modelled. This paper adopts the First Order Second Moment method in order to get the statistical properties of the output variables reflecting data uncertainty.

Verbic *et al.* (2006) presents an application of the approach described in Lien (2005) to take into account the uncertainties in the Optimal Power Flow problem, namely, on demand and supply bid uncertainty prices. In this work the stochastic behaviour of market participants is introduced in the OPF calculation by means of a two-estimate method. Every uncertain variable is replaced by only two deterministic points placed on each side of the corresponding mean, which enables the use of the deterministic OPF. The results are the moments of the variables of interest that correspond in this work to locational marginal prices. The deterministic OPF is then run twice for each uncertain variable, once for the value below the mean, and another for the value above the mean, with all other variables kept at their corresponding mean value. This means that this approach needs 2n runs of the deterministic OPF given that n represents the number of uncertain variables. Following the presented results, the authors concluded that this

approach is accurate if the number of uncertain parameters is not too large. The computational effort is more reduced when the number of uncertain parameters is low, since the computational time is directly dependent on the number of variables affected by uncertainty.

3.2.2. Fuzzy models

There are situations in which the uncertainty is related with the incomplete characterization of the phenomenon under analysis or derives from the lack of information required to build probability distributions, as it happens in very low frequency phenomena (Merrill *at al.*, 1990). In other cases, uncertainty is related with vagueness in the sense that human language has an intrinsic subjective nature that turns each user a different user of language. In this sense, expressions as “larger than”, “close to”, “more or less” or “approximately” are inherently vague and their use does not reflect an historic average of past values but it rather corresponds to a subjective evaluation of each user.

In the above cases, probability theory is not fully adequate to model this type of uncertainty. In this sense, since the 80’s of the last century, Fuzzy Set models are under development and application to power systems aiming at providing a new framework to model the vague or the ill-defined nature of some phenomena namely in Fuzzy Power Flows, Fuzzy Optimal Power Flows, risk analysis and reinforcement strategies, generation planning (Muela *et al.*, 2007), reliability models, fuzzy reactive power control, fuzzy dispatch and fuzzy clustering of load curves (Saraiva *et al.*, 1993) or even in transient or steady state stability. In this context, in the following sections we will detail several contributions in the areas considered as the ones of larger importance within the subject of this Thesis.

3.2.2.1. Fuzzy DC and AC Power Flow

Data in general fields of human science is deterministic, random or uncertain. Power system analysis is no exception to this rule, but system models so far being used or even considered incorporate only deterministic or probabilistic approaches. However, since in forecasting or planning problems projecting data from past to future cannot be considered as a consistent procedure, in early 90’s it was developed a new perspective over the power system planning problem that adopts a conceptual framework appropriate to assess the possibility of events based on the Fuzzy Set theory. In this context, Miranda *et al.* (1989) details the first DC and AC incremental models admitting that at least one generation or demand is modelled by trapezoidal fuzzy numbers. For the AC version of the Fuzzy Power Flow, the authors used the algorithm proposed by Allan *et al.* (1976a) in the context of the AC Probabilistic Power Flow. As a consequence, as in the Probabilistic Power Flow context, voltage possibility distributions results also show a shift regarding the values determined with the conventional deterministic analysis. In this work the authors also described an operational procedure to derive fuzzy load diagrams associated with different types of energy demand.

In Miranda *et al.* (1990) the previous algorithms were enhanced by considering new linearized techniques for the AC version of the algorithm. In fact, in this new algorithm the active and reactive branch flows, the generated active power in the slack bus and the reactive power in the slack and PV buses nonlinear functions were linearized considering the first terms of their expansions in Taylor series around the corresponding deterministic values. Since this technique does not perform well in case of branch currents and losses (specially on lightly loaded branches or branches in which reversing of power flow may occur), in this cases it was adopted a new technique that considers an approximation of the injected power deviations regarding the deterministic values that lead to the extreme values under consideration. Once these deviations are identified, a new set of injected powers can be obtained and used as data in a deterministic power flow study (Saraiva *et al.*, 1991). This technique can then be adopted considering successive α-cuts in the possibility distributions of the injected power deviations in order to build the output membership functions.

In the next paragraphs we detail the mains steps of the Fuzzy DC Power Flow algorithm (Miranda *et al.*, 1992).

1. Perform a deterministic DC load flow using the central values of the possibility distribution functions of the injected active power to obtain the crisp vector of voltage phase angles and active power flows.
2. Evaluate the possibility distribution deviations of voltage phase angles, $\left[\Delta\tilde{\theta}\right]$, and active power flows, $\left[\Delta\tilde{P}_{ik}\right]$, considering the DC model matrix [B], the sensitivity coefficient matrix [A] and the possibility distribution deviations of the active injected power $\left[\Delta\tilde{P}\right]$ regarding their deterministic values.

$$\left[\Delta\tilde{\theta}\right] = [B]^{-1}\left[\Delta\tilde{P}\right] \tag{3.1}$$

$$\left[\Delta\tilde{P}_{ik}\right] = [A]\left[\Delta\tilde{P}\right] \tag{3.2}$$

3. The possibility distributions of the voltage phase angles, $\tilde{\theta}$, and of the active power flows, $\tilde{P}_{ik}$, are obtained by superimposing their increments ($\Delta\tilde{\theta}$ and $\Delta\tilde{P}_{ik}$, respectively) to the respective deterministic values ($\theta^{ctr.}$ and $P_{ik}^{ctr.}$, respectively) (3.3) and (3.4).

$$\tilde{\theta} = \theta^{ctr.} + \Delta\tilde{\theta} \tag{3.3}$$

$$\tilde{P}_{ik} = P_{ik}^{ctr.} + \Delta\tilde{P}_{ik} \tag{3.4}$$

In this context, in the next paragraphs we will present the mains steps of the Fuzzy AC Power Flow algorithm (Saraiva *et al.*, 1991).

1. Obtain a crisp vector of nodal injections departing from the specified fuzzy membership functions (3.5). In this expression CV denotes the Central Value operator that returns the central values, $P^{ctr.}$ and $Q^{ctr.}$, of the $\tilde{P}$ and $\tilde{Q}$ injected powers.

$$\begin{bmatrix} P^{ctr} \\ Q^{ctr} \end{bmatrix} = \begin{bmatrix} CV(\tilde{P}) \\ CV(\tilde{Q}) \end{bmatrix} \tag{3.5}$$

2. Using this vector, perform a crisp AC Power Flow run using an iterative algorithm (such as the Newton-Raphson, for example). In the end, it is obtained an initial crisp operation point characterized by crisp voltages and phases ($V^{ctr.}$ and $\theta^{ctr.}$), crisp active and reactive branch flows ($P_{ik}^{ctr.}$ and $Q_{ik}^{ctr.}$), generations ($P_g^{ctr.}$ and $Q_g^{ctr.}$) and losses ($P_{loss}^{ctr.}$ and $Q_{loss}^{ctr.}$).

3. $\Delta\tilde{\theta}$ and $\Delta\tilde{V}$ deviations are computed using the inverted Jacobian matrix $[J]^{-1}$ built in the last iteration of the previous crisp Newton-Raphson run (3.6). The membership functions of $\tilde{\theta}$ and $\tilde{V}$ are computed as the addition of the crisp initial values ($\theta^{ctr.}$ and $V^{ctr.}$) with the corresponding deviations ($\Delta\tilde{\theta}$ and $\Delta\tilde{V}$) (3.7) and (3.8), respectively.

$$\begin{bmatrix} \Delta\tilde{\theta} \\ \Delta\tilde{V} \end{bmatrix} = [J]^{-1}.\begin{bmatrix} \Delta\tilde{P} \\ \Delta\tilde{Q} \end{bmatrix} \tag{3.6}$$

$$\left[\tilde{\theta}\right] = \left[\theta^{ctr.}\right] + \left[\Delta\tilde{\theta}\right] \tag{3.7}$$

$$\left[\tilde{V}\right] = \left[V^{ctr.}\right] + \left[\Delta\tilde{V}\right] \tag{3.8}$$

4. Active and reactive branch flows, losses and branch currents are nonlinear functions of voltage magnitudes and phases angles at the extreme nodes of each branch. As an example, the active power flow between nodes i and k is given by (3.9) and so its deviation can be approximated using the linear terms of its Taylor series expansion (3.10).

$$P_{ik} = -g_{ik}.V_i^2 + V_i.V_k(g_{ik}.\cos\theta_{ik} + b_{ik}.\sin\theta_{ik}) \tag{3.9}$$

$$\Delta P_{ik} \approx \frac{\partial P_{ik}}{\partial V_i}.\Delta V_i + \frac{\partial P_{ik}}{\partial V_k}.\Delta V_k + \frac{\partial P_{ik}}{\partial \theta_i}.\Delta\theta_i + \frac{\partial P_{ik}}{\partial \theta_k}.\Delta\theta_k \tag{3.10}$$

In these expressions:

V_i and V_k - are the voltage magnitudes on buses *i* and *k*, respectively;
g_{ik} - is the conductance of the branch linking buses *i* and *k*;
b_{ik} - is the susceptance of the branch linking nodes *i* and *k*;
θ_{ik} - is the difference between phase angles in nodes *i* and *k*.

Since it is possible to obtain linear expressions for ΔV_i, ΔV_k, $\Delta\theta_i$ and $\Delta\theta_k$ in terms of active and reactive deviations of nodal injections directly from the $[J]^{-1}$ matrix, substituting these expression on (3.10) leads to (3.11).

$$\Delta\tilde{P}_{ik} = \sum_j SP_{ik,j}.\Delta\tilde{P}_j + \sum_j SQ_{ik,j}.\Delta\tilde{Q}_j \tag{3.11}$$

In this expression, $SP_{ik,j}$ and $SQ_{ik,j}$ represent sensitivity coefficients relating the active flow in branch i-k with the active and reactive injections in node j.

The fuzzy description of the i-k active power flow, $\tilde{P}_{ik}$, is given by the fuzzy addition of its crisp value, $P_{ik}^{ctr.}$, (output of step 2) with the corresponding fuzzy deviation, $\Delta\tilde{P}_{ik}$ (3.12).

$$\tilde{P}_{ik} = P_{ik}^{ctr.} + \Delta\tilde{P}_{ik} \tag{3.12}$$

5. The active generation in the slack bus and the reactive generation in the slack and PV buses are nonlinear functions of the voltage and phase angles in all nodes and so their expressions will be also linearized by considering the first terms of their expansion in Taylor series around the associated deterministic values, like it was done in step 4 for the active branch flows.

6. Since the linearization procedure doesn't give full satisfactory results for branch currents and losses, namely for lightly loaded lines or lines where reversion of power flow may occur, the corrective algorithm described in (Saraiva *et al.*, 1991) can be applied.

Recognizing that this linearization method could produce errors which are function of the deterministic power flow initially performed and of the data uncertainty, Saraiva *et al.* (1991) presented a work in which the results obtained from the Fuzzy AC Power Flow (thin line) model are compared with the ones obtained from a Monte Carlo simulation method (strong line) and with the ones obtained from two deterministic power flows studies (using the Newton-Raphson method) considering the maxima and minima values for generated powers and demand of each possibility distribution (extreme case values). Figure 3.2 illustrates the membership functions obtained for the generated power in bus 1 using these three approaches as indicated in Saraiva *et al* (1991).

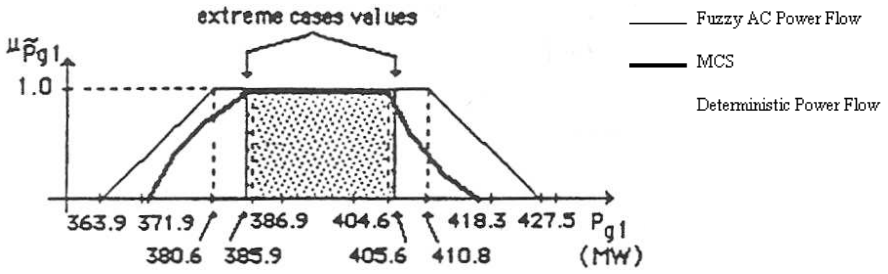

Figure 3.2: Possibility distribution of the generated active power at bus 1 (source: Saraiva *et al.*, 1991).

As a summary, the authors conclude that the results of the Fuzzy AC Power Flow have the same or even larger level of quality of information and they can be achieved with less computational effort when compared with the other approaches.

As it was previously presented, the original Fuzzy AC Power Flow model didn't consider the possibility of specifying any kind of correlation between fuzzy membership functions. However, correlations exist in many situations as, for instance, in the generation of several wind farms geographically located in a given region, in the generation of some hydro stations located in the same downstream hydro, in the solar energy used by photovoltaic panels located in a given region and also in loads located in a certain specific region as a consequence of atmospheric or human behaviour patterns.

In this context, Saraiva *et al.* (2004b) presented a modified Fuzzy AC Power Flow algorithm that can consider this type of uncertainty correlations. More in particular, the algorithm admits that there are only correlated active power data, correlated reactive power data, or instead, correlations between active and reactive data. As expected, correlations contribute to narrow the membership functions of the results as illustrated in Figure 3.3 for three distinct situations of correlation.

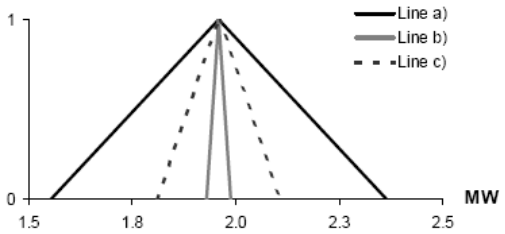

Figure 3.3: Triangular fuzzy numbers for the active power flow in line 4 without correlation data (case a), with fully correlated data (case b) and with a mixed situation (case c) (source: Saraiva *et al.*, 2004b).

As we know, in the deterministic case the slack bus only compensates losses. However, in Fuzzy Power Flow it also compensates load uncertainties that come from all the other buses. Previously it was also described a corrective procedure that partially addresses this problem (Saraiva *et al.*, 1991). In this context, Matos *et al.* (2008) presented an alternative approach that completely solves this problem. The proposed method consists of solving several linear optimization problems to determine the maximum and minimum value of the fuzzy injected power variables for each α level. This formulation can eventually consider branch limit constraints to evaluate the effect of these limits on the power flow results. The problem is then formulated as (3.13) to (3.16) (in order to obtain $\tilde{P}_k^{\min}(\alpha)$ it must be solved a minimization linear optimization problem instead of a maximization).

$$\max \quad \tilde{P}_k(\alpha) = \tilde{P}_k^{\max}(\alpha) = \sum_{i \neq Slack} A_{ki}.P_i \tag{3.13}$$

$$st: P_i \in \tilde{P}_i(\alpha) \quad all \quad buses \quad i \tag{3.14}$$

$$\sum_i P_i = 0 \tag{3.15}$$

$$\left|A.P\right| \leq P_{LIM} \tag{3.16}$$

In this formulation,

$\tilde{P}_k^{\max}(\alpha)$ - is the maximum value of the power flow in branch k in the α-level interval;

$\tilde{P}_i(\alpha)$ - is the α-level interval of the nodal injected power $\tilde{P}_i$;

A - is the sensitivity matrix;

P - is the vector of P_i;

P_{LIM} - is the vector of branch limits.

Besides identifying the congested branches, the model can be used to check if the demand or generation can be accepted or accommodated by the transmission network and, if not, it returns the repressed load or generation (3.17) to (3.20)

$$\max \quad \tilde{P}_i^{final}(\alpha) \tag{3.17}$$

$$st: P_i \in \tilde{P}_i(\alpha) \quad all \quad buses \quad i \tag{3.18}$$

$$\sum_i P_i = 0 \tag{3.19}$$

$$\left|A.P\right| \leq P_{LIM} \tag{3.20}$$

The values of $\tilde{P}_i^{final}$ will then describe the true injection allowed by the transmission network in the present circumstances. If $\tilde{P}_i^{final} \neq \tilde{P}_i$ one can say that the transmission network is not completely adequate, since generation or load in node i are repressed. Based on these results the authors define the *degree of repression* and *severity of the repression* indices to quantify the adequacy of the transmission network. The first one was defined as the maximum value of α for which there is no repressed generation/demand in any node. The second one was defined as the sum of the repressed load/generation quantities.

Recognizing, for one side, that the Fuzzy Power Flow linearization model fails when the system becomes more stressed and, for another, that any fuzzy number can be decomposed into two fuzzy numbers with complementary uncertainties with smaller associated uncertainty than the original one, Saavedra *et al.* (2007) proposed a multi-linearized procedure (more in particular a bi-linearized procedure) to solve the Fuzzy Power Flow problem (multi-linearized Fuzzy Power Flow). In this approach, the mean values of the two decomposed possibility distributions of active and reactive power (loads or generations) are used as linearization points. Taking as reference the results obtained for a 30 bus/41 branch power system, the authors concluded that the proposed methodology outperforms the classical linearization approach and provides good quality solutions.

Mangueira *et al.* (2008) presented a work that aims at evaluating the impact of wind generation (modelled via fuzzy numbers, since they could enclose meteorological data, wind generation operator data and forecast accuracy data) on the network using the multi-linearized Fuzzy Power Flow previously mentioned.

Other contributions to this subject were also presented by several authors, like Bijwe *et al.* (2005) and Das *et al.* (1999). However, since they are directed specifically to distribution networks they will not be detailed in this work.

3.2.2.2. Fuzzy DC Optimal Power Flow

A subsequent step was given by Miranda *et al.* (1992) with the presentation of the first Fuzzy DC Optimal Power Flow model admitting that at least a demand was represented by a fuzzy number. In Figure 3.4 it is presented the flowchart of the proposed algorithm.

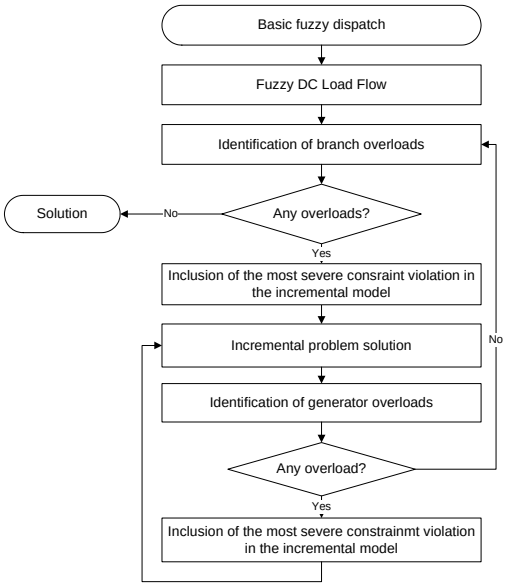

Figure 3.4: Fuzzy DC Optimal Power Flow algorithm (source: Miranda *et al.*, 1992).

This algorithm starts at an operation point that satisfies the power balance equation. The violated limits of generation and power flows are then identified. After selecting the most severe power flow or generation violation one gets the deviation of the initial generation needed to cancel the selected violation. As, in general, the number of violated limits is only a small percentage of the total possible ones, the algorithm presents the advantage of determining the optimal solution by solving problems of small dimension when compared with the complete ones. In accordance with what was defined by Merrill *et al.* (1990), in this work the authors also show how the system robustness and exposure indices can be determine and used to define hedging strategies.

The algorithm previously presented was revised originating a new one whose flowchart is presented in Figure 3.5 (Saraiva *et al.*, 1994a). Although a more complete description of this approach is included in Section 5, we will now briefly summarize it. According to Figure 3.5, this new algorithm starts with a deterministic DC OPF identifying a feasible and optimal solution, according to the minimum and/or maximum capacity limits of each generator or branch and the active power balance equation. To get this solution it was adopted a Linear Programming formulation for the central values of the possibility distributions of the injected power. To take into account the specified uncertainties in loads, this approach:

- Identifies a number of vertices of the hipervolume enclosing all possible load values by checking, for each branch and generator, which combination of load values maximizes and minimizes branch flows or power injections;
- For each vertex, varying a parameter that is associated with the membership value of the possibility distributions, it identifies the optimal dispatches for all load scenarios lying on the line between the vertex and the central value initially computed;
- Aggregates the results of the studies obtained for each analysed vertex leading to the possibility distributions of generations, branch flows and power not supplied.

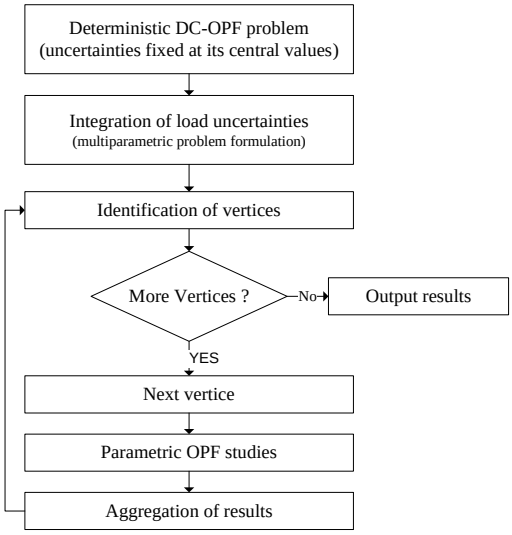

Figure 3.5: Fuzzy DC Optimal Power Flow algorithm (source: Saraiva *et al.*, 1994a).

Following Guan *et al.* (1995) and Liu *et al.* (1996), the conventional OPF problems comprise two types of inequality constraints. Physical limits on the control variables (hard constraints) as, for instance, the capacity of generation units and, on the other hand, operating limits (soft constraints) like, for instance, transmission branch flows for which small violations may be sometimes acceptable. This has a clear correspondence to the practice in power system operation when defining normal and emergency limits for several components. In this sense, the algorithms proposed in these two references use Fuzzy Set theory to model soft constraint limits. However, the algorithm proposed by the second author also uses this theory to model control action curtailment, since the total number of control actions (such as, generation unit output, phase shifter angles, transformer tap positions, shunt capacitors/reactors, etc) is approximated by a smooth nonlinear function. As a consequence, while in the first mentioned work the implemented OPF aims at reducing "*the cost as much as possible, while satisfying the soft constraints as much as possible, and while enforcing the hard constraints exactly"*, the second mentioned work aims at reducing *"the cost as much as possible without moving too many control settings, while satisfying the soft constraints as much as possible and enforcing the hard constraints exactly"*.

As expected the authors concluded that a significant cost saving can be obtained by using Fuzzy OPF when small violations of the normal operational limits are admitted. It is also important to refer the fact that when no feasible solution exists for the crisp OPF version, the fuzzy OPF can obtain a more realistic solution, since it distributes the violations of the operational limits instead of violating a single operational limit. As expected, Liu *et al.* (1996) also show that the total number of control actions can be reasonably reduced with small cost increase or violations of soft constraints.

Recognizing that all previously proposed OPF's were applied to the centralized dispatch in the vertically integrated structure, Chayakulkheeree *et al.*, (2005) presented a Fuzzy Constrained Optimal Power Dispatch (FCOPD) that is formulated as a fuzzy optimization problem for the active energy and the ancillary markets, namely for automatic generation control (AGC), 10 minutes spinning reserve and 30 minutes operating reserve markets. The proposed FCOPD problem is decomposed into a sub problem that maximizes a fuzzified social welfare function, which is solved by mixed-integer fuzzy linear programming, and into another sub problem that minimizes real power losses. This second sub problem is solved by linear programming and its solution is performed iteratively with the mixed integer sub problem.

In this sense, the market clearing price is obtained using the Lagrange multiplier of the real power balance constraint, obtained by solving the social welfare fuzzy maximization sub problem. In the end, the proposed FCOPD algorithm gives the accepted real power demand bids, accepted real power generation bids, accepted AGC quantities, accepted 10 minute spinning reserve quantities, accepted 30 minute operation reserve quantities, AGC on/off status, generator's on/off status and 30 minutes operation reserve selected status that satisfies both sub-optimization problems and also the technical operation limits of the system.

3.2.2.3. Risk analysis and reinforcement strategies

Planning in a power system environment involves a wide range of options, conflicting objectives of different stakeholders (investors, employees, environmentalists, customers of various classes, etc.) and many uncertainties. In this context, it seems useful to clarify the distinction between risk and uncertainty. Uncertainties correspond to factors which can have a major influence on a company but are not under its direct control or cannot be predicted with certainty. Risk, on its turn, is the hazard to which a company is exposed if it selects one plan or a course of action instead of another because of uncertainty. Risk has to do with attributes, but even more, with decisions. Since uncertainty cannot be eliminated, managers would need to have the ability to characterize, quantify and manage risk. Risk is frequently discussed on two dimensions: robustness (if the plan represents a reasonable trade off for all possible values of uncertainties) and exposure (a measure of "for what outcomes of uncertainty is a particular plan unattractive?") (Merril *et al.*, 1990; Crousillat *et al.*, 1993).

Based on these concepts, Saraiva *et al.* (1994a) uses the Fuzzy DC OPF presented in Figure 3.5 to determine the exposure index (defined as the highest α-cut of the power not

supplied possibility distribution for which this power not supplied has non-zero values) and the robustness index (1-α), defined as the lowest α-cut level for which the system still accommodates data uncertainties at that level. These indices were then used to help the decision maker to select power system expansion plans.

In Saraiva *et al.* (1994c) it was presented a model to derive reinforcement plans driven by economic criterion and integrating representation of load uncertainties. In this approach the described Fuzzy DC OPF approach is used to determine the most economic reinforcement strategy since the objective function to be optimized was formulated in terms of the costs inherent to expand the generation and branch flow capacities. As a consequence, in this case the objective function is formulated as (3.21).

$$z = \sum c_{gi}.\Delta P_{gi} + \sum c_{bi}.\Delta P_{bj} \tag{3.21}$$

In this expression,

- c_g - is the investment to expand generation capacities;
- c_b - is the investment to expand branch capacities;
- ΔP_{gi} - is the generation expansion capacities;
- ΔP_{bi} - is the branch expansion capacities.

In this formulation, as in the one presented in Saraiva *et al.* (1994a), constraints related to generation capacity limits and branch flow limits are also modified in order to integrate the variables related with the generation expansion capacities and branch expansion capacities, ΔP_{gi} and ΔP_{bi}, respectively.

Recognizing that system component outages are more adequately represented by probabilistic models and that load uncertainties are more adequately represented by fuzzy numbers, Saraiva *et al.* (1996a) presented a new approach where the Fuzzy DC OPF model was integrated in a Monte Carlo simulation as a way to obtain the expected values of the output variables reflecting fuzzy loads and reliability equipment data modelled with the usual probability based approaches. In this sense, this model has a hybrid nature, since it aggregates fuzzy and probabilistic models. The mentioned Fuzzy DC OPF model was also integrated in a methodology to identify the most adequate expansion plan so that the risk of not being able to meet the demand gets reduced while accommodating the inherent uncertainty (Saraiva *et al.*, 1996b).

3.2.3. Interval arithmetic models

Wang *et al.* (1992) described a new method based on interval arithmetic to take into account uncertainty in input data (represented by arithmetic intervals) during power flow simulations. In this approach the power flow problem is solved by first linearizing the problem and then the resulting linear equations are solved by means of a Gauss Seidel iterative process. Following the authors, the solution obtained is conservative because it

contains all solution points, but also some non-solution points as well, situation that results from the attempt to express solutions as simple intervals when in reality they are not. According to the authors this conservative nature worsens as data uncertainty increases.

Taking into account the presented methodology, one of the major critics that the authors faced was related to the fact that interval arithmetic is not the adequate way to model uncertainties, since it does not allow to represent any kind of qualitative information on the phenomena to be modelled (differently from what happens with fuzzy numbers, for example) or even the knowledge related with some kind of repetitive events as it happens with random numbers which come associated with probability distributions.

Das (2002) presents a method for radial distribution system power flow based on interval arithmetic that replaces the real interval arithmetic calculation used by Wang *et al.* (1992) by complex interval arithmetic calculations to represent uncertainties in the input load parameters. Taking as reference the results obtained for a 30 bus and also for a 68 bus balanced radial distribution system, the authors concluded that the solution obtained with this approach encompasses all the solutions obtained from a 5 millions repeated power flow simulations.

Chaturvcedi (2006) also presented an interval arithmetic-based distribution power flow to evaluate the effects of the input uncertainties. In this algorithm the probabilistic variation of load uncertainty (load parameter is considered varying according to a Gaussian probability distribution) is linearized at multi-points to find bounded intervals, as depicted in Figure 3.6. In this Figure $\alpha_{PL}(k)$ represents the degree of membership and it takes any value between $\alpha_{PL}(k) \cong \alpha_{PL\max} / N_L$ to $\alpha_{PL}(k) \cong \alpha_{PL\max}$.

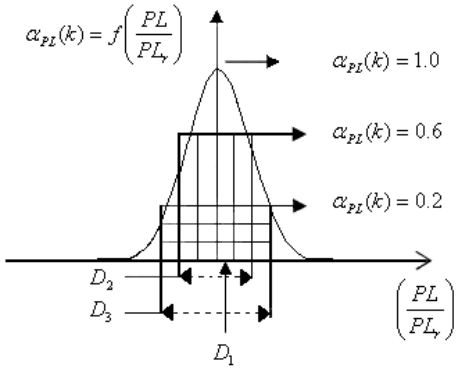

Figure 3.6: Gaussian distribution of load demand with N_L points of linearization (source: Chaturvedi, 2006).

According to Figure 3.6, the linearization process is conducted at three points resulting in three distinct load intervals (regions), such that:

$$D_1 \rightarrow \quad \{PL_r(i), PL_r(i)\}, \text{ point interval (or singleton) for } k = 1; \tag{3.22}$$

$$D_2 \rightarrow \quad \{PL_r(i)[1-\delta_2], PL_r(i)[1+\delta_2]\}, \text{ for } k = 2; \tag{3.23}$$

$$D_3 \rightarrow \quad \{PL_r(i)[1-\delta_3], PL_r(i)[1+\delta_3]\}, \text{ for } k=3; \tag{3.24}$$

Equations (3.22) to (3.24) indicate that D_1, D_2, and D_3 are in a bound form and, hence, an interval arithmetic operation has to be performed to incorporate these variations in the power flow problem. Following this author, this approach is three times faster than the one developed by Das (2002).

3.2.4. Boundary Load Flow models

Another kind of approach presented in literature (Dimitrovski *et al.*, 2004) corresponds to an extension of the Boundary Power Flow method previously presented in Section 3.2.1.2. In fact, this method corresponds to an extension of the idea presented by Allan *et al.* (1981) in the context of the Probabilistic Power Flow where the algorithm was applied to determine the ranges of values of the state and output variables, given the range of the input variables from their probability distribution. The results were then used to determine multiple points of linearization for the power flow equations in order to improve the accuracy of the Probabilistic Power Flow solutions in the tail regions of probability distributions.

In its initial formulation, the algorithm corresponds to an iterative process in which, at each iteration, a new solution of the power flow problem is determined and a new point of linearization is evaluated. The maximum and minimum values of the state variables associated with these linearization processes are then determined considering a sensitivity coefficient matrix that includes the partial derivatives of the state variables with respect to the input variables evaluated at each point of linearization. In this sense, for positive sensitivity coefficients the state variables will be maximum (minimum) where the input variables are maximum (minimum). In each iteration, the algorithm finds the boundary values of each state variable. A similar process is then applied to determine the boundary values of the output values from the values of the state variables in each point of linearization. In this new approach, however, it is used the Jacobian matrix together with the sensitivity coefficient matrix (partial derivatives of the output variables in order to the state variables). The iterative process ends when the partial derivatives are positive and the associated variable is at a minimum, the partial derivatives are negative and the associated variable is at a maximum or the partial derivatives are zero.

According to Dimitrovski *et al.* (2004) some convergence difficulties arise especially when determining the range of values of the voltage magnitudes and reactive power flows given their higher nonlinear degree.

As it was described, this approach is computationally intensive since the procedure to determine the boundary values comprises several power flow solutions for each variable. Following the authors, the proposed algorithm may occasionally fail to find the right solution if the function exhibits extreme changes during the course of solution.

As we know almost every power flow algorithm including uncertainties uses the traditional deterministic problem definition, that is, load buses are defined as PQ buses, generator buses are defined as PV buses and one of these buses is assumed to be a slack bus to balance the active and reactive power in the system. While this definition of the power flow problem is appropriate for a deterministic solution, it has an inherent drawback when dealing with uncertain input variables. In fact, in this case the slack bus has to absorb not only power losses, but also all uncertainties arising from the solution and thus it will have the widest possibility (or probabilistic) distribution in the system that frequently contain values beyond the margins of the generator connected to it. Recognizing these concerns, Dimitriovski *et al.* (2005) proposed two different approaches to deal with this problem within the context of Boundary Load Flow algorithm. The first one considers a conversion of the slack bus to PV bus and PV bus back to slack bus and the second one considers a distributed slack bus modelling.

The first approach is similar to the PV bus to PQ bus conversion used in traditional steady state analysis, that is, if the slack bus real power generation exceeds its predefined limits, it is fixed at the violated limit and some other PV bus must be relaxed in order to be able to solve the power flow problem. Obviously, the PV bus to choose corresponds to the one that has the highest margin from the current generation to either its lower or upper limit. With a new PV bus as slack bus, the power flow problem has to be redefined by swapping only the equation of the real power at the chosen PV bus with the equation of the slack bus real power. Another approach within this method consists of relaxing the voltage angle of the slack bus and declare the voltage angle of the PV bus with relaxed real power as reference, which can be interpreted as a complete conversion from slack bus to PV bus and PV bus to slack bus. In these two approaches, if there is no such PV bus available the problem is unfeasible.

In the second approach, one selects a number of PV buses that will share the slack function in a distributed and predetermined way. A possible rule corresponds to assign the power proportionally to the current injections or proportionally to the margin between the current injections and the lower or upper generation limits. It is clear that to maintain the feasibility of the problem, the available generation should always match the demand.

CHAPTER IV Parametric and Multiparametric Analysis – Theoretical Concepts

4. Parametric and multiparametric analysis - theoretical concepts

4.1. General aspects

As a consequence of changes on the formulation of optimisation problems, or due to the possibility of production of new goods or services or even to the modification of the allocation of resources to each activity, it can be necessary to integrate in the linear programming model additional variables or constraints or, eventually, proceed to the modification of elements in the independent vector and/or on the objective function coefficients. Obviously that, in any of these situations, one can chooses solving the entire linear optimization problem from the beginning. However, given the inefficiency of such procedure and given the fact that in any Simplex tableau the information related with the set of operations performed from the beginning of the solution is saved on the initial tableau identity matrix columns, B^{-1} matrix, the effects of these modifications can be more easily obtained by affecting that matrix of the corresponding modification vector and, in case the solution loses its optimality and/or feasibility, proceed to Simplex tableau modifications until the optimality and feasibility conditions are again recovered.

Not less important than obtaining the range of values that a given variable can assume taking into account the optimality and feasibility criterions (sensibility analysis) is the procedure performed to attain new optimal and feasible solutions when a parameter modification occurs (parametric and multiparametric analysis). This second type of procedures analyses the effects of the continuous variation of the objective function coefficients, of the independent vector terms, or of both of them simultaneously (Taha, 2003). In this sense it must be emphasized that the knowledge of these intervals and solutions assume extreme importance, since they can help the decision maker in selecting optimal production levels or available resources, as well as to evaluate the consequences of their variations in scenarios characterized by large uncertainties.

In the parametric and multiparametric analysis, the objective function coefficients or the independent vector coefficients, c and b, respectively, are replaced by parameterized functions $c(v)$ and $b(\lambda)$, where v and λ represent the variation parameters. Mathematically these parameters can assume positive or negative values.

In this context, in the following Sections of this document we will detail the theorical concepts of the techniques previously mentioned, namely, the parametric and multiparametric techniques.

4.2. Independent vector parameterization

The knowledge of the independent vector parameter intervals for which a given solution remains optimal and feasible assumes extreme importance, since it can help the decision maker in the definition of the proper available resource levels, as well as to evaluate the consequences of their expansion or reduction.

In the case of the independent vector parameterization, the solution remains feasible provided that all feasibility conditions are satisfied, that is, until the independent vector elements remain nonnegative.

From the geometric point of view, the systematic parameterization means that the solution space K is partitioned into critical regions, R_ρ, in such a way that two critical regions R_i and $R_j \subset K$ are distinct and so they not overlap. From a mathematical point of view, the systematic parameterization represents the procedure following which it is possible to successively determine all neighbor regions starting from an initial optimal and feasible basis. In this context, it is assumed that the dependency of the independent vector terms in relation to a scalar is described by expression (4.1).

$$b(\lambda) = b + f.\lambda \tag{4.1}$$

In this expression, $f = (f_1,..., f_m)^T$ represents the λ parameter vector coefficients. Let us now consider that $\underline{\lambda}$ and $\overline{\lambda}$ represent the extreme vertices, inferior and superior, respectively, of the critical region. Denoting this interval by $M = [\underline{\lambda}, \overline{\lambda}]$ it follows that $K^* = K \cap M$ represents the unique region of K that has to be analyzed since it is the only one that has values in common with M. According to Gal (1979), the mathematical solution procedure to adopt to solve this kind of problems comprises two distinct phases:

- Determine an initial optimal and feasible basis, B_0;
- Systematically search for the neighbour regions starting from B_0.

In this scope, Gal (1979) proposes the independent vector parameterization solution algorithm detailed in the next paragraphs.

Phase I:

1. Transform the inequalities into equations (by means of slack and artificial variables) and place the term $f.\lambda$ on the right side of the equations;

2. Set $\lambda = 0$ and solve the linear optimization problem (4.2) to (4.4):

$$\min \quad z = c^T.x \tag{4.2}$$

$$Subj.:$$

$$A.x = b \tag{4.3}$$

$$x \geq 0 \tag{4.4}$$

2.1 Once an optimal and feasible solution associated with the basis B_0 in step 2 is identified, then Phase I is finished, since B_0 represents the initial optimal and feasible basis. Go to Phase II;

Phase II:

1. In the Simplex tableau corresponding to B_0 determine the interval $R_0 = [\underline{\Theta}_0, \overline{\Theta}_0]$ in which the basis remains optimal and feasible. The minimum and maximum values of this interval $\underline{\Theta}_0$ and $\overline{\Theta}_0$, respectively, should be computed using the feasibility condition as described in (4.5).

$$B_{\rho}^{-1}.b(\lambda_k) = B_{\rho}^{-1}(b + b'(\lambda_k)) \geq 0 \qquad (4.5)$$

In this expression,

B - is an optimal and feasible basis;
ρ - is the index for the corresponding set of basic variables;
λ - is the parameter that models the right hand side uncertainties;
b - is the right hand side vector.

1.1 Let us now consider that $\underline{\Theta}_0$ and $\overline{\Theta}_0$ are finite. If it was used a pivot element to determine the neighbour basis corresponding to $\underline{\Theta}_0$, the procedure is called descending, since it aims at determining smaller values of λ. Oppositely, if it aims at determining basis corresponding to $\overline{\Theta}_0$ the process is called ascending. The chosen process is, however, irrelevant for the final results;

1.2 If $\underline{\Theta}_0 = -\infty$, $\underline{\Theta}_0 \leq \underline{\lambda}$ or $\overline{\Theta}_0 = +\infty$, $\overline{\Theta}_0 \geq \overline{\lambda}$, then the descendant or ascendant process, respectively, is finished.

Considering the ascendant procedure and that the optimal and feasible basis B_k was already determined, the algorithm proceeds as follows:

2. The pivot row corresponds to that where the $\overline{\Theta}_k$ was determined;
3. In the pivot row, the negative elements ${}^{k}a_{ij}$ are potential candidates to be selected, with exception to those that belong to artificial variables;
   3.1 If there are no negative elements on the pivot row, there are no neighbours for $\lambda = \overline{\Theta}_k$. The ascendant process is finished. Go to 7.
4. Determine the smallest ratio computed in step 3. The corresponding column becomes the pivot column;
5. Performing a Dual Simplex step (considering the pivot element previously determined) over B_k, it is possible to obtain B_{k+1};
6. Determine $\overline{\Theta}_{k+1}$, where $\underline{\Theta}_{k+1} = \overline{\Theta}_k$
   6.1 If $\underline{\Theta}_{k+1}$ is finite, repeat steps 2 to 5 of Phase II regarding the basis ρ_{k+1};
   6.2 If $\overline{\Theta}_{k+1} = +\infty$ or $\overline{\Theta}_{k+1} \geq \overline{\lambda}$, then the ascendant process is finished.

The described procedure must be repeated in relation to the base B_k until $\overline{\Theta}_k = +\infty$, $\overline{\Theta}_k \geq \overline{\lambda}$ or all elements of the pivot row are nonnegative.

7. Go back to the Simplex tableau associated to the basis B_0 and consider the row in which the ratio $\underline{\Theta}_0$ was determined as pivot row;
8. Determine the pivot element in accordance with steps 2 to 4 of Phase II;
9. Performing a Dual Simplex step (considering the pivot element previous determined) over B_t, it is possible to obtain B_{t+1} (taking into account that $\underline{\Theta}_0 \in [\underline{\lambda}, \overline{\lambda}]$);
10. Determine $\underline{\Theta}_{t+1}$, where $\overline{\Theta}_{t+1} = \underline{\Theta}_t$;

Steps 8 to 10 must be repeated until in basis B_t $\underline{\Theta}_t = -\infty$, $\underline{\Theta}_t \leq \underline{\lambda}$, or all pivot row elements are nonnegative.

4.3. Independent vector multiparameterization

If more than one element of the independent vector b is affected by uncertainty and these uncertainties are represented in b as linear functions of the parameters λ_i, $i=1,...,s$, the independent vector terms could be represented by expression (4.6) (Gal, 1979):

$$b_i(\lambda)=\sum_{k=i}^{s} f_{ik}.\lambda_k \ , \ i=1,...,m \tag{4.6}$$

In this expression,

- f_{ik} - represents the coefficients of the λ_k parameter vector, $i=1,...,m$, $k=1,...,s$;
- λ_k - represents an element of the λ parameter vector, $k=1,...,s$.

In this sense, the algorithm proposed by Gal (1979) aims at systematically identifying all regions associated to optimal and feasible basis $K \subseteq R^s$ of the linear multiparametric programming problem represented, in a condensed way, by (4.7) to (4.9). In this sense, the problem will have an optimal and feasible solution for each $\lambda \in K, \lambda \in R^s$ and for $\lambda \in R^s, \lambda \notin K$ the referred problem will have no solution.

$$Max \ \ z=c^T.x \tag{4.7}$$

Subj.:

$$A.x=b+F.\lambda \tag{4.8}$$

$$x \geq 0 \tag{4.9}$$

In this expression,

- A - represents the coefficients constraint matrix, with elements $A=a_{ij}$, $i=1,...,m$, $j=1,...,N$;
- F - represents the coefficients vector of the independent vector parameters, with elements $F=f_{ik}$, $i=1,...,m$, $k=1,...,s$;
- λ - represents the parameter vector, this is, $\lambda=(\lambda_1,...,\lambda_s)^T$;
- c^T - represents the objective function coefficients vector;
- x - represents the decision variables vector;
- b - represents the vector of independent terms.

In this problem, the coefficients of the vectors and matrixes c, A, b and F are constant and so the independent vector terms can be represented as a linear function of the parameters λ as described in expression (4.10).

$$b(\lambda)=b+F.\lambda \tag{4.10}$$

Additionally, the parameters vector must satisfy the constraints (4.11), that is, the set defined by (4.11) is a closed convex polyhedron set in R^s.

$$G.\lambda \leq d \tag{4.11}$$

In which,

$G = g_{ik}$, $i = 1,...,r$, $K = 1,...,s$ and $d \in R^r$, constant.

According to Gal (1979), two regions are classified as neighbours if it is possible to pass from one to the other by means of a single iteration of the Dual Simplex method (in case of right hand side parameterization). In this sense, two neighbour regions differ only in one basic variable. This author represents the optimal and feasible basis by means of a non-oriented graph in which:

- S represents the set of vertices. One vertex, ρ_i, is associated to the indices of a set of basic variables forming an optimal and feasible basis for, at least, one vector $\lambda \in K^*$;
- $X(\rho_i)$ represents the set of vertices connected to the vertex ρ_i by means of a branch. There is a branch connecting the vertices ρ_i and ρ_j whenever their associated bases are neighbors. In this situation these two vertices are considered adjacent;
- The distance between the vertices ρ_i and ρ_j is given by the number of elements in ρ_i (this is, the basic decision variables in the basis associated to ρ_i) that are different regarding the elements in ρ_j (that is, the basic decision variables in the basis associated to ρ_j).

Starting from one region $R_{\rho 0}$ associated to the vertex ρ_0 and identifying neighbor regions R_ρ associated to optimal and feasible basis not yet analyzed, Gal (1979) shows that it is possible to create a sub-graph of G(S,X), $G_0(S_0,X_0)$, connected and in which condition (4.12) holds. If dual degeneracy does not occur, that is, if there isn't more than one optimal and feasible solution in relation to any critical region R_ρ it is verified that G and G_0 coincide.

$$\bigcup_{\rho \in S_0} R_{\rho 0} \cup R_\rho = K^* \tag{4.12}$$

In next paragraphs it is presented the solution algorithm proposed by Gal (1979) for the systematic identification of all critical regions R_ρ and their corresponding optimal and feasible basis.

1. Determine the vertex ρ_0 associated to the optimal and feasible basis of the region R_0;
2. Initialize the set V_0 comprising the vertices that belong to the graph in the current iteration:

$$V_0=\{\rho_0\} \tag{4.13}$$

3. Initialize the set W_0 comprising all vertices of $T(\rho_0)$ such that, starting from the optimal and feasible basis associated to the vertex ρ_0 it is possible to obtain the basis associated to the vertex $T(\rho_0)$ by means of a Dual Simplex iteration. In this sense, the graph will have branches connecting the vertex ρ_0 to the vertex $T(\rho_0)$.

$$W_0 = \{T(\rho_0)\} \tag{4.14}$$

4. Let us now consider that in iteration $k-1$ it was identified the vertex ρ_{k-1} and formed the V_{k-1} and W_{k-1} sets.

   4.1. If $W_{k-1} = \varnothing$, then $V_{k-1} = S_0$ and so the iterative process is finished;

   4.2. If $W_{k-1} \neq \varnothing$, select the vertex $\rho_k \in W_{k-1}$ having the smaller distance in relation to ρ_{k-1};

   4.3. Form the sets V_k and W_k and return to 4.1 incrementing k by one unity.

$$V_k = V_{k-1} \cup \{\rho_k\} \tag{4.15}$$

$$W_k = [W_{k-1} \cup \{T(\rho_k)\}] / V_k \tag{4.16}$$

This author presents two algorithms termed F and F_D for the solution of the linear multiparametric optimization problems considering independent vector parameters. In this work, however, it will be only presented the F approach, since it was the one adopted in the algorithms developed in this Thesis.

In this context, the solution of a linear multiparametric optimization problem considering independent vector uncertainty parameters comprises two important steps:

- Determine a initial optimal and feasible solution (x^0, λ^0), considering $\lambda_s = 0, \ \forall s$;
- Determine all critical regions and its associated optimal and feasible basis. Each of these critical regions, R_ρ, is a polyhedron defined by (4.17).

$$-B_\rho^{-1}.F.\lambda \leq 0 \Leftrightarrow -\sum_{k=1}^{s} {}^{\rho} f_{ik}.\lambda_k \leq 0, \quad i=1,...,m, \quad k=1,...,s \tag{4.17}$$

Since each critical region R_ρ forms a polyhedron in R^s, from the geometrical point of view the problem of determining all adjacent nodes of a given node $\rho \in S$ could be seen as how to determine the face of the corresponding polyhedron for which an optimal basis

can be assigned. Mathematically and according with Gal (1979), this corresponds to the problem of determining redundant inequalities, which could be defined as the problem (4.18) to (4.20).

$$\min \quad \underset{i \in P_\rho}{\varepsilon_i} \tag{4.18}$$

Subj.:

$$-\sum_{k=1}^{s}{}^{\rho} f_{ik}.\lambda_k + \varepsilon_i = 0, \qquad i = 1,...,m, \; k = 1,...,s \tag{4.19}$$

$$\varepsilon_i \geq 0, \qquad i = 1,...,m \tag{4.20}$$

In this expression:

P_ρ - is the number of faces of the polyhedron that defines the node $\rho \in S$;

ε - is a slack variable.

As we can see the problem of determining redundant inequalities corresponds, in fact, to the minimization of the slack variables related with the inequalities that define the corresponding polyhedron. This problem will have a solution, that is, will determine non-redundant inequalities, if and only if $\min \; \varepsilon_t = \varepsilon_t^0 \geq 0$ and ε_t is a basic variable of the problem (4.18) to (4.20).

In next paragraphs it is presented the solution algorithm of the linear multiparametric optimization problem considering that the terms of the independent vector are represented by linear expressions of the λ parameters (Gal, 1979).

Phase I Determine an initial optimal and feasible solution for $\lambda_1^* = ... = \lambda_s^* = 0$, this is, a vertex $\rho_0 \in S_0$:

1. Set $\lambda_1^* = ... = \lambda_s^* = 0,$ that is, $\lambda^* = (0,...0)^T$;
2. Determine an optimal and feasible solution of the linear optimization problem (4.21) to (4.22).

$$\min \quad z = c^T.x \tag{4.21}$$

Subj.:

$$A.x = b, \quad x \geq 0 \tag{4.22}$$

3.1 Once an optimal and feasible associated with basis B_0 is identified in step 2, then phase I is finished. The solution of this problem represents the basis associated to the first vertex, ρ_0, such that, $\rho_0 \in S_0$. The critical region R_0 is a polyhedron in R^s, being defined by inequalities (4.23).

$$-F.\lambda \leq 0 \tag{4.23}$$

Phase II Determine all critical regions and their associated optimal and feasible basis on the solution space:

The solution algorithm of this phase is analogous to the one previously presented for the systhematic identification of all critical regions and their corresponding optimal and feasible basis considering that, in this case, however, it will be used the auxiliary problem (4.18) to (4.20) to determine all adjacent nodes in each iteration.

4.4. Objective function coefficients parameterization

If there exists some kind of uncertainty related to the coefficient of a given decision variable x_i in the objective function and this uncertainty is represented by a linear parameter, it becomes essential to determine the interval of variation of this parameter for which there is an optimal and feasible solution.

In this sense, the solution algorithm of this type of problems aims at determining the regions $\overline{R}_\rho \subseteq R^s$, $v \in \overline{R}_\rho$, such that the linear parametric optimization problem (4.24) to (4.26) has an optimal and feasible solution corresponding to the basis B_ρ and for $v \notin \overline{R}_\rho$ the referred basis doesn't correspond to an optimal solution.

$$Max \quad w = (c + H.\Delta)^T.x \tag{4.24}$$

Subj.:

$$A.x = b \tag{4.25}$$

$$x \geq 0 \tag{4.26}$$

In this formulation A is the constant coefficients matrix of the constraints, H is a vector of the parameter coefficients, b is the independent vector, c is the objective function coefficient vector and $v \in R^s$ is the objective function vector parameter.

As it can be seen, the objective function coefficients vector is represented by expression (4.27).

$$c(v) = c + H.\Delta \tag{4.27}$$

Additionally, the parameters vector must satisfy the constraint (4.28), that is, the set defined by (4.28) is a closed convex polyhedron set in R^s:

$$G.\Delta \leq d \tag{4.28}$$

In which,

$G = g_{ik}$, $i = 1,...,r$, $K = 1,...,s$ and $d \in R^r$, constant.

Similarly to what was detailed in Section 4.2, also in this case and from the geometrical point of view, the systematic parameterization corresponds to a procedure by which they are computed all admissible values of a scalar parameter of the problem (4.24) to (4.26). This corresponds to a systematic procedure to cover all the solution space $\overline{K}$ by critical regions (intervals) $\overline{R}_\rho$ such that two mutually different critical regions do not overlap. From the mathematical point of view, this systematic parameterization represents a procedure that allows to successively determine all neighbour regions and their corresponding optimal and feasible basis starting from the initial optimal and feasible basis.

If $M = [\underline{v}, \bar{v}]$ denotes the total region for the scalar parameter v, then $\overline{K}^* = \overline{K} \cap M$ represents the region of $\overline{K}$ with common points with M. The solution algorithm comprises two distinct phases. The first one aims at determining an initial optimal and feasible basis B_0. In the second, they are successively determined all neighbor regions, $\overline{R}_\rho$, starting from B_0. In next paragraphs it will be presented the algorithm proposed by Gal (1979) for the solution of this kind of problems.

Phase I:

1. Transform the inequalities into equations (by means of slack and artificial variables);
2. Set $v = 0$ and solve the linear optimization problem (4.29) to (4.31):

$$Max \quad c^T.x; \tag{4.29}$$
$$Subj.:$$
$$A.x = b \tag{4.30}$$
$$x \geq 0 \tag{4.31}$$

3.1 If there is an optimal and feasible solution associated with the basis B_0 in step 2, then the Phase I is finished. Go to Phase II;

Phase II:

1. In the tableau corresponding to B_0 determine the interval $\overline{R}_0 = [\underline{\psi}_0, \overline{\psi}_0]$ in which the basis remains optimal and feasible. The minimum and maximum values of this interval $\underline{\psi}_0$ and $\overline{\psi}_0$, respectively, should be computed using the optimality condition as described in (4.32).

$$C^T(\Delta_k) - C_0^T.B_\rho^{-1}.A = (c + c'(\Delta_k)) - C_0^T.B_\rho^{-1}A \geq 0 \tag{4.32}$$

In this expression,

- B - is an optimal and feasible basis;
- ρ - is the index for the corresponding set of basic variables;
- Δ - is the objective function uncertainty vector parameters;
- A - is the columns of the non-basic variables in the Simplex tableau;
- C_0 - is the cost vector of the basic variables;
- C^T - is the cost vector of the non-basic variables.

1.1 Let us now assume that $\underline{\psi}_0$ and $\overline{\psi}_0$ are finite. If it was used a pivot element to determine the neighbour basis of $\underline{\psi}_0$ the process is called descendant, since it aims at determining values smaller than Δ. Oppositely, if it aims at determining the neighbour basis of $\overline{\psi}_0$ the process is called ascendant. The chosen process is, however, irrelevant regarding to the final results;

1.2 If $\underline{\psi}_0 = -\infty$, $\underline{\psi}_0 \leq \underline{\Delta}$ or $\overline{\psi}_0 = +\infty$, $\overline{\psi}_0 \geq \overline{\Delta}$, then the descendant or ascendant process, respectively, is finished.

Considering the ascendant process and that the optimal basis B_k was already determined, the algorithm proceeds as follows:

2. The column of the Simplex tableau in which the ratio $\overline{\psi}_k < \overline{\Delta}$ was determined will be considered as pivot column;
3. They are identified all positive elements of ${}^{k}a_{ij}$ in the pivot column. They become the denominators of the ratios whose numerators correspond to the ${}^{k}b_i$ elements;

   3.1 If there aren't elements ${}^{k}a_{ij} > 0$ then they there aren't neighbour regions of $\Delta = \overline{\psi}_k$. The ascendant process is finished. Go to 7;
4. Determine the smaller ratio between those computed in Step 3. The corresponding row becomes the pivot row;
5. Perform a Primal Pivot step over B_k (considering the pivot element previously determined) to obtain B_{k+1};
6. Determine $\overline{\psi}_{k+1}$, where $\underline{\psi}_{k+1} = \overline{\psi}_k$;

   6.1 If $\overline{\psi}_{k+1} < \overline{\Delta}$ is finite, repeat steps 2 to 5 of Phase II in relation to the basis indices ρ_{k+1};

   6.2 If $\overline{\psi}_{k+1} = +\infty$ or $\overline{\psi}_{k+1} \geq \overline{\Delta}$ the ascendant process is finished. Go to 7.

The described procedure must be repeated to the basis B_k, until $\overline{\psi}_k = +\infty, \overline{\psi}_k \geq \Delta$ or all elements of the pivot columns are non-positive.

7. Go back to the initial Simplex tableau corresponding to basis B_0 and perform the descendant process assuming that the basis B_t was already determined.
8. Determine the pivot element according to steps 2 to 4 of Phase II;
9. Perform a Primal Pivot step over B_t (considering the pivot element previous determined) to obtain B_{t+1};
10. Determine $\underline{\psi}_{t+1}$, where $\overline{\psi}_{t+1} = \underline{\psi}_t$;

Steps 8 to 10 are repeated until in basis B_t, $\underline{\psi}_t = -\infty$, $\underline{\psi}_t \leq \underline{\Delta}$ or all elements of the pivot columns are non-positive.

4.5. Objective function coefficients multiparameterization

In optimization problems where the profit maximization represents an objective to attain, it is eventually possible to arise questions related, for instance, to the individual profits or to the way following which the operation program should be planned. In the linear programming terminology, this means that the cost coefficients are in these cases unknown or, eventually, that there is some uncertainty related to their definition. In this context, the objective function could be expressed in terms of its parameters dependency, as described by expression (4.33):

$$z(\Delta) = \sum_{j=1}^{N} \sum_{k=1}^{S} h_{jk}.\Delta_k.x_j \tag{4.33}$$

In this expression,

h_{jk} - represents the coefficient of the v_k parameter vector, $j = 1,...,m,\ k = 1,...,s$;

Δ_k - represents an element of the Δ parameter vector, $k = 1,...,s$.

x_j - represents an element of decision variable vector.

In this sense, the linear programming problem will consist of determining all values of the parameters Δ_k for which there are optimal and feasible solutions. If, for instance, it was identified a critical region $\overline{R}_\rho$, then each vector $(\Delta_1,...,\Delta_s)^T \in \overline{R}_\rho$ represents the S vector dimension of the cost function.

Similarly to what was presented for the linear multiparametric optimization problems considering independent vector parameters, in this case Gal (1979) also presents two distinct algorithms for the solution of this kind of problems. The author calls them H and H_D algorithms. The H method could be described as an approach to compute a region $\overline{K} \subseteq R^s$ in such a way that the linear multiparametric maximization problem (4.34) to (4.36) has an optimal and feasible solution for each $\Delta \in \overline{K}, \Delta \in R^s$ and for each $\Delta \in R^s, \Delta \notin \overline{K}$, the problem doesn't not have any optimal and feasible solution.

$$\min \quad z(\Delta) = (H.\Delta)^T.x \tag{4.34}$$

Subj.:

$$A.x = b \tag{4.35}$$

$$x \geq 0 \tag{4.36}$$

Similarly to the F algorithm previously detailed for the linear multiparametric optimization problem considering independent vector parameters, the H algorithm also comprises two different important steps:

- Determine an initial optimal and feasible solution (x^0, v^0), considering $\Delta_s = 0, \ \forall s$;
- Determine all critical regions and their associated optimal and feasible basis. Each critical region $\overline{R}_\rho$ is defined by the expression (4.37):

$$-H.\Delta \leq 0 \tag{4.37}$$

Since each critical region $\overline{R}_\rho$ forms a polyhedron in R^s, according to Gal (1979), the process to adopt in order to determine all adjacent nodes of a given node $\rho \in S$ corresponds to solve the problem (4.38) to (4.40).

$$\min \quad \underset{j \in P_\rho}{\varepsilon_j} \tag{4.38}$$

Subj.:

$$-\sum_{k=1}^{s} {}^{\rho} h_j^k.\Delta_k + \varepsilon_j = 0 \qquad j = 1,...,m, \ k = 1,...,s \tag{4.39}$$

$$\varepsilon_j \geq 0 \qquad j = 1,...,m \tag{4.40}$$

In this expression:

P_ρ - is the number of faces of the polyhedron that defines the node $\rho \in S$;
ε - is a slack variable.

This problem will have a solution, if and only if, min $\varepsilon_j = \varepsilon_j^0 \geq 0$, and ε_j was a non-basic variable of the problem (4.38) to (4.40).

In next paragraphs it is detailed the solution algorithm of the H method (Gal, 1979).

Phase I Determine an initial optimal and feasible solution for $v_1^* = ... = v_s^* = 0$, that is, a vertex $\rho_0 \in S_0$:

1. Set $\Delta_1^* = ... = \Delta_s^* = 0$, that is, $\Delta^* = (0,...0)^T$;
2. Determine an optimal and feasible solution of the linear optimization problem (4.41) to (4.43).

$$\min \quad z = c^T.x \tag{4.41}$$

Subj.:

$$A.x = b \tag{4.42}$$

$$x \geq 0 \tag{4.43}$$

2.2 Once obtained a solution (x^0, Δ^0) go to Phase II.

The solution of this problem represents the basis associated to the first vertex, ρ_0, such that, $\rho_0 \in S_0$. The critical region $\overline{R}_0$ is a polyhedron in R^s, that is defined by inequalities (F4.44).

$$-H.\Delta \leq 0 \tag{4.44}$$

Phase II Determine all critical regions and their associated optimal and feasible basis.

The solution algorithm of this phase is analogous to the one presented for the systematic identification of all critical regions and their corresponding optimal and feasible basis (Section 4.3). However, in this case, it must be considered that in step 3 it is applied a Primal Simplex step instead of a Dual Simplex step and the auxiliary problem to be solved corresponds to (4.38) to (4.40).

4.6. Simultaneous parameterization of c and b vectors

Typically the interdependence of prices and goods or product volumes to be sold or produced in a given company is high. Prices, costs and/or profits, by one side, and sales, demand, offer availability and/or raw-material quantities, by another, could depend on external factors or on one another. In such a system, it must be taken into account the sub-systems interrelations, as well as the relation of the system with its involving environment.

The analysis of such relations could be seen as a production adaptation to some modifications that eventually occurred (a *posteriori* analysis), or as an analysis performed in advance (*a priori* analysis) allowing to perform some sensitivity analysis, such as, production or market conditions in relation to a given system and/or take management decisions. If these influences are described by parameters in a linear model, the cost vector and the independent term vector could, in a general form, be written as a function of two parameters, this is, $c(v)$ and $b(\lambda)$, which can be dependent or independent between them.

If the function $F(v,\lambda)=0$ exists, the vectors v and λ as considered as dependent parameters. Oppositely, they will be called independent. Similarly to what was described in Sections 4.2 and 4.4 the solution algorithm for the linear parametric optimization problems considering, simultaneously, independent parameters modeling independent vector uncertainties and objective function vector uncertainties comprises three different phases:

- Determine an initial optimal and feasible solution considering $\lambda=0$ and $v=0$;
- Perform an independent vector parameterization analysis;
- Perform an objective function parameterization analysis.

In the next paragraphs it is presented the solution algorithm for the linear parametric optimization problem considering, simultaneously, parameters on the independent vector coefficients and on the objective function coefficient vector (Gal, 1979).

Phase I:

1. Transform the inequalities into equations (by means of slack and artificial variables);
2. Set $\Delta=\lambda=0$ and solve the linear optimization problem (4.45) to (4.47):

$$\min\ c^T.x; \qquad (4.45)$$

$$Subj.:$$

$$A.x=b \qquad (4.46)$$

$$x\geq 0 \qquad (4.47)$$

3.1 Once an optimal and feasible solution associated to the base B_0 in step 2, then Phase I is finished, since B_0 represents the searched initial optimal and feasible basis. Go to Phase II;

Phase II:

This phase comprises the independent vector parameterization analysis as previously described in Section 4.2.

Phase III:

This phase comprises the objective function coefficients parameterization analysis as previously described in Section 4.4.

4.7. Simultaneous multiparametrization of the independent vector and of the objective function coefficients

The algorithm to be used to solve linear multiparametric optimization problems considering, simultaneously, parameters on the independent vector and on the objective function vector coefficients is presented in next paragraphs. As described in Section 4.6., in this case the algorithm can also be divided in three distinct steps:

- Determine an initial optimal and feasible solution considering $\lambda_s=0$ and $v_s=0$;
- Perform an independent vector multiparametric analysis;
- Perform an objective function multiparametric analysis.

In this context, in next paragraphs it is presented the algorithm proposed by Gal (1979) for the solution of this type of problems.

Phase I Determine an initial optimal and feasible solution for $\Delta_1^* = ... = \Delta_s^* = 0$ and $\Delta_1^* = ... = \Delta_s^* = 0$, that is, determine the vertex $\rho_0 \in S_0$:

1. Set $\Delta_1^* = ... = \Delta_s^* = 0$, that is, $\Delta^* = (0,...0)^T$ and $\Delta_1^* = ... = \Delta_s^* = 0$, that is, $\Delta^* = (0,...0)^T$;
2. Determine an optimal and feasible solution of the linear optimization problem (4.48) to (4.50).

$$Max \quad z = c^T.x \tag{4.48}$$

Subj.:

$$A.x = b \tag{4.49}$$

$$x \geq 0 \tag{4.50}$$

3.2 If there is a solution $(x^0, \Delta^0, \lambda^0)$, then go to Phase II.

The solution of this problem represents the basis associated to the first vertex, ρ_0 such that, $\rho_0 \in S_0$. The critical region $\overline{R}_0^*$ is a polyhedron in R^s, that is defined by inequalities (4.51) to (4.52).

$$-H.\Delta \leq 0 \tag{4.51}$$

$$-F.\lambda \leq 0 \tag{4.52}$$

Phase II Determine all critical regions and their associated optimal and feasible basis in the solution space with respect to the independent vector multiparameterization.

The solution algorithm of this phase is analogous to the one presented for the systematic identification of all critical regions and their corresponding optimal and feasible basis. However, in this case, it must be considered, simultaneously, the auxiliary problems (4.18) to (4.20) and (4.38) to (4.40) to determine all adjacent vertices in each iteration..

Phase III Determine all critical regions and their associated optimal and feasible basis in the solution space with respect to the objective function coefficient multiparameterization.

The solution algorithm of this phase is analogous to the one presented in Figure 4.2 (considering in step 3. a Primal Simplex step instead of a Dual Simplex step). However, in this case, it must be considered, simultaneously, the auxiliary problems (4.18) to (4.20) and (4.38) to (4.40) to determine all adjacent vertices in each iteration.

CHAPTER V Problem Formulation

5. Problem formulation

5.1. Fuzzy Optimal Power Flow model

As previously mentioned in Chapter 3, during the 90's several contributions were published aiming at including in several power system operations and planning models load uncertainties represented by trapezoidal fuzzy numbers. In this context, Miranda *et al.* (1992) and Saraiva, *et al.* (1994a) described the Fuzzy DC OPF model admitting that the demand vector can be affected by uncertainties. This formulation used the DC model to represent the operation of the transmission system and its solution algorithm is presented in Figure 5.1.

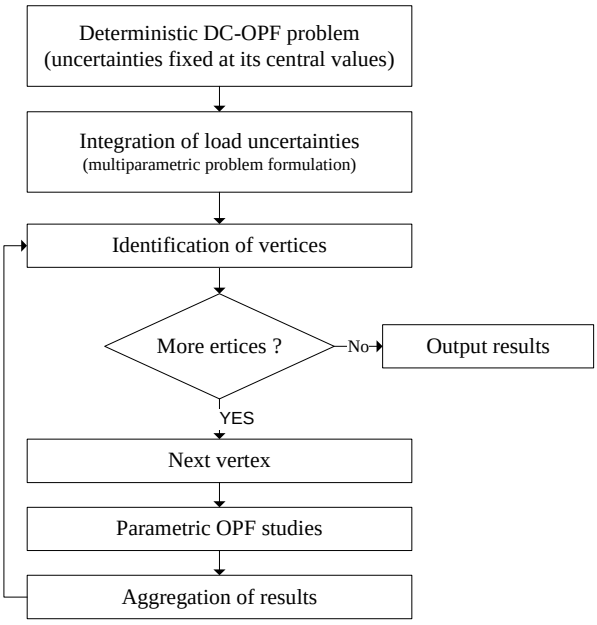

Figure 5.1: Algorithm of the original Fuzzy DC Optimal Power Flow model (source: Saraiva *et al.*, 1994a).

This algorithm starts by solving a deterministic DC OPF in which the fuzzy numbers that represent loads are substituted by their corresponding central values. This leads to the linear optimization problem (5.1) to (5.7).

$$\min \; z = \sum_{i=1}^{nb}\sum_{k=1}^{ngi} CP_{ik}.P_{Gik} + G.\sum_{i=1}^{nb} PNS_i \tag{5.1}$$

Subj.:

$$\sum_{i=1}^{nb}\sum_{k=1}^{ngi} P_{Gik} + \sum_{i=1}^{nb} PNS_i = \sum_{i=1}^{nb} P_{Li}^{ctr} \tag{5.2}$$

$$P_{Gik} \le P_{Gik}^{máx} \qquad i = 1,...,nb; \;\; k = 1,...,ngi \tag{5.3}$$

$$P_{Gik} \ge P_{Gik}^{\min} \qquad i = 1,...,nb; \;\; k = 1,...,ngi \tag{5.4}$$

$$PNS_i \le P_{Li}^{ctr} \qquad ,i=1,...,nb \tag{5.5}$$

$$\sum_{i=1}^{nb} S_{dcbi} \cdot \left(\sum_{k=1}^{ngi} P_{Gik} - P_{Li}^{ctr} + PNS_i \right) + Vf_{b1} = P_b^{máx}, \ j=1,...,nr \tag{5.6}$$

$$-\sum_{i=1}^{nb} S_{dcbi} \cdot \left(\sum_{k=1}^{ngi} P_{Gik} - P_{Li}^{ctr} + PNS_i \right) + Vf_{b2} = P_b^{máx}, \ j=1,...,nr \tag{5.7}$$

In this problem,

- nr - represents the number of branches in the system;
- nb - represents the number of buses in the system;
- P_{Li}^{ctr} - represents the central value of the trapezoidal fuzzy number of the load specified to bus i;
- ngi - represents the number of generators, each one associated with a linear cost function, connected to bus i;
- CP_{ik} - represents the incremental cost of the generator k in bus i;
- P_{Gik} - represents the active power generation of the generator k connected to bus i;
- PNS_i - represents the active power generation of the fictitious generator used to model the Power Not Supplied in bus i;
- G - represents the cost assigned to the Power Not Supplied in the system;
- S_{dcbi} - represents the sensibility matrix element that relates the active power flow on branch b with the injected active power on bus i;
- Vf_{b1} - represents the slack variable related with the maximum limit constraint of the active power flow on branch b;
- Vf_{b2} - represents the slack variable related with the minimum limit constraint of the active power flow on branch b;
- $P_b^{máx}$ - represent the maximum branch capacity limit of a branch b. In this model it is also assumed that the minimum branch capacity limit is symmetric of the corresponding maximum value;
- $P_{Gik}^{máx}, P_{Gik}^{\min}$ - represent the maximum and minimum generation capacity limit, respectively, of the generator k connected to bus i.

With the solution of this linear optimization programming problem it will be possible to obtain the values of P_{Gik} related with the minimum generation cost, while respecting the active power balance equation (5.2), the maximum and minimum capacity limits of generators (5.3), (5.4) and (5.5), respectively, and the maximum and minimum capacity limits of branch active power flows (5.6) and (5.7), respectively. In the scope of this deterministic DC-OPF study, the active loads to be considered correspond to the central values of their respective trapezoidal fuzzy membership functions.

From the point of view of its computational implementation, the solution of the linear optimization programming problem (5.1) to (5.7) can be obtained considering the well known Simplex method, and so, it will not be further detailed in this document.

In order to integrate the uncertainties that affect demand we must then consider that the membership functions of the active loads can be expressed as a function of its central value as defined in (5.8).

$$\lambda_i = \tilde{P}_{Li} \Theta P_{Li}^{ctr} \tag{5.8}$$

In this context, the deviations corresponding to the 0.0 membership degree of the active load connected to bus i can be obtained considering a parameter, λ_i, according with expression (5.9).

$$\tilde{P}_{Li} = P_{Li}^{ctr} + \lambda_i, \qquad \lambda_i \in S\left(\tilde{P}_{Li} \Theta P_{Li}^{ctr} \right) \tag{5.9}$$

In this way, the DC-OPF problem integrating uncertainties associated with the 0.0 membership degree can be formulated as a linear multiparametric optimization problem represented in a condensed way by (5.10) to (5.12). In this formulation, b and $b'(\lambda)$ are vectors representing the right hand side terms of the constraints given that some of them are independent and some others are dependent on the parameters λ_i used to model load uncertainties.

$$\min \quad z = c^T.X \tag{5.10}$$

Subj.:

$$A.x = b + b'(\lambda) \tag{5.11}$$

$$\lambda_i^{\min} \le \lambda_i \le \lambda_i^{máx}, \quad i = 1,...,nb \tag{5.12}$$

In this problem,

- c - represents the cost vector of the system generators;
- X - represents the active power generation of the system generators;
- A - represents the constant coefficient matrix of the constraints;
- b - represents the right hand side vector of the constraints that are independent from the parameters that model loads uncertainties;
- $b'(\lambda)$ - represents the right hand side vector of the constraints that depend on the parameters that model load uncertainties;
- λ - represents the parameters that model load uncertainties;
- nb - represents the number of buses in the system.

Since the optimal solution of the crisp problem may not be feasible for all possible load combinations associated with (5.12), once the linear multiparametric programming problem is defined the algorithm proceeds identifying vertices of the hypervolume defined by (5.12). As a general rule, these vertices correspond to feasible solutions leading to maximum or minimum values of each basic variable of the initial solution or, instead, to vertices corresponding to unfeasible solutions. In the end of this process, all

vertices that lead to individual extreme values of the basic variables or, instead, to non-feasible solutions are identified. Afterwards, the algorithm proceeds by running a set of two consecutive parametric DC-OPF studies for each identified vertex. As an example, let us consider that Figure 5.2 represents the rectangles enclosing all possible load combinations for the 0.0 and 1.0-cuts for a system with two trapezoidal fuzzy loads defined by (5.13) and (5.14).

$$P_{L1} = P_{L1}^{ctr} + (\lambda_{11};\lambda_{12};\lambda_{13};\lambda_{14}) \text{ MW} \quad (5.13)$$

$$P_{L2} = P_{L2}^{ctr} + (\lambda_{21};\lambda_{22};\lambda_{23};\lambda_{24}) \text{ MW} \quad (5.14)$$

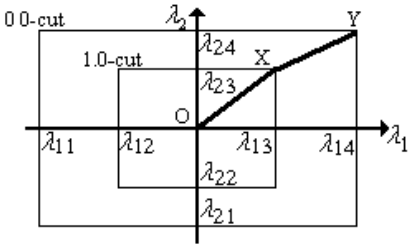

Figure 5.2: Rectangles enclosing all possible load combinations in the 0.0 and 1.0-cuts for a system with two trapezoidal fuzzy loads.

Taking Figure 5.2 as reference and vertex Y as an illustration, the first parametric study analyses load combinations on the segment OX considering that points O and X correspond, respectively, to α = 1.0 and α = 0.0 in the linear parametric optimization problem (5.15) to (5.17).

$$\min f = c^t.X \quad (5.15)$$

Subj.

$$A.X = b + b'(1.0 - \alpha) \quad (5.16)$$

$$0.0 \le \alpha \le 1.0 \quad (5.17)$$

When point X is reached, the optimal and feasible solution is given by (5.18).

$$X_{opt} = B^{-1}.(b + b'(1.0 - \alpha)) \quad (5.18)$$

In the second parametric study, points X and Y correspond to α = 1.0 and α = 0.0, respectively. Performing another parametric DC-OPF study, it is possible to obtain the solution for Y, where the optimal and feasible basis is given by (5.19).

$$X_{opt} = B^{-1}.(b + b' + b''(1.0 - \alpha)) \quad (5.19)$$

These parametric studies are formulated in such a way that it is possible to guarantee that the values obtained in the first one are assigned to 1.0 membership degree while the values related with the second one have a membership degree that corresponds to the value of α, and so, it decreases from 1.0 to 0.0 membership degree (points X and Y, respectively). The final membership functions of branch flows, generations and Power

Not Supplied can then be obtained by aggregating the partial membership functions of each variable obtained in each set of parametric studies using the fuzzy union operator.

5.2. New Fuzzy DC Optimal Power Flow model

5.2.1. General aspects

The development of electricity markets and the volatility of fuel prices place a new emphasis on power system planning and operation activities, as well as, in the liquidity of the market. Recognizing these concerns, the New Fuzzy Optimal Power Flow, NFOPF, approach aims at, in first place, extending the original concept by translating to the results not only load uncertainties, but also generation costs uncertainties. Secondly, since computational resources are nowadays more powerful than in the past, the NFOPF model also enables obtaining a more accurate solution for this type of problems, since it adopts linear multiparametric optimization techniques. The application of these techniques leads to the identification of a number of critical regions covering all the uncertainty space meaning that it effectively covers all the combinations of values of the parameters affected by uncertainties. This has an important consequence, since that the algorithm developed back in 90's and previously presented in Section 5.1, differently to the new developed one, adopted a simplified approach to build the membership functions for generations, branch flows and Power Not Supplied. As a consequence, the range of possible values obtained at that time may, in some cases, not correspond to the widest possible behaviour of the problem outputs.

As described in Chapter 4., the algorithms used to solve the linear multiparametric problems were originally proposed by Gal (1975). Starting at the initial optimal and feasible solution of the deterministic optimization problem (5.1) to (5.7), these algorithms identify critical regions in the uncertainty space. This means that they search all the combination of values of the parameters affected by uncertainties for which there is an optimal and feasible basis. When running this process, the feasibility (5.20) and optimality (5.21) conditions are extended so that they become function of λ_k (parameters modeling load uncertainties) or Δ_k (parameters modeling generation cost uncertainties) or both. Then, starting at the optimal and feasible solution of the initial deterministic DC-OPF problem and considering each of these conditions, the algorithm proceeds finding the set of other optimal and feasible solutions provided they are valid in some region of the uncertainty space. These regions are called critical regions and this process is conducted by pivoting over the initial basis as well as over all the new ones identified during the search process.

From a mathematical point of view, let B be an optimal and feasible basis, ρ the index for the corresponding set of basic variables, A the columns of the non-basic variables in the Simplex tableau, c_0 the cost vector of the basic variables, c^T the cost vector of the non-basic variables, λ_k the parameters that model load uncertainties, Δ_k the parameters that model generation cost uncertainties, b the right hand side vector of the constraints and c the objective function coefficient vector. The feasibility and optimality conditions for a

minimization linear optimization problem can then be defined in terms of λ_k and Δ_k by (5.20) and (5.21), respectively.

$$B_{\rho}^{-1}.b(\lambda_k) = B_{\rho}^{-1}(b + b'(\lambda_k)) \geq 0 \tag{5.20}$$

$$C^T(\Delta_k) - C_0^T.B_{\rho}^{-1}.A = (c + c'(\Delta_k)) - C_0^T.B_{\rho}^{-1}A \geq 0 \tag{5.21}$$

Since the dual solution does not depend on λ_k for right hand side parameterizationm, a critical region, i.e., a region in the uncertainty space where B remains optimal and feasible, can be uniquely defined by the conditions in (5.20). By analogy, since the primal solution does not depend on Δ_k for cost parameterization, a critical region can be defined by the conditions (5.21). Apart from these conceptual aspects, two optimal and feasible basis, B_1 and B_2, are considered neighbor ones, if and only if one can pass from B_1 to B_2 performing one dual pivot step in case of right hand side parameterization, one primal pivot step in case of cost vector parameterization or one step of each type if we are addressing the simultaneous parameterization of cost and load uncertainties.

As a final comment, the ultimate objective to attain when solving a linear multiparametric optimization problem is to find all possible optimal solutions, their corresponding optimal values and critical regions, which can be defined as a closed nonempty polyhedron, that is, a set of linear inequalities in λ_k, Δ_k, or both. Mathematically, this set of constraints can be expressed as the equivalent set of non-redundant constraints, which in turn can be identified through a non-redundant test for linear inequalities, like the one proposed by Gal (1975) and already detailed in Section 4.

5.2.2. Integration of load uncertainties

As stated in Section 5.2.1. the developed NFOPF approach does not include any kind of simplification (apart from adopting the DC Model), and so, the corresponding linear multiparametric optimization problem is treated by linear multiparametric optimization techniques (according to what was described in Section 4.3) in order to obtain the widest possible behavior of each variable on the uncertainty space. In this sense, the algorithm developed to solve the NFOPF problem is presented in Figure 5.3. As it can be observed, this new algorithm also starts by solving the deterministic Fuzzy DC-OPF problem (5.1) to (5.7) considering the central values of the fuzzy numbers that represent loads. After obtaining an optimal and feasible solution for this deterministic problem, the algorithm integrates the parameters that model load uncertainties in the initial deterministic Fuzzy DC-OPF problem, leading to the condensed linear multiparametric optimization problem (5.10) to (5.12), whose complete formulation is presented in (5.22) to (5.27).

$$\min \; z = \sum_{i=1}^{nb}\sum_{k=1}^{ngi} CP_{ik}.P_{Gik} + G.\sum_{i=1}^{nb} PNS_i \tag{5.22}$$

Subj.:

$$\sum_{i=1}^{nb}\sum_{k=1}^{ngi} P_{Gik} + \sum_{i=1}^{nb} PNS_i = \sum_{i=1}^{nb}(P_{Li}^{ctr} + \lambda_i) \tag{5.23}$$

$$P_{Gik} \leq P_{Gik}^{máx} \qquad i = 1,...,nb; \;\; k = 1,...,ngi \tag{5.24}$$

$$P_{Gik} \geq P_{Gik}^{\min} \qquad i=1,...,nb;\ k=1,...,ngi \tag{5.25}$$

$$PNS_i \leq P_{Li}^{ctr} + \lambda_i \qquad i=1,...,nb \tag{5.26}$$

$$\sum_{i=1}^{nb} S_{dcbi} \cdot \left(\sum_{k=1}^{ngi} P_{Gik} - P_{Li}^{ctr} + PNS_i \right) + Vf_{b1} = P_b^{máx} + \sum_{i=1}^{nb} S_{dcbi} . \lambda_i, \quad j=1,...,nr \tag{5.27}$$

$$-\sum_{i=1}^{nb} S_{dcbi} \cdot \left(\sum_{k=1}^{ngi} P_{Gik} - P_{Li}^{ctr} + PNS_i \right) + Vf_{b2} = P_b^{máx} - \sum_{i=1}^{nb} S_{dcbi} . \lambda_i, \quad j=1,...,nr \tag{5.28}$$

The presence of the parameters λ_i $(i=1,...,s)$ in this linear optimization problem originates situations in which the optimal and feasible basis identified in the initial deterministic Fuzzy DC-OPF problem will not be feasible in some regions of the hypervolume associated to (5.12). Following the algorithm in Figure 5.3, it will now be identified a set of non-redundant constraints defining new critical regions considering the inequalities associated with the feasibility condition (5.20). If there are no non-redundant constraints, the algorithm stops. Otherwise, it performs a dual pivoting over the initial optimal and feasible basis to identify new critical regions. This process is repeated until no non-redundant constraints exist or until all identified critical regions correspond to already known ones. When this process is completed all the uncertainty space was covered and they were identified all critical regions in which a basis B of the problem (5.22) to (5.28) remains feasible and optimal.

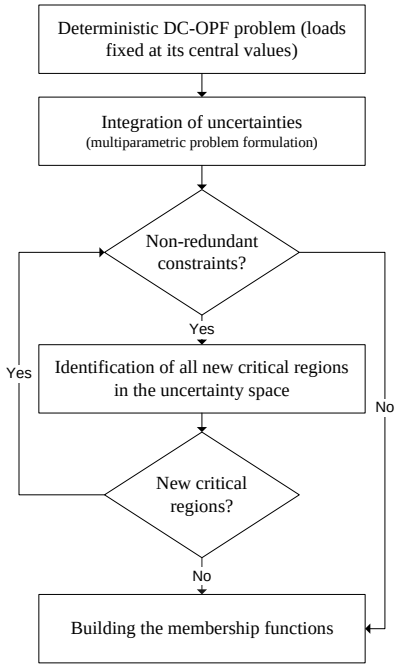

Figure 5.3: Solution algorithm for the New Fuzzy DC Optimal Power Flow model integrating active load uncertainties.

For a better understanding of this procedure, Figure 5.4 depicts the rectangles enclosing all possible load combinations in the 0.0 and 1.0-cuts for a system supplying two trapezoidal fuzzy loads. In this Figure, lines “a” and “b” represent constraints, for instance, related with branch flow or generator capacity limits, point O corresponds to the

optimal and feasible solution of the initial deterministic DC-OPF problem and the dashed lines define the range of values of the uncertainties associated with the i^{th} cut of the fuzzy load membership functions. From Figure 5.4 it becomes clear that the non-redundant constraints, such as the one associated with line "a", can define any critical regions, such as, R_i and R_j indicated in this Figure. The process to identify these regions is implemented using the feasibility condition (5.20) described by the parameters that model load uncertainties. In a systematic way, all critical regions are obtained by performing a dual pivoting over each of the optimal and feasible identified basis.

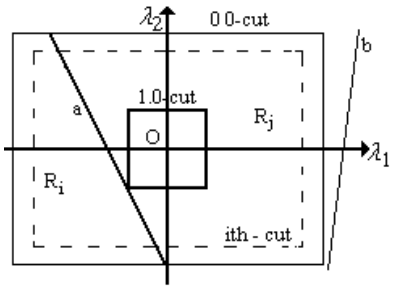

Figure 5.4: Critical regions in the uncertainty space.

In order to build the membership functions of the output variables (generations, branch flows and Power Not Supplied) it is important to identify their extreme possible behaviours reflecting data uncertainty. Since the problem is linear, each variable in each critical region is represented by a linear expression. As a result, if we want to capture the widest possible behaviour of a variable represented by a linear function of the uncertainty parameters λ_1 and λ_2, say $v(\lambda_1, \lambda_2)$, we will then have to solve the problem (5.29) to (5.32).

$$\min/\max \quad f = v(\lambda_1, \lambda_2) \tag{5.29}$$

Subj.:

$$k_{1i}.\lambda_1 + k_{2i}.\lambda_2 \le b_i \tag{5.30}$$

$$\lambda_1^{\min\ i^{th}-cut} \le \lambda_1 \le \lambda_1^{máx\ i^{th}-cut} \tag{5.31}$$

$$\lambda_2^{\min\ i^{th}-cut} \le \lambda_2 \le \lambda_2^{máx\ i^{th}-cut} \tag{5.32}$$

This problem can be formulated for some α-cuts of the specified load uncertainties, meaning that, in some way, each fuzzy load is discretized in a number of intervals, each one associated with a α-cut. Once this discretization is completed, we reflect the uncertainties now represented by α-cuts, in the output variables of the problem. This corresponds to minimize and to maximize the linear expressions of each of these variables, subjected to the constraints modelling the non-redundant conditions (5.30), where k_{1i} and k_{2i} are real numbers, together with the possible ranges of the input uncertainties regarding the i^{th} cut under analysis (5.31) and (5.32). After solving these minimization and maximization problems for the selected cuts, it is possible to build the membership function of v in the critical region under analysis. Once all regions are analyzed, the final membership function of v is obtained applying the fuzzy union

operator to the partial membership functions obtained for that variable in each critical region.

5.2.3. Integration of generation cost uncertainties

In this case and similarly to what was described in the previous Section, the membership functions related to the generation costs can be expressed as a function of their central values, as described by (5.33).

$$\Delta_i = \tilde{CP}_i \ \Theta CP_i^{ctr} \tag{5.33}$$

The 0.0 cut values of the generation cost membership function of a given generator connected to bus i, can then be obtained considering a parameter, Δ_i, according to expression (5.34).

$$\tilde{CP}_{ci} = CP_{ci}^{ctr} + \Delta_i, \qquad \Delta_i \in S\left(\tilde{CP}_i \ \Theta CP_i^{ctr} \right) \tag{5.34}$$

The parameters $\Delta_i \quad (i = 1,...,nb)$ can be integrated in the objective function coefficients of the initial deterministic DC-OPF problem. Similarly to what was described in the previous section, it is formulated a linear multiparametric optimization problem represented in a condensed way by (5.35) to (5.37). In this formulation $c^T(\Delta)$ is a vector integrating the parameters dependent of $\Delta_i \quad (i = 1,...,s)$ in the objective function.

$$\min \quad z = c^T(\Delta).X \tag{5.35}$$

Subj.:

$$A.x = b \tag{5.36}$$

$$\Delta_i^{\min} \le \Delta_i \le \Delta_i^{máx} \tag{5.37}$$

The complete formulation of the Fuzzy DC-OPF problem integrating generation cost uncertainties corresponds to the mathematical problem described in (5.38) to (5.44).

$$\min \ z = \sum_{i=1}^{nb} \sum_{k=1}^{ngi} (CP_{ik} + \Delta_i).P_{Gik} + G.\sum_{i=1}^{nb} PNS_i \tag{5.38}$$

Subj.:

$$\sum_{i=1}^{nb} \sum_{k=1}^{ngi} P_{Gik} + \sum_{i=1}^{nb} PNS_i = \sum_{i=1}^{nb} P_{Li}^{ctr} \tag{5.39}$$

$$P_{Gik} \le P_{Gik}^{máx} \qquad i = 1,...,nb; \quad k = 1,...,ngi \tag{5.40}$$

$$P_{Gik} \ge P_{Gik}^{\min} \qquad i = 1,...,nb; \quad k = 1,...,ngi \tag{5.41}$$

$$PNS_i \le P_{Li}^{ctr} \qquad i = 1,...,nb \tag{5.42}$$

$$\sum_{i=1}^{nb} S_{dcbi} \cdot \left(\sum_{k=1}^{ngi} P_{Gik} - P_{Li}^{ctr} + PNS_i \right) + Vf_{b1} = P_b^{máx}, \qquad j = 1,...,nr \qquad (5.43)$$

$$-\sum_{i=1}^{nb} S_{dcbi} \cdot \left(\sum_{k=1}^{ngi} P_{Gik} - P_{Li}^{ctr} + PNS_i \right) + Vf_{b2} = P_b^{máx}, \qquad j = 1,...,nr \qquad (5.44)$$

With the solution of this linear multiparametric optimization problem we will obtain the values of the active generations and of the active branch power flows related with minimum costs for different α - cuts of $\Delta_i \quad (i = 1,...,s)$.

In order to solve the linear multiparametric optimization problem (5.38) to (5.44), we must recall the algorithm presented in Section 4.5 together with the algorithm presented in Figure 5.3 that is still valid provided that some adaptations are made. In this context, after identifying an optimal and feasible basis of the problem (5.1) to (5.7) formulated for the central values of the fuzzy numbers that represent generation costs, we include in the formulation the parameters that represent generation cost uncertainties leading to the linear multiparametric optimization problem (5.38) to (5.44). In this case, however, the process of identifying the non-redundant constraints that leads to the definition of the critical regions in the uncertainty space will be conducted by the optimality condition (5.21) in terms of the parameters Δ_k. In this case, the critical regions are identified performing a primal pivoting over the initial optimal and feasible basis as well as over all new optimal and feasible basis identified along the search procedure.

When solving problems as (5.38) to (5.44), we should recall that each variable (generations, branch flows and Power Not Supplied) is constant for all generation cost combinations inside each critical identified region. Therefore, the values of these output variables will only change if there is a basis change, which means moving from one critical region to another. Accordingly, for each critical region, the partial membership function of any variable is built considering the non-redundant inequalities defining that region and the maximum membership degree of that output variable. This is simply done solving the linear system formed by the inequalities that define each critical region to check if, at least, one point of a given cut level belongs to the critical region under analysis. Once all these pairs are obtained, they are aggregated using the fuzzy union operator to obtain the final membership function of the output variable under analysis.

Therefore, when addressing generation cost uncertainties, the possible behaviour of the output variables is represented by pairs including the value of the output variable and the corresponding membership degree. This result corresponds, in some way, to the dual of the type of results obtained for load uncertainties. This should not be an entire surprise since when addressing load uncertainties we are multiparameterizing the right hand side vector, while for generation cost uncertainties we are running a cost function multiparameterization study. From a conceptual point of view, this means that these two problems correspond to a primal and dual version of the same problem.

5.2.4. Simultaneous integration of generation cost and load uncertainties

If we represent the membership functions of generation costs and active loads as a function of the parameters Δ_i and λ_i, respectively, we can formulate the problem related with the 0.0-cut level of the respective membership functions as a linear multiparametric optimization problem represented in a condensed way by (5.45) and (5.48).

$$\min \quad z = C^T(\Delta).X \tag{5.45}$$

Subj.:

$$A.x = b + b'(\lambda) \tag{5.46}$$

$$\lambda_i^{\min} \le \lambda_i \le \lambda_i^{máx} \tag{5.47}$$

$$\Delta_i^{\min} \le \Delta_i \le \Delta_i^{máx} \tag{5.48}$$

The complete formulation of the Fuzzy DC-OPF problem integrating, simultaneously, active load and generation cost uncertainties corresponds to the problem given by (5.49) and (5.55).

$$\min \quad z = \sum_{i=1}^{nb}\sum_{k=1}^{ngi}(CP_{ik} + \Delta_i).P_{Gik} + G.\sum_{i=1}^{nb} PNS_i \tag{5.49}$$

Subj.:

$$\sum_{i=1}^{nb}\sum_{k=1}^{ngi} P_{Gik} + \sum_{i=1}^{nb} PNS_i = \sum_{i=1}^{nb}(P_{Li}^{ctr} + \lambda_i) \tag{5.50}$$

$$P_{Gik} \le P_{Gik}^{máx} \qquad i = 1,...,nb; \quad k = 1,...,ngi \tag{5.51}$$

$$P_{Gik} \ge P_{Gik}^{\min} \qquad i = 1,...,nb; \quad k = 1,...,ngi \tag{5.52}$$

$$PNS_i \le P_{Li}^{ctr} \qquad i = 1,...,nb \tag{5.53}$$

$$\sum_{i=1}^{nb} S_{dcbi}.\left(\sum_{k=1}^{ngi} P_{Gik} - P_{Li}^{ctr} + PNS_i\right) + Vf_{b1} = P_b^{máx} + \sum_{i=1}^{nb} S_{dcbi}.\lambda_i, \quad j = 1,...,nr \tag{5.54}$$

$$-\sum_{i=1}^{nb} S_{dcbi}.\left(\sum_{k=1}^{ngi} P_{Gik} - P_{Li}^{ctr} + PNS_i\right) + Vf_{b2} = P_b^{máx} - \sum_{i=1}^{nb} S_{dcbi}.\lambda_i, \quad j = 1,...,nr \tag{5.55}$$

The presence of the parameters $\Delta_i \quad (i = 1,...,s)$ and $\lambda_i \quad (i = 1,...,s)$ in this problem will eventually turn the optimal and feasible basis identified for the initial deterministic DC-OPF problem as non optimal or unfeasible in some regions of the hypervolume related with (5.47) and (5.48).

The process to identify non-redundant constraints is implemented using both the inequalities given by the feasibility (5.20) and optimality (5.21) conditions expressed as linear functions of the uncertainty parameters λ_i and Δ_i, respectively. As a result of the increased number of parameters modeling data uncertainties, the search of all critical regions should now be conducted in a more structured way. This leads to the adoption of

a search tree as illustrated in Figure 5.5, where ρ_i defines the index of the set of basic variables in a given critical region i.

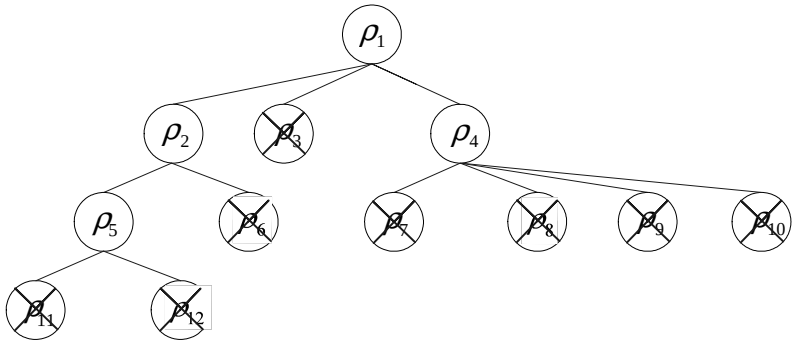

Figure 5.5: Search tree to illustrate the search procedure.

Departing from one node in the tree, one can find two kinds of neighbour basis. The first one is determined by the application of the feasibility condition (5.20) (in Figure 5.5 these basis correspond to nodes at the left of its departure node). The second type results from the optimality condition (5.21) (in Figure 5.5 these basis correspond to nodes on the right side of its departure node) as described in Section 4.7. This process is repeated for each new node until no non-redundant constraints exist or all the identified critical regions correspond to already known ones. In Figure 5.5 and for illustration purposes, the crosses denote basis that are not new regarding the previously identified ones. Similarly to the algorithms described in Sections 5.2.1 and 5.2.2, each critical region is defined by a set of inequality conditions related, in this case, both with the feasibility and optimality conditions.

Once all critical regions are identified, the algorithm proceeds with the construction of the membership function of the final results. In order to do this, we once again recognize that in each region, the behaviour of each variable is expressed by a linear expression and so, they are solved for each of them and for each critical region optimization problems as (5.29) to (5.32) to identify the widest possible behaviour of that variable in that region. In this case, however, the number of constraints is larger given that we are now considering all the non-redundant inequalities given by (5.20) and (5.21). Finally, the partial membership functions built for each variable in each region are aggregated using the fuzzy union operator.

CHAPTER VI Nodal Marginal Price Computation

6. Nodal marginal price computation

6.1. General aspects

The implementation of market mechanisms in the electricity industry aims at developing procedures to turn electricity closer to a commodity to be traded in open markets. In this context, the access to the transmission network corresponds to a crucial issue since the access must be guaranteed in order to create conditions for the proper development of market mechanisms. As it was mentioned in Chapter 2, the literature on this area already describes several tariff methods to allocate transmission costs to network users, namely, the average, incremental and marginal approaches.

Marginal pricing is broadly recognized as the core approach to the economic evaluation of generation and transmission services. In this context, optimal power flow analysis becomes an adequate tool to identify power system operation points driven by economic criteria. These studies contribute to obtain information about optimal generation strategies at the same time that the computation and the decomposition of nodal marginal prices provide adequate economic signals for transmission and generation investments.

In this context, the next sections detail the algorithms developed in order to build the membership functions of the nodal marginal prices if loads, generation prices or both are affected by uncertainties.

6.2. Model A

As it was previously presented in Chapter 5, the DC-OPF model can be mathematically described by the formulation (5.1) to (5.7). In this context, if it was not considered any estimation of the active branch losses in the OPF formulation, the nodal marginal prices geographical dispersion would only become a consequence of branch congestions that eventually occur in the system. If one wants to include an estimation of the active branch losses, one can select several approaches, namely the models known as Models A or B as described in (Saraiva *et al.*, 2002). In this work we will adopt Model A to include in the usual results of the developed DC-OPF model an estimate of active branch losses.

Addmiting that nodal voltages are at 1.0 pu, the active losses in each branch of the system are given by expression (6.1).

$$losses_{ij} = 2.g_{ij}.\left(1-\cos(\theta_i - \theta_j\right) \qquad (6.1)$$

In this expression,

g_{ij} - represents the conductance of the branch linking nodes *i* and *j;*

θ_i and θ_j - represent the voltage phases in nodes *i* and *j*, respectively.

This expression is directly obtained from the exact expression of the active power losses in a given branch admitting that voltage magnitudes in nodes *i* and *j* are 1.0 p.u.

Following this model the integration of an estimate of the active losses in the linear programming model (5.1) to (5.7) can be implemented as an iterative procedure in which, at the end of each iteration, it is computed the active power losses in each branch of the system using (6.1). Then, half of active losses computed for each branch is added to the active load in the extreme buses of that branch. Since the total load of the system changes regarding the value initially considered, it is necessary to run a new DC-OPF problem to change the generation values. The process finishes if, in two successive iterations, the difference between voltage phases in all nodes gets smaller than a specified value.

In this context, Model A can be synthesized by the algorithm presented in the next paragraphs (Paiva, J. P., 2005). According to our experience and to other published experiences, this algorithm typically converges in three to five iterations.

1. Perform a deterministic DC-OPF study (5.1) to (5.7);
2. Compute the nodal voltage phases according to the DC model;
3. Estimate the active losses in each branch of the system;
4. Add half of the active losses estimated for each branch to the load connected to the corresponding extreme buses;
5. Perform a new deterministic DC-OPF study to establish a new set of generation values;
6. Compute the nodal voltage phases according to the DC model;
7. Finish if the difference between every nodal voltage phases in two successive iterations is smaller than a specified value. Otherwise, return to step 3.

As we know, the nodal marginal price in bus i is defined as the derivate of the objective function, z, regarding a load variation in node i, P_{Li} as expressed in (6.2).

$$\rho_i = \frac{\partial z}{\partial P_{Li}} \tag{6.2}$$

Since this model doesn't include any kind of information related with the reactive power flows, voltage regulation or nodal power injections uncertainties, the computed marginal prices will only correspond to the active energy prices.

Assuming the formulation (5.1) to (5.7) and the algorithm previously presented to include an estimate of the active losses, the marginal price in bus i can be computed using the dual variables of the optimization problem that are obtained when the iterative process previously presented converges.

For a better understanding of the computation of nodal marginal prices and also to establish a general expression to compute them, let us now analyse the impact of a load variation in bus i on the objective function. In order to do this analysis, we will consider each of the constraints (5.2) to (5.7) of the optimization problem (5.1) to (5.7) in a successive way.

6.2.1. Equality constraint

Regarding the equality constraint (5.2), we can immediately conclude that the independent term corresponds to the total active load of the system. Taking into account the marginal price definition (6.2) we must investigate the impact felt by the objective function, z, when the active power connected to bus i experiments a variation. Since varying this load by one unit corresponds to a unit variation of the independent term of this constraint, the effect of this change will be exactly captured by the dual variable, γ, of this constraint. In this sense, γ corresponds to the first term of the expression of the marginal price in bus i as presented in (6.3).

$$\frac{\partial z}{\partial P_{Li}} = \gamma + ... \tag{6.3}$$

We can also observe that this term is independent from the bus under analysis and it coincides with the marginal price in all buses of the system admitting a single bus configuration, this is, if all generators and loads are connected to the some bus or, when there is no binding branch limit constraints and the active losses are neglected. Under these conditions, γ is numerically and conceptually equal to the system lambda, λ, used in several Lagrangian based formulations of the OPF problem.

6.2.2. Generation limit constraints

The independent terms of constraints (5.3) and (5.4) correspond to the minimum and maximum limits of the active power produced in each generator. In these conditions, changing the active load in a given bus i has no impact on the independent term of these constraints, and so, the corresponding dual variables will not be part of the marginal price expression.

6.2.3. Power Not Supplied constraint

Let us now consider that the constraint associated with the Power Not Supplied in bus i (5.5) is binding, that is, the Power Not Supplied value in bus i is equal to its corresponding limit. In these conditions, the constraint is verified in equality terms and so a unit change in the active power connected to bus i will originate a similar modification in the independent term of that constraint. In this context, the dual variable associated with the constraint related with bus i, σ_i, corresponds to another term of the nodal marginal price on bus i according with expression (6.4).

$$\frac{\partial z}{\partial P_{Li}} = \gamma + \sigma_i + ... \tag{6.4}$$

6.2.4. Maximum branch power flow constraints

Let us now consider an operation situation in which the power flow in branch b is on its maximum limit, that is, a situation in which the maximum branch power flow limit constraint is binding because it is satisfied in equality terms. In this situation, constraint (5.6) can be re-written according to (6.5).

$$\sum_{i=1}^{nb} S_{dcbi}(\sum_{k=1}^{ngi} P_{Gik} + PNS_i) = P_b^{máx} + \sum_{i=1}^{nb} S_{dcbi}.P_{Li}^{ctr} \tag{6.5}$$

It is then clear that an increment of one unit in the load of bus i does not cause a unit increment in the independent term of this constraint. In fact, a unit variation of P_{Li}^{ctr} originates a variation of S_{dcbi} in the independent term of (6.5). Therefore, the impact felt by the objective function, z, as a consequence of a unit load variation in bus i is given by the product of S_{dcbi} by the dual variable associated with this constraint, $\eta_b^{máx}$. Accordingly, the expression of the nodal marginal price in bus i includes this new component and so it is given by (6.6). In this new expression, this term corresponds to the summation extended to all branches regarding which the active branch flow is at the maximum limit.

$$\frac{\partial z}{\partial P_{Li}} = \gamma + \sigma_i + \sum_{all\ branches} \eta_b^{máx}.S_{dcbi} + ... \tag{6.6}$$

Finally it should be noted that the sensibility coefficient, S_{dcbi}, corresponds to the symmetric of the derivate of the active power flow in branch b regarding the active load in node i, and so, expression (6.6) can be re-written as (6.7).

$$\frac{\partial z}{\partial P_{Li}} = \gamma + \sigma_i - \sum_{all\ branches} \eta_b^{máx}.\frac{\partial P_b}{\partial P_{Li}} + ... \tag{6.7}$$

6.2.5. Minimum branch power flow constraint

Let us now consider that the active power flow in branch b achieves its minimum limit and so constraint (6.8) is verified in equality terms.

$$\sum_{i=1}^{nb} S_{dcbi}(\sum_{k=1}^{ngi} P_{Gik} + PNS_i) = -P_b^{máx} + \sum_{i=1}^{nb} S_{dcbi}.P_{Li}^{ctr} \tag{6.8}$$

Similarly to what was presented for the maximum power flow constraints, the impact felt by the objective function, z, as a consequence of a unit variation of the load in bus i is given by the product of S_{dcbi} by the corresponding dual variable, $\eta_b^{\min}$. Therefore, the expression of the nodal marginal price in bus i will now include a new term as presented in (6.9).

$$\frac{\partial z}{\partial P_{Li}} = \gamma + \sigma_i - \sum_{all\ branches} \eta_b^{máx} . \frac{\partial P_b}{\partial P_{Li}} - \sum_{all\ branches} \eta_b^{\min} . \frac{\partial P_b}{\partial P_{Li}} + ... \qquad (6.9)$$

6.2.6. Evaluation of the impact of active branch power losses

The last term of the nodal marginal price in bus i aims at evaluating the impact felt by the objective function, z, as a consequence of the active losses change resulting from a marginal variation of the load connected to bus i. This term doesn't translate the absolute value of the active power losses in the system but, simply, the cost of an active power loss change when the load connected to bus i is changed by one unit. In this context, the impact felt by the objective function, z, can be represented by (6.10).

$$\frac{\partial z}{\partial P_{Li}}(losses) = \frac{\partial z}{\partial losses} . \frac{\partial losses}{\partial P_{Li}} \qquad (6.10)$$

In this expression,

losses - represents a function depending on the voltage phases and it corresponds to an estimation of the losses in the whole transmission system.

As we previously mentioned, according to Model A the active losses in each branch are added to the active load in the corresponding extreme buses. This means that active losses are effectively treated as loads, and so, the first term of the second member of (6.10) corresponds to the dual variable, γ, that is, to the dual variable associated with the equality constraint (5.2).

Regarding the second term, the function *losses* corresponds to the summation of the losses in all branches, and so, expression (6.10) leads to (6.11) in which $losses_b$ represents the active power losses in branch b, which is assumed to have buses *m* and *n* as extreme buses. Using the expression of active losses (6.1), we can write (6.12) and taking its derivative regarding the load in bus i, we get expression (6.13).

$$\frac{\partial z}{\partial P_{Li}}(losses) = \gamma . \sum_{all\ branches} \frac{\partial losses_b}{\partial P_{Li}} \qquad \Leftrightarrow \qquad (6.11)$$

$$\Leftrightarrow \quad \frac{\partial z}{\partial P_{Li}}(losses) = \gamma . \sum_{all\ branches} \frac{\partial (2.g_{mn}.[1-\cos(\theta_m - \theta_n)])}{\partial P_{Li}} \qquad \Leftrightarrow \qquad (6.12)$$

$$\Leftrightarrow \quad \frac{\partial z}{\partial P_{Lm}}(losses) = \gamma . \sum_{all\ branches} 2.g_{mn}.\sin(\theta_m - \theta_n).\left[\frac{\partial \theta_m}{\partial P_{Li}} - \frac{\partial \theta_n}{\partial P_{Li}}\right] \qquad (6.13)$$

Since the voltage phases in buses *m* and *nj* regarding the load in bus i can be given, in DC model, by the product of the B inverse matrix (once eliminated one line and one column) by the injected power vector, we can finally write expression (6.14) to compute the

impact on the objective function of a change in the active branch losses due to a change in the load in bus i.

$$\frac{\partial z}{\partial P_{Li}}(losses) = \gamma . \sum_{all\ branches} 2.g_{mn}.\sin(\theta_m - \theta_n).(-Z_{mi} + Z_{ni}) \tag{6.14}$$

In this expression:

Z_{mi} - is the element of line *m*, column *i* of the B inverse matrix;

Z_{ni} - is the element of line *n*, column *i* of the B inverse matrix.

6.2.7. Nodal marginal price expression

According to Model A, aggregating all terms previously referred, the nodal marginal price in bus i is given by (6.15).

$$\frac{\partial Z}{\partial P_{Li}} = \gamma + \sigma_i - \sum_{all\ branches} \eta_b^{máx} . \frac{\partial P_b}{\partial P_{Li}} - \sum_{all\ branches} \eta_b^{\min} . \frac{\partial P_b}{\partial P_{Li}} + \gamma . \frac{\partial losses}{\partial P_{Li}} \tag{6.15}$$

This expression can then be simplified if we attain to the fact that a given branch power flow can not achieve its minimum and its maximum limit capacity simultaneously. In these conditions, the third and forth terms of expression (6.15) can then be replaced by a unique term so that we obtain (6.16).

$$\frac{\partial Z}{\partial P_{Li}} = \gamma + \sigma_i - \sum_{all\ branches} \eta_b . \frac{\partial P_b}{\partial P_{Li}} + \gamma . \frac{\partial losses}{\partial P_{Li}} \tag{6.16}$$

Having established the expression of the active power nodal marginal price according to Model A, it is important to refer that the nodal marginal prices computed in this way depend on the bus selected as slack. This situation derives directly from the fact that the model includes one unique and global balance equation, and also, from the fact that the impact of losses is computed using (6.14) that uses the elements of the B inverse matrix. The inversion of this matrix requires eliminating a row and a column of the B matrix which implicitly means that we are selecting the slack bus. This marginal variation is then valued at price γ that corresponds to the generation cost of the marginal generator. This ultimately means that Model A assumes that variations of active branch losses are being balanced at the slack bus (bus related with the line and the column eliminated from the B matrix) while these changes are being valued at the price of the marginal generator.

Using this model and if one wants to compute nodal marginal prices accurately, it would be necessary to select the slack bus carefully so that it coincides with the bus where the marginal generator is connected to. This condition is not always easy or even possible to guarantee since, for example, there are situations in which the marginal generator changes due to different system operation conditions or, when there is more than one generator performing these functions. However, the experience indicates that if this point

is important from a conceptual point of view it is, in practice, responsible for small changes on nodal marginal prices given the small influence of losses in the values of the nodal marginal prices.

According to Rivier *et al.* (1993) the decomposition of the energy marginal price is of extreme importance for several reasons. In the first place, because even in markets based on marginal prices it occurs, frequently, the separated computation of generation and transmission energy prices. In fact, even in systems where the energy transactions are paid at marginal prices (similar to what happens in Chile), it frequently occurs that only one node, given its importance as central load in the market (which in case of Chile corresponds to Santiago), is chosen as reference for the marginal and transmission tariff prices computation. This suggests that γ can be adopted as the marginal price in that node. There are also systems where the electricity prices are not based on marginal principles existing, however, the need to establish reliable transmission cost computation methods, situation that could, for instance, result from the open market process. Finally, it must be mentioned that in any marginal price computation method all price components must be properly organized and computed so that each user contribution is adequately identified and understood.

When a network is congested and transmission constraints become active, large differences between nodal marginal prices may exist with the creation of "economic islands", that is, sets of nodes with nodal marginal prices that only depend on their local generators and so they are not related to the rest of the system. When these conditions exist, the differences between the average system marginal price and most of the nodal marginal prices, ρ_k, may be large, therefore resulting in large individual contributions and credits of most of the individual market agents to the network entity. Although a large part of these contributions and credits will typically cancel out, the total net revenue from variable charges will be also large under these circumstances (Rivier *et al.*, 1993).

A possible solution to this problem, which does not change the total value of the marginal remuneration given by (2.24) or the total economic signal ρ_k to each participant, but does change the individual contributions to the network and the total net value of the variable network charges, consists of defining local values of γ for the well identified "economic islands", therefore resulting in a redefinition of the marginal price network component without changing the nodal marginal price. Following Rivier *et al.*, (1993) this reduction in the network variables charges should be compensated by the corresponding increment in complementary charges in accordance with the regulatory principles.

The described marginal price methodology also has several disadvantages. In the first place, the marginal price based tariffs could create perverse effects, since that not investment originates the increasing of the company's remuneration as a result of the global increase of system congestion as well as losses. In the second place, the tariffs based on this kind of methodologies don't allow the recovery of all investment costs, namely those performed in a centralized planning era. In the third place, marginal prices

present high spatial and temporal volatility, and so their computation should include the integration of uncertainties, such as (Saraiva, 1999b):

- Load uncertainties especially in a liberalized market environment;
- Generation cost uncertainties;
- Uncertainties related with the equipments availability. The non-ideal characteristic of these equipments, that is, its reliability is usually modeled by probabilistic methods that take into account data, such as, outadge and repair rates.

Additionally, Oren *et al.* (1995) indicates that the application of marginal price tariff based methodologies to meshed networks seems inappropriate, since those structures will not be able to create proper incentives to investment decisions, because:

- The marginal price differences between extreme nodes of any non congested branch could be greater than marginal loss values as a consequence of a congestion occurring in any other system branch;
- In accordance with the optimal dispatch and several network constraints, the energy could flow from nodes with higher prices to nodes with lower prices giving origin to negative transmission prices.

The practical implementation of this kind of methodologies could be time fastidious given the high number of nodes existent in real systems. In this context, alternative methodologies like, for instance, zonal or area prices instead nodal prices (Stoft *et al.*, 1997) were suggested and implemented in several countries and systems as, for instance, in the Nordpool.

6.2.7.1. Revenue Reconciliation problem

Read (1988) shows that the methodology related to short-term marginal prices only allow obtaining a fraction usually not larger than 30% of the regulated costs. In accordance with Shirmohammadi *et al.* (1996) in practice, however, this fraction is between 10 and 30%. This can be explained due to the conditions following which the first author performed this study. In fact, Read (1998) based his analyses in a scenario that includes, simultaneously, optimal expansion conditions and system economies of scale not considering the fact that real systems have, in general, excess capacity due to several reasons.

The revenue reconciliation problem of the wiring companies implies, subsequently, the existence of supplementary tariffs to be solved. In this context, Odériz *et al.* (2000), Saraiva *et al.* (2002) and Rudnick *et al.* (1995), after having analysed different models adopted in the definition of the mentioned supplementary tariff in several power systems all over the world, concluded that there are essentially three different possible approaches to solve this problem:

- Marginal prices adjustments: the marginal prices are modified in accordance with some criterion (an additive or multiplicative term, Ramsay prices, between others) in such a way that they will allow the total remuneration of the network costs;
- Use concept extension: the supplementary fraction is allocated between different users based on the use that they effectively make of the network;
- Allocation by benefit: the supplementary tariff is defined between different users depending on the economical benefit that each of them obtains from the use of the existent network.

In accordance with these authors, the marginal price adjustment methods are not recommendable and were not applied given the enormous difference that normally exists between the remuneration obtained by the marginal approach and the network regulated costs. In accordance with Saraiva *et al.* (2002), the application of this method could modify, distort or even remove the economical signals produced by the nodal marginal prices geographical dispersion and the numerical relation between them. In this context, there are three methods typically adopted in an attempt to solve the revenue reconciliation problem:

- Influence Areas or Marginal Participation Factors;
- Mean Participation Factors;
- Beneficiary or Benefit Factors method.

The first two methods could be interpreted as representing the application of the extension concept and the third as the application of the benefit allocation concept. As main advantages and disadvantages underlined on the application of these referred methods, Odériz *et al.* (2000) concludes that:

- Since the Influence Areas method is based on simple engineering principles, it is easily understood by technical personal. However, this method doesn't create proper economical signals, it is computationally demanding (because it doesn't allow the computation of participation factors for a unique branch without analysing the whole system) and it also doesn't recognize sunk flows which can represent a problem if a line is heavily loaded during most of the year;
- The Mean Participation Factors method is simple to implement and it allows the identification of sunk flows. However, it doesn't present any kind of economical or technical foundation;
- The Beneficiary or Benefit Factors method presents as advantages the fact that it doesn't change the investment efficiency decisions and also the fact that it can allocate costs to each branch individually. However, it is computationally demanding since it requires running simulations for an annual period and, in some specific situations, it could also produce allocation factors of difficult understanding given that a simple branch removal could imply high levels of Power Not Supplied.

Finally, Odériz *et al.* (2000) concludes that the Mean Participation Factors method is conceptually the most adequate one, since it is the method that more largely meets

performance criteria as efficiency (create proper economical signals to system agents avoiding decision making distortions), objectivity (a good method must be based on sounded economical and technical principles) and simplicity (requiring reduced data and being of simple implementation and understanding).

6.2.7.2. Short-term marginal price volatility

The short-term marginal prices are influenced by the power system reliability, by the generation cost uncertainties, by the load level, by the geographic dispersion of loads and generators and by the branch flow limits. Analyzing in a more detailed way these factors we can see that (Saraiva *et al.*, 2002):

- Load level: modifying the system load level could, in some circumstances, originate the need to start some more costly generators, leading to new congestions on the transmission system and to the modification of the active transmission losses. In this context, depending on system conditions in the period that preceded these load variation, there could eventually happen an increase or a reduction of the short-term marginal prices;
- System equipment reliability: the unavailability of several system equipments (generators, lines, transformers, between others) due to forced outages or maintenance reasons, could originate large nodal marginal price variations;
- Generation costs: the modification of the optimal generation strategy due to generation costs variations will always produce short-term marginal prices variations.

The nodal short-time marginal price volatility makes it difficult to predict the marginal remuneration that could be obtained by a given wiring company by its transmission activity (Saraiva *et al.*, 2002). In this sense and given that an adequate system coordination can only be achieved if the economical price signals include information related with uncertainties (Kaye *et al.*, 1989), several works were developed in order to integrate these uncertainties in the marginal prices computation. In this line of research, we must emphasize the works developed by Baughman *et al.*, 1992, Rivier *et al.*, 1994, Saraiva, 1999b, Certo *et al.*, 2001, Leão *et al.*, 2003 and Jesus *et al.*, 2004.

In general, these works treat load uncertainties using probabilistic distribution models (Rivier *et al.*, 1990, Baughman *et al.*, 1992; Certo *et al.*, 2001) or using fuzzy numbers (Saraiva, 1999b; Leão *et al.*, 2003). The adoption of fuzzy representations is justified since, in several situations, the future is not just a repetition of the past (Kaye *et al.*, 1989). However, it is common to all models the consideration of data related with the equipments reliability like, for instance, repair rates and outage rates. This topic and the corresponding models will be more detailed in the next Chapter of this work.

6.3. Consideration of uncertainties in the computation of nodal marginal prices

6.3.1. General aspects

As it was previously mentioned, marginal pricing is broadly recognized as the core approach to the economic evaluation of generation and transmission services. However, marginal price approaches have several drawbacks. In the first place, a marginal price tariff scheme may lead to perverse effects since, for example, more frequent transmission congestion could increase the nodal marginal price dispersion, and so, increase the marginal remuneration or congestion rent. Secondly, pure short term nodal marginal prices do not take into account transmission investment costs and so it would not be possible to recover these costs. This under recovery problem is well known in the literature and it is termed as the Revenue Reconciliation problem. Thirdly, since marginal prices depend on several factors they are typically very volatile. Therefore, their computation should also be able to integrate the following data:

- Uncertainties clearly affect load values especially in market environment. Therefore, load uncertainties and their consequences on nodal marginal prices are certainly a major issue that should be investigated;
- Uncertainties may also affect generation costs. Changes on generation costs will likely change the dispatch policy and thus the marginal prices;
- Marginal prices depend on the system components that are available in instant t. Therefore, the consequence of the non ideal nature of the system components, that is, their reliability on nodal marginal prices computation should be investigated.

In the next sections we will describe the algorithm developed in order to integrate load and/or generation cost uncertainties in nodal marginal price computation considering that these uncertainties are represented by fuzzy numbers, more in particular, by trapezoidal fuzzy numbers. This means that we can use the New Fuzzy Optimal Power Flow algorithm already described in Chapter 5 to treat these uncertainties and to compute, at the end, the corresponding nodal marginal prices.

6.3.2. Consideration of load uncertainties

As described in Chapter 5, the NFOPF problem corresponds to an optimization problem aiming at identifying the best generation strategy according to a generation cost function if, at least, one generation cost and/or load are represented by fuzzy numbers. Following the algorithm presented in Figure 5.3, the NFOPF algorithm adopts the DC approach to model the operation conditions of the network. In the first step, the NFOPF runs a deterministic DC-OPF study for the central values of the fuzzy numbers that represent costs and/or loads. After performing this study and having identified a feasible and optimal solution for it, the uncertainty parameters are integrated in the original optimization problem leading to a multiparametric linear formulation. The presence of these parameters can turn the crisp solution non-feasible or non-optimal in some regions of the uncertainty space and so the algorithm proceeds by identifying regions of the uncertainty space according to the algorithms that were detailed in Chapters 4 and 5.

Once all these critical regions are determined, the algorithm can proceed in one of the four following different directions:

- It can immediately build the membership functions of generations, branch flows and PNS based on the obtained results;
- It can compute an estimate of losses and then build the corresponding membership functions of the results;
- It can compute and build the membership functions of the nodal marginal prices without considering the effect of active losses;
- It can compute and build the membership functions of the nodal marginal prices considering the effect of active losses.

Figure 6.1 presents the algorithm developed for the implementation of these procedures when we are only considering load uncertainties. This algorithm, in fact, corresponds to a more detailed view of the module *building the membership functions* of the algorithm presented on Figure 5.3. The algorithm presented on Figure 6.1 can be described as follows:

i. If the objective is to build the membership functions of generations, branch flows and PNS, the algorithm runs, for each cut level, several minimization/maximization linear optimization problems (5.29 - 5.32) to determine the minimum and maximum values of each variable in each cut level;
ii. If the objective is to integrate the effect of the active branch losses on the results, then the algorithm runs, in the first place and for each cut level, several minimization/maximization linear optimization problems (5.29 - 5.32) to determine the minimum and maximum value of each variable in each cut level and then, for each corresponding combination of loads in each cut level it is run the algorithm presented in Section 6.2 in order to determine an estimate of the active branch losses and the new corresponding values of the output variables, since the new system load will determine changes in the generation values;
iii. If the objective is to compute and build the membership functions of the nodal marginal prices without taking into account the impact of active losses, then the algorithm runs, in the first place, the procedures described in i. and then, for each corresponding critical region identified, it determines the nodal marginal prices using expression (6.16), considering that the term $\gamma.\frac{\partial losses}{\partial P_{Li}}$ is zero;
iv. If the objective is to compute and build the membership functions of the nodal marginal prices considering the impact of the active branch losses, then the algorithm runs, in the first place, the procedures described in ii. and then, for each corresponding critical region identified, it determines the nodal marginal prices using expression (6.16).

In all these four situations, it is obtained in the first place the partial membership functions of all variables comprising, each of them, ordered pairs power/price, membership value. In this context, the final membership function of each variable is then obtained applying the fuzzy union operator to all the partial membership functions obtained.

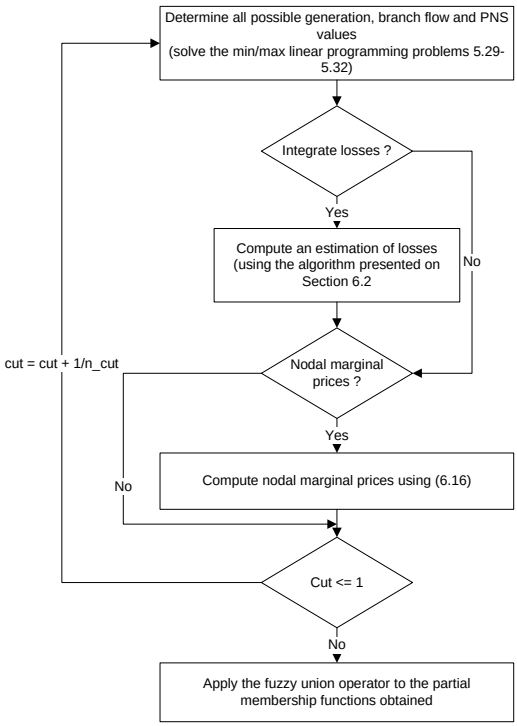

Figure 6.1: Algorithm developed to build the membership functions of all variables when load uncertainties are considered.

It is also important to mention that different kinds of results are obtained depending on the variables under analysis. In fact, we must recall that since we are using a linear model, each variable in each critical region is represented by a linear expression and so generations, active branch flows and PNS are described by linear (at least by segments) membership functions. In a different way, since nodal marginal prices are related with the dual variables of this optimization problem, their corresponding membership functions are described by ordered pairs including price/membership value. These aspects will be analysed in a more detailed way in Chapter 8.

6.3.3. Consideration of generation cost uncertainties

Similarly to what was described in Section 6.3.2, in this case once all critical regions are identified they are built the partial membership functions of generations, branch flows and PNS, although with different assumptions, considerations and results. Figure 6.2 presents the algorithm developed for the implementation of these procedures which, once again, corresponds to a more detailed view of the module *building the membership functions* of the algorithm presented in Figure 5.3 for the case of generation cost uncertainty modelling.

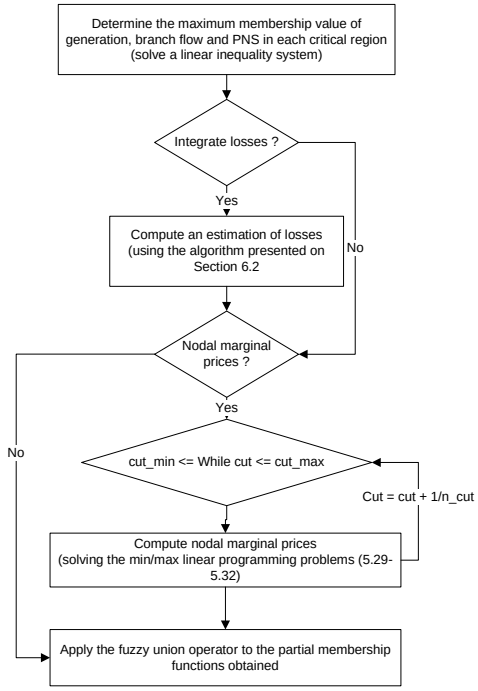

Figure 6.2: Algorithm developed to build the membership functions of all variables when generation cost uncertainties are modelled.

When comparing this algorithm with the one presented in Figure 6.2, we can see that the main difference relies on the fact that, in this case, the value of each primal variable is constant inside each critical region. As a consequence, in this case the four situations described in Section 6.3.2 are now implemented as follows:

i. If the objective is to build the membership function of generations, branch flows and PNS, the algorithm only needs to solve a linear problem including the inequalities that define each critical region in order to determine the maximum membership value of each variable inside each critical region;
ii. If the objective is to integrate the effect of the active losses then the algorithm solves, in the first place, a linear problem that includes the inequalities that define each critical region in order to determine the maximum and minimum values of generation prices in each critical region. Then, based on these results, we compute an estimate of the active system losses in each critical region under analysis;
iii. If the objective is to compute and build the membership function of nodal marginal prices without integrating the impact of active branch losses, the algorithm runs, in the first place, the procedures described in i. Secondly, for each cut level it runs several minimization/maximization linear optimization problems (5.29) to (5.32) to determine the minimum and maximum value of each dual variable in each cut level. Based on these results the algorithm determines the minimum/maximum values of the nodal marginal using (6.16);
iv. If the objective is to compute and build the membership function of nodal marginal prices integrating the impact of active branch losses, then the algorithm runs, in the first place, the procedures described in ii. Then, for each

cut level, it runs several minimization/maximization linear optimization problems (5.29) to (5.32) to determine the minimum and maximum value of each dual variable in each cut level. Based on these results the algorithm determines the minimum/maximum values of the nodal marginal prices using (6.16).

For a given output variable, once all partial membership functions are built, the algorithm uses the fuzzy union operator to aggregate all of them to ensure that its final result displays the widest possible behaviour in the specified uncertainty space.

As we previously mentioned, when considering generation cost uncertainties, the value of each primal variable (generations, branch flows and power not supplied) is constant inside each critical region. This means that their corresponding membership functions are described by ordered pairs of power/membership value. Since the nodal marginal prices are related with the dual variables of the original problem, in this case the membership functions of nodal marginal prices are described by linear (at least by segments) membership functions.

6.3.4. Consideration of load and generation cost uncertainties

As it was previously mentioned, the simultaneous integration of load and generation cost uncertainties into the same problem turns it more complex, since it acquires characteristics of the two previous developed models. This means that critical regions are, in this case, defined by both the optimality and feasibility conditions. As a consequence, both primal and dual variables of the original problem are represented by linear expressions of the parameters that model load and generation cost uncertainties.

Similar to what was described in previous Sections, in this case the algorithm developed for the computation of the membership functions of the output variables presents four distinct possibilities:

i. If the objective is to build the membership functions of generations, branch flows and PNS then, for each cut level the algorithm runs several minimization/maximization linear optimization problems (5.29) to (5.32) in order to determine the minimum and maximum values of each variable in each cut level;
ii. If the objective is to integrate the impact of active branch losses on these results then, in the first place and for each cut level, the algorithm runs several minimization/maximization linear optimization problems (5.29) to (5.32) to determine the minimum and maximum value of each variable in each cut level. Then, for each corresponding critical region and for each cut level, it runs the algorithm presented in Section 6.2 in order to determine an estimate of the active branch losses and the new corresponding values of the output variables;
iii. If the objective is to compute and build the membership function of nodal marginal prices without considering the impact of active branch losses, then for each cut level the algorithm runs several minimization/maximization linear optimization problems (5.29) to (5.32) in order to determine the minimum and

maximum value of each dual variable in each cut level. Then, based on these results it determines the minimum/maximum values of the nodal marginal prices using (6.16);

iv. If the objective is to compute and build the membership function of nodal marginal prices considering the impact of active branch losses then, in the first place, the algorithm runs the procedures described in ii. Afterwards, for each cut level, it runs several minimization/maximization linear optimization problems (5.29) to (5.32) to determine the minimum/maximum values of each dual variable in each cut level. Finally, based on these results, it determines the minimum/maximum values of the nodal marginal prices using (6.16).

The additional complexity presented by this case when compared with the two previous ones, obviously derives from the number of parameters that model load and generation cost uncertainties. The final membership function of each variable is obtained applying the fuzzy union operator to the partial membership functions of each variable obtained in each critical region. Figure 6.3 presents the algorithm developed to implement the above procedures.

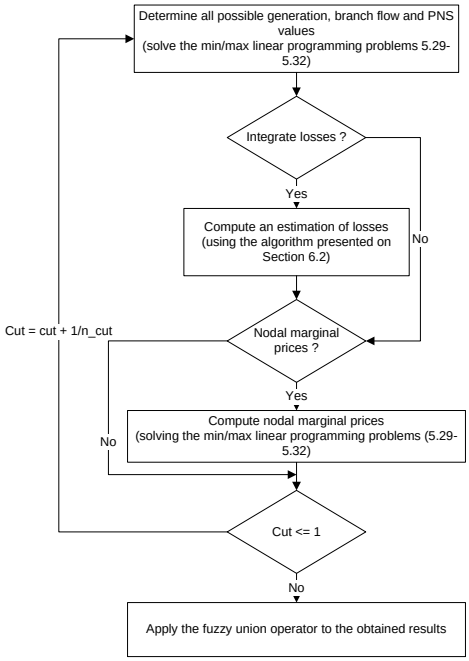

Figure 6.3: Algorithm developed to build the membership functions of all variables when considering, simultaneously, load and generation cost uncertainties.

CHAPTER VII Reliability and Risk Evaluation of Generation / Transmission Systems

7. Reliability and risk evaluation of generation / transmission systems

7.1. General aspects

Generally static reserve and reliability studies of power systems ignore, in a first analysis, the transmission system influence corresponding to what is known as *Hierarchical Level I*. The reliability studies addressing the composite generation/transmission system correspond to the *Hierarchical Level II* that usually include complex and laborious analysis, several of them including a sampling process of states within the entire population of possible residence states of the system under analysis. In this sense, the *Hierarchical Level II* has as limits the main substations connected to the distribution networks, since it comprises the generation and transmission systems.

It must be also mentioned that this stratified arrangement typically excludes the small stations of dispersed nature (like, for instance, wind farms, small hydro stations or cogeneration plants, among others) that, in general, are directly connected to the distribution grids. In recent years, the installed capacity of this type gained an increased importance in such a way that the extension of the reliability studies to the *Hierarchical Level III*, including the generation, transmission and distribution systems turned a clear requirement (Schilling *et al.*, 1995).

Additionally, in this kind of studies it is also common to express the reliability of a given power system in terms of the expected values of the results of the steady state system analysis. These indices could, in turn, be classified in four distinct classes (Pereira *et al.*, 1992a):

- System problem indices;
- System steady state reliability indices, basically, *Loss of Load Probability*, LOLP, *Expected Power Not Suplied*, EPNS, *Loss of Load Frequency*, LOLF, and *Loss of Load Duration*, LOLD*;*
- Point steady state reliability indices per load bus, basically, *Loss of Load Probability*, LOLP, *Expected Power Not Suplied*, EPNS, *Loss of Load Frequency*, LOLF, and *Loss of Load Duration*, LOLD;
- Point sensitivity indices that, even in an indirect way, are able to provide information related with the spatial distribution of the steady-state reliability helping identifying areas which may need reinforcement. In this class, we can include nodal marginal prices, marginal benefit of generation reinforcement for each candidate site for expansion and marginal benefit of transmission reinforcement for each candidate right-of-way.

In this classification they are obviously omitted the reliability indices deduced using customer and load data as, for example, the System Average Interruption Frequency Index (SAIFI) and others, that clearly would conduct us to a more detailed description of this topic that are, however, out of the main focus of this thesis.

7.1.1. Hierarchical Level I

As it was previous mentioned, in the *Hierarchical Level I* it is only considered the generation system. In this context, power systems can be modelled by a single node at which all generators and loads are connected as it is illustrated in Figure 7.1.

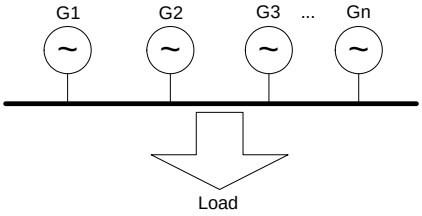

Figure 7.1: Single node model.

In the power system sketched in Figure 7.1 the load diagram typically comprises the peak daily active power values of the demand and generators are represented by two distinct states, called Operation and Failure. It is also admitted that a given generator can go from the Operation state to the Failure state randomly as a result of a non-programmable incident with a failure rate λ (measured in failures by year). On the other hand, the same generator can return from the Failure state back to the Operation state in accordance with its repair rate, μ, which corresponds to the inverse of the Mean Time To Repair (MTTR), r., that is, $\mu = 1/r$. Figure 7.2 illustrates, schematically, this behaviour.

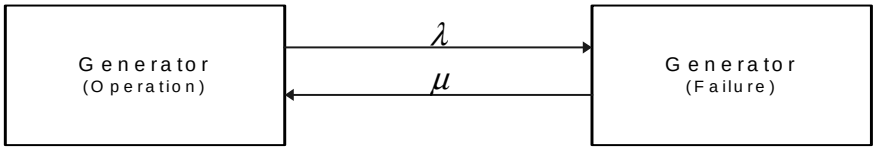

Figure 7.2: Generator state.

In this context, the probability of the Failure and Operation states can be determined by expressions (7.1) and (7.2), respectively.

$$P_F = \frac{\lambda}{\lambda + \mu} \tag{7.1}$$

$$P_O = \frac{\mu}{\lambda + \mu} \tag{7.2}$$

The probability of a given generator being on the Failure state, F, is well known in the literature and it is termed by *Forced Outage Rate*, FOR. It can be estimated using the historical incidents record data during a given company operation period or, as it happens in planning environment, by analogy with existent generators and through the consultancy of the generator manufacturer data.

It should be also observed that, in general, λ is much smaller than μ , and so we can approximate (7.1) by (7.3).

$$F.O.R. = P_F \approx \lambda.r \tag{7.3}$$

Expression (7.3) shows the importance that a good maintenance policy, technical knowledge and human skills of a given company can play in order to reduce the F.O.R value of the equipments, for instance, generators in a given company.

7.1.2. Hierarchical Level II

The interest in the composite reliability studies, that is, in the interaction between generation and transmission systems started in the late of 60's, mostly in Europe (Italy and France) and in North America, however, following different approaches. Europe favored the Monte Carlo approach, whereas analytical methods were favored in North America (Pereira *et al.,* 1992a). Nevertheless, the interest on this kind of studies had only increased during the 80's in North America, mostly due to changes in the business and regulations of the utility industry. In this context, the following areas were identifying as requiring composite reliability studies:

- Transfer capability objectives (determine transfer capability for both internal transmission and interconnection additions);
- Internal transmission reinforcements (compare transmission line alternatives, determine long-term transmission needs, determine the effect of load management on transmission systems, among others);
- Effect of generation sitting (evaluate the reliability impact of different sites for generators);
- Generation and transmission trade-offs (determine trade-off between generation and internal transmission).

As we previously mentioned, in *Hierarchical Level I* the transmission system analysis was ignored or, in other terms, the transmission network was considered 100% reliable, and so it did not impose any kind of limitation in supplying energy from the generators to the demand. Nevertheless, in several cases such a consideration is not acceptable. In fact, the transmission network can affect the reliability of demand supply by three distinct manners:

- The occurrence of branch failures;
- The existence of technical limits imposing limits to the branch power flows.

In this context, several studies show that in numerous real situations the most severe incidents from the Power Not Supply point of view take place when there are simultaneously generator and branch failures, that is, in a situation of a combined contingency in the generation and transmission sub-systems. For this reason, several

researchers and power companies started to adopt the *Hierarchical Level II* as a standard for the development of their planning studies.

As it was previously mentioned, to perform this kind of studies two different types of models were developed as a way to achieve satisfactory results, not only regarding the numerical values, but also regarding the computational efficiency. The second aspect represented an important stimulus factor for the development of new approaches since that, in real situations, the *Hierarchical Level II* analysis represents a large computational effort. Accepting that each component has two possible states (Operation and Failure), in a network having *n* components there are 2^n different possible states to be analyzed. Each of these 2^n possible states should then be analyzed running an Optimal Power Flow study in order to evaluate, for instance, the Power Not Supplied.

The two different types of models previously mentioned were termed as *analytical* and *simulation models*. The first ones try to obtain the combined generation/transmission system reliability indices through mathematical models. The second ones adopt the Monte Carlo simulation method to estimate reliability indices analyzing not the entire population of possible system states, but only a sample of elements in this population. As a consequence of the computational effort associated to the Monte Carlo simulation method, the analytical methods were the preferred ones until the 80's, especially in the U.S.A. and Canada. However, in Europe and Brazil several companies were more devoted to the simulation methods. Given the remarkable increase of the computation capacity and the development of new convergence acceleration techniques, in recent years the Monte Carlo method gained a renewed interest. As in many other areas, nowadays researchers and users in general try to take advantage of the developments made by the two different approaches as an attempt to obtain the best of each of them. In this context, Figure 7.3 presents, schematically, the suitable simulation alternatives regarding the state space size, the system reliability and the modeling complexity.

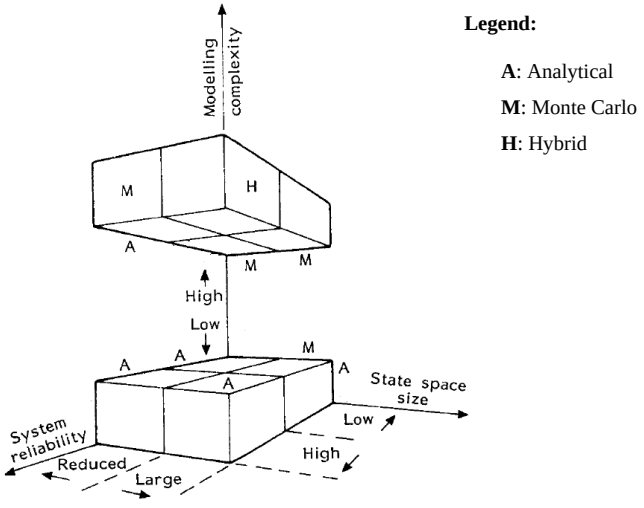

Figure 7.3: Adequate simulation methods (source: Schilling *et al.*, 1995).

As it can be easily understood, the most precise and rigorous model corresponds to the one that uses the AC approach to model the system operation conditions, since it

incorporates the active and reactive branch power flows and nodal voltages. This kind of formulation, however, is more complex and computational intense, namely if such model has to be solved some thousand times in the scope of a Monte Carlo analysis. As a consequence, in a planning environment largely dominated by uncertainties running AC models, for instance, power flow or OPF AC models, is seen as unnecessary. This means that it is very typical to adopt simplified DC approaches to model the operation conditions of the power system for planning purposes.

7.2. Failure modes

Following Schilling *et al.* (1995), the causes of power system failure modes may be broadly classified in three categories:

- Environmental causes, which correspond to those usually caused by climatic or atmospheric conditions (unavailability of the required minimum level of water in a given reservoir, lack of wind, presence of pollution, among others);
- Socieconomical causes, which correspond to those that stem from direct human interference, as for example, lack of fuel, social turmoil, human errors, among others;
- Systemic causes, which correspond to those directly related to the electrical system and/or equipment, such as equipment malfunction, equipment outages or unexpected operation points. It must be noted that failures caused by load behaviour may be classified by systemic, however, they are primarily associated with environmental or social factors.

Regarding the failure mode consequences, they are usually classified as:

- Primary level or **integrity**, in which only continuity of supply is taken into account, regardless of any consideration with respect to the degree of quality with which the load is supplied, as for example, partial load interruption, loss of interconnections, among others;
- Secondary level or **adequacy**, in which the main concern is the supply quality, as, for instance, overloads, undervoltages, overvoltages, occurrence of uneconomical operational conditions, among others;
- Tertiary level or **security** in which the dynamic behaviour of the system is the main concern. In this context, a failure may be defined when the system operational point is such that loss of synchronism may occur or when the system enters in a region where the voltage may suddenly collapse. In this context, the security indices give a measure of the system stability level.

Given these definitions we could then describe a failure mode state space as depicted in Figure 7.4. In this Figure, State 1 represents the normal state when the system is intact, adequate and secure. State 2 referred to as inadequate, depicts the situation where some level of inadequacy occurs, but the system as a whole is still intact and dynamically secure. State 3, termed as insecure, represent a situation where the system, although still intact and adequate, is insecure from the dynamic point of view. State 4 corresponds to an emergency situation where the system is both inadequate and insecure, but all loads are

still being completely served. States 5 to 8 represent situations where system complete integrity is lost, but parts of the system may be still operating under adequate and/or secure conditions.

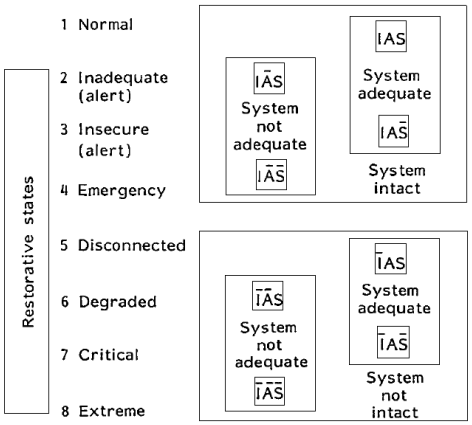

Figure 7.4: Failure modes state space (source: Schilling *et al.*, 1995).

It must be also emphasized that reliability indices would become meaningless if the time frames associated with their evaluation and application are not precisely defined. In this context, Figure 7.5 gives a schematic picture of reliability time frames for potential application in pre-operational horizons such as short-term operations, operational planning and expansion planning.

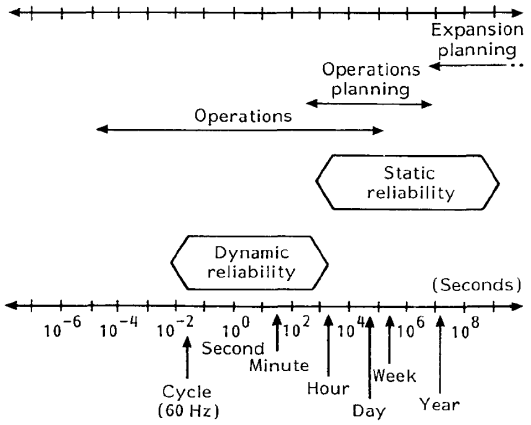

Figure 7.5: Reliability time frames (source: Schilling *et al.*, 1995).

7.3. Monte Carlo simulation method

7.3.1. General aspects

The Monte Carlo method allows evaluating reliability indices of a power system constituted by a given number of components. The method simulates an experience during a previously fixed period of time. During the experience, the method tries to simulate situations close to reality. At the end of the process, the obtained results allow the estimation of system reliability by adequate statistical treatment (Sousa, 1997). The method presents several advantages, namely:

- It allows the use of any probability distribution;
- It is easy to include any relation of dependency between events;
- It can be easily adjusted to system changes.

However, it also presents several disadvantages, namely:

- It requires a large number of experiments to obtain meaningful results;
- If the analysis of each ample state is complex and time-consuming, the method will require a large computational effort.

In general, we can say that the Monte Carlo method comprises the following stages:

- Sampling the states to analyze;
- Analysis of each sampled state by a function related with the variable to be estimated;
- Along with the analysis of the sampled states, update the estimate of the variables under analysis;
- Perform a convergence test in order to check if the current estimate has the required quality.

As we mentioned above, the Monte Carlo method is a very flexible tool that allows the representation of several operation aspects of a power system not always easily captured by analytical models. However, running a Monte Carlo simulation can be computational heavy. On the other hand, although sometimes insufficient to model the system operation conditions, analytical models can contribute to speed up the convergence of the Monte Carlo simulation. This leads to hybrid approaches in the sense that the incorporation of analytical techniques in the Monte Carlo simulation can increase the efficiency of the simulation process.

7.3.2. Method description

As we previous mentioned, Monte Carlo simulation is often used when complex operation conditions are involved and/or the number of severe events is relative large, reason by which it is commonly used in the bulk electric power system reliability evaluation. There are three basic Monte Carlo approaches, designated as the sequential, nonsequential (Billinton *et al.,* 2005) and pseudo-sequential simulation techniques (Mello *et al.,* 1994). This latest approach is in fact an hybrid method in the sense that it uses a nonsequential simulation to select failure states and a sequential simulation only in the neighbor of the selected failure states in order to define previous and posterior sequences regarding that failure state.

In the nonsequential approach the states of all components are sampled and a nonchronological system state sequence is determined. In the sequential approach, the operation and failure cycles of all components are simulated and the system operating cycle is determined by combining all the component cycles. In this context, the sequential simulation technique provides an opportunity to incorporate chronological factors and, as a consequence, it allows a more accurate computation of reliability frequency related indices but, instead, requires a larger computation time effort.

The Monte Carlo simulation method starts by sampling a power system state. In the nonsequential version, each component can be in one of two possible states, Operation or Failure. Each state is characterized by a vector $X = [x_1, x_2, ..., x_m]$, whose elements, x_i, represent the residence state of each system component i. Considering that failures correspond to random and independent events, the probability of occurrence of a system state x is given by (7.4).

$$p(x) = [\prod_{i=1}^{n1} (1.0 - p_i(F))].[\prod_{i=n_1+1}^{n} (p_i(F))] \tag{7.4}$$

In this expression it was considered that the n_1 first components are in the Operation state and that the remainder ones are in the Failure state. $p_i(F)$ represents the failure probability of the component i. In the universe X of system states there are states in which some system components are unavailable and so it is important to study the system performance in face of such unavailability through the statistical evaluation of the expected value of a system analysis function or test function, $F(x)$. For example, $F(x)$ can measure the system operation cost or the Power Not Supplied. The probabilistic analysis of a power system could then be viewed as the computation of the expected value of the function $F(x)$, that is the computation of (7.5).

$$E(F) = \sum_{x \in X} F(x).p(x) \tag{7.5}$$

In this expression:

$E(F)$ - is the expected value of F;
x - is one residence state of the system under analysis;
X - is the set of all residence states of the system under analysis;
$p(x)$ - is the probability of the residence state x given by (7.4).

As a consequence of the large number of possible residence system states, expression (7.5) is typically inadequate for realistic sized systems. In this sense, the Monte Carlo simulation method estimates the expected value of F, $E(F)$, considering only a sample of N states in X considering the individual probability of failure of each component. In this context, $\hat{E}(F)$ is estimated by (7.6).

$$\hat{E}(F) = \frac{1}{N}\sum_{i=1}^{N} F(x_i) \tag{7.6}$$

In this expression:

$\hat{E}(F)$ - is the expected value of F obtained from a sample of X with dimension N;
x_i - represents the state i of the system.

In fact the value obtained from expression (7.6) will not exactly correspond to the value of $E(F)$ as given by (7.5). As a consequence, it is important to compute the sample size that guaranties an estimation error not larger than a pre-specified value. In this context, let $\hat{V}(F)$ and $\hat{V}(\hat{E}(F))$ be the variance of F and the variance of the expected values of F obtained with different samples extracted from X, respectively. It this sense, we can define the relative uncertainty or variation coefficient of the estimation of $\hat{E}(F)$ as the value β defined by (7.7).

$$\beta^2 = \frac{\hat{V}(\hat{E}(F))}{N.\hat{E}(F)^2} \tag{7.7}$$

Since $\hat{V}(\hat{E}(F))$ is given by (7.8), and $\hat{V}(F)$ is given by (7.9), we can estimate the required size of the sample, N, to ensure a specified level of β using expression (7.10).

$$\hat{V}(\hat{E}(F)) = \frac{\hat{V}(F)}{N} \tag{7.8}$$

$$\hat{V}(F) = \frac{1}{N-1}\sum_{i=1}^{N}(F(x_i) - \hat{E}(F))^2 \tag{7.9}$$

$$N = \frac{V(F)}{(\beta.\hat{E}(F))^2} \tag{7.10}$$

This expression is important, since it allows to estimate the sample size as a function of the maximum value allowed for β. Given the Monte Carlo method disadvantages previously mentioned, one of the challenges consists, precisely, of reducing the sample dimension (and so the computational effort) for the same level of uncertainty, which is usually adopting techniques to reduce the value of the variance, $\hat{V}(F)$.

In this domain, three techniques are commonly used and described in literature (Oliveira *et al.*, 1989; Pereira *et al.*, 1992a): the antithetic sampling approach, the control variable technique and the importance sampling method. All of them aim at speeding up the convergence of the Monte Carlo method, and so, reducing its computational effort. In the following sections we will describe in a more detailed way the control variable technique, since it corresponds to the one that was implemented in the developed approach.

In an attempt to clarify the main steps of the nonsequential Monte Carlo simulation approach, in the next paragraphs it is presented its corresponding algorithm (Billinton *et al.*, 2005).

1. A system state issampled. This is simply done by sampling a value ε using a pseudorandom generator and comparing it with the equipment failure rate, λ. If $\varepsilon \geq \lambda$, the equipment is in operation, otherwise, it is failure state. However, because λ is usually small, the large majority of samplings indicates that the equipment is operating.
2. If the system is in a normal state, then there is no load curtailment. Go back to step 1. for the next sampling. If the sampled state is a contingency state, load curtailment may be required. In this case, a power flow analysis or an optimal power flow analysis is conducted;
3. If constraints occur such as line overload, corrective actions, that is, generation rescheduling or load curtailment may be needed to alleviate the constraints;
4. Reliability indexes are calculated and updated. Steps 1 to 3 are repeated until the relative uncertainty coefficient is smaller than a specified tolerance.

As it was previously mentioned the sequential or state duration approach is based on sampling the probability distributions of the component state durations, and so, chronological load models can also be easily incorporated as an attempt to model all contingencies and operating characteristics inherent to the system. In this context, in next paragraphs it is presented the corresponding algorithm (Billinton *et al.*, 2005).

1. Specify the initial state of each component. Usually, it is assumed that all components are in the normal state (operating state);
2. Simulate the duration of each state component residing in its present state and the distribution functions of the component failure and repair rates. For example, given an exponential distribution function, that

is, $f(t) = \lambda.e^{-\lambda.t}$, then the sampled value of the state duration for component i, Ti, is given by $T_i = -\ln(U_i)/\lambda_i$, where U_i is a uniformly distributed random number in $[0,1]$ corresponding to the ith component. λ_i is a failure rate or repair rate depending on the current state of the ith component;

3. Repeat step 2 in a given time span, normally a year (8760 h). A chronological up and down sequence of states for each component is then constructed in a given time span. Chronological hourly load models (if available) can be incorporated to calculate annual indexes. Annualised indexes can be calculated using a constant load, usually at the peak level;
4. The simulated operation is assessed for each hour during a given time span. If constraints occur, corrective actions may be required to alleviate the constraints and the load may be curtailed if necessary;
5. At the end of each simulated year, the reliability indices are calculated and updated. Steps 2. to 4. are repeated until the relative uncertainty coefficient is smaller than a specified tolerance .

7.3.3. Control variable method

Let $F(x)$ be the function we want to estimate. $Z(x)$ is a function that approximates $F(x)$ and that has an expected value $E(Z)$ that is possible to compute by an external analytical process. Let $\xi(x)$ be the difference between $F(x)$ and $Z(x)$ and let $F^*(x)$ be a new estimator given by the addition of $\xi(x)$ and $Z(x)$. Given these indications, we can write the following relations.

$$\xi(x) = F(x) - Z(x) \tag{7.11}$$

$$F^*(x) = \xi(x) + E(Z) = F(X) - Z(x) + E(Z) \tag{7.12}$$

The mean values of $F(x)$ and $F^*(x)$ are equal, but the variance of $F^*(x)$ is equal to the variance of $\xi(x)$ because the variance of $E(Z)$ is zero, since $E(Z)$ is a constant.

If the correlation between $Z(x)$ and $F(x)$ is positive and high, that is, if $Z(x)$ represents a good approximation of $F(x)$, then the variance of $\xi(x)$, $V(\xi)$ will be small. In this context, the variance of $F^*(x)$ will be smaller than the variance of $F(x)$.

This technique implies the analytical computation of the value of $Z(x)$ for each sampled state of the system and its corresponding expected value. The expression to use to compute the expected value of $F(x)$ would then be given by:

$$\hat{E}(F) = E(Z) + \frac{1}{N}.\sum_{i=1}^{N}(F(x_i) - Z(x_i)) \tag{7.13}$$

Following Oliveira *et al.* (1989) the choice of the regression function z(x) to apply to a given system should be oriented by the correlation. Typically, pure generation or transmission variables are used as regression functions. However, there are situations in which more complex regression functions are more effective than the simple ones previously mentioned, which in fact suggests that this selection should be guided by the planner's experience and prior numerical simulations (Pereira *et al.*, 1992b).

7.3.3.1. Power Not Supplied function as F(x)

Let us considerer that part of the Power Not Supplied is, in each analysed state, mainly due to contingencies on the generation sub-system. In these cases, it would be possible to use the Power Not Supplied only due to the generation sub-system, PNS_g, as an approximate function of the power in fact not supplied by the composite generation/transmission system. In this context, the methodology to estimate the expected value of the Power Not Supplied of the composite generation/transmission system is described as follows:

i. Compute $E(PNS_g)$ using an analytical method independent and external to the Monte Carlo simulation;
ii. Obtain a state of the generation system using the FOR of each generator;
iii. Compute the Power Not Supplied of the generation system, PNS_g, as described by (7.14):

$$PNS_g^i = \max\left\{0, D - \sum_{j=1}^{ng} P_{\max_j}\right\} \tag{7.14}$$

In this expression D is the system load and $P_{\max_j}$ is the capacity of the jth generator in operation in the ith state;

iv. Obtain a state of the transmission system using the FOR of each transmission component. Compute the Power Not Supplied of the ith state, PNS^i, using this state together with the generation state obtained in ii. The value obtained for PNS will be due to contingencies in both the generation and transmission systems;
v. Compute the residue, that is, the difference between PNS^i and PNS_g^i as described by (7.15);

$$\xi^i = PNS^i - PNS_g^i \tag{7.15}$$

vi. Repeat steps ii. to v. N times and compute $E(PNS)$ using (7.16):

$$E(PNS) = E(PNS_g) + \frac{1}{N}.\sum_{i=1}^{N} \xi^i \tag{7.16}$$

vii. Evaluate the convergence of the simulation computing the relative uncertainty coefficient and comparing it with the corresponding maximum specified value. If convergence was not yet reached go back to step ii.

In this context, it is also important to mention that, in general, PNS_g is strongly correlated with PNS, since the FOR of branches is typically much smaller than the FOR of generators. This fact strengthens the idea of choosing PNS_g to approximate PNS since that $V(\xi)$ will be smaller, and so, the number of states to analyze would be also smaller than it would be necessary to analyze if we did not use this approximate function. Figure 7.6 describes the Monte Carlo algorithm when it is considered this control variable convergence speed up technique.

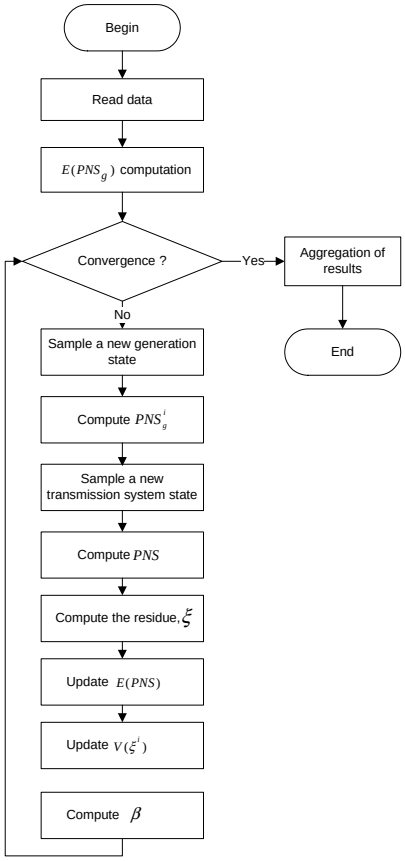

Figure 7.6: Monte Carlo algorithm when it is implemented the control variable speed up technique.

7.3.3.2. Nodal marginal price approximation function

As we know the regression function technique or control variable technique requires the use of an external evaluation function that constitutes a good approximation of the function to analyze (Oliveira *et al.*, 1989). In the previous section we saw that when computing the Power Not Supply expected value this function corresponds to the Power Not Supply due only to the generation sub-system. Now we will also see that in the case of the nodal marginal price expected value computation it can also be used the generation sub-system, that is, the nodal marginal price due only to this sub-system, ρ_k^{Gen}, as an approximate function. In this scope, the nodal marginal price in each bus of the system,

for instance k, due only to the generation sub-system in each analysed state i, $\rho_{k,i}^{Gen}$, can be determined by a deterministic dispatch study. In this sense, $\rho_{k,i}^{Gen}$ will correspond to the generation cost of the marginal generator or to the PNS cost if the system is unable to accommodate the system load. In this context, it is important to note that $\rho_{k,i}^{Gen}$ is the same for all system buses and it represents an approximation of $\rho_{k,i}$. Once again, if this approximation is of good quality, the residuals will be smal and the variance of the sample will also be reduced. Using this approximation, the estimation of the expected value of the nodal marginal price in node k can be determined by (7.17).

$$E(\rho_k) = E(\rho_k^{Gen}) + \frac{1}{N}.\sum_{i=1}^{N}(\rho_{k,i} - \rho_{k,i}^{Gen}) \tag{7.17}$$

As we can see, the use of expression (7.17) requires the knowledge of $E(\rho_k^{Gen})$, that is, the expected value of the regression function. This can be done by means of analytical techniques external to the Monte Carlo simulation.

The exact expression to evaluate the expected value of the nodal marginal price due to the generation sub-system, $E(\rho_k^{Gen})$, is given by (7.18).

$$E(\rho_k^{Gen}) = \sum_{i=1}^{N} \rho_{ki}^{Gen}.p(x_i) \tag{7.18}$$

In this expression,

$E(\rho_k^{Gen})$ - is the expected value of the nodal marginal price due to the generation sub-system;

ρ_{ki}^{Gen} - is the nodal marginal prices on bus *k* in state *i* when it is only considered the generation sub-system;

$p(x_i)$ - is the probability of the state *i* under analysis.

This expression is not easy to apply, since it requires the enumeration of all possible combinations of the generators in the Operation and Failure states. In practice, however, it would be sufficient to consider a smaller set of states including the following ones:

- The state in which all system components are in operation;
- The state in which at least N_G generators are in the Failure state (N_G should be specified by the user). In general, it is not necessary to use a large value for N_G because if a very large number of generators are unavailable in a given state, the probability $p(x_i)$ of that state will be very small and the nodal marginal price will tend to the PNS cost. This means that as the number N_G increases the product $\rho_{ki}^{Gen}.p(x_i)$ will not increase and for large N_G values it will even

decrease. In this sense, the impact of the terms associated with very large N_G values will be less and less reduced, which means that they could be ignored without compromising the accuracy of the expected values to compute.

Similarly to what was presented for the PNS approximation function, in this situation the convergence can also be evaluated by means of the uncertainty coefficient β computed for each node as described by (7.19).

$$\beta_k^2 = \frac{V(\rho_k)}{N.[E(\rho_k)]^2} \tag{7.19}$$

In this sense, β is computed using the variance of the nodal marginal price in node k, $V(\rho_k)$, of each sampled state, the current value of its expected value, $E(\rho_k)$, and also the number of sampled states, N. The simulation ends when the computed value of β for all buses is smaller than the maximum pre-specified value.

7.4. Fuzzy Monte Carlo algorithm

7.4.1. General aspects

As we know one of the objectives of a power system planning problem is to determine the sequence of equipment additions required for an economic and reliable supply of the predicted system demand. These objectives are conflicting since a higher reliability level requires system reinforcements, which could, in turn, result in higher customer rates. The responsibility of the system planner is then to achieve the best possible trade-off between cost and reliability, recognizing the uncertainties with respect to load fluctuations, generation costs and equipment availability (Pereira *et al.*, 1992a). In this context, several methods have been developed in order to integrate load uncertainties in the traditional composite reliability studies. These methods can then be classified as deterministic, probabilistic, hybrid (loads are modeled by fuzzy numbers and reliability data is modeled by probabilistic distributions) or fuzzy (given the uncertainties present in some reliability data, such as in failure and repair rates several authors (Verma *et al.*, 2002) presented a fuzzy reliability evaluation model).

In the deterministic approaches the performance of a candidate system design is evaluated for several different scenarios, representing different operation conditions. A system will be acceptable if it is able to supply the load under all scenarios. In this case, the planner will select the most economic plan among those candidates found to be acceptable under deterministic criteria. This kind of approach is straightforward to implement and easy to understand, however it has several limitations. One of then is related with it incapacity to determine safety margins of a given plan and the other one is related with the fact that they typically lead to uneconomic plans (usually overdesign) as a consequence of the underperformance of the approach under the scenarios evaluation (Pereira *et al.*, 1992b).

In the probabilistic and hybrid approaches the stochastic aspects of the problem are explicitly represented. The main difference between them relies on the way by which load uncertainties are represented. In probabilistic approaches both equipment availability and load uncertainties are represented by probabilistic distribution functions (Allan, *et al.*, 2000). In the hybrid approaches, as it is the case of the Fuzzy Monte Carlo algorithm (Saraiva *et al.*, 1996b) equipment availability is considered using random variables and, consequently, represented by probabilistic distribution functions, and load uncertainties are represented by fuzzy numbers.

These methods and techniques assume in fact extreme importance since, as indicated by Allan *et al.* (2000), the system organization and the operational environment in which it operates changed and continues to change motivated by evolutionary or even revolutionary processes as it is the case of the unbundling, re-regulation, privatization and restructuring processes, the economic and environmental constraints and the increased amount of renewable energy generation and new players on the energy supply industry. All these new aspects impose, in fact, new paradigms. Firstly, power systems are now characterized by a number of independent generators competing with each other and there is a need to retain confidentiality about their investments and operating decisions. Secondly, since small-scale generation embedded or distributed within distribution systems is now playing a significantly developing role, bulk supply points will change and so will the power flows in the transmission networks. Additionally, Billinton *et al.* (1997) mentioned that this kind of approaches will in fact play an important role in the future planning and operation of power systems since, for example, it is expected that, in the future, operating points would be judged as acceptable depending on the level of risk and the economic benefits associated with them and not simply based on operating reliability criteria. Following this author, in the near future the question of balancing security and profit should be approached in such a manner that conforms quite naturally to the new competitive structure by providing economic incentives to induce participants (both suppliers and demanders) to include in their decision making the effects of those decisions on system security levels, which could be, for example, achieved by including a security-related component in the price of the transmission service.

Recognizing that reliability and economics must be treated together in order to perform objective cost-benefit studies and that probably the reliability worth will be driven by markets, in next sections of this work it will be presented an upgraded version of the Fuzzy Monte Carlo algorithm that admits that both loads and/or generation costs are represented by fuzzy numbers.

The Fuzzy Monte Carlo algorithm was originally developed by Saraiva *et al.* (1996b) and corresponds to an hybrid reliability evaluation method where the states to analyze are obtained by a random process based on the Forced Outage Rate of the system components. The main difference of this approach when compared with the one described in 7.3 is that, in this case, in each sampled state it is performed a Fuzzy Optimal Power Flow algorithm or, as it is the case of this work, a New Fuzzy Optimal Power Flow algorithm, since we admit that both loads and/or generation costs are represented by fuzzy numbers. In this sense, the Fuzzy Monte Carlo algorithm can be interpreted as an

extension of the classical Monte Carlo algorithm previously described in previous Sections.

7.4.2. Convergence analysis

As described in section 7.3.2, the Fuzzy Monte Carlo algorithm also uses expression (7.7) to monitor the convergence of the simulation. However, in this case that expression should be rearranged in order to accommodate the fuzzy nature of the functions under analysis as described in (7.20).

$$\beta^2 = \frac{V(\hat{E}(\tilde{F}^{ctr}))}{N.[\hat{E}(\tilde{F}^{ctr})]^2} \tag{7.20}$$

In this expression $\hat{E}(\tilde{F}^{ctr})$ represents the central value of the current estimate of the expected value of $\tilde{F}$, which is computed considering the central values of $\tilde{F}$ obtained for each state using the NFOPF algorithm. The simulation ends whenever the current value computed for β becomes smaller than a pre-specified value.

7.4.2.1. Convergence speed up method: regression function technique

As we also saw in section 7.3.3, this technique uses a regression function to obtain an approximation of the expected value of the function *F* to analyze. However, in case of the Fuzzy Monte Carlo algorithm two situations should be considered as a way to apply this technique:

- The choice of the regression function;
- The fuzzification of the regression function in order to incorporate the information related with the fuzzy loads and/or generation costs.

Taking the cases of the Power Not Supplied and of the nodal marginal prices due to the generation sub-system once again as approximate functions, we can then state that if loads and/or generation costs are represented by fuzzy numbers, than $E(\tilde{PNS})$ and $E(\tilde{\rho}_k)$ should be given by (7.21) and (7.22), respectively:

$$E(\tilde{PNS}) = E(\tilde{PNS}_g) \oplus \frac{1}{N}.\sum_{i=1}^{N}\left[\tilde{PNS}_i \ominus \tilde{PNS}_{g_i}\right] \tag{7.21}$$

$$E(\tilde{\rho}_k) = E(\tilde{\rho}_{kg}) \oplus \frac{1}{N}.\sum_{i=1}^{N}\left[\tilde{\rho}_{ki} \Theta \tilde{\rho}_{kg_i}\right] \tag{7.22}$$

In these expressions,

- $E(\tilde{PNS})$ - is the expected value of the PNS membership function;
- $E(\tilde{PNS}_g)$ - is the expected value of the PNS membership function due only to the generation sub-system;
- $\tilde{PNS}_i$ - is the fuzzy number that represents the PNS in state *i*;
- $\tilde{PNS}_{g_i}$ - is the fuzzy number that represents the PNS in state *i* due only to the generation sub-system;
- $E(\tilde{\rho}_k)$ - is the expected value of the nodal marginal price function on bus *k*;
- $\tilde{\rho}_{ki}$ - is the fuzzy number that represents the nodal marginal price on bus *k* in state *i*;
- $\tilde{\rho}_{kg_i}$ - is the fuzzy number that represents the nodal marginal price on bus *k* in state *i* due only to the generation sub-system.

In these expressions $\oplus$ represents the addition of two fuzzy numbers and Θ represents the deconvolution operation. In accordance with what was previously mentioned, $\tilde{PNS}_i$ and $\tilde{\rho}_{ki}$ are obtained from the NFOPF algorithm and $\tilde{PNS}_{g_i}$ is obtained considering only generator outages as described in (7.23).

$$\tilde{PNS}_{g_i} = f(\tilde{P}_1 \Theta P_g^{máx} \oplus P_{g_i}^{out}) \tag{7.23}$$

In this expression:

- $\tilde{P}_1$ is the fuzzy number that describes the total active load of the system;
- $P_g^{máx}$ is the system generation installed capacity;
- $P_{g_i}^{out}$ is the total generation capacity out of service in the ith state;
- f is the fuzzy function that cancels the membership function for negative values of its argument.

Regarding $\tilde{\rho}_{kg_i}$, nodal marginal prices are determined taking into account what was described in section 7.3.3.2 considering, in this case, that loads and/or generation costs are represented by fuzzy numbers, and so, in each analyzed state it should be performed a NFOPF algorithm.

7.4.3. Risk indices

Apart from computing reliability indices, when considering load uncertainties, for instance, one can also be interested in evaluating the capacity that the system has in accommodating the specified load or, in other way, in characterizing the risk of not being able to meet the demand. This leads to the computation of risk indices, namely, the exposure and the robustness indices, $I_{\exp}$ and I_{rob}, respectively. The first one is defined as the lowest level of uncertainty at which the system is still able to accommodate the load without performing any kind of load shedding. The second one is defined as the difference to one of the exposure index and it gives information related with the level of uncertainty above which the system can operate without having Power Not Supplied. In this context, when it is analysed the system behaviour considering load and/or generation cost uncertainties the same kind of knowledge could be applied to determine these risk indices given the specified load and/or generation cost uncertainties together with the non-ideal nature of the system components. As expected, in these cases the problem becomes more complex meaning that:

- For α cut levels larger than $I_{\exp}$ the system will still be able to accommodate the specified load uncertainty without violating any kind of branch and/or generation capacity limits. In this sense, for these uncertainty levels, independently of the load and/or generation cost combinations we could conclude that the PNS value would be always zero;
- For α cut levels smaller than $I_{\exp}$ the system will lose its ability to completely accommodate all load and/or generation cost uncertainties, and so, for these values there are combinations of loads and/or generation costs that will originate non-zero values for PNS.

Taking into account what was previously mentioned together with the situation presented in Figure 7.7, we could conclude that in the case represented on this Figure the exposure index is equal to α and that the robustness index is equal to $1-\alpha$.

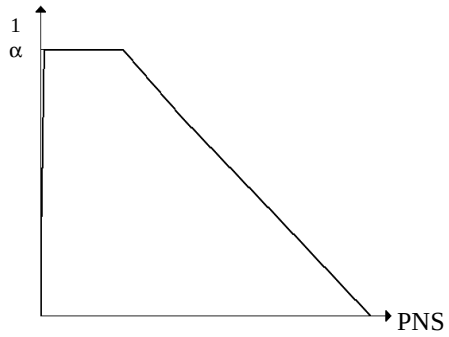

Figure 7.7: Exposure index.

For each analysed state, the NFOPF algorithm gives the values of the exposure and robustness indices and the membership function of the Power Not Supplied and of the

nodal marginal prices. In this context, once N states are sampled and analysed, the expected values of these variables can be computed using (7.24), (7.25) and (7.21), (7.22), respectively.

$$E(I_{rob}) = \frac{1}{N} . \sum_{i=1}^{N} I_{rob\,i} \tag{7.24}$$

$$E(I_{\exp}) = \frac{1}{N} . \sum_{i=1}^{N} I_{\exp_i} \tag{7.25}$$

In these expressions $I_{rob\,i}$ and $I_{\exp_i}$ represent the robustness and exposure indices, respectively.

Regarding the membership function of the Power Not Supplied it is also important to refer that, when the deterministic solution of the OPF problem or the NFOPF solution leads to load shedding, the solution could eventually, not be unique (Braga, 2004b). In fact, there may exist several solutions that minimize the Power Not Supplied, and so, the individual Power Not Supplied values in each load bus of the system lose relevance and, consequently, turn the global system Power Not Supplied more relevant. As we previously mentioned, these partial results are aggregated using the fuzzy union operator. However, in this particular case, this aggregation must be conducted carefully as an attempt to not artificially enlarge the final membership function. As an attempt to illustrate this situation, in Figures 7.9 and 7.10 we represent the aggregated membership functions as a result of different procedures of aggregation of the individual Power Not Supplied membership functions presented in Figure 7.8.

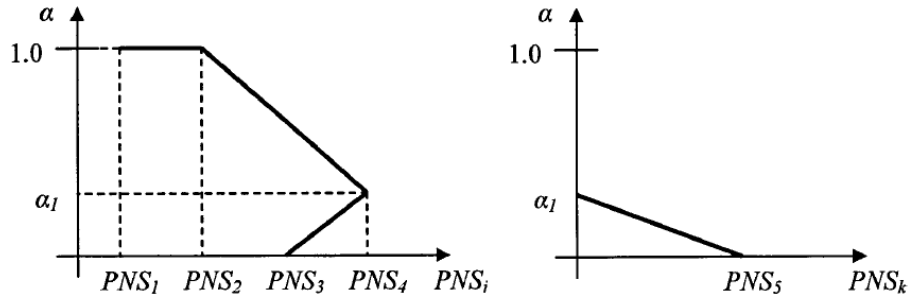

Figure 7.8: Membership functions of the power not supplied on buses *i* and *k* (source: Braga, 2004b).

Figure 7.10 shows a situation in which, for membership values smaller than α_1, the Power Not Supplied minimization strategy leads to a situation where the Power Not Supplied in bus i decreases and in bus *k* increases.

In Figures 7.9 and 7.10 we can see two possible Power Not Supplied aggregated membership functions. In case of Figure 7.9 the aggregation was applied after the application of the Maximum operator at each partial membership function. As a result the

aggregated membership function corresponds to an artificial enlargement of the expected membership function, since that the combination of PNS_4 and PNS_5 never occurs.

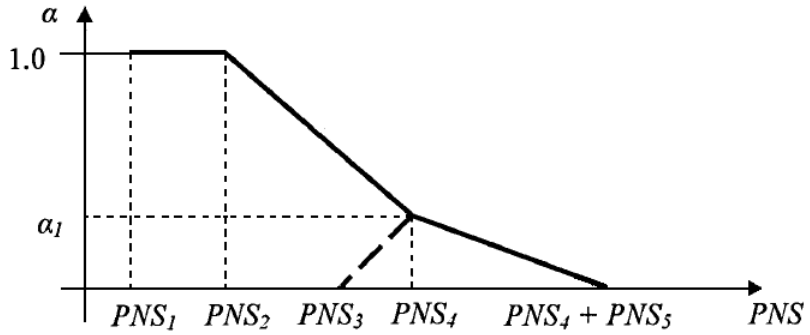

Figure 7.9: Final Membership function obtained through application of the maximum operator followed by the fuzzy union operator (source: Braga, 2004b).

On the other hand, Figure 7.10 presents a situation where the final membership function was obtained through the addition of the individual Power Not Supplied membership functions followed by the application of the Maximum operator.

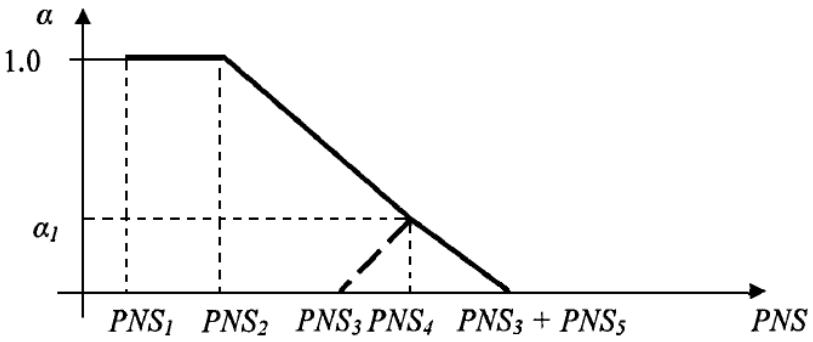

Figure 7.10: Final Membership function obtained through application of the addition of the individual power not supplied membership functions followed by the application of the fuzzy union operator (source: Braga, 2004b).

As we can now see from Figure 7.10 this strategy avoids the artificial enlargement that occurred on Figure 7.9, and so, it corresponds to the adopted procedure.

CHAPTER VIII Results

8. Results

For a better understanding of the solution algorithms described in the previous Chapters, in the present Chapter we will present some case studies. In Section 8.1 it will be presented a full didactic example based on a three bus/three branch power system that, although small, has the advantage of allowing the reader to follow the solution of the problems while being possible to interpret the results in a clear and direct way. In Section 8.2 it will be considered an illustrative example, based on a six bus/eight branch power system that, even still being a small example, will help the reader to fully understand all the developed features of the proposed algorithms. Finally, in Section 8.3 it will be presented an example based on the IEEE 24 bus/38 branch power system to illustrate the potential of the developed algorithms. The technical characteristics of these power systems are detailed in Appendices A, B and C, respectively.

8.1. Three bus/three branch power system

In order to describe the developed algorithms, in the present Section it will be presented the mathematical formulations of the linear multiparametric optimization problems corresponding to the NFOPF model when considering loads and/or generation costs uncertainties. In Appendix A of this Thesis we present the technical characteristics, loads and generation data of this system.

8.1.1. Integration of load uncertainties

In the first place, let us consider that the active loads in buses 2 and 3 of the system presented on Appendix A are represented by the trapezoidal fuzzy numbers (8.1) and (8.2), respectively, and that the generation cost of the generator at bus 2 is the double of the generation cost of the generator at bus 1.

$$P_{L2} = (0,0;1,5;2,5;4,0) \quad MW \tag{8.1}$$

$$P_{L3} = (2,0;3,0;4,0;5,0) \quad MW \tag{8.2}$$

According with Section 5.2.2, the formulation of the linear multiparametric Fuzzy DC-OPF problem integrating load uncertainties corresponds to the mathematical problem (8.3) to (8.13), where λ_2 and λ_3 represent the parameters that model load uncertainties on buses 2 and 3, respectively. In this formulation we adopted bus 3 as reference.

$$\min \quad z = CP_1.P_{G1} + CP_2.P_{G2} \tag{8.3}$$

Subj.:

$$P_{G1} + P_{G2} = 5,5 + \lambda_2 + \lambda_3 \tag{8.4}$$

$$P_{G1} \leq 6,0 \tag{8.5}$$

$$P_{G2} \leq 6,0 \tag{8.6}$$

$$\frac{1}{3}.P_{G1} - \frac{1}{3}.P_{G2} \leq \frac{4}{3} - \frac{1}{3}.\lambda_2 \tag{8.7}$$

$$-\frac{1}{3}.P_{G1}+\frac{1}{3}.P_{G2}\le\frac{8}{3}+\frac{1}{3}.\lambda_2 \quad (8.8)$$

$$\frac{2}{3}.P_{G1}+\frac{1}{3}.P_{G2}\le\frac{17}{3}+\frac{1}{3}.\lambda_2 \quad (8.9)$$

$$-\frac{2}{3}.P_{G1}-\frac{1}{3}.P_{G2}\le\frac{13}{3}-\frac{1}{3}.\lambda_2 \quad (8.10)$$

$$\frac{1}{3}.P_{G1}+\frac{2}{3}.P_{G2}\le\frac{19}{3}+\frac{2}{3}.\lambda_2 \quad (8.11)$$

$$-\frac{1}{3}.P_{G1}-\frac{2}{3}.P_{G2}\le\frac{11}{3}-\frac{2}{3}.\lambda_2 \quad (8.12)$$

$$P_{G1,}P_{G2}\ge 0 \quad (8.13)$$

In this context, the solution of the linear multiparametric optimization problem (8.3) to (8.13) leads to the identification of a first critical region, R_0, in the uncertainty space where the generation at buses 1 and 2 are represented by the linear expressions (8.14) and (8.15), respectively.

$$P_{G1}=4{,}75+0{,}5.\lambda_3 \quad \text{MW} \quad (8.14)$$

$$P_{G2}=0{,}75+\lambda_2+0{,}5\lambda_3 \quad \text{MW} \quad (8.15)$$

Running the non-redundant constraints identification algorithm, as well as the identification of all new critical regions on the uncertainty space algorithm, it was possible to find a new critical region, R_1, neighbour of the first one, R_0, in which the variables P_{G1} and P_{G2} are described by the linear expressions (8.16) and (8.17), respectively.

$$P_{G1}=5{,}5+\lambda_2+\lambda_3 \quad \text{MW} \quad (8.16)$$

$$P_{G2}=0 \quad \text{MW} \quad (8.17)$$

Taking into account the previous results, Figure 8.1 presents the rectangles enclosing all possible load combinations between the 0.0 and 1.0-cuts and the corresponding critical regions for which they were identified optimal and feasible basis. This Figure also indicates that the optimal and feasible basis obtained from the initial deterministic run (point O) remains feasible in the region termed as R_0. To the left hand side of line r (related with the capacity limit of branch 1-2), the value of one basic variable gets negative indicating that the current basis is no longer feasible. This means that we have to use the Dual Simplex algorithm to recover feasibility, thus defining a new critical region, R_1.

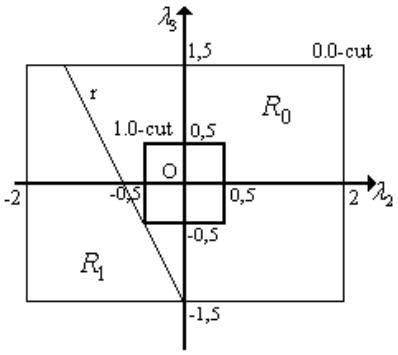

Figure 8.1: Rectangles enclosing all possible load combinations between the 0.0 and 1.0-cuts and the corresponding critical regions in the uncertainty space for which they were identified optimal and feasible basis.

According with Section 5.2.2, the partial membership functions of P_{G1} and P_{G2} can now be obtained solving a set of linear maximization/minimization problems ((5.29) to (5.32)) considering the linear expressions associated to these variables and the non-redundant inequalities in each critical region, together with the possible ranges of the input uncertainties regarding the i^{th} cut levels under analysis. Once all partial membership functions were obtained, it was applied the fuzzy union operator in order to get the widest possible behavior of these variables given the specified uncertainties. This procedure leads to the membership functions presented in Figure 8.2 for the generations at buses 1 and 2.

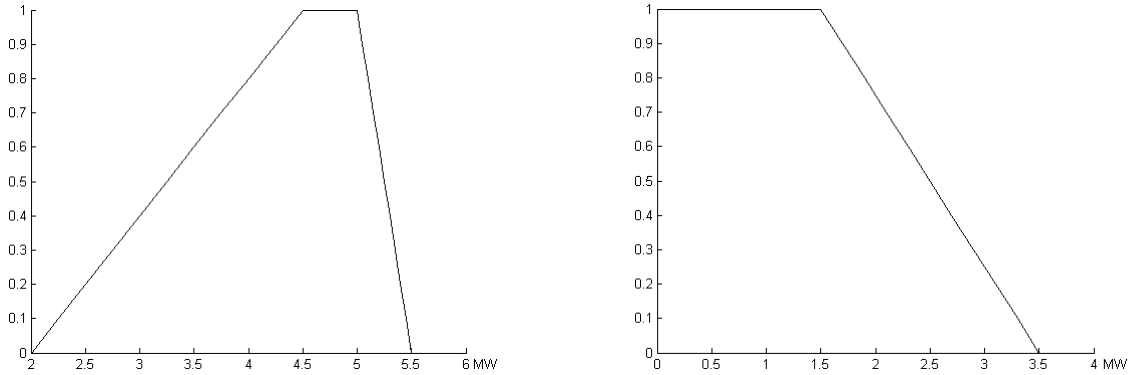

Figure 8.2: Membership functions of P_{G1} (at left) and P_{G2} (at right), when modelling load uncertainties.

As we can see from this Figure, for the central values of loads generator 1 is at 4,75 MW and generator 2 is only at 0,75 MW giving its generation cost and the maximum limit capacity of branch 1-2. It can also be seen that load variations are accommodated by both generators, however, tacking into account the analysis previously presented, we can also see that for load combinations corresponding to the ones within the critical regions R_1 only generator 1 operates while for load combinations corresponding to the ones within region R_0 both generators will operate.

8.1.2. Integration of generation cost uncertainties

Let us now consider again the three bus/three branch power system presented in Appendix A. In this case, the generation costs of the generators located at buses 1 and 2 are represented by the trapezoidal fuzzy numbers (8.18) and (8.19), respectively, and $\left|P_{12}^{máx}\right| = 5 \;\; MW$.

$$CP_{G1} = (5.0;15.0;25.0;35.0) \quad €/\text{MWh} \tag{8.18}$$

$$CP_{G2} = (15.0;25.0;35.0;45.0) \quad €/\text{MWh} \tag{8.19}$$

In this context, and according with what was described in Section 5.2.3, the mathematical formulation of the linear multiparametric Fuzzy DC-OPF problem integrating generation cost uncertainties corresponds to the mathematical problem (8.20) to (8.30).

$$\min \;\; z = (20 + \Delta_1).P_{G1} + (30 + \Delta_2).P_{G2} \tag{8.20}$$

Subj.:

$$P_{G1} + P_{G2} = 5{,}5 \tag{8.21}$$

$$P_{G1} \leq 6{,}0 \tag{8.22}$$

$$P_{G2} \leq 6{,}0 \tag{8.23}$$

$$\frac{1}{3}.P_{G1} - \frac{1}{3}.P_{G2} \leq \frac{13}{3} \tag{8.24}$$

$$-\frac{1}{3}.P_{G1} + \frac{1}{3}.P_{G2} \leq \frac{17}{3} \tag{8.25}$$

$$\frac{2}{3}.P_{G1} + \frac{1}{3}.P_{G2} \leq \frac{17}{3} \tag{8.26}$$

$$-\frac{2}{3}.P_{G1} - \frac{1}{3}.P_{G2} \leq \frac{13}{3} \tag{8.27}$$

$$\frac{1}{3}.P_{G1} + \frac{2}{3}.P_{G2} \leq \frac{19}{3} \tag{8.28}$$

$$-\frac{1}{3}.P_{G1} - \frac{2}{3}.P_{G2} \leq \frac{11}{3} \tag{8.29}$$

$$P_{G1,}P_{G2} \geq 0 \tag{8.30}$$

The solution of the initial deterministic Fuzzy DC-OPF problem associated with the central values of the generation costs allows us to obtain the results (8.31) and (8.32) for the generations at buses 1 and 2, respectively, in the critical region $\overline{R}_0$.

$$P_{G1} = 5{,}5 \;\; \text{MW} \tag{8.31}$$

$$P_{G2} = 0 \;\; \text{MW} \tag{8.32}$$

According with the algorithm presented in Section 5.2.3, we could also verify the existence of another critical region, $\overline{R}_1$, neighbour of $\overline{R}_0$, where:

$$P_{G1} = 0 \quad \text{MW} \tag{8.33}$$

$$P_{G2} = 5{,}5 \quad \text{MW} \tag{8.34}$$

Taking into account these results, Figure 8.3 presents the rectangles enclosing all possible generation cost combinations between the 0.0 and 1.0-cuts and the corresponding critical regions, $\overline{R}_0$ and $\overline{R}_1$, for which they were identified optimal and feasible basis. Similarly to what was presented in Figure 8.1, this Figure also indicates that the optimal and feasible basis obtained from the initial deterministic DC-OPF problem (point O) remains feasible and optimal within the region $\overline{R_0}$. However, in this situation, in the right hand side of line r the value of one dual variable gets negative indicating that the current solution is no longer optimal. In this context, it was performed a Primal Simplex step to recover the optimality of the solution, thus defining a new critical region, $\overline{R_1}$.

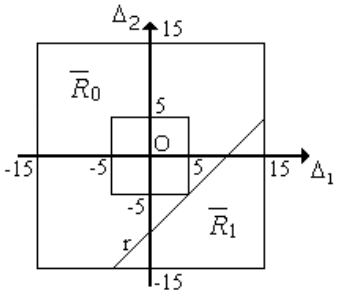

Figure 8.3: Rectangles enclosing all possible generation cost combinations between the 0.0 and 1.0-cuts and the corresponding critical regions in the uncertainty space for which were identified optimal and feasible basis.

Since there are no active constraints due to the minimum and maximum capacity branch limits, the previous solution can be easily understood if we consider that the $\overline{R}_0$ region is related with the uncertainty space where the generation cost of the generator located at bus 1 is smaller than the generation cost of the generator located at bus 2. In the opposite case, the critical region $\overline{R}_1$ corresponds to the uncertainty space where the generation cost of generator at bus 1 is larger than the corresponding generation cost of generator at bus 2. As it was previously mentioned, in this example it is clear that when modeling generation cost uncertainties, the generation, as well as the branch power flows, is described by means of ordered pairs generation/membership values in each of the identified critical regions. The application of the fuzzy union operator to the results previously presented leads to the membership functions of the generations at buses 1 and 2 as presented in Figure 8.4.

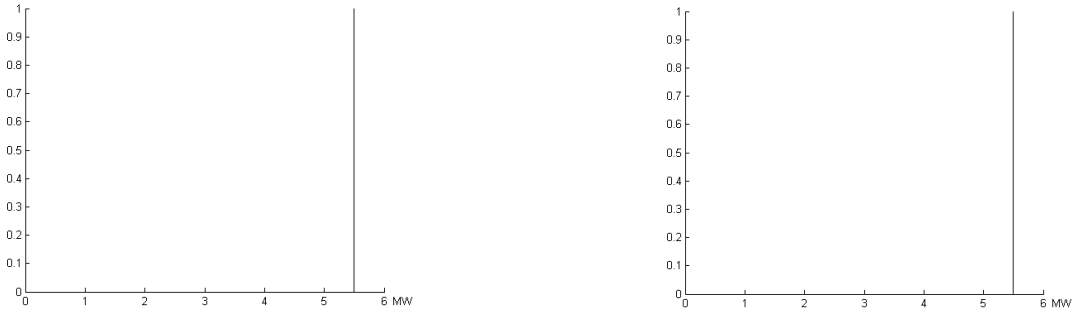

Figure 8.4: Membership functions of P_{G1} (at left) and P_{G2} (at right), when modeling generation cost uncertainties.

8.1.3. Simultaneous integration of loads and generation costs uncertainties

For a better understanding of the solution algorithms presented in Section 5.2.4, let us now consider, once again, the three buses/three branch power system presented in Appendix A. In this case, however, we will consider that the active load in bus 2 and the cost of the generator at bus 1 are described by the trapezoidal fuzzy numbers (8.35) and (8.36), respectively. The active load at bus 3 was fixed at 3,5 MW and the generation cost of generator at bus 2 was fixed at 30 €/MWh.

$$P_{L2} = (0{,}0;1{,}5;2{,}5;4{,}0) \quad \text{MW} \tag{8.35}$$

$$CP_{G1} = (5.0;15.0;25.0;35.0) \quad €/\text{MWh} \tag{8.36}$$

In this context and according to what was described in Section 5.2.4, the mathematical formulation of the linear multiparametric Fuzzy DC-OPF integrating, simultaneously, active load and generation cost uncertainties corresponds to (8.37) to (8.47).

$$\min \quad z = (20 + \Delta_1).P_{G1} + 30.P_{G2} \tag{8.37}$$

Subj.:

$$P_{G1} + P_{G2} = 5{,}5 + \lambda_2 \tag{8.38}$$

$$P_{G1} \leq 6{,}0 \tag{8.39}$$

$$P_{G2} \leq 6{,}0 \tag{8.40}$$

$$\frac{1}{3}.P_{G1} - \frac{1}{3}.P_{G2} \leq \frac{4}{3} - \frac{1}{3}.\lambda_2 \tag{8.41}$$

$$-\frac{1}{3}.P_{G1} + \frac{1}{3}.P_{G2} \leq \frac{8}{3} + \frac{1}{3}.\lambda_2 \tag{8.42}$$

$$\frac{2}{3}.P_{G1} + \frac{1}{3}.P_{G2} \leq \frac{17}{3} + \frac{1}{3}.\lambda_2 \tag{8.43}$$

$$-\frac{2}{3}.P_{G1} - \frac{1}{3}.P_{G2} \leq \frac{13}{3} - \frac{1}{3}.\lambda_2 \tag{8.44}$$

$$\frac{1}{3}.P_{G1}+\frac{2}{3}.P_{G2}\le\frac{19}{3}+\frac{2}{3}.\lambda_2 \quad (8.45)$$

$$-\frac{1}{3}.P_{G1}-\frac{2}{3}.P_{G2}\le\frac{11}{3}-\frac{2}{3}.\lambda_2 \quad (8.46)$$

$$P_{G1,}P_{G2}\ge 0 \quad (8.47)$$

The integration of load and generation cost uncertainties in the solution of the initial deterministic DC-OPF problem associated with the central values of the active load in bus 2 and the generation cost in bus 1 allows us to obtain the results given by expressions (8.48) and (8.49) for the generations at buses 1 and 2, respectively.

$$P_{G1}=4{,}75 \quad \text{MW} \quad (8.48)$$

$$P_{G2}=\lambda_2+0{,}75 \quad \text{MW} \quad (8.49)$$

The algorithm also determines three additional critical regions, $\overline{R}_1^*$, $\overline{R}_2^*$ and $\overline{R}_3^*$, neighbours of $\overline{R}_0^*$, in which the generations at buses 1 and 2 are described by expressions (8.50) and (8.51), (8.52) and (8.53), and (8.54), (8.55), respectively.

$$\begin{cases} P_{G1}=\lambda_2+5{,}5 \quad MW & (8.50) \\ P_{G2}=0 \quad MW & (8.51) \end{cases}$$

$$\begin{cases} P_{G1}=0 \quad MW & (8.52) \\ P_{G2}=\lambda_2+5{,}5 \quad MW & (8.53) \end{cases}$$

$$\begin{cases} P_{G1}=-0{,}5+\lambda_2 \quad MW & (8.54) \\ P_{G2}=6 \quad MW & (8.55) \end{cases}$$

Figure 8.5 presents the rectangles enclosing all possible combinations of loads and generation cost uncertainties between the 0.0 and 1.0-cut, as well as the corresponding critical regions for which they were determined optimal and feasible basis of the linear multiparametric Fuzzy DC-OPF problem integrating, simultaneously, active load and generation cost uncertainties. Similarly to what was presented in Figures 8.1 and 8.3, this Figure also indicates that the optimal and feasible basis obtained from the initial deterministic DC-OPF problem (point O) remains feasible and optimal in the uncertainty space region $\overline{R}_0^*$. However, in this case, there are situations where a given variable gets negative indicating that the current solution is no longer feasible and others where a dual variable gets negative indicating that the current solution is no longer optimal. In this context, they were performed Primal and Dual Simplex steps in order to recover the optimality or the feasibility of the solution, thus defining new critical regions, such as $\overline{R}_1^*$, $\overline{R}_2^*$ and $\overline{R}_3^*$.

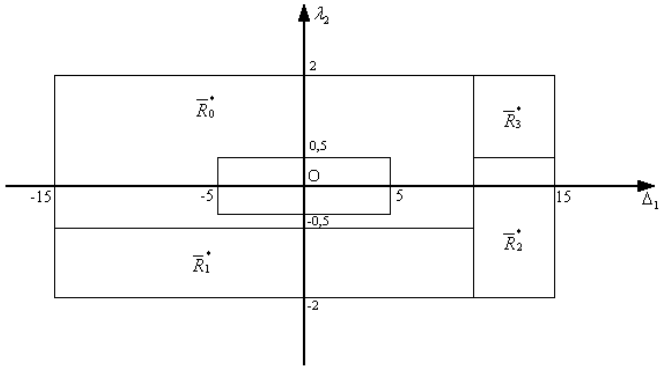

Figure 8.5: Rectangles enclosing all possible loads and generation costs combinations between the 0.0 and 1.0-cut and the corresponding critical regions in the uncertainty space for which they were identified optimal and feasible basis.

In order to build the membership function of each variable, it was once again recognized that in each region the behaviour of the output variables are expressed by linear expressions, and so, they are solved for each of them and for each critical region optimization problems as (5.29) to (5.32) to identify the widest possible behaviour of these variables in each critical region. As mentioned in Section 5.2.4, in this case it should be considered all the non-redundant inequalities related both with the feasibility and optimality conditions (5.20 and 5.21, respectively). Once all partial membership functions are obtained, it was applied the fuzzy union operator in order to get the membership functions of P_{G1} and P_{G2} presented in Figure 8.6.

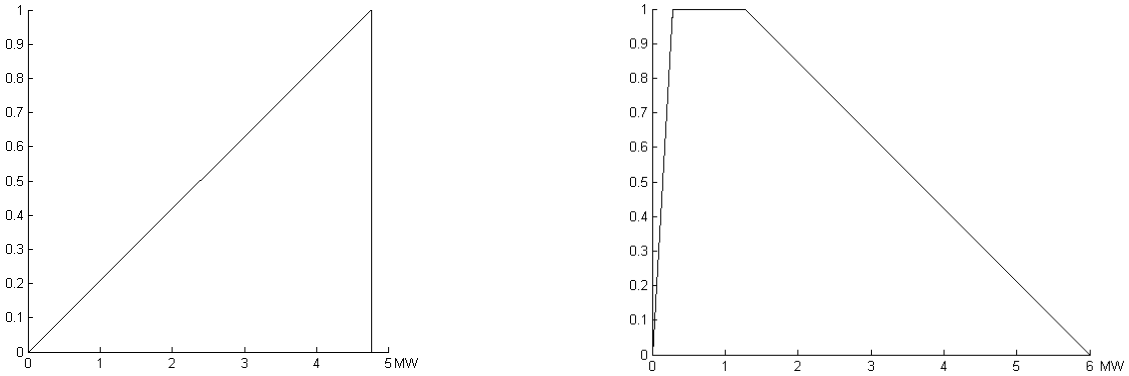

Figure 8.6: Membership functions of P_{G1} (at left) and P_{G2} (at right), when they are modelled, simultaneously, loads and generation costs uncertainties.

In this sense it is possible to describe the power system behaviour in the presence of these uncertainties in the following way:

- For the system active load between 3.5 and 4.75 MW ($-2{,}0 \le \lambda_2 \le -0{,}75$) and generation cost of generator at bus 1 between 5,0 and 30,0 €/MWh ($-15{,}0 \le \Delta_1 \le 10{,}0$) the generation at bus 1 will vary from 3,5 to 4,75 MW ($P_{G1} = \lambda_2 + 5{,}5 \;\; MW$) and the generation at bus 2 will be zero. This operation strategy is related with the critical region $\overline{R}_1^*$;

- Taking into account the generation cost of the previous situation ($-15{,}0 \le \Delta_1 \le 10{,}0$) and considering that the system active load varies between 4,75 and 7,5 MW ($-0{,}75 \le \lambda_2 \le 2{,}0$), generator at bus 2, the most expensive one, will start to generate reaching the value of 2,75 MW ($P_{G2} = \lambda_2 + 0{,}75 \;\; MW$). The generator at bus 1 will maintain a constant generation of 4,75 MW given the maximum capacity limit of branch 1-2. This situation corresponds to the one related with the critical region $\overline{R}_0^*$;
- If the generation cost of generator at bus 1 takes values between 30,0 and 35,0 €/MWh ($10{,}0 \le \Delta_1 \le 15{,}0$), it gets more expensive than the generator at bus 2. Under these conditions, there will be an inversion on the generation schedule and generator at bus 1 goes to zero. This situation will be maintained until the system active load achieves the value of 6,0 MW ($-2{,}0 \le \lambda_2 \le 0{,}5$). As a consequence, generator at bus 2 will also reach its maximum generation capacity. This situation is associated with the critical region $\overline{R}_2^*$;
- Taking into account the generation cost of the previous situation ($10{,}0 \le \Delta_1 \le 15{,}0$) and considering that the system active load will continue to increase till its maximum value of 7,5 MW ($0{,}5 \le \lambda_2 \le 2{,}0$), generator at bus 2 will maintain its generation level of 6,0 MW and generator at bus 1 will increase its generation till 1,5 MW ($P_{G1} = \lambda_2 - 0{,}5 \;\; MW$). This situation corresponds to the one related with the critical region $\overline{R}_3^*$.

8.2. Six bus/eight branch power system

In order to clarify the theoretical developments presented in previous Chapters, in this section we will present results obtained for a case study based on a six bus, eight branches power system, whose technical characteristics, loads and generation data are presented on Appendix B of this Thesis.

8.2.1. Considering load uncertainties

In order to model load uncertainties, loads at buses 2, 4 and 5 were defined by the trapezoidal fuzzy numbers (8.56) to (8.58).

$$P_{L2} = (1.0, 2.0, 6.0, 7.0) \text{ MW} \tag{8.56}$$

$$P_{L4} = (1.5, 3.0, 5.0, 6.5) \text{ MW} \tag{8.57}$$

$$P_{L5} = (2.0, 3.5, 4.5, 6.0) \text{ MW} \tag{8.58}$$

Figures 8.7 and 8.8 present the membership functions of $P_{G1/1}$, $P_{G2/1}$ and $P_{G5/1}$ considering the transmission losses effect and when this effect is not considered. In the right side of Figure 8.8 it is also presented the membership function of the nodal marginal price at bus 3 when considering the transmission losses effect and when this effect is not considered.

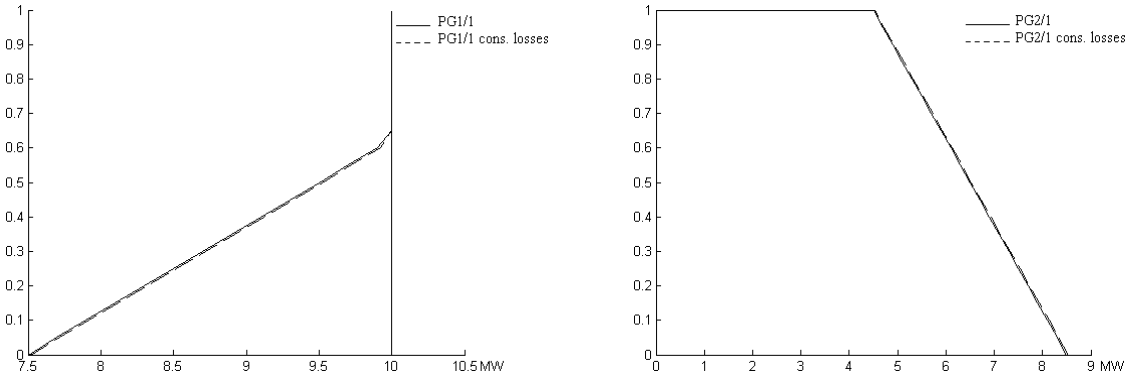

Figure 8.7: Membership functions of generators at buses 1 (at left) and 2 (at right) when the transmission losses effect is considered and when this effect is not considered (load uncertainties modelling).

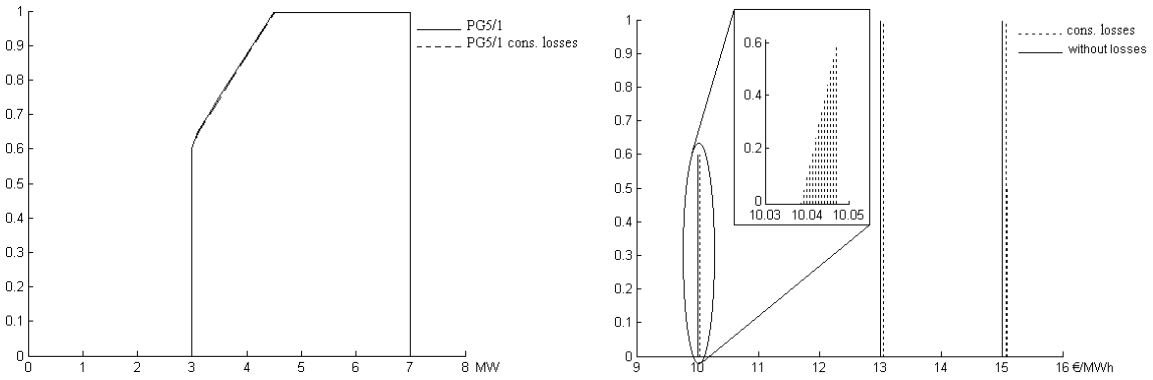

Figure 8.8: Membership functions of generator at bus 5 (at left) and of the nodal marginal price on bus 3 (at right) when the transmission losses effect is considered and when it is not considered (load uncertainties modelling).

As we can see from Figures 8.7 and 8.8 load variations are followed by variations, firstly, on generators at buses 1 and 5, and then by the generator at bus 2 that, for larger values of load becomes the marginal one and for smaller values is at 0,0 MW. The membership function of the generator at bus 6 is not represented since it is always zero (it is the most expensive one among all generators). From these Figures it is also possible to see that the effect of the transmission losses corresponds, as expected, to a general increase of the generation value of each generator (when compared with the situation where they are not considered) for the same level of uncertainty.

In Figure 8.8 (at right) we can also see the membership function of the nodal marginal price at bus 3. As expected this Figure shows three different nodal marginal prices deriving from the explanation previously presented. This price corresponds to 10,0 €/MWh when generator at bus 1 is the marginal generator, 13,0 €/MWh when generator at bus 5 is the marginal one and, finally, 15,0 €/MWh when generator at bus 2 is the marginal generator. When the transmission losses are considered, the marginal price at this bus increases meaning that a load increase in this bus imposes a general transmission losses increase. In this Figure it is also represented a detail of this marginal price increase due to transmission losses.

In order to evaluate the reliability and risk indices of this small power system regarding the reliability data presented on Appendix B and the specified load uncertainties, it was performed the Fuzzy Monte Carlo algorithm presented on Chapter 7. In this context, it was possible to obtain some risk indices, such as, the exposure and robustness indices and the Power Not Supplied expected value. In fact, under the specified conditions and after running this algorithm it was obtained a value of 0,8821 for the expected robustness index and a value of 0,1179 for the expected exposure index. Figure 8.9 presents the membership function of the Power Not Supplied expected value.

In order to evaluate the behaviour of the model regarding parameter variations it was also simulated a situation in which branch capacity limits were reduced to 6 MW. In this case, the expected values of the robustness index reduced to 0,8561 and the expected value of the exposure index increased to 0,1439. According to this Figure, reducing the branch limit implies that for the same PNS value, the membership value is larger, namely on the right hand side of membership functions. This means that the reduction of the branch limit increases the risk of the system not being able to supply the demand.

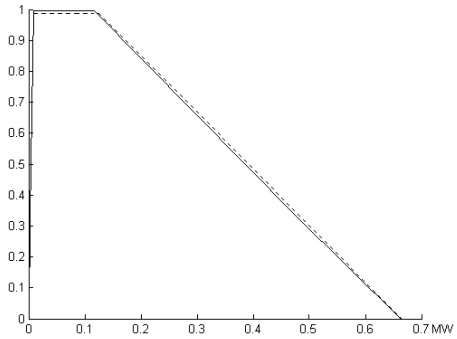

Figure 8.9: Membership function of the PNS expected value when considering a branch capacity limit of 8 MW (continuous line) and 6 MW (dashed line) (load uncertainties modelling).

Figure 8.10 presents the evolution of the β coefficient within the Fuzzy Monte Carlo simulation process, showing in this way the evolution of the convergence of this algorithm.

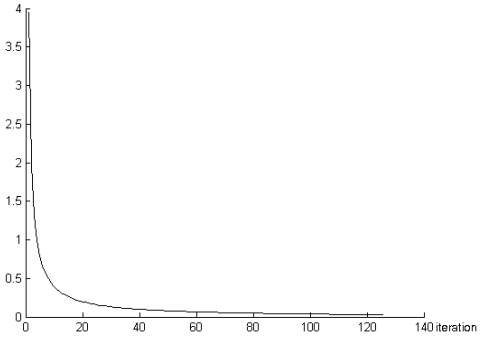

Figure 8.10: Fuzzy Monte Carlo convergence behaviour.

As we saw on Figure 8.8 when we are modelling load uncertainties, nodal marginal prices are represented by ordered pairs of price/membership values as a consequence of

the different generation strategies imposed by load values and generation/branch contingencies. In this context, Figure 8.11 presents the membership functions of the expected values of the nodal marginal prices at buses 1 (8 MW branch limit capacity). As it can be seen from this Figure, the nodal marginal price expected value reflects the occurrence of some PNS values different from zero. In fact, the largest values presented on this Figure correspond to the marginal price when PNS is different from zero.

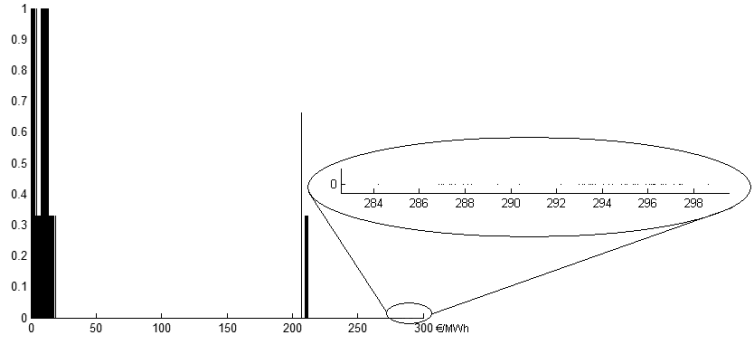

Figure 8.11: Membership function of the expected value of the nodal marginal price on bus 1 when modelling load uncertainties.

In this situation it was also performed a simulation with the branch capacity limits set at 6 MW. Figure 8.12 presents the obtained results for buses 1 and 2.

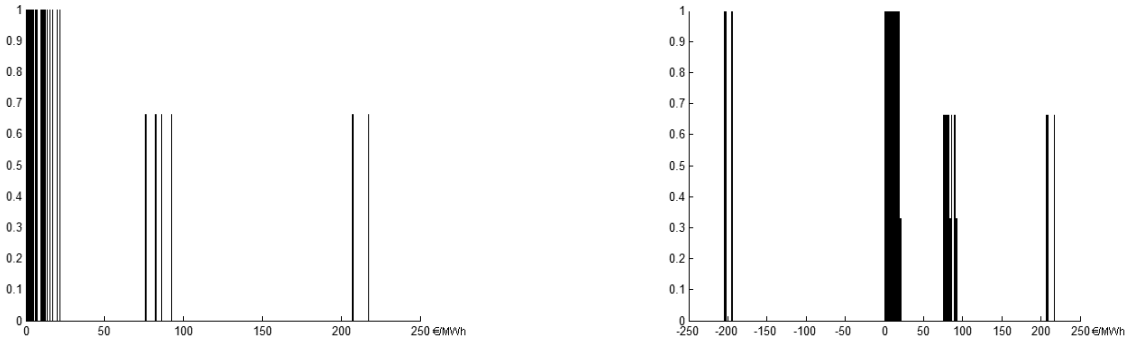

Figure 8.12: Membership function of the expected values of the nodal marginal prices on buses 1 and 2 when modelling load uncertainties.

As we can see from Figure 8.12 one of the main differences of these results when compared with the ones presented on Figure 8.11 is related with the ordered pairs with price larger than 50 €/MWh, whose presence is now more visible and also in some other pairs having negative values for the nodal price. Together, these ordered pairs show us that branch congestion increases the volatility of the nodal marginal prices and that depending on the branch and/or generator out of service, the price in a given bus could increase or decrease as an economical signal inducing more efficient behaviours on these situations.

8.2.2. Considering generation cost uncertainties

In order to evaluate the system behaviour in the presence of generation costs uncertainties, the costs of generators at buses 1, 2 and 5 were modelled by the trapezoidal fuzzy numbers (8.59) to (8.61), respectively.

$$C_{P_{G1/1}} = (5.0,7.5,12.5,15.0)\ €/\text{MWh} \tag{8.59}$$

$$C_{P_{G2/1}} = (9.0,12.0,18.0,21.0)\ €/\text{MWh} \tag{8.60}$$

$$C_{P_{G5/1}} = (12.0,12.5,13.5,14.0)\ €/\text{MWh} \tag{8.61}$$

Figures 8.13 and 8.14 present the membership functions of the generators at buses 1, 2, 5 and 6 considering these generation cost uncertainties.

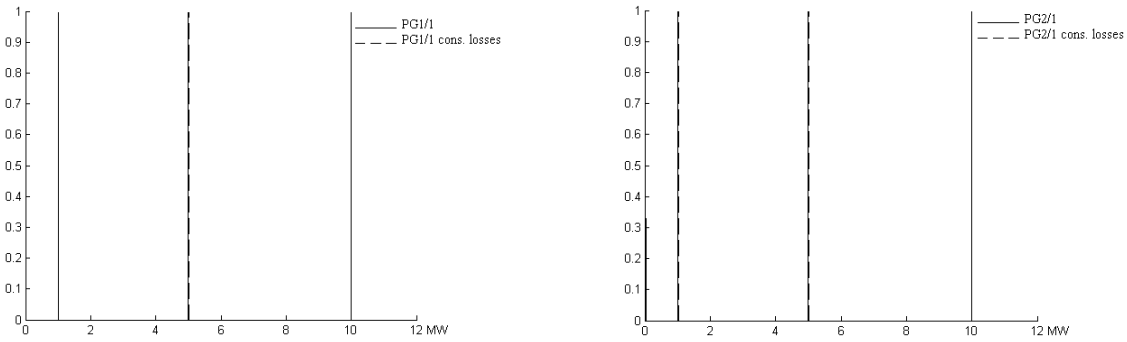

Figure 8.13: Membership functions of the generators at buses 1 (at left) and 2 (at right) when considering the transmission losses effect and when not considering this effect (generation cost uncertainties modelling).

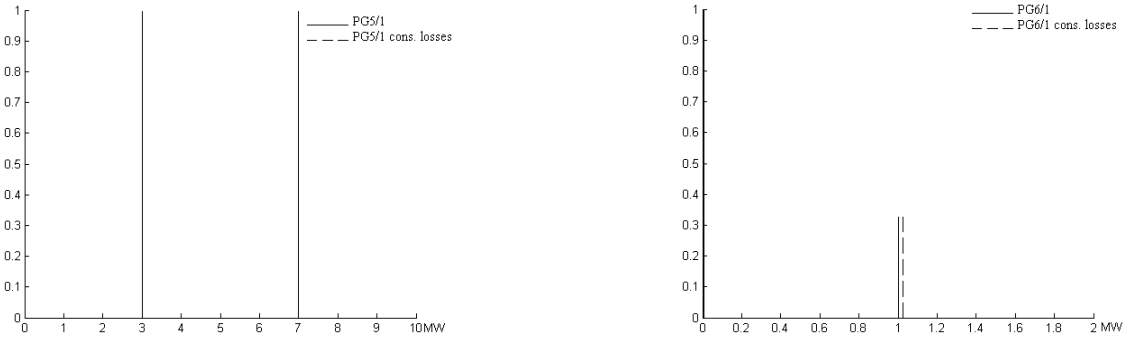

Figure 8.14: Membership functions of the generators at buses 5 (at left) and 6 (at right) when considering the transmission losses effect and when not considering this effect (generation cost uncertainties modelling).

As we can see from Figures 8.13 and 8.14, when we are modelling generation cost uncertainties the generator membership functions are no longer represented by linear expressions, but instead, by ordered pairs of generation/membership value. We can also see that for the specified uncertainties, the membership function of the generator at bus 6 is not always zero since that, for some uncertainty values, the generator at bus 2 becomes more expensive than the generator at bus 6, and so, for these uncertainty values this generator becomes the marginal one.

As expected, the integration of the transmissions losses originates an increase in the generation value of some generators for some levels of uncertainty. Nevertheless, this only occurs in specific situations (this is, in some ordered pairs) since, transmission losses are compensated by the marginal generators.

Figure 8.15 presents the membership function of the nodal marginal price at buses 1 and 3 when considering the transmission losses effect and when this is not considered.

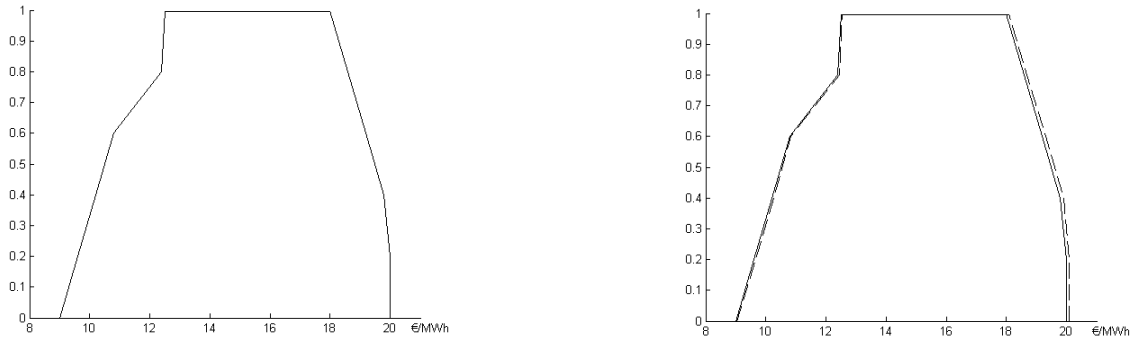

Figure 8.15: Membership functions of nodal marginal prices at buses 1 (at left) and 3 (at right) when considering the transmission losses effect and not considering this effect (generation cost uncertainties modelling).

From Figure 8.15 we can see that nodal marginal prices exhibit a variation from 9,0 €/MWh to 20,0 €/MWh at the zero membership value and from 12,5 €/MWh to 18,0 €/MWh at the 1.0 membership value at buses 1 and 3. These values correspond to the minimum and maximum generation cost of the marginal generators in each of the mentioned uncertainty levels.

As expected, in bus 3 the integration of transmission losses is followed by an increase of the marginal price in this bus, meaning that a load increase in this bus implies an increase of transmission losses. In this context, it is also important to mention that in opposition to what happens when not considering the transmission losses effect, in this case marginal prices differ from bus to bus reflecting different impacts of local variations in transmission losses. From this Figure it is also possible to see that the marginal price on bus 1 did not exhibit any kind of variation when it was considered the transmission losses effect. This situation results, however, directly from the model used to compute the nodal marginal prices (model A), since this bus is the system slack bus.

In order to evaluate the reliability and risk indices of this power system regarding the reliability data presented on Appendix B and the specified generation cost uncertainties, it was performed the Fuzzy Monte Carlo algorithm presented on Chapter 7. In this context, it was possible to obtain some risk indices, such as, the expected value of the robustness index that, in this case, takes the value of 0,9931 and the expected value of the exposure index that takes the value of 0,069. Figure 8.16 presents the membership function of the expected value of PNS.

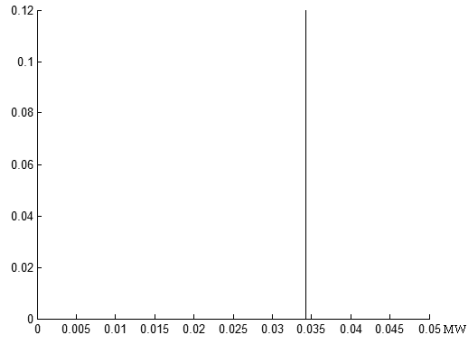

Figure 8.16: Membership function of the expected value of PNS when modelling generation cost uncertainties.

Figure 8.17 displays the behaviour of the β coefficient within the Fuzzy Monte Carlo simulation process showing the convergence behaviour of this algorithm.

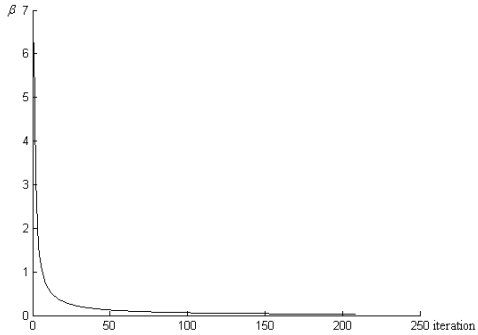

Figure 8.17: Fuzzy Monte Carlo convergence behaviour.

Figure 8.18 presents the membership functions of the expected value of the nodal marginal prices on buses 1 and 3 considering the specified generation cost uncertainties and the non-ideal nature of the system components.

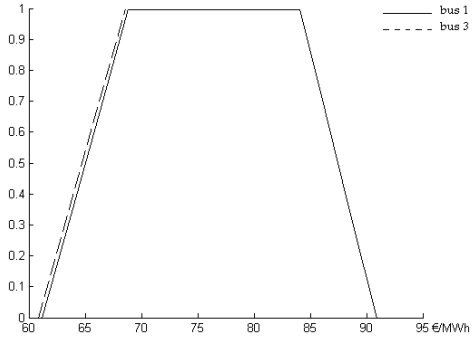

Figure 8.18: Membership function of the expected value of the nodal marginal prices on buses 1 and 3 when modelling generation cost uncertainties.

As an attempt to test the algorithm for different operation conditions, the branch capacities were set at 6 MW. In this case, Figure 8.19 presents the membership function of the expected value of PNS. The expected values of the robustness and exposure indices are, in this case, 0,9847 and 0,0153, respectively. As expected the robustness index is now smaller than what it was when it was considered an 8 MW capacity branch limit.

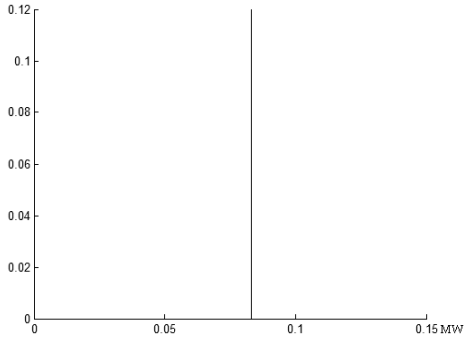

Figure 8.19: Membership function of the expected value of PNS when modelling generation cost uncertainties.

Figures 8.20 and 8.21 present the membership functions of the expected value of the nodal marginal prices at buses 1 and 2, 3 and 6, respectively.

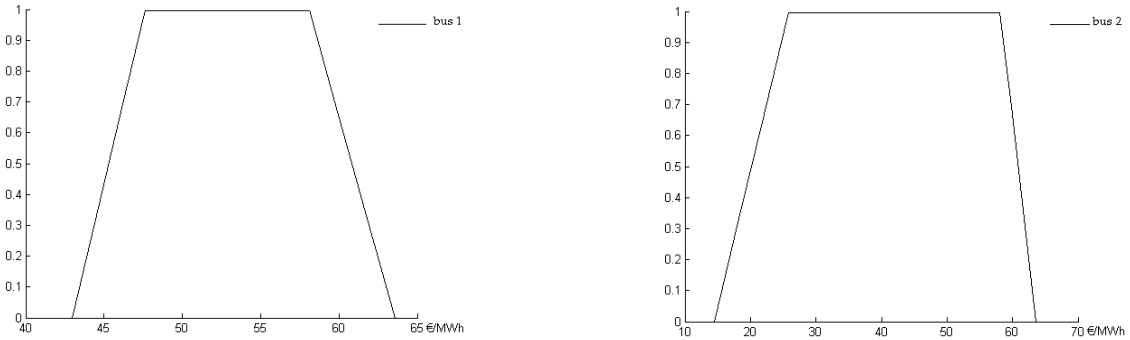

Figure 8.20: Membership function of the expected values of the nodal marginal prices on buses 1 (at left) and 2 (at right) when modelling generation cost uncertainties.

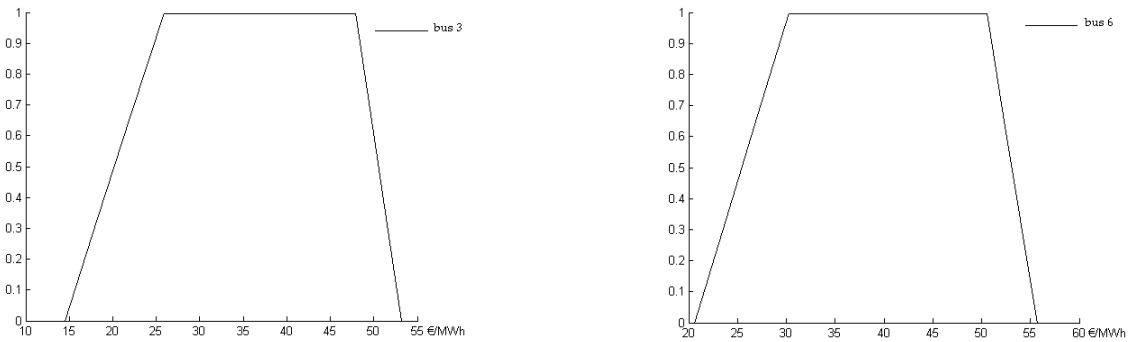

Figure 8.21: Membership function of the expected value of the nodal marginal prices on buses 3 (at left) and 6 (at right) when modelling generation cost uncertainties.

As we can see from Figures 8.20 and 8.21, when using a branch capacity limit of 6 MW, membership functions of nodal marginal prices display larger differences from bus to bus

than the ones presented in Figure 8.18, since now the transmission sub-system imposes different nodal marginal price values. The occurrence of smaller nodal marginal prices means that on these buses a load increase or a generation decrease would largely benefit the system, reflecting in this way the larger influence of the transmission sub-system.

8.2.3. Considering load and generation cost uncertainties simultaneously

In order to model load and generation costs simultaneously, load at buses 2, 4 and 5 and generation costs of generators at buses 1, 2 and 5 where modeled by the trapezoidal fuzzy numbers (8.56) to (8.58) and (8.59) to (8.61), respectively. Figures 8.22 and 8.23 present the membership functions of generators at buses 1, 2, 5 and 6 when considering the transmission losses effect and when this effect is not considered.

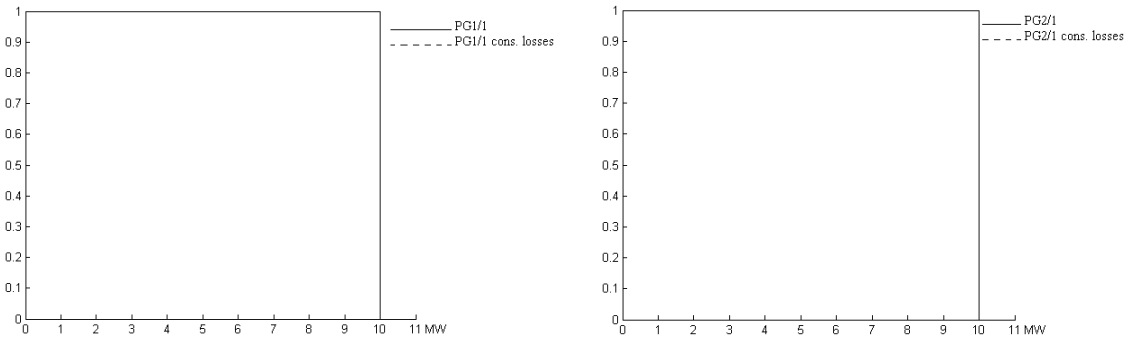

Figure 8.22: Membership functions of generators at buses 1 (at left) and 2 (at right) when considering the transmission losses effect and when not considering this effect (loads and generation costs uncertainties modelling).

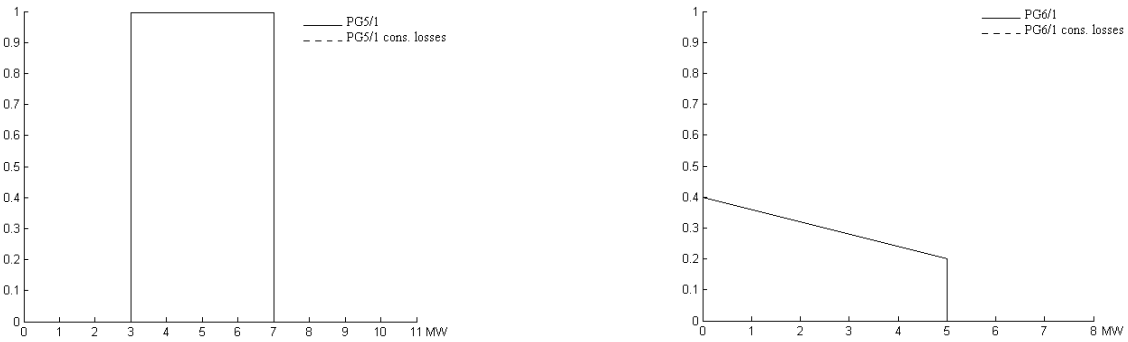

Figure 8.23: Membership functions of generators at buses 5 (at left) and 6 (at right) when considering the transmission losses effect and when not considering this effect (loads and generation costs uncertainties modelling).

As we can see, in this new situation the membership function of the generator at bus 6 is not always zero as it was in the results of Section 8.2.1 neither it presents a constant value of 1 MW as it was the case of Section 8.2.2. In fact the result presented in Figure 8.23 clearly reveals the combined effect of the specified uncertainties for the load and generation costs. Additionally, these Figures present another important result. In fact, these Figures do not display differences between the membership functions when considering the transmission losses effect and when they are not considered. In this context, it is important to clarify that this occurred because the extreme values of these

membership functions always correspond to the maximum/minimum generation capacity of each generator, and so, the differences imposed by transmission losses are not directly visible.

Figure 8.24 presents the membership functions of the nodal marginal prices in this situation when considering the transmission losses effect and when they are not considered.

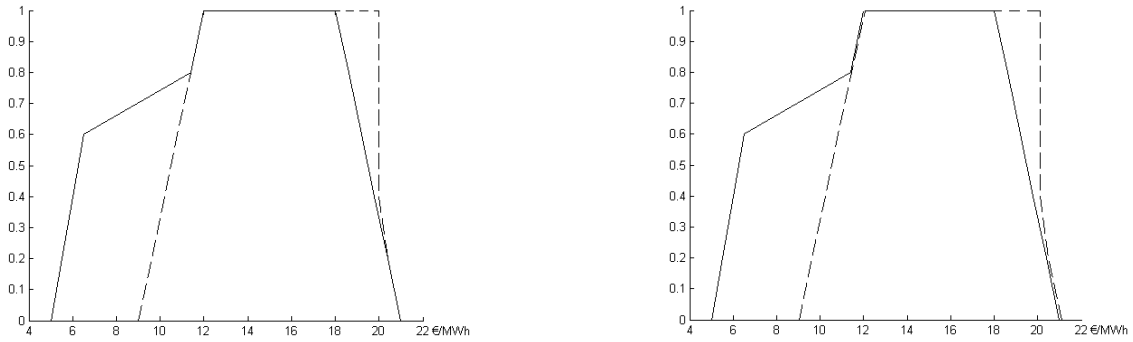

Figure 8.24: Membership functions of nodal marginal prices at buses 1 (at left) and 3 (at right) when considering the transmission losses effect and when they are not considered (loads and generation costs uncertainties modelling).

When we compare these results with the ones presented on Figure 8.15 we see that they have similar behavior, however, with different values. This happens because the compensation of load variations within different generation prices values originates different generation strategies as, for example, the one that forces generator at bus 2 to operate and, consequently, defining a new maximum nodal marginal price value (at the 0.0 membership value). Another situation, for example, corresponds to the case where the generator at bus 1, forced by the minimum generation capacity of the generator at bus 5, becomes the marginal generator defining a new minimum nodal marginal price (at the 0.0 membership value). In fact when considering the transmission losses effect this situation did not occur and, as a consequence of the elimination of this generation strategy, the minimum marginal price at all buses increase. As it can be seen from these Figures, a similar situation occurs regarding the maximum value of the marginal prices at the 1.0 membership value.

As we mentioned on Section 8.2.1 these Figures also present another important aspect. In fact, comparing these results and ignoring the differences inherent to the questions mentioned on the previous paragraph, we can see that the nodal marginal price on bus 1 did not change with the integration of the transmission losses effect (since it is the slack bus) and that a marginal load increase in bus 3 imposes an increase of the transmission losses, since the nodal marginal price on this bus increase when considering the transmission losses effect.

In order to evaluate the reliability and risk indices of this power system regarding the reliability data presented on Appendix B and the specified load and generation cost uncertainties, it was run the Fuzzy Monte Carlo algorithm presented on Chapter 7. In this context, it was possible to obtain some risk indices, such as the expected value of the robustness index that, in this case, takes the value of 0,8439 and the expected value of the

exposure index that takes the value of 0,1561. Figure 8.25 presents the membership function of the expected value of PNS and Figure 8.26 displays the behaviour of the β coefficient within the Fuzzy Monte Carlo simulation process showing the convergence of the simulation.

As expected the robustness index obtained for this case corresponds to a value smaller than the ones obtained for the load and generation cost uncertainties when modelled separately, meaning that, this reflects the simultaneous effect of modelling both kinds of uncertainties.

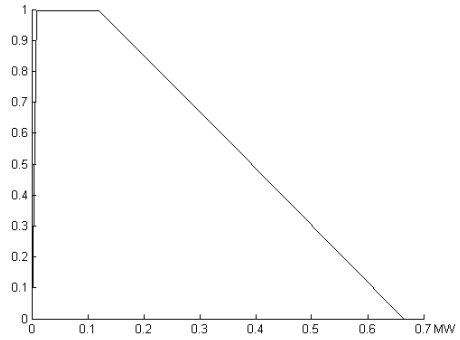

Figure 8.25: Membership function of the PNS expected value when modelling, simultaneously, load and generation cost uncertainties.

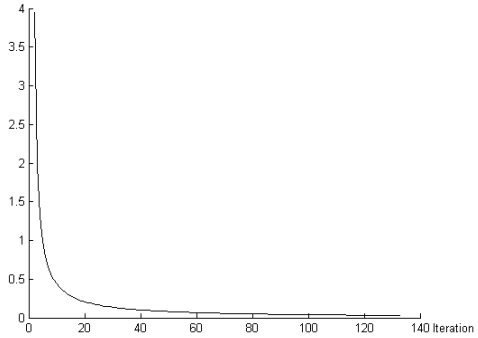

Figure 8.26: Fuzzy Monte Carlo convergence behaviour.

Figure 8.27 presents the membership functions of the expected values of the nodal marginal prices at buses 1 and 5. As it can be seen from this Figure, the occurrence of some PNS values different from zero originates the increase of the nodal prices.

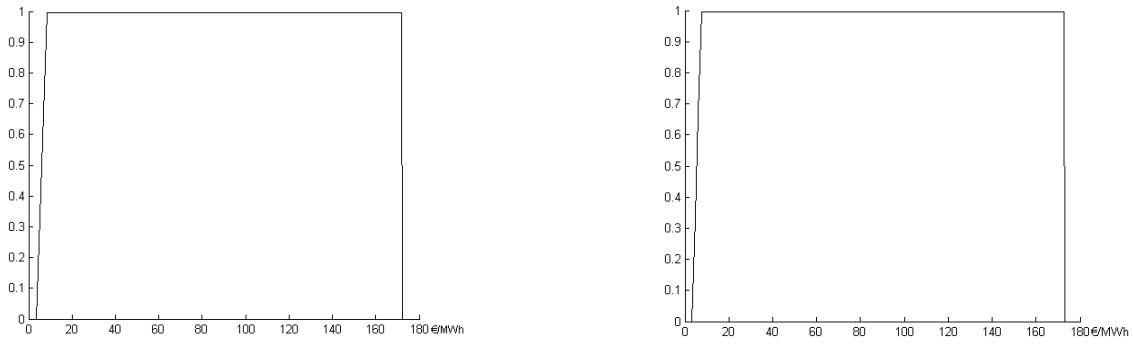

Figure 8.27: Membership function of the expected value of the nodal marginal prices on buses 1 (at left) and 5 (at right) when modelling, simultaneously, loads and generation cost uncertainties.

As an attempt to test the algorithm for different operation conditions, the branch capacities were set at 6 MW. In this case, Figure 8.28 presents the membership function of the expected value of PNS. The expected values of the robustness and exposure indices are, in this case, 0,8359 (smaller than the one previously obtained) and 0,1641, respectively.

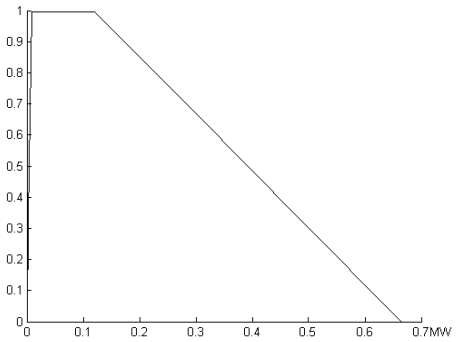

Figure 8.28: Membership function of the PNS expected value when modelling, simultaneously, load and generation cost uncertainties.

Figure 8.29 presents the nodal marginal prices on buses 1 and 5 for this new situation.

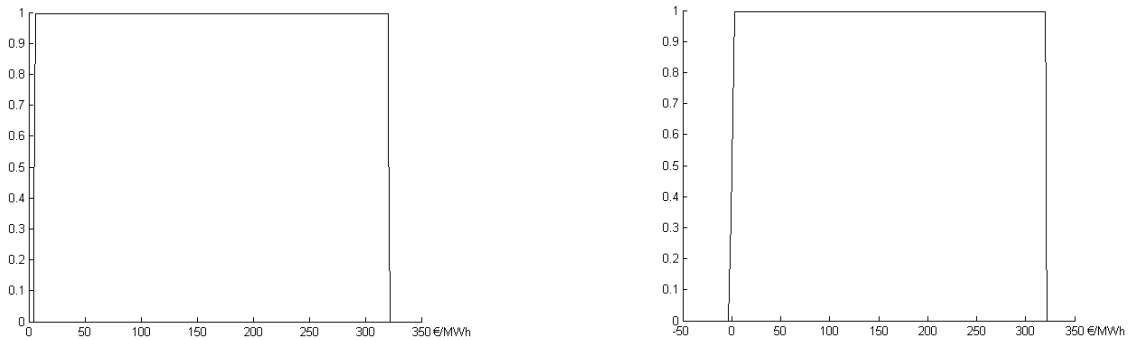

Figure 8.29: Membership function of the expected value of the nodal marginal prices on buses 1 (at left) and 5 (at right) when modelling, simultaneously, loads and generation cost uncertainties.

Comparing Figures 8.29 and 8.27 we can see that their maximum values increase meaning that the system is now less reliable and so marginal prices will generally

increase. Additionaly, this Figure also shows that the branch limit capacity reduction will also impose larger differences between nodal marginal prices. For instance in bus 5 it is possible to obtain negative nodal marginal prices.

8.3. Examples considering the IEEE 24 bus /38 branch test system

The algorithms described so far were used to build the membership functions of generations, branch flows, PNS and nodal marginal prices considering a case study based on the IEEE 24 bus/38 branch test system, whose technical characteristics, loads and generation data are presented on the Appendix C of this Thesis.

8.3.1. Considering load uncertainties

In order to test the algorithm presented in Section 5.2.2, we considered trapezoidal fuzzy numbers to model loads. At the 0.0 level the uncertainty of these numbers ranges from +/-10 per cent of their central values and at the 1.0 level the uncertainty ranges from +/- 5 per cent of their central values. Figure 8.30 presents the membership functions of the generators 19/1 and 21/1 considering and not considering the transmission losses effect.

As expected, the load variation determines changes on the generation of generator 21/1 since it is the marginal one. When this generator reaches its maximum capacity of 800,0 MW, generator 19/1 becomes the marginal one. Another important point illustrated by these functions is related with the impact of the transmission losses. In this case, these generators have larger generation values for the same level of uncertainty due to the compensation of losses.

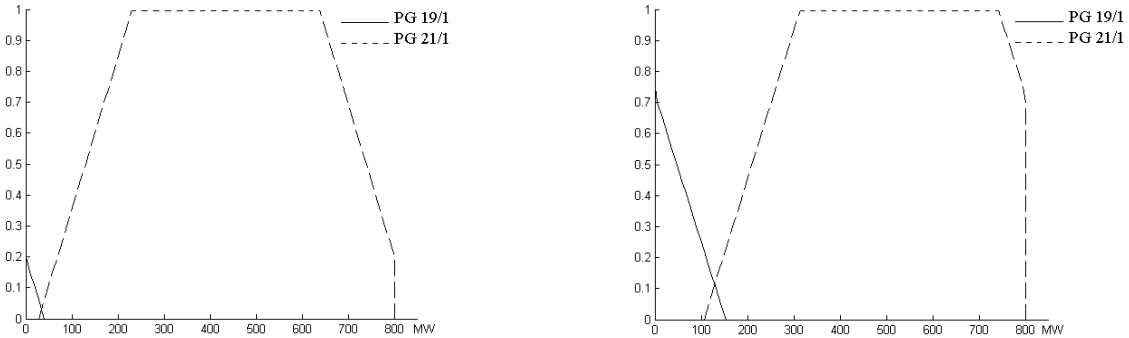

Figure 8.30: Membership functions of generators 19/1 and 21/1 not considering the effect of the transmission losses (at left) and considering this effect (at right) (loads uncertainty modelling).

Figure 8.31 presents the nodal marginal prices at node 1 for the two situations previously presented. As mentioned in Section 6.3.2, since nodal marginal prices are related with the dual variables of the original problem, their membership functions are described by pairs of price/membership values. From Figure 8.31 it is possible to see that, neglecting the transmission losses, branch congestions or PNS effect, the marginal price in node 1 equals the generation cost of the marginal generator (21/1 or 19/1). When the effect of transmission losses is considered the nodal marginal prices increase or decrease

depending on the impact of load variations in transmission losses. For instance, when generator 19/1 is the marginal one, an increase of the load in node 1 increases transmission losses, and so, the nodal marginal price in node 1 also increases.

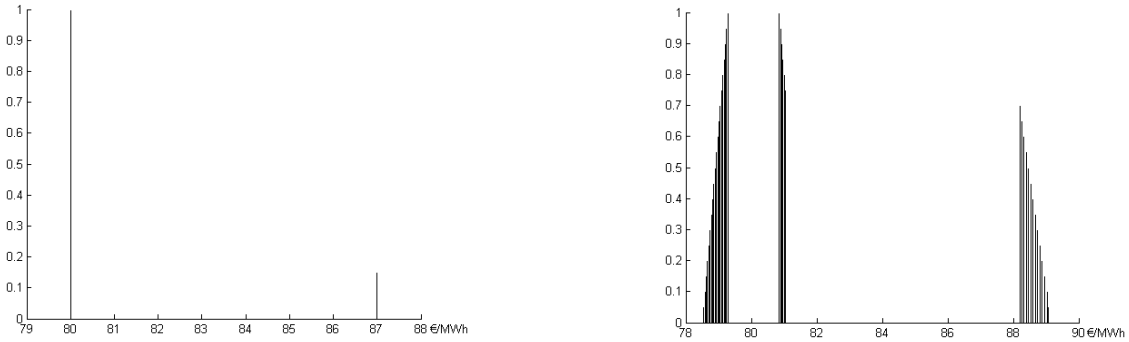

Figure 8.31: Membership functions of the nodal marginal price in node 1 not considering the effect of transmission losses (at left) and considering this effect (at right) (loads uncertainty modelling).

In order to evaluate the impact of congested branches, the flow limit of the two branches between nodes 15 and 21 was reduced to 350,0 MW. As a consequence, for some combination of loads these branches get congested. Figure 8.32 presents the membership functions of generators 19/1 and 21/1 and of the marginal price in bus 15 in this case.

The analysis of these results indicates that the congestion on branches 15-21 implies a change on the marginal prices in most of the buses, but more in particular in the ones that are closer to the congested branches. In case of bus 15 in Figure 8.32, the marginal price increase means that a generation increase or a load reduction in this bus contributes to alleviate the congestion. The membership function of generator 21/1 in Figure 8.32 reveals that now this generator doesn't reach its maximum limit of 800,0 MW, differently from what was indicated in Figure 8.30. This is due to the congestion of branches 15-21.

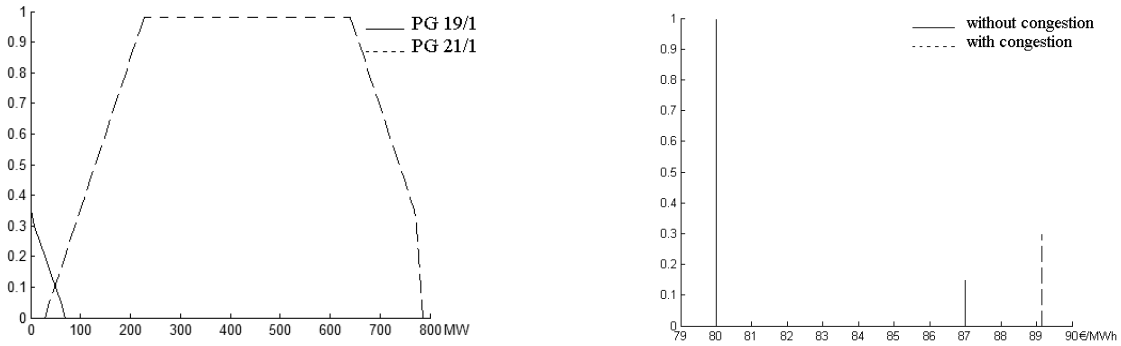

Figure 8.32: Membership functions of generators 19/1 and 21/1 (at left) and of the nodal marginal price in bus 15 (at right) (loads uncertainty modelling).

In order to evaluate the reliability and risk indices of this power system regarding the reliability data presented on Appendix C and the specified load uncertainties, it was run the Fuzzy Monte Carlo algorithm presented on Chapter 7. In this context, it was possible to obtain some risk indices, such as, the expected value of the robustness index that, in this case, takes the value of 0,9111 and the expected value of the exposure index that takes the value of 0,0889. In this context, Figure 8.33 (at the left side) presents the membership function of the expected value of PNS.

To evaluate the performance of the algorithm with respect to different conditions and parameters, it was also analysed a situation in which the generator 23/1 (800 MW) was removed from the system. In this context, it was obtained an expected value of the robustness index of 0,8857 (as expected smaller than the previous one) and an expected value of the exposure index of 0,1143 showing, in this way, that the system is now more exposed. In Figure 8.31 (right side) it is presented the expected value of the PNS membership function obtained for this situation.

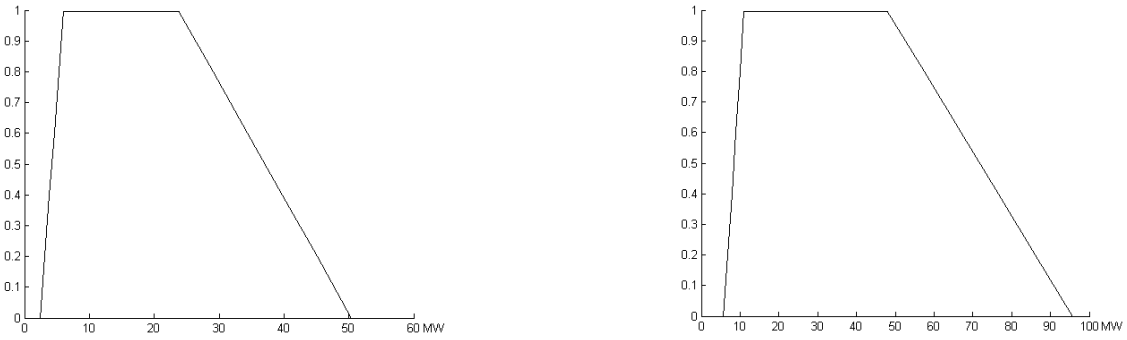

Figure 8.33: Membership function of the PNS expected value when the 23/1 generator is available (at left) and when it is not available (at right) (modelling load uncertainties).

As expected, this Figure also shows that when the system generation capacity decreases the PNS expected value increases for the same level of uncertainty meaning that the system are now less reliable.

Figure 8.34 presents the membership functions of the expected values of the nodal marginal prices on buses 1 and 5 for the specified load uncertainties and reliability data. Figure 8.35 presents similar membership functions, however, in this case not considering generator 23/1. In this context, from this Figure we can see, once again, that volatility increases and that the possibility of occurring large nodal marginal prices also increases as presented in Figure 8.35.

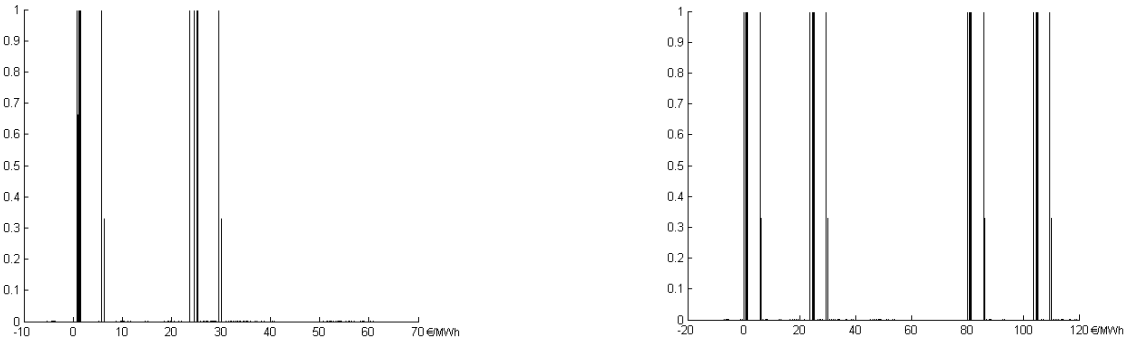

Figure 8.34: Membership function of the expected value of the nodal marginal price on buses 1 (at left) and 5 (at right) when modelling load uncertainties.

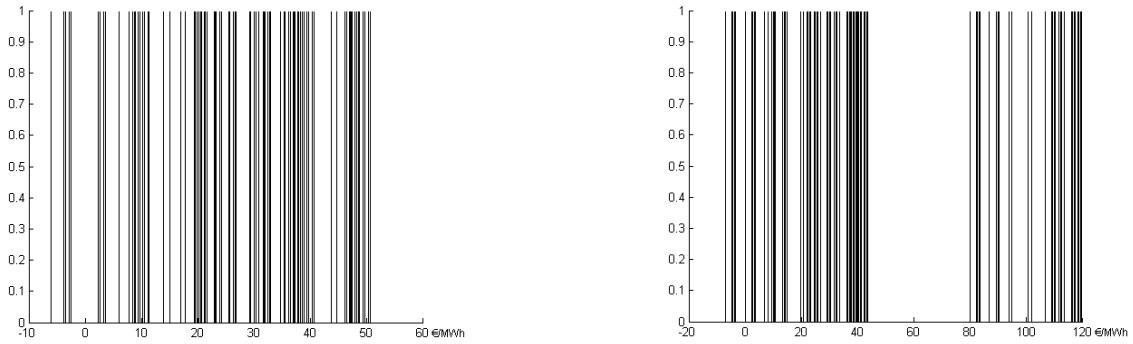

Figure 8.35: Membership function expected value of the nodal marginal price on buses 1 (at left) and 5 (at right) when the generator 23/1 is not available (loads uncertainty modelling).

8.3.2. Considering generation cost uncertainties

In this simulation, the trapezoidal fuzzy numbers (8.62) to (8.67) were used to model the generation cost of generators 1/1, 2/1, 7/1, 19/1, 22/2 and 23/2. Figure 8.36 presents the membership functions of generators 19/1 and 21/1 for this situation.

$$CP_{G1/1} = (26.0,27.5,32.5,34.0)\ €/MWh \quad (8.62)$$

$$CP_{G2/1} = (33.0,34.5,37.5,39.0)\ €/MWh \quad (8.63)$$

$$CP_{G7/1} = (42.0,43.5,46.5,48.0)\ €/MWh \quad (8.64)$$

$$CP_{G19/1} = (74.0,82.0,92.0,100.0)\ €/MWh \quad (8.65)$$

$$CP_{G22/2} = (14.0,15.5,18.5,20.0)\ €/MWh \quad (8.66)$$

$$CP_{G23/2} = (46.0,47.5,50.5,52.0)\ €/MWh \quad (8.67)$$

As it was mentioned in Section 5.2.3, in the case of generation cost uncertainty modeling the membership functions of generators are represented by pairs of power/membership values. The functions in Figure 8.36 reflect two different generation strategies according to the specified generation cost uncertainties. In fact, when the cost of generator 19/1 is smaller than 80,0 €/MWh (which corresponds to the generation cost of generator 21/1) this generator will generate 434,05 MW. For larger costs, this generator will be at 0,0 MW and generator 21/1 will generate 434,05 MW.

Figure 8.36 also indicates that when transmission losses are included there is, in general, an increase of generation values. This increase depends, however, on the adopted generation strategy because of their different impacts on transmission losses.

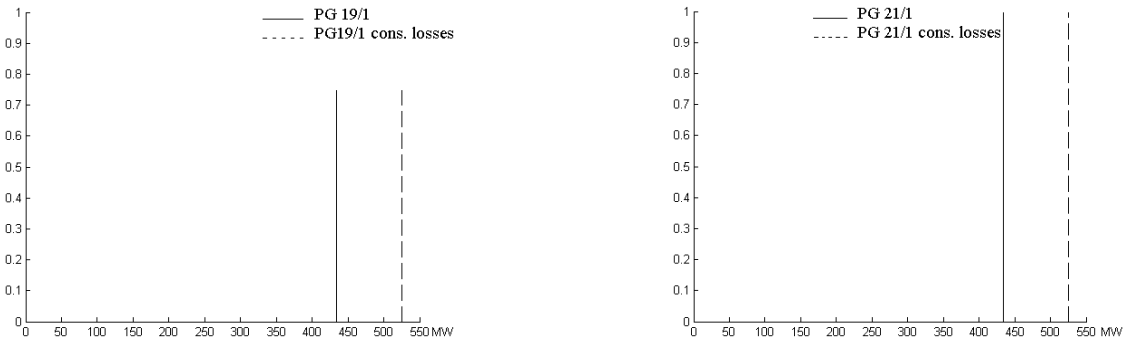

Figure 8.36: Membership functions of generators 19/1 and 21/1 considering and not considering the transmission losses effect when modelling generation cost uncertainties.

Figure 8.37 presents the marginal price of node 1 in these two situations. As mentioned in Section 6.3.3, when we are modelling generation costs uncertainties the membership functions of the nodal marginal prices are linear, at least by segments. Considering the effect of transmission losses, there is an increase of the marginal price in bus 1. These results are in line with the ones in Figure 8.31 since we observed that a load increase in bus 1 contributed to increase the overall system transmission losses.

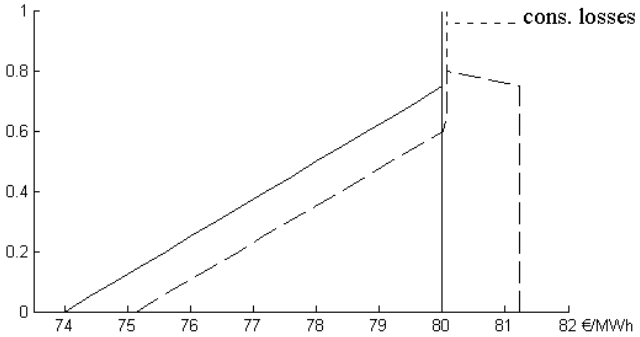

Figure 8.37: Membership function of the nodal marginal price at bus 1 considering and not considering the transmission losses effect (generation cost uncertainties modelling).

In order to evaluate the reliability and risk indices of this power system regarding the reliability data presented on Appendix C and the specified generation cost uncertainties, it was run the Fuzzy Monte Carlo algorithm presented on Chapter 7. In this context, it was possible to obtain some risk indices, such as, the expected value of the robustness index that, in this case, takes the value of 0,9898 and the expected value of the exposure index that takes the value of 0,0102. In this context, Figure 8.38 presents the membership function of the expected value of PNS for two different situations. In fact, to evaluate the performance of the algorithm with respect to different operation conditions and parameters, it was also analysed a situation in which the generator 23/1 (800 MW) was removed from the system. In this context, it was obtained an expected value of the robustness index of 0,9718 (as expected smaller than the previous one) and an expected value of the exposure index of 0,0282 showing, in this way, that the system are now more exposed. In Figure 8.38 (at right) it is presented the expected value of the PNS membership function obtained for this situation.

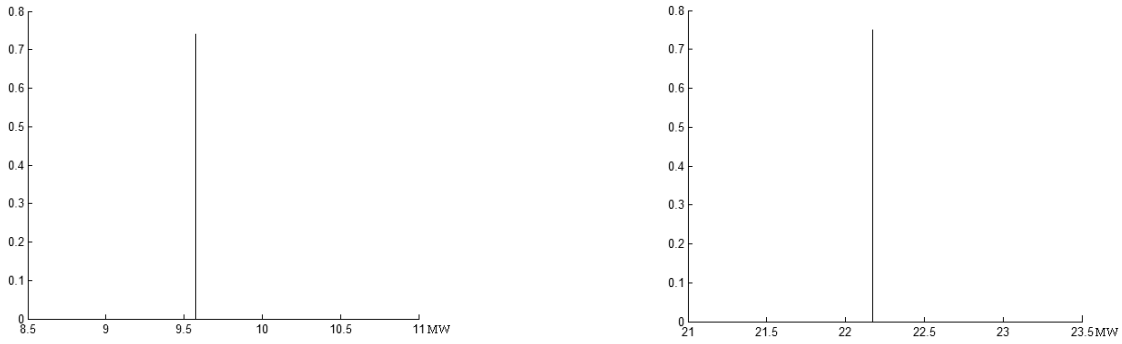

Figure 8.38: Membership function of the PNS expected value when generator 23/1 is available and when it is not available (at right) (modelling generation costs uncertainties).

Similarly to what happened for the load uncertainty modelling, Figure 8.38 also shows that when the system generation capacity decreases the expected value of the Power Not Supplied increases.

Figure 8.39 presents the membership functions of the expected values of the nodal marginal prices on buses 1, 22 and 24. From this Figure we can also see that reliability data has large influence on the nodal marginal price values, since they now exhibit much larger values reflecting the occurrence of PNS values different from zero.

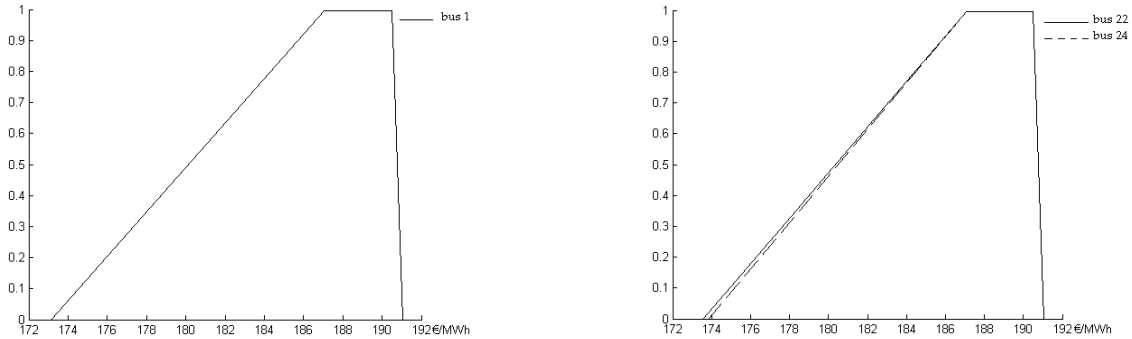

Figure 8.39: Membership function of the expected value of the nodal marginal price on bus 1, 22 and 24 (modelling generation costs uncertainties).

To evaluate the performance of the algorithm with respect to different conditions and parameters, it was also analysed a situation in which generator 23/1 (800 MW) was removed from the system. In this context, Figure 8.40 presents the expected value of the nodal marginal prices at buses 1 (at left), 22 and 24 (at right) for this situation.

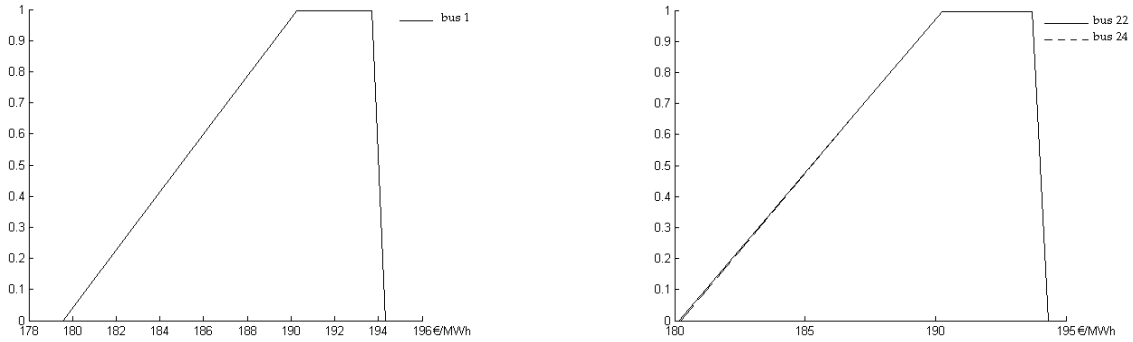

Figure 8.40: Membership function of the expected value of the nodal marginal price on bus 1, 22 and 24 when generator 23/1 is not available (modelling generation costs uncertainties).

As expected, from this Figure is possible see that as a consequence of this new power system condition the nodal marginal price on these buses exhibit larger values than in the previous case (Figure 8.39).

8.3.3. Considering load and generation cost uncertainties simultaneously

In this simulation, we considered that loads uncertainties are represented by trapezoidal fuzzy numbers in such a way that at the 0.0 level the uncertainty of these numbers ranges from +/-5 per cent of their central values and at the 1.0 level the uncertainty ranges from +/- 2,5 per cent of their central values. We also considered the generation cost uncertainties presented in Section 8.3.2. In this context, Figure 8.41 presents the membership functions of the generators 13/3, 19/1 and 21/1 considering and not considering the transmission losses effect.

As we can see from the results, simultaneously modelling load and generation cost uncertainties turns the problem and the results more complex since they reflect characteristics of both cases analysed in Sections 8.3.1 and 8.3.2. In fact, the different generation strategies and generation values become function not only of load uncertainties, but also of the generation cost uncertainties. As a result, for some combinations of the specified uncertainties there is congestion on the branches 16-19 and 11-13. The congestion on branches 16-19 and 11-13 prevents generators 19/1 and 13/3 from having larger outputs. If transmission losses are considered as in the right side of Figure 8.41, the generation values are larger for the some uncertainty levels.

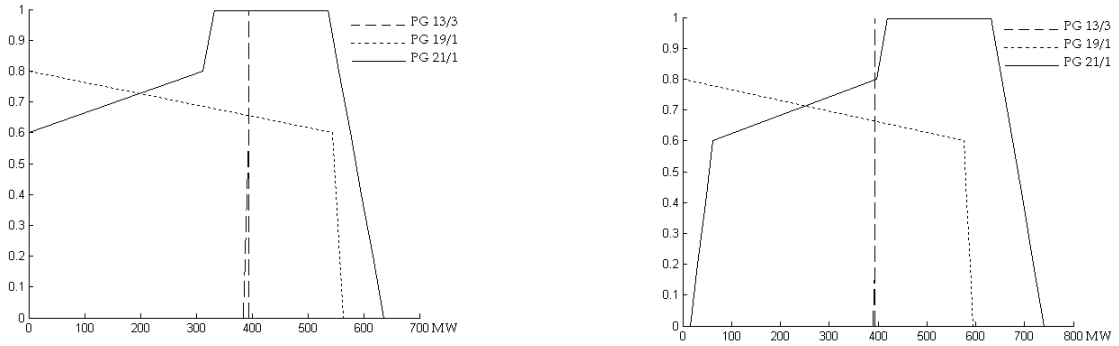

Figure 8.41: Membership functions of the generators 13/3, 19/1 and 21/1 not considering the transmission losses effect (at left) and considering this effect (at right) (loads and generation cost uncertainties modelling).

Figure 8.42 (at left) presents the membership functions of the nodal marginal prices in buses 15 and 21. This Figure indicates that these two nodal marginal prices are similar. This was expected since the nodal marginal prices incorporate the dual variable of the generation/load balance equation and the impact of increasing the load regarding congestions. For buses 15 or 21 this impact is very similar, explaining that these two membership functions are similar.

From the right hand side of Figure 8.42 we can also see the impact of the transmission losses on the nodal marginal prices of these buses. In this context, we can see that a load increase in these buses has different impacts on the overall system transmission losses. In fact, we can see that for some generation strategies (such as the ones corresponding to the definition of the left side of these memberships functions) a load increase on these buses implies a generalized system transmission losses increase since marginal prices on these buses increases. Nevertheless, for other generation strategies (such as the ones responsible for the definition of the right hand side of these membership functions) a load increase on these buses originates a decrease of transmission losses since marginal prices decreases.

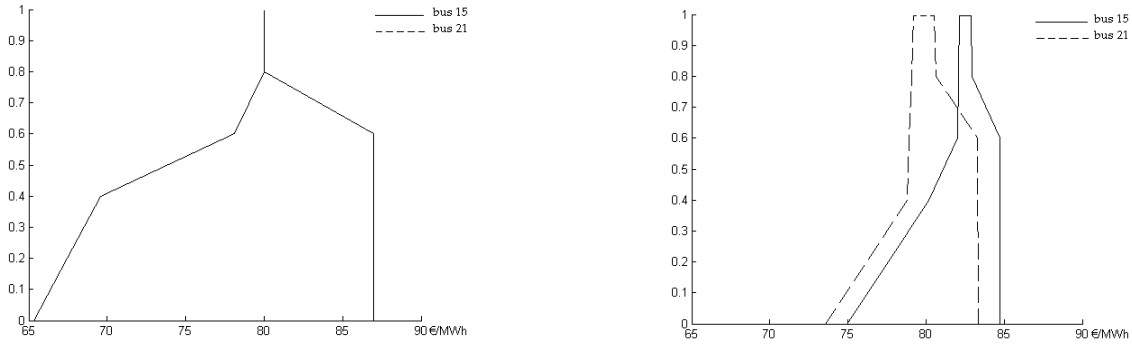

Figure 8.42: Membership functions of the nodal marginal prices on buses 15 and 21 considering the transmission losses effect (at right) and not considering this effect (at left) (loads and generation cost uncertainties modelling).

In line with what was mentioned in Section 8.3.1, Figure 8.43 presents the results obtained when the limits of branches 15-21 are reduced to 300,0 MW. From this Figure we can see that this new situation has the effect of reducing the maximum generation levels of generator 21/1.

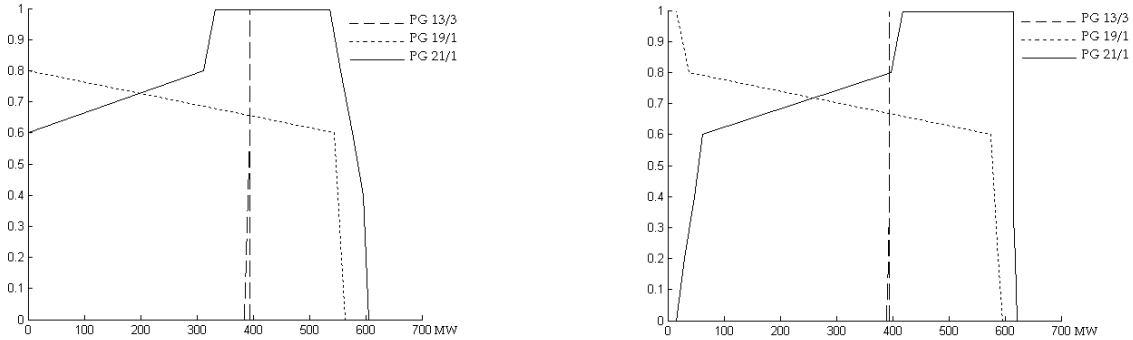

Figure 8.43: Membership functions of the generators 13/3, 19/1 and 21/1 when not considering the transmission losses effect (at left) and when this effect is considered (at right) (loads and generation cost uncertainties modelling).

Finally, Figure 8.44 presents the membership functions of the nodal marginal prices on buses 15 and 21 when the limits of branches 15-21 are set at 300,0 MW. As expected the membership functions of these prices are no longer similar, as they were on Figure 8.42. The congestion of branches 15-21 determines a maximum price of 87,0 €/MWh for bus 21 and a value larger than 100,0 €/MWh for bus 15. This situation is in line with what was mentioned in Section 8.3.1, because the nodal marginal price increases in bus 15 means that a generation increase or a load reduction in this bus contributes to alleviate congestion in branches 15-21.

Comparing the membership functions on the right side of Figure 8.44 with the ones presented in Figure 8.42 (at right) we can conclude that the left side of these membership functions are similar. However, the right side of these membership functions exhibit different behaviours reflecting the occurrence of branch congestions.

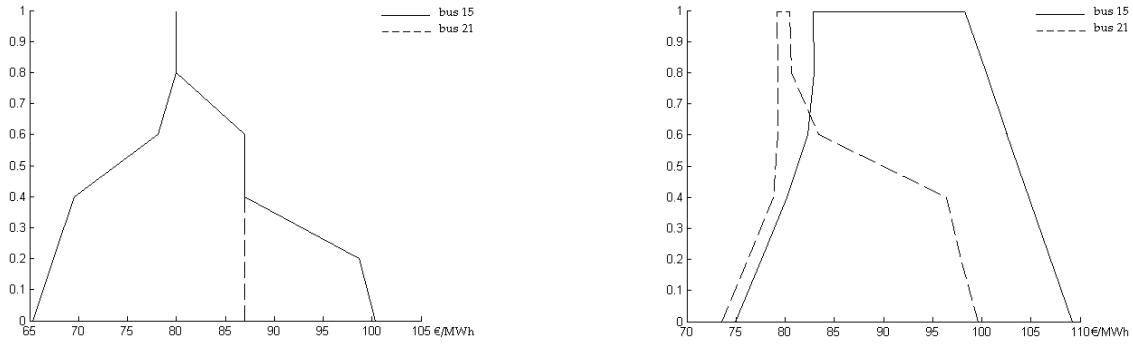

Figure 8.44: Membership functions of nodal marginal prices on buses 15 and 21 when considering the transmission losses effect (at right) and when not considering (at left) (loads and generation cost uncertainties modelling).

In order to evaluate the reliability and risk indices of the corresponding power system regarding the reliability data presented on Appendix C and the specified load and generation cost uncertainties, it was run the Fuzzy Monte Carlo algorithm presented on Chapter 7. In this context, it was possible to obtain some risk indices, such as, the expected value of the robustness index that, in this case, takes the value of 0,90 and the expected value of the exposure index that takes the value of 0,1.

To evaluate the performance of the algorithm with respect to different conditions and parameters, it was also analysed a situation in which the generator 23/1 (800 MW) was removed from the system. In this context, it was obtained a robustness index of 0,8571 (as expected smaller than the one previously obtained) and an exposure index of 0,1429 showing, in this way, that the system are now less robust. In Figure 8.45 (right side) it is presented the expected value of the PNS membership function obtained for this situation.

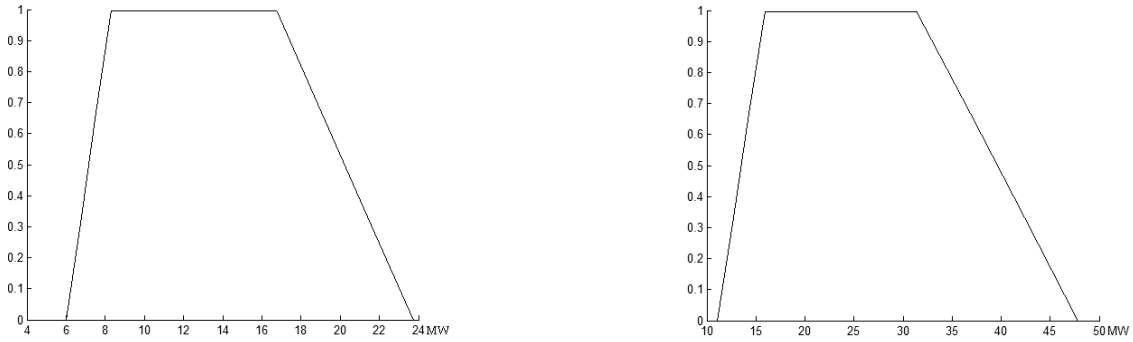

Figure 8.45: Membership function of the PNS expected value when generator 23/1 is available (at left) and when it is not available (at right) (modelling load and generation cost uncertainties).

Figure 8.46 presents the membership functions of the expected values of the nodal marginal prices on buses 22 and 24. From this Figure we can also see that reliability data has large influence on the nodal marginal price values, since they now exhibit much higher values reflecting the occurrence of PNS values different from zero.

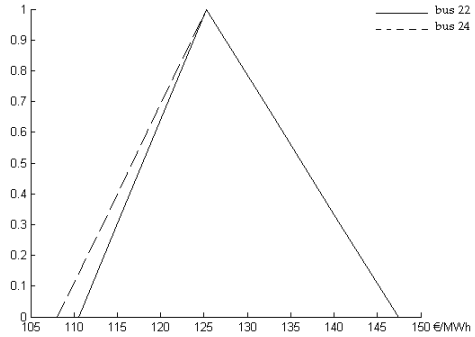

Figure 8.46: Membership function of the expected value of the nodal marginal price on buses 21 and 24 (modelling loads and generation cost uncertainties simultaneously).

If the generator 23/1 (800 MW) is not available, Figure 8.47 presents the expected value of the nodal marginal prices at buses 21 and 24 for this situation.

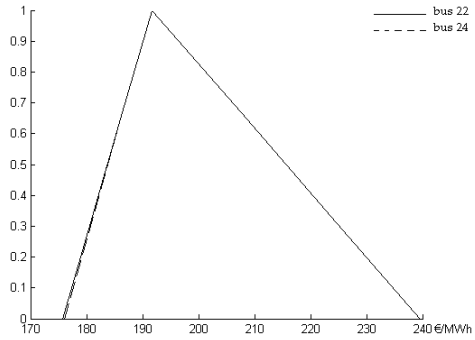

Figure 8.47: Membership function of the expected value of the nodal marginal price on buses 21 and 24 when it is not considered the generator 23/1 (modelling loads and generation costs uncertainties simultaneously).

As expected, from this Figure is possible see that as a consequence of removing generator 23/1 nodal marginal price on these buses exhibit larger values than in the previous case displayed in Figure 8.46.

CHAPTER IX Conclusions and Future Work

9. Conclusions and future work

The open access to the transmission networks is a crucial issue that must be guaranteed in order to create the proper conditions for the development of electricity markets. In this context, along this Thesis we had the opportunity to present and analyse some of the most commonly proposed and adopted methodologies for allocating transmission costs among system users. Within this description, marginal approaches deserved special attention since they are commonly pointed as the most economicaly sounded methodology.

We also described some of the traditional uncertainties present on power systems, as well as the new challenges that power systems are now facing deriving directly from a growing consciousness regarding environmental concerns, and by the global economy conjuncture reflected on primary energy uncertainty prices or even on load uncertainty levels. In this context, we presented several methodologies available in the literature regarding the uncertainty modelling on power system planning and operation, namely, probabilistic, interval arithmetic, boundary and Fuzzy models. This last approach deserved special attention in the last decade, since it is extremely adequate to model very low frequency or not completely characterized phenomena's, such as the ones previously mentioned.

In this context, in this Thesis we presented a new methodology, the New Fuzzy DC Optimal Power Flow, for modelling loads and/or generation cost uncertainties on the operation and planning of power systems, admitting that they are represented by fuzzy numbers. This new methodology besides allowing the independent or simultaneous modelling of load and generation cost uncertainties also uses linear multiparametric optimization techniques to systematically search all the uncertainty space allowing, in this way, to obtain more accurate results with respect to the variables under analysis. Additionally, they were also presented the algorithms developed in order to integrate the effect of the transmission losses on the results and to compute the nodal marginal prices when considering the mentioned uncertainties. Per last, it was also presented a reviewed version of an hybrid model, the Fuzzy Monte Carlo algorithm that, taking the NFOPF as the base algorithm, allows to model the reliability data of the system components (probabilistic), simultaneously with the uncertainty data specified for loads and/or generation cost (described by fuzzy numbers) in order to evaluate the system behaviour in presence of such uncertainties. As a result it was possible to obtain expected values of the overall system Power Not Supplied, of the nodal marginal prices and also of some risk indices like the exposure and robustness indices.

In this context, these algorithms can perform an important role in the current power system planning and operation environment since, for one side, when anticipating the nodal marginal price volatility we are addressing one of the most serious drawbacks associated with this transmission cost allocation methodology and, for another, when analysing the reliability of a power system together with all mentioned uncertainties we are contributing to give a positive answer to power system planners who certainty wish to take decisions based on a broader vision of their possible future impacts.

Following the European Union Directive 2003/54/EC, *each transmission system operator shall be responsible for ensuring the long-term ability of the system to meet reasonable demands for the transmission of electricity.* In this context and given the characteristics of the developed models, the author believes that, the in future, the developed methodologies will be useful for several entities in the power system sector, namely, for regulatory entities, for transmission and distribution companies and also for generation companies. In this context, regulatory entities and transmission and distribution companies would benefit from their capacity on the nodal marginal prices analysis domain and on the reliability and operation condition analysis domain. For generation companies these characteristics will certainly play an important function to maximize profits in environments characterized by several uncertainties like the ones described along this Thesis

With this Thesis the author, departing from a well know methodology termed as Fuzzy DC Optimal Power Flow, developed a new contribution to a such important topic as it is the uncertainty modelling in power system operation and planning. Its contribution could, obviously, be measure directly from the obtained results, but also from the results that, although not so clear, can be viewed as an indirect consequence of the first effort. In this Section, this kind of results could, eventually, be termed as *future work*, since they could be viewed as a continuation of the developed and presented work. In this sense, the author would like to mentioned that in future it should be investigated the impact of several co-related uncertainty parameters such as, co-related load uncertainty parameters (as it happens, for instance, with loads dependent on weather conditions within a given region), co-related generation cost parameters (as it happens, for instance, between generators operated by gas and fuel), co-related generation cost and load parameters (which could be also viewed as an attempt to model the elasticity of load regarding generation costs) or correlated availability of some primary resources in a given geographic region, namely, when talking about wind parks and hydro stations.

Given the new kind of uncertainties currently present on power systems, the developed algorithms can also be used to investigate the impact of some of the new market environment mechanisms in the power systems planning and operation. This can be done, by clearly defining generation cost parameters related with these market mechanisms. Since it is now unrealistic not considering the dispersed generation effect on power system planning and operation, one of the future challenges will certainly be the analysis of the behaviour of power systems operation regarding the uncertainty intrinsic to this kind of generation. At last, it should be also mentioned that the simultaneously modelling of all these uncertainties can also be an interesting work to develop in the future.

The application of more developed programming techniques like parallel programming ones to the developed algorithms would certainly contribute to reduce the computational effort and, consequently, turn it more adapted to the real sized networks. The author also believes that if this kind of techniques is effectively applied, methodologies like the one presented along this Thesis could be converted in powerful and accurate tools at the disposal of the real operation and planning power system problems.

BIBLIOGRAPHY

Bibliography

Aboytes, F. (1977), “Stochastic Contingency Analysis”, ibid., PAS-97, 1977.

Acevedo, J., Pistikopoulos, Efstratios N. (1997), “A Multiparametric Programming Approach for Linear Process Engineering Problems Under Uncertainty”, American Chemical Society, 1997.

Allan, R. N., Borkowska, B., Grigg, C. H. (1974), ”Probabilistic Analysis of Power Flows”, Proceedings of the IEE, Vol. 121, No. 12, December 1974.

Allan, R. N., Al-Shakarchi, M. R. G. (1976a), ”Probabilistic a.c. Load Flow”, Proceedings of the IEE, Vol. 123, No. 6, June 1976.

Allan, R. N., Grigg, C. H., Newey, D. A., Simmons, R. F. (1976b), “Probabilistic Power-Flow Techniques Extended and Applied to Operation Decision Making”, Proceedings of the IEE, Vol. 123, No. 12, December 1976.

Allan, R. N., Al-Shakarchi, M. R. G. (1977), ”Probabilistic Techniques in a.c. Load Flow Analysis”, Proceedings of the IEE, Vol. 124, No. 2, February 1977.

Allan, R. N., Grigg, C. H., Prato-Garcia, J. A. (1979), “Effect of Network Outages in Probabilistic Load Flow Analysis”, IEEE PES Winter Meeting, New York, February 1979.

Allan, R. N., Leite da Silva, A. M., Burchett, R. C. (1981a), “Evaluation Methods and Accuracy in Probabilistic Load Flow Solutions”, IEEE Transactions on PAS, Vol. PAS-100, 1981.

Allan, R. N., Leite da Silva, A. M. (1981b), “Probabilistic Load Flow Using Multilinearisations”, IEE Proceedings, Vol. 128, Pt. C, No. 5, 1981.

Allan, R., Billinton, R. (2000), “Probabilistic Assessment of Power Systems”, Proceedings of the IEEE, Vol. 88, No. 2, February 2000.

Agência Nacional de Energia Eléctrica – ANEEL (1999a), “Manual da Metodologia Nodal para Cálculo de Tarifas de Uso dos Sistemas Eléctricos”, (in Portuguese), Brasília, 1999.

Agência Nacional de Energia Eléctrica – ANEEL (1999b), “Resolução nº 281 – Estabelece as Condições Gerais de Contratação do Acesso, Compreendendo o Uso e a Conexão, aos Sistemas de Transmissão e Distribuição de Energia Eléctrica”, (in Portuguese), October 1999.

Agência Nacional de Energia Eléctrica – ANEEL (2004), “Resolução Normativa nº 117 – Altera a Sistemática de Cálculo das Tarifas de Uso do Sistema de Transmissão – TUST”, (in Portuguese), December 2004.

Bakirtziz, A., Biskas, P., Maissis, A., Coronides, A., Kabouris, J., Efstathiou, M. (2001), "Comparasion of Two Methods for Long-Run Marginal Cost-Based Transmission Use-of-System Pricing", IEE Proc.-Gener. Transm. Distrib., Vol. 148, N0. 4, July 2001.

Bandemer, H., Nather, W. (1992), "Fuzzy Data Analysis", Kluwer Academic Publishers, cop. 1992.

Baran, M. E., Banunarayanan, V., Garren, K. E. (1999), "A Transaction Assessment for Allocation of Transmission Services", IEEE Transactions on Power Systems, Vol. 14, No. 3, August 1999.

Barbosa, F. Maciel (2005), "Fiabilidade do Sistema de Produção/Transporte", (in Portuguese) Faculdade de Engenharia da Universidade do Porto, 2005.

Baughman, Martin L., Siddiqi, Shams N. (1991), "Real-Time of Reactive Power: Theory and Case Study Results", IEEE Transactions on Power Systems, Vol. 6, No. 1, February 1991.

Baughman, Martin L., Lee, Walter W. (1992), "A Monte Carlo Model for Calculating Spot Market Prices of Electricity", IEEE Transactions on Power Systems, Vol. 7, No. 2, May 1992.

Bayona, G. L., Arriaga, I. J. P. (1994), "Chopin, a Heuristic Model for Long Term Transmission Expansion Planning", IEEE Transactions on Power Systems, Vol. 9, No. 4, November 1994.

Bijwe, P. R., Hanmandlu, M., Pande, V. N. (2005), "Fuzzy Power Flow Solutions with Reactive Limits and Multiple Uncertainties", Electrical Power Systems Research, Vol. 76, September 2005.

Billinton, R., Salvaderi, L., McCalley, J. D., Chao, H., Seitz, Th., Allan, R. N., Odom, J., Fallon, C. (1997), "Reliability Issues in Today's Electric Power Utility Environment", IEEE Transactions on Power Systems, Vol. 12, No 4, November 1997.

Billinton, R., Tang, X. (2004), "Selected Considerations in Utilizing Monte Carlo Simulation in Quantitative Reliability Evaluation of Composite Power Systems", Electric Power Systems Research, 2004.

Billinton, R., Wangdee, W. (2005), "Impact of Utilising Sequential and Nonsequential Simulation Techniques in Bulk-Electric-System Reliability Assessment", IEE Proceedings Generation, Transmission and Distribution, Vol. 152, No. 5, September 2005.

Blyth, W., Bradley, R., Bunn, D., Clarke, C., Wilson, T., Yang, M. (2007), "Investment Risks Under Uncertain Climate Change Policy", Energy Pol*icy*, Vol. 35, pp 5766-5773, November 2007.

Borkowska, B. (1974), "Probabilistic Load Flow", IEEE Transactions on PAS, Vol. PAS-93, 1974.

Braga, A. S., Saraiva, J. T. (2003), "Transmission Expansion Planning and Long Term Marginal Prices Calculation Using Simulated Annealing", IEEE Bologna PowerTech Conference, June 2003.

Braga, A. S., Saraiva, J. T. (2004a), "Long Term Transmission Expansion Planning – A Simulated Annealing Based Multiyear Algorithm Including Long Term Marginal Prices" 8th International Conference on Probabilistic Methods Applied to Power Systems, September 2004.

Braga, A. (2004b), "Metodologia de Planeamento da Expansão e Tarifação do Uso de Redes de Transporte de Energia Eléctrica em Ambiente Reestruturado", (in Portuguese), PhD Thesis, Faculdade de Engenharia da Universidade do Porto, May 2004.

Braten, J. (1997), "Transmission Pricing in Norway", Utilities Policy, Vol. 6, No. 3, 1997.

Bronson, R., Naadimuthu, G. (2001), "Investigação Operacional - Segunda edição", (in Portuguese) Mcgraw-Hill de Portugal, Lda., 2001.

Calviou, M. C., Dunnett, R. M., Plumptre, P. H. (1993), "Charging for Use of a Transmission System by Marginal Cost Methods", 11th PSCC, August 1993.

Caramanis, M. C., Bohn, R. E., Schweppe, F. C. (1982), "Optimal Spot Pricing: Practice and Theory", IEEE Transactions on Power Apparatus and Systems, Vol. PAS-101, No. 9, September 1982.

Caramanis, M. C., Roukos, N., Schweppe, F. C. (1989), "Wrates: A Tool for Evaluating the Marginal Cost of Wheeling", IEEE Transactions on Power Systems, Vol. 4, No. 2, May 1989.

Certo, J., Saraiva, J. T. (2001), "Evaluation of Target Prices for Transmission Congestion Contracts Using a Monte Carlo Accelerated Approach", IEEE Porto Power Tech Conference, September 2001.

Chattopadhyay, D., Bhattacharya, K., Parikh, Jyoti (1995), "Optimal Reactive Power Planning and its Spot-Pricing: An Integrated Approach", IEEE Transactions on Power Systems, Vol. 10, No. 4, November 1995.

Chaturvedi, A., Prasad, K., Ranjan, R. (2006), "Use of Interval Arithmetic to Incorporte the Uncertainty of Load Demand for Radial Distribution System Analysis", IEEE Transactions on Power Delivery, Vol. 21, No. 2, April 2006.

Chayakulkheeree, C., Ongsakul, W. (2005), “Fuzzy Constrained Optimal Power Dispatch for Competitive Electricity and Ancillary Services Markets”, Electrical Power Components and Systems, Vol. 33, 2005.

Chair, James D. M., Asgarpoor, S., Gedra, T., Halpin, M., Saini, N. K., Schrameyer, M. H. (1997), “Second Bibliography on Transmission Access Issues”, IEEE Transactions on Power Systems, Vol. 12, No. 4, November 1997.

Chen, L., Suzuki, H., Wachi, T., Shimura, Y. (2002), “Components of Nodal Prices for Electric Power Systems”, IEEE Transactions on Power Systems, Vol. 17, No. 1, February 2002.

Crousillat, Enrique O., Dorfner, P., Alvarado, P., Merrill, Hyde M. (1993), “Conflicting Objectives and Risk in Power System Planning”, IEEE Transactions on Power Systems, Vol. 8, No. 3, August 1993.

Dantzig, George B. (1956), “Recent Advances in Linear Programming”, Management Science, 1956.

Das, D., Ghosh, S., Srinivas, D. K. (1999), “Fuzzy Distribution Load Flow”, Electric Machines and Power Systems, Vol. 27, 1999.

Das, Biswarup (2002), “Radial Distribution System Power Flow Using Interval Arithmetic”, Electrical Power and Energy Systems, Vol. 24, 2002.

Dimitrovski, A., Ackovski, R. (1996), “Probabilistic Load Flow in Radial Distribution Networks”, Proceedings of the 1996 14th IEEE Transmission Distribution Conference, 1996.

Dimitrovski, A., Matos, M. A. (2000), “Fuzzy Engineering Economic Analysis”, IEEE Transactions on Power Systems, Vol., 15, No. 1, February 2000.

Dimitrivski, A., Tomsovic, K. (2004), “Boundary Load Flow Solutions”, IEEE Transactions on Power Systems, Vol. 19, No. 1, February 2004.

Dimitrivski, A., Tomsovic, K. (2005), “Slack Bus Treatment in Load Flow Solutions with Uncertain Nodal Powers”, Electrical Power and Energy Systems, Vol. 27, November/December, 2005.

Directiva 2003/54/CE do Parlamento Europeu e do Conselho (2003), “que estabelece as regras comuns para o mercado interno da electricidade”, (in Portuguese), 26 de Junho de 2003.

Directiva 2003/55/CE do Parlamento Europeu e do Conselho (2003), “que estabelece as regras comuns para o mercado interno do gás natural”, (in Portuguese), June 2003.

Directiva 2004/8/CE do Parlamento Europeu e do Conselho (2004), "relativa à promoção da cogeração baseada na utilização do calor no mercado interno da energia", (in Portuguese) February 2004.

Dubois, D., Prade, H. (1980), "Fuzzy Sets and Systems", Academic Press Inc., 1980.

El-Hawary, M. E., Mbamalu, G. A. N. (1989), "Stochastic Optimal Load Flow Using a Combined Quasi-Newton and Conjugated Gradient Technique", Electric Power & Energy Systems, Vol. 11, No. 2, April 1989.

El-Keib, A. A., Ma, X. (1997), "Calculating Short-Run Marginal Costs of Active and Reactive Power Production", IEEE Transactions on Power Systems, Vol. 12, No. 2, May 1997.

Farinelli, U., Johansson, T. B., McCormick, K., Mudanca, L., Oikonomou, V., Ortenvik, M., Patel, M., Santi, F. (2005), "White and Green: Comparison of Market-Based Instruments to Promote Energy Efficiency", Journal of Cleaner Production, vol. 13, pp 1015-1026, August/September 2005.

Farmer, E. D., Perera, B. L. P. P., Cory, B. J. (1995), "Optimal Pricing of Transmission Services: Application to Large Power Systems", IEE Proc.-Gener. Transm. Distrib., Vol. 142, No. 3, May 1995.

Finney, John D., Othman, Hisham A., Rutz, William L. (1997), "Evaluating Transmission Congestion Constraints in System Planning", IEEE Transactions on Power Systems, Vol. 12, No. 3, August 1997.

Freund, Robert M. (1985), "Postoptimal Analysis of a Linear Program Under Simultaneous Changes in Matrix Coefficients", Mathematical Programming Study, October, 1985.

Gal, Tomas, Nedoma, Josef (1972), "Multiparametric Linear Programming", Management Science, Vol. 18, No. 7, March 1972.

Gal, Tomas (1975), "Rim Multiparametric Linear Programming", Management Science, Vol. 21, No. 5, January 1975.

Gal, Tomas (1979), "Postoptimal Analyses, Parametric Programming, and Related Topics", Mcgraw-Hill International Book Company, 1979.

Gal, Tomas (1993a), "Selected Bibliography on Degeneracy", Annals of Operations Research, No. 46, 1993.

Gal, Tomas (1993b), "Degeneracy Graphs: Theory and Application. An Updated Survey", Annals of Operations Research, No. 46, 1993.

Galetovic, A., Montecinos, Cristián M. (2006), "The New Chilean Transmission Charge Scheme as Compared With Current Allocation Methods", IEEE Transactions on Power Systems, Vol. 21, No. 1, February 2006.

Gil, Hugo A., Galiana, Francisco D., Silva, Edson L. (2006), "Nodal Price Control: A Mechanism for Transmission Network Cost Allocation", IEEE Transactions on Power Systems, Vol. 21, No. 1, February 2006.

Gomes, Bruno A. (2005), "Simulator of the Market and System Operators in Electricity Markets Considering Inter-temporal Constraints", (in Portuguese), MSc Thesis, Faculdade de Engenharia da Universidade do Porto, September 2005.

Gomes, B. A., Saraiva, J. T. (2007), "Calculation of Nodal Marginal Prices Considering Load and Generation Price Uncertainties", Proceedings of the IEEE Lausanne Power Tech, Lausanne, Switzerland, 2007.

Gomes, Bruno A., Saraiva, J. T., Neves, L. (2008), "Modelling Costs and Load Uncertainties in Optimal Power Flow Studies", 5th International Conference on the European Electricity Market, Portugal, May, 2008.

Gribik, P. R., Shirmohammadi, D., S. Hao, Thomas, C. L. (1990), "Optimal Power Flow Sensitivity Analysis", IEEE Transactions on Power Systems, Vol. 5, August 1990.

Green, Richard (1997a), "Transmission Pricing in England and Wales", Utilities Policy, Vol. 6, No. 3, 1997.

Green, Richard (1997b), "Electricity Transmission Pricing: An International Comparison", Utilities Policy, Vol. 6, No. 3, 1997.

Guan, Xiaohong, Liu, W. H. Edwin, Papalexopolus, Alex D. (1995), "Application of a Fuzzy Set Method in an Optimal Power Flow", Electric Power System Research, Vol. 34, No. 1, July 1995.

Hadigheh, Alireza G., Terlaky, T. (2005), "Sensitivity Analysis in Linear Optimization: Invariant Support Set Intervals", European Journal of Operational Research, July 2005.

Hao, S., Papalexopoulos, A. (1997), "Reactive Power Pricing and Management", IEEE Transactions on Power Systems, Vol. 12, No. 1, February 1997.

Happ, H. H. (1994), "Cost of Wheeling Methodologies", IEEE Transactions on Power Systems, Vol. 9, No. 1, February 1994.

Harris, Phillip G. (2000), "Impacts of Deregulation on the Electric Power Industry", IEEE Power Engineering Review, October 2000.

Hu, Z., Wang, X. (2006), "A Probabilistic Load Flow Method Considering Branch Outages", IEEE Transactions On Power Systems, Vol. 21, No. 2, May 2006.

Imbert, J-L., Hentenryck, P. Van (1996), "Redundancy Elimination with a Lexicographic Solved Form", Annals of Mathematics and Artificial Intelligence, 1996.

Jansen, B., Jong, J. J., Roos, C., Terlaky, T. (1996), "Sensitivity Analysis in Linear Programming: Just be Careful!", European Journal of Operational Research, May 1996.

Jesus, Paulo M., Leão, T. (2004), "Impact of Uncertainty and Elastic Response of Demand in Short Term Marginal Prices", 8th International Conference on Probabilistic Methods Applied to Power Systems, Ames, Iowa, September, 2004.

John, R., Coupland, S. (2007), "Type-2 Fuzzy Logic: A Historical View", IEEE Computational Intelligence Magazine, February 2007.

Jones, C. N., Kerrigan, E. C., Maciejowski, J. M. (2007), "Lexicographic Perturbation for Multiparametric Linear Programming with Applications to Control", Automatica Oct., January 2007.

Karakatsanis, T. S., Hatziargyriou, N. D. (1994), "Probabilistic Constrained Load Flow Based on Sensitivity Analysis", IEEE Transactions on Power Systems, Vol. 9, No. 9, 1994.

Kaye, R., Outhred, H. R. (1989), "A Theory of Electricity Tariff Design for Optimal Operation and Investment", IEEE Transactions on Power Systems, Vol. 4, No. 2, May 1989.

Kaye, R. John, Wu, F. F., Varaiya, P. (1995), "Pricing for System Security", IEEE Transactions on Power Systems, Vol. 10, No. 2, May 1995.

Katz, S., Risman, L. J., Rodeh, M. (1980), "A System for Constructing Linear Programming Models", IBM System Journal, Vol. 19, No .4, 1980.

Kaufman, A., Gupta, M. M. (1988), "Fuzzy Mathematical Techniques Models in Engineering and Management Science", North Holland, Amesterdam, 1988.

Kovacs, Ross. R., Leverett, A. (1994), "A Load Flow Based Method for Calculating Embedded, Incremental and Marginal Cost of Transmission Capacity", IEEE Transactions on Power Systems, Vol. 9, No. 1, February 1994.

Krause, Thilo (2003), "Evaluation of Transmission Pricing Methods for Liberalized Markets – A Literature Survey", EEH-Power Systems Laboratory and ETH-Swiss Federal Institute of Technology, Zurich, July 2003.

Lamont, John W., Fu, J. (1999), "Cost Analysis of Reactive Power Support", IEEE Transactions on Power Systems, Vol. 14, No. 3, August 1999.

Lankford, Craig B., MacCalley, James D., Saini, Narinder K. (1996), "Bibliography on Transmission Access Issues – by the Bibliography Subcommitee of the IEEE Task Force on Transmission Access and Nonutility Generation", IEEE Transactions on Power Systems, Vol. 11, No. 1, February 1996.

Leão, M. T. P. (1995), "Planeamento de Redes de Distribuição com Produção Independente", (in Portuguese), PhD Thesis, Faculdade de Engenharia da Universidade do Porto, 1995.

Leão, M. T. P. (1999), "Marginal Cost Computation Using Simulated Annealing", IEEE Power Tech '99 Conference, Budapest, August - September, 1999.

Leão, M. T. P., Saraiva, J. T. (2000), "A Simulated Annealing Approach to Evaluate Long Term Marginal Costs and Investment Decisions", IEEE Power Engineering Society Summer Meeting, Conference Proceedings, 2000.

Leão, M. T. P., Saraiva, J. T. (2003), "Solving the Revenue Reconciliation Problem of Distribution Network Providers Using Long-Term Marginal Prices", IEEE Transactions on Power Systems, Vol. 18, No. 1, February 2003.

Leite da Silva, A. M., Allan, R. N., Soares, S. M., Arienti, V. L. (1985), "Probabilistic Load Flow Considering Network Outages", IEE Proceedings, 132, Pt. C, 1985.

Leite da Silva, A. M., Ribeiro, S. M. P., Arienti, V. L., Allan, R. N., Couto Filho, M. B. (1990a), "Probabilistic Load Flow Techniques Applied to Power System Expansion Planning", IEE Transactions on Power Systems, Vol. 5, No. 4, November 1990.

Leite da Silva, A. M., Arienti, V. L. (1990b), "Probabilistic Load Flow by a Multilinear Simulation Algorithm", IEE Proceedings, Vol. 137, Pt. C., No. 4, 1990.

Leite da Silva, A. M., Perez, G., Lima, Maragon J. W., Mello, J. C. O. (1997), "Loss of Load Costs in Generating Capacity Reliability Evaluation", Electric Power Systems research, 1997.

Leite da Silva, A. M., Manso, L. A. F., Anders, G. J. (2004), "Evaluation of Generation and Transmission Maintenance Strategies Based on Reliability Worth", Electric Power System Research, 71, 2004.

Li, Y. Z., David, A. K. (1993), "Pricing Reactive Power Conveyance", IEE Proceedings-C, Vol. 140, No. 3, May 1993.

Li, Y. Z., David, A. K. (1994a), "Wheeling Rates of Reactive Power Flow Under Marginal Cost Pricing", IEEE Transactions on Power Systems, Vol. 9, No. 3, August 1994.

Li, Y. Z., David, A. K. (1994b), "Optimal Multi-Area Wheeling", IEEE Transactions on Power Systems, Vol. 9, No. 3, August 1994.

Lien, Chun (2005), "Probabilistic Load Flow Computation Using Point Estimate Method", IEEE Transactions on Power Systems, Vol. 20, No. 4, November 2005.

Lima, J.W. Marangon, Pereira, M. V. F., Pereira, J. L. R. (1995), "An Integrated Framework for Cost Allocation in a Multi-Owned Transmission System", IEEE Transactions on Power Systems, Vol. 10, No. 2, May 1995.

Lima, J.W. Marangon (1996), "Allocation of Transmission Fixed Charges: An Overview", IEEE Transactions on Power Systems, Vol. 11, No. 3, August 1996.

Lima, J. W. Marangon, Oliveira, E. J. (1998), "The Long-Term Impact of Transmission Pricing", IEEE Transactions on Power Systems, Vol. 13, No. 4, November 1998.

Lin, Benjamin W. Y. (1977), "Development of a Parametric Generating Procedure for Integer Programming Test Problems", Journal of the Association for Computing Machinery, Vol. 24, No. 3, July, 1977.

Lin, Benjamin W. Y., Rardin, Ronald L. (1997), "Development of a Parametric Generating Procedure for Integer Programming Test Problems", Journal of the Association for Computing Machinery, Vol. 24, No. 3, July 1997.

Liu, W. H. Edwin, Guan, Xiaohong (1996), "Fuzzy Constraint Enforcement and Control Action Curtailment in an Optimal Power Flow", IEEE Transactions on Power Systems, Vol. 11, No. 2, May 1996.

Lobo, L. V. (2000), "Determinação de Índices de Fiabilidade em Sistemas Eléctricos Utilizando o Método de Monte Carlo", (in Portuguese) MSc Thesis, Faculdade de Engenharia da Universidade do Porto, September 2000.

Ma, X., El-Keib, A. A., Haskew, Tim A. (1998), "Marginal Cost-Based Pricing of Wheeling Transactions and Independent Power Producers Considering Security Constraints", Electric Power Systems Research, February 1998.

Machado, J. T. P., Areias, L. E., Marzano, L. G. B., Ribeiro, P. M., Caldas, R. P. (2001), "Generation Investments in the Brazilian New Electric Sector Model: An Analysis of Transmission Tariffs", IEEE Porto Power Tech Conference, September 2001.

Madansky, A. (1962), "Methods of Solution of Linear Programs Under Uncertainty", Operations Research, 1962.

Madrigal, M., Ponnambalam, K., V. H. Quintana (1998), "Probabilistic Optimal Power Flow", Proceedings IEEE Canadian Conference on Electrical and Computer Engineering, Waterloo, Canada, 1998.

Mangueira, Heitor H. D., Saavedra, Osvaldo R., Pessanha, José E. O. (2008), "Impact of Wind Generation on the Dispatch of the System: A Fuzzy Approach", Electrical Power and Energy Systems, Vol. 30, 2008.

Manso, L. A. F., Leite da Silva, A. M., Mello, J. C. O. (1999), "Comparasion of Alternative Methods for Evaluating Loss of Load Costs in Generation and Transmission Systems", Electric Power Systems research, 50, 1999.

Marannino, P., Vailati, R., Zanellini, F., Bompard, E., Gross, G. (2001), "OPF Tools for Optimal Pricing and Congestion Management in a Two Sided Auction Market Structure", IEEE Porto Power Tech Conference, September 2001.

Matos, Manuel A. (2004), "Normas para apresentação de dissertações – Bases essenciais", (in Portuguese) Faculdade de Engenharia da Universidade do Porto, January 2004.

Matos, Manuel A. (2008), Gouveia, Eduardo M., "The Fuzzy Power Flow Revisited", IEEE Transactions on Power Systems, Vol. 23, No 1, February 2008.

Mello, J. C. O., Pereira, M. V. F., Leite da Silva, A. M. (1994), "Evaluation of the Reliability Worth in Composite Systems Based on Pseudo-Sequential Monte Carlo Simulation", IEEE Transactions on Power Systems, Vol. 9, No., 3, August 1994.

Mendel, Jerry M. (2007), "Type-2 Fuzzy Sets and Systems: An Overview", IEEE Computational Intelligence Magazine, February 2007.

Merrill, H. M., Erickson, B. W. (1989), "Wheeling Rates Based on Marginal-Cost Theory", IEEE Transactions on Power Systems, Vol. 4, No. 4, October 1989.

Merrill, Hyde M., Wood, Allen J. (1990), "Risk and Uncertainty in Power System Planning", 10th Power Systems Computation Conference, PSCC, August, 1990.

Miranda, V., Matos, Manuel A. (1989), "Distribution System Planning With Fuzzy Models and Techniques", 10th International Conference on Electricity Distribution - CIRED, 1989.

Miranda, V., Matos, M. A., Saraiva, J. T. (1990), "Fuzzy Load Flow - New Algorithms Incorporating Uncertain Generation and Load Representation", Proceedings of the 10th PSCC, Butterworths, London, 1990.

Miranda, V., Saraiva, J. T. (1992), "Fuzzy Modelling of Power System Optimal Load Flow, IEEE Transactions on Power Systems, 7, 1992.

Monteiro,. Cláudio (2002), "Fuzzy Spatial Load Forecasting", PhD Thesis, Faculdade de Engenharia da Universidade do Porto, 2002.

Muela, E., Schweickardt, G., Garcés, F. (2007), "Fuzzy Possibilistic Model for Medium-Term Power Generation Planning With Environmental Criteria", Energy Policy, Vol. 35, 2007.

Munasinghe, M. (2001), “Principles of Modern Electricity Pricing”, Proceedings of the IEEE, Vol. 69, No 3, March 2001.

Murphy, L., Kaye, R. J., Wu, F., F. (1994), “Distributed Spot Pricing in Radial Distribution Systems”, IEEE Transactions on Power Systems, Vol. 9, No. 1, February 1994.

Murtagh, Bruce A. (1981), “Advanced Linear Programming: Computation and Practice”, Mcgraw-Hill International Book Company, 1981.

Narayan, S. Rau (1989), “Certain Considerations in the Pricing of Transmission Service”, IEEE Transactions on Power Systems, Vol. 4, No. 3, August 1989.

Odériz, J. R, Arriaga, I. J. P. (2000), “Marginal Pricing of Transmission Services: A Comparative Analysis of Network Cost Allocation Methods”, IEEE Transactions on Power Systems, Vol. 15, No. 1, February 2000.

Oliveira, G. C., Pereira, M. V. F., Cunha, S. H. F. (1989), “A Technique For Reducing Computational Effort in Monte-Carlo Based Composite Reliability Evaluation”, IEEE Transactions on Power Systems, Vol. 4, No. 4, October 1989.

Oren, Shamuel S., Spiller, Pablo T., Varaiya, P., Wu, F. (1995), “Nodal Prices and Transmission Rights: A Critical Appraisal”, The Electricity Journal, April 1995.

Paiva, José P. (2005), “Redes de Energia eléctrica – Uma Análise Sistémica”, (in Portuguese) IST Press, Abril 2005.

Pan, J., Teklu, Y., Rahman, S. (2000), “Review of Usage-Based Transmission Cost Allocation Methods Under Open Access”, IEEE Transactions on Power Systems, Vol. 15, No. 4, November 2000.

Patton, A. D., Blackstone, J. H., Balu, N. J. (1988), “A Monte Carlo Simulation Approach to the Reliability Modeling of Generation Systems Recognizing Operation Considerations”, IEEE Transactions on Power Systems, Vol. 3, No. 3, August 1988.

Paulraj, S., Chellappan, C., Natesan, T. R. (2006), “A Heuristic Approach for Identification of Redundant Constraints in Linear Programming Models”, International Journal of Computer Mathematics, Vol. 83, No. 8-9, August-September 2006.

Pereira, M. V., Maceira, M. E. P., Oliveira, G. C., Pinto, L. M. V. G., “Combining Analytical Models and Monte Carlo Techniques in Probabilistic Power System Analysis”, IEEE Transactions on Power Systems, Vol. 7, No. 1, February, 1992.

Pereira, M. V., Balu, N. J. (1992a), “Composite Generation/Transmission Reliability Evaluation”, Proceedings of the IEEE, Vol. 80, No. 4, April 1992.

Pereira, M. V., Pinto, L. M. V. G. (1992b), "A New Computational Tool for Composite Reliability Evaluation", IEEE Transactions on Power Systems, Vol. 7, No. 1, February 1992.

Pérez-Arriaga, Ignácio J., Rubio, F. J., Puerta, J. F., Marín, Arceluz J. (1995), "Marginal Pricing of Transmission Services: An Analysis of Cost Recovery", IEEE Transactions on Power Systems, Vol. 10, No. 1, February 1995.

Pérez-Arriaga, Ignácio J., Rudnick, H., Stadlin, Walter O. (1999), "International Power System Transmission Open Access Experience", IEEE Transactions on Power Systems, Vol. 10, No. 1, February 1999.

Rathmann, M. (2007), "Do Support Systems for RES-E Reduce EU-ETS-Driven Electricity Prices?", Energy Policy, Vol. 35, pp 342-349, January 2007.

Read, E. G., Sell, D. P. M. (1988), "Pricing and Operation of Transmission Services": Short-Run Aspects", Principles of Pricing Electricity Transmission, 1988.

Read, E. G. (1990), "Transmission Pricing in New Zeland", Utilities Policy, Vol. 6, No. 3, 1997.

Rivier, M., Pérez-Arriaga, I. J., Luengo, G. (1990), "JUANAC: A Model for Computation of Spot Prices in Interconnected Power Systems", 10th PSCC Conference, Graz, Austria, August 1990.

Rivier, M., Pérez-Arriaga, I. J. (1993), "Computation and Decomposition of Spot Prices for Transmission Pricing", 11th Power Systems Computation Conference, PSCC, Avignon, França, 1993.

Rivier, M., Pérez-Arriaga, I. J. Sánchez, P. Ramos, A., Gomez, T. (1994), "An Improved Version of the Model JUANAC: Applications to Network Adequacy and Economic Studies in Large Interconnected Power Systems", 4th Probabilistic Methods Applied to Power Systems Conference, PMAPS, Rio de Janeiro, Brazil, September 1994.

Rudnick, H., Palma, R., Fernández, J. E. (1995), "Marginal Pricing and Supplement Cost Allocation in Transmission Open Access", IEEE Transactions on Power Systems, Vol. 10, No. 2, May 1995.

Rudnick, H., Raineri, R. (1997), "Transmission Pricing Practices in South America", Utilities Policy, Vol. 6, No. 3, 1997.

Ruspini, Enrique H., Bonissone, Piero P., Pedrycz, W. (1998), "Handbook of Fuzzy Computation", Institute of Physics Publishing, 1998.

Ruth, M., Gabriel, S. A., Palmer, K.L., Burtraw, D., Paul, A., Chen, Y., Hobbs, B. F., Irani, D., Michael, J., Ross, K. M., Conklin, R., Miller, J. (2008), "Economic and Energy Impacts From Participation in the Regional Greenhouse Gas Initiative: A Case Study of the State of Maryland", Energy Policy, Vol. 36, pp 2279-2289, April 2008.

Saavedra, O. R., Mangueira, H. H. D., Chalco-cano, Y., Roman-Flores, H. (2007), "Solution of Non-Linear Fuzzy Systems by Decomposition of Incremental Fuzzy Numbers", Information Sciences, Vol. 177, October 2007.

Salvaderi, Luigi, Billinton, Roy (1985), "A Comparasion Between Two Fundamentally Different Approaches To Composite System Reliability Evaluation", IEEE Transactions on Power Apparatus and Systems, Vol. PAS-104, No. 12, December 1985.

Saraiva, J. T., Miranda, V., Matos, Manuel A. (1991), "Generation and Load Uncertainties Incorporated in Load Flow Studies", Proceedings of the 6th Mediterranean Electrotechnical Conference – Melecon, May, 1991.

Saraiva, J. T. (1992), "Aplicação de Conjuntos Imprecisos na Modelização e Planeamento de Sistemas Eléctricos", (in Portuguese) PhD Thesis, Faculdade de Engenharia da Universidade do Porto, 1992.

Saraiva, J. Tomé, Miranda, Vladimiro (1993), "Impacts in Power System Modeling From Including Fuzzy Concepts in Models", Proceedings of Athens Power Tech, September 1993.

Saraiva, J. T., Miranda, V. (1994a), "Impact in Some Planning Decisions From a Fuzzy Modelling of Power Systems", IEEE Transactions on Power Systems, Vol. 9, No. 2, May 1994.

Saraiva, J. T., Miranda, V. (1994b), "Evaluation of the Performance of a Fuzzy Optimal Power Flow Algorithm", Proceedings of the Mediterranean Electrotechnical Conference - MELECON, 1994.

Saraiva, J. T., Miranda, V. (1994c), "Flexible Power System Reinforcement Planning Under Uncertainty Proceedings of the Mediterranean Electrotechnical Conference - MELECON, 1994.

Saraiva, J. T., Miranda, V. (1996a), "Identification of Hedging Policies in Generation/Transmission Systems", 12th Power Systems Computation Conference, Dresden, August 1996.

Saraiva, J. T., Miranda, V., Pinto, L. M. V. G. (1996b), "Generation/ Transmission Power System Reliability Evaluation by Monte-Carlo Simulation Assuming a Fuzzy Load Description", IEEE Transaction on Power Systems, Vol. 11, 1996.

Saraiva, J. T. (1999a), "Modelo de Cálculo de Preços Spot e Integração de Incertezas", 4º Encontro Luso-Afro-Brasileiro e Exploração de Redes de Energia - ELAB'99, Junho 1999.

Saraiva, J. T. (1999b), "Evaluation of the Impact of Load Uncertainties in Spot Prices Using Fuzzy Set Models", 13th PSCC in Trondheim, July 1999.

Saraiva, J. T., Silva, J. P., Leão, M. T. (2001), "Evaluation of the Marginal Based Remuneration – A Case Study Using the Portuguese Transmission Network", IEEE Porto Power Tech Conference, September 2001.

Saraiva, J. T., Silva, P., Leão, M. T. (2002), "Mercados de Electricidade – Regulação e Tarifação de Uso das Redes", FEUP edições, 2002.

Saraiva, J. T., Sá, André F. (2004a), "Evolution of the Marginal Based Remuneration of the Portuguese Transmission Network From 1998 to 2001", IX Simpósio de Especialistas em Planejamento da Operação e Expansão Eléctrica - SEPOPE, Rio de Janeiro, Maio 2004.

Saraiva, J. T., Fonseca, N., Matos, M. A. (2004b), "Fuzzy Power Flow - An AC Model Adrdressing Correlated Data", 8th International Conference on Probabilistic Methods Applied to Power Systems, September, 2004.

Schellenberg, A., Rosehart, W., Aguado, J. (2005), "Cumulant-Based Probabilistic Optimal Power Flow (P-OPF) with Gaussian and Gamma Distributions", IEEE Transactions on Power Systems, 20, 2005.

Schilling, M. Th., Billinton, R., Leite da Silva, A. M., El-Kady, M. A. (1989), "Bibliography on Composite System Reliability", IEEE Transactions on Power Systems, Vol. 4, No 3, August 1989.

Schilling, M. Th., Leite da Silva, A. M., Billinton, R., Allan, R. N. (1995), "An Integrated Approach to Power System Reliability Assessment", Electric Power & Energy Systems, Vol. 17, No. 6, 1995.

Schweppe, Fred C., Caramanis, Michael C., Tabors, Richard D., Bohn, Roger E. (1988), "Spot Pricing of Electricity", Kluwer Academic Publishers, March 1988.

Silva, J. P., Saraiva, J. T., Leão, M. T. (2001), "Use of Power Flow Based Embedded Methods to Set Tariffs for Use of Networks – A Case Study Using the Portuguese Transmission Company", IEEE Porto Power Tech Conference, September 2001.

Shirmohammadi, D., Gribik, Paul R., Law, Eric T. K., Malinowski, James H., O'Donnell, Richard E. (1989), "Evaluation of Transmission Network Capacity Use for Wheeling Transactions", IEEE Transactions on Power Systems, Vol. 4, No. 4, October 1989.

Shirmohammadi, D., Rajagopalan, C., Alward, Eugene R., Thomas, Chifong L. (1991), "Cost of Transmission Transactions: An introduction", IEEE Transactions on Power Systems, Vol. 6, No. 4, November 1991.

Shirmohammadi, D., Gorenstin, Xisto V., Pereira, Mário V. P. (1996), "Some Fundamental Technical Concepts about Cost Based Transmission Pricing", IEEE Transactions on Power Systems, Vol. 11, No. 2, May 1996.

Soderholm, P. (2008), "The Political Economy of International Green Certificates Market", Energy Policy, vol. 36, pp 2051-2062, June 2008.

Sousa, António T. (1997), "Estudos de Fiabilidade Utilizando o Método de Simulação de Monte Carlo Integrando Informação Expressa sob a Forma de Números Imprecisos", (in Portuguese) MSc Thesis, September 1997.

Spinney, Peter J., Watkins, G. Campbell (1996), "Monte Carlo Simulation Techniques and Electric Utility Resource Decisions", Energy Policy, Vol. 24, No 2, 1996.

Stoft, S., Webber, C., Wiser, R. (1997), "Transmission Pricing and Renewables: Issues, Options, and Recommendations", University of California, California, May 1997.

Sugihara, Kokichi (1999), "Exact Computation of 4-D Convex Hulls with Perturbation and Acceleration", Proceedings, 7th Pacific Conference on Computer Graphics and Applications, 1999.

Tabors, Richard D., Schweppe, F. C., Caramanis, M. C. (1989), "Utility Experience With Real Time Rates", IEEE Transactions on Power Systems, Vol. 4, No. 2, May 1989.

Tabors, Richard D. (1994), "Transmission System Management and Pricing: New Paradigms and International Comparisons", IEEE Transactions on Power Systems, Vol. 9, No. 1, February 1994.

Taha, H. (2003), "Operations Research: An Introduction – Seventh Edition", Prentice Hall, 2003.

Task Force of Application Probabilistic Methods Subcommittee (1979), "IEEE Reliability Test System", IEEE Transactions PAS, Vol. PAS-98, No. 6, November - December 1979.

Telgen, Jan (1983), "Identifying Redundant Constraints and Implicit Equalities in Systems of Linear Constraints", Management Science, Vol. 29, N0 10, October 1983.

Tsukamoto, Y., Iyoda, I. (1996), "Allocation of Fixed Transmission Cost to Wheeling Transactions by Cooperative Game Theory", IEEE Transactions on Power Systems, Vol. 11, No. 2, May 1996.

UNIPEDE System Tariff Issues Working Group (1997), “Principles of Transmission Pricing”, May 1997.

Verbic, G., Canizares, Claudio A. (2006), “Probabilistic Optimal Power Flow in Electricity Markets Based on a Two-Point Estimate Method”, IEEE Transactions on Power Systems, Vol. 21, No. 4, November 2006.

Verma, Ajit. K., Srividya, A. (2002), “A Framework Using Uncertainties in the Composite Power System Reliability Evaluation”, Electric Power Components and Systems, 30:679-691, 2002.

Vojdani, A. F., Imparato, C. F., Saini, N. K., Wollenberg, B. F., Happ, H. H. (1996), “Transmission Access Issues”, IEEE Transactions on Power Systems, Vol. 11, No. 1, February 1996.

Wang, Z., Alvarado, Fernando L., “Interval Arithmetic in Power Flow Analysis”, Transactions on Power Systems, Vol. 7, No. 3, August 1992.

Wang, P., Billinton, R. (2003), “Reliability Assessment of a Restructured Power System Using Reliability Network Equivalent Techniques”, IEE Proceedings on Generation, Transmission and Distribution, Vol. 150, No 5, September 2003.

Zadeh, L.A. (1965), “Fuzzy Sets, Information and Control”, No 8, 1965.

Zadeh, L.A., “Fuzzy Sets as a Basis for a Theory of Possibility”, Fuzzy Sets and Systems, Vol. 1, No. 1, 1999.

Zhang, P., Lee, S. T. (2004), “Probabilistic Load Flow Computation Using the Method of Combined Cumulants and Gram-Charlier Expansion”, IEEE Transactions on Power Systems, Vol. 19, No. 1, February 2004.

Zimmermann, H. J. (1991, “Fuzzy Sets, Decision Making and Expert Systems”, Kluwer, imp., 1991.

Web site list

Aneel	-	Agência Nacional de Energia Eléctrica, http://www.aneel.gov.br/, Brasil
Cne	-	Comisión Nacional de Energía, http://www.cne.es/, Spain
Cne	-	Comisión Nacional de Energía, http://www.cne.cl/, Chile
Elkraft System	-	Transmission and System Operator, http://www.eng.elkraft-system.dk/, Denmark
Eltra	-	Transmission and System Operator, http://www.eltra.dk/, Denmark
Enre	-	Entidad Nacional Reguladora de la Electricidad, http://www.enre.gov.ar/, Argentina
Erse	-	Entidade Reguladora dos Serviços Energéticos, http://www.erse.pt, Portugal
Euroelectric	-	Union of the Electricity Industry, http://unipede.euroelectric.org/
Fingrid	-	Transmission and System Operator, http://www.fingrid.fi/, Finland
Ngc	-	National Grid Company, http://www.nationalgrid.co.uk/, United Kingdom
Offgem	-	Office of Gas and Electricity Markets, http://www.ofgem.gov.uk/, United Kingdom
Ree	-	Red Eléctrica de España, http://www.ree.es/, Spain
Ren	-	Redes Energéticas Nacionais, http://www.ren.pt/, Portugal
Statnett	-	Transmission and System Operator, http://www.statnett.no/, Norway
Svenska Kraftnat	-	Transmission and System Operator, http://www.svk.se/, Sweden

APPENDIX A **3 bus/3 branch power system**

In Figure A.1 it is presented the three bus/three branch power system used in Section 8.1 and their corresponding characteristics.

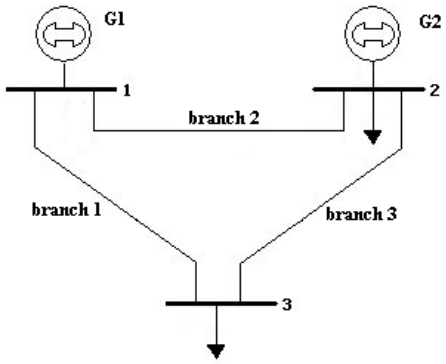

$$P_{G1}^{máx} = 6 \quad MW$$
$$P_{G2}^{máx} = 6 \quad MW$$
$$\left|P_{12}^{máx}\right| = 2 \quad MW$$
$$\left|P_{13}^{máx}\right| = 5 \quad MW$$
$$\left|P_{23}^{máx}\right| = 5 \quad MW$$

Figure A.1: Three bus/three branch power system.

Table A.1 presents the system data. It should be referred that the per unit reactance of branches are in a 10 MVA base.

Table A.1: Resistance, reactance and shunt admittance of the power system branches.

Branch	Extreme nodes		r [pu]	x [pu]	Ysh/2 [pu]
1	1	3	0.05	1.0	0.0
2	1	2	0.05	1.0	0.0
3	2	3	0.05	1.0	0.0

APPENDIX B 6 bus/8 branch power system

In Figure B.1 it is presented the three bus/three branch power system used in Section 8.2 and their corresponding characteristics.

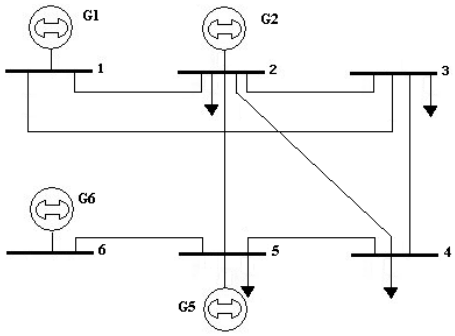

Figure B.1: Six bus/eight branches power system.

Table B.1 presents the load central values, the per unit branch reactances in a 100 MVA base, the capacity limits of the generators, the central values of their generation cost and the Forced Outage Rate of branches and generators. Finally, it should be referred that the branch capacities were set at 8 MW.

Table B.1: Load central values, per unit reactance, capacity limits of generators, central values of generation costs and FOR of the system components.

Bus	Load [MW]	Branch	Reactance [pu]	FOR	Bus/Gen	P_G^{max}/P_G^{min} [MW]	Cost [€/MWh]	FOR
1	0.0	1-2	0.06	0.01	1/1	10/0	10.0	0.10
2	4.0	1-3	0.24	0.01	2/1	10/0	15.0	0.05
3	6.0	2-3	0.18	0.01	5/1	7/3	13.0	0.20
4	4.0	2-4	0.18	0.01	6/1	5/0	20.0	0.10
5	4.0	2-5	0.12	0.01	--	--	--	--
6	0.0	3-4	0.03	0.01	--	--	--	--
--	--	4-5	0.24	0.01	--	--	--	--
--	--	5-6	0.03	0.01	--	--	--	--

APPENDIX C IEEE 24 bus/38 branch power system

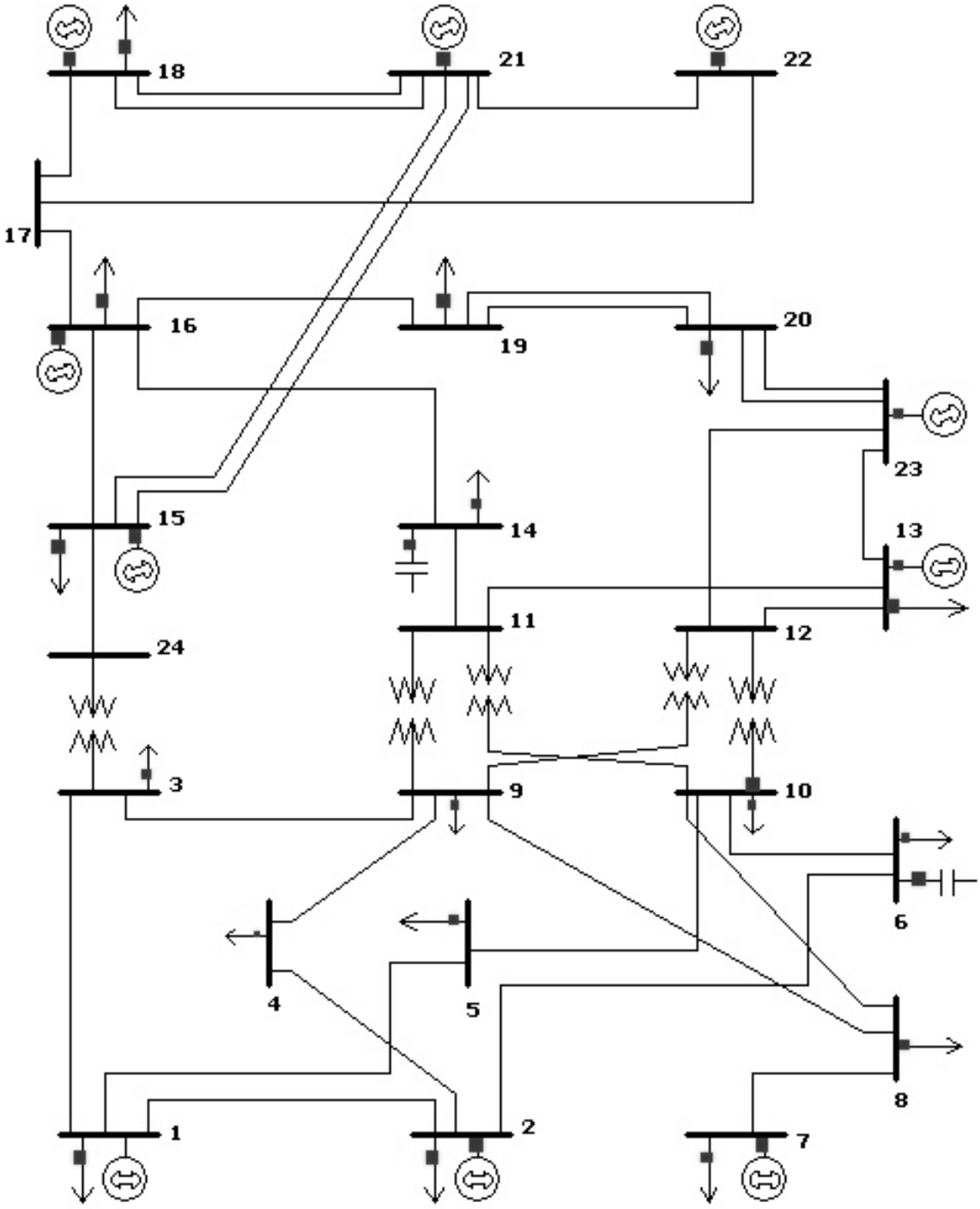

Figure C.1: IEEE 24 bus/38 branch power system.

For this power system it was adopted a base power of 500,0 MVA. In Tables C.1 and C.2 are presented the branch and the transformer technical characteristics, respectively, of this power system.

Table C.1: Resistance, reactance and shunt admittance of the power system branches.

Branch	Extreme nodes		Type	V_n [kV]	r [pu]	x [pu]	$y_{sh}/2$ [pu]	P_{max} [MW]	F.O.R
1	1	2	cable	138.0	0.0130	0.0695	0.04611	175	0.00044
2	1	3	line	138.0	0.2730	1.0560	0.00572	175	0.00059
3	1	5	line	138.0	0.1090	0.4225	0.00229	175	0.00038
4	2	4	line	138.0	0.1640	0.6335	0.00343	175	0.00045
5	2	6	line	138.0	0.2485	0.9600	0.00520	175	0.00055
6	3	9	line	138.0	0.1540	0.5950	0.00322	175	0.00043
8	4	9	line	138.0	0.1340	0.5185	0.00281	175	0.00041
9	5	10	line	138.0	0.1140	0.4415	0.00239	175	0.00039
10	6	10	cable	138.0	0.0695	0.3025	0.24590	175	0.00132
11	7	8	line	138.0	0.0795	0.3070	0.00166	175	0.00034
12	8	9	line	138.0	0.2135	0.8255	0.00447	175	0.00050
13	8	10	line	138.0	0.2135	0.8255	0.00447	175	0.00050
18	11	13	line	230.0	0.0305	0.2380	0.00999	500	0.00050
19	11	14	line	230.0	0.0270	0.2090	0.00879	500	0.00049
20	12	13	line	230.0	0.0305	0.2380	0.00999	500	0.00050
21	12	23	line	230.0	0.0620	0.4830	0.02030	500	0.00065
22	13	23	line	230.0	0.0555	0.4325	0.01818	500	0.00062
23	14	16	line	230.0	0.0250	0.1945	0.00818	500	0.00048
24	15	16	line	230.0	0.0110	0.0865	0.00364	500	0.00041
25	15	21	line	230.0	0.0315	0.2450	0.01030	500	0.00052
26	15	21	line	230.0	0.0315	0.2450	0.01030	500	0.00052
27	15	24	line	230.0	0.0335	0.2595	0.01091	500	0.00052
28	16	17	line	230.0	0.0165	0.1295	0.00545	500	0.00044
29	16	19	line	230.0	0.0150	0.1155	0.00485	500	0.00043
30	17	18	line	230.0	0.0090	0.0720	0.00303	500	0.00040
31	17	22	line	230.0	0.0675	0.5265	0.02212	500	0.00068
32	18	21	line	230.0	0.0165	0.1295	0.00545	500	0.00044
33	18	21	line	230.0	0.0165	0.1295	0.00545	500	0.00044
34	19	20	line	230.0	0.0255	0.1980	0.00833	500	0.00048
35	19	20	line	230.0	0.0255	0.1980	0.00833	500	0.00048
36	20	23	line	230.0	0.0140	0.1080	0.00455	500	0.00043
37	20	23	line	230.0	0.0140	0.1080	0.00455	500	0.00043
38	21	22	line	230.0	0.0435	0.3390	0.01424	500	0.00057

Table C.2: Transformers characteristics.

Branch	Extreme nodes		Type	V_{np}/V_{ns}	r [pu]	x [pu]	$y_{sh}/2$ [pu]	P_{max} [MW]	F.O.R
7	3	24	Transf.	138.0/230.0	0.0	0.4195	0.0	400.0	0.00175
14	9	11	Transf.	138.0/230.0	0.0	0.4195	0.0	400.0	0.00175
15	9	12	Transf.	138.0/230.0	0.0	0.4195	0.0	400.0	0.00175
16	10	11	Transf.	138.0/230.0	0.0	0.4195	0.0	400.0	0.00175
17	10	12	Transf.	138.0/230.0	0.0	0.4195	0.0	400.0	0.00175

Regarding the original data presented in Task Force (1979), the load was increased to 4060,05 MW. Table C.3 presents the installed capacities and the central values of the generation costs and Table C.4 indicates the central values of loads. The total installed capacity is 5226,0 MW according with the data in Table C.3. Branch data can be obtained from Task Force (1979) considering that the transformers have a capacity of

400,0 MW, the capacity of the branches 1 to 6 and 8 to 13 was set at 175,0 MW and the capacity of the remaining branches was set at 500,0 MW.

Table C.3 Installed system capacity and central values of generation costs.

Bus/Gen	Capacity [MW]	Cost [€/MWh]	F.O.R.	Bus/Gen	Capacity [MW]	Cost [€/MWh]	F.O.R.
1/1	40.0	30.0	0.10	16/1	310.0	55.0	0.04
1/2	40.0	32.0	0.10	19/1	800.0	87.0	0.12
1/3	152.0	40.0	0.02	21/1	800.0	80.0	0.12
1/4	152.0	43.0	0.02	22/1	100.0	15.0	0.01
2/1	40.0	36.0	0.10	22/2	100.0	17.0	0.01
2/2	40.0	38.0	0.10	22/3	100.0	19.0	0.01
2/3	152.0	41.0	0.02	22/4	100.0	15.0	0.01
2/4	152.0	42.0	0.02	22/5	100.0	17.0	0.01
7/1	150.0	45.0	0.04	22/6	100.0	25.0	0.01
7/2	200.0	43.0	0.04	23/1	200.0	50.0	0.04
13/1	250.0	61.0	0.05	23/2	50.0	49.0	0.04
13/2	394.0	62.0	0.05	23/3	310.0	47.0	0.08
13/3	394.0	67.0	0.05	-- -	- -	- -	

Table C.4 Load central values.

Bus	Load [MW]	Bus	Load [MW]	Bus	Load [MW]
1	220.48	9	385.82	17	0.00
2	270.80	10	216.49	18	226.76
3	3.94	11	40.00	19	265.53
4	32.67	12	10.00	20	103.92
5	105.94	13	162.45	21	50.00
6	187.65	14	262.88	22	10.00
7	218.77	15	650.36	23	0.00
8	398.09	16	225.50	24	12.00

APPENDIX D Fuzzy Sets

D. 1 Fuzzy Set theory

D.1 General aspects

There are two important kinds of uncertainty, which could be classified as *linguistic* and *random.* The former is associated with words since words can mean different things to different people and the latter is associated with unpredictability. Probability theory is used to handle random uncertainty and Fuzzy Sets are used to handle linguistic uncertainty. Sometimes Fuzzy Sets can also be used to handle both kinds of uncertainty, because a Fuzzy system may use noise measurements or operate under disturbances (Mendel, J., 2007).

Within probability theory one begins with a probability density function that embodies total information about random uncertainties. However, in most practical applications, it is impossible to know or determine the probability density function, so the fact that a probability density function is characterized by all of its moments is used. For most probability density functions an infinite number of moments are required. Unfortunately, it is not possible, in practice, to determine a number of moments, so instead, enough moments are computed to extract as much information as possible from the data. Typically, two moments are used – the mean and the variance. Just using first moments would not be very useful because random uncertainty requires an understanding of dispersion about the mean and this information is provided by the variance. So the accepted probabilistic modelling of random uncertainty focuses, to large extent, on methods that use at least the first two moments of a probabilistic distribution function.

Fuzzy Set theory whose definitions and basic concepts were given by Zadeh (1965) could be interpreted as an generalization of the classical theory of the rigid sets (related with the Boolean logic) in such a way that its principles and theorems are reduced to the theory of the rigid sets when their application are reduced to that level (Saraiva, 1995).

The main characteristic of the Fuzzy Sets is related with the fact that they admit the existence of a continuous interval of membership degrees of an element to a set varying between the extreme situations of full membership to complete lack of membership. This generalization makes that the scope of application of Fuzzy Sets is wider than the classical theory in modelling systems having high levels of complexity or in areas in which there is a subjective evaluation of some characteristics and properties of systems or even when there is incomplete information with respect to the behaviour of some variables.

Fuzzy Sets is adequate to represent the uncertainty associated with the vague character of a knowledge given the existence of a gradual and continuous transition between the 0.0 and 1.0 membership function.

The operational rules associated with Fuzzy Sets can be considered as a generalization of the concepts associated to the interval analyses. Consequently, a Fuzzy Set can be interpreted as a set of nested intervals having, each of them, a given membership value. For one side, the membership value can be considered as a measure of the more or less

uncertainty in the knowledge of the precise value of the variable. By another, each of these intervals correspond, in the scope of Fuzzy Set theory at a given cut-level α.

At another level, Fuzzy Sets can also be considered as related with the sensibility studies frequently performed in several different types of analysis. Consequently, the data represented by Fuzzy Sets in several studies can be interpreted as allowing performing a systematic sensibility analysis.

The possibility and probabilistic theories represent two different kinds of uncertainties. In this context, it can be said that under the probabilistic theory all the events are well defined and that probabilistic concepts wish to quantify the uncertainty with respect to the event that will occur. Differently, the possibility theory is related with entities that are not precisely defined and so it can happen that it is not possible to select the confidence to associate to a given knowledge between the values of the classical logic. Regarding this issue, Zadeh (1978) stated the Consistence Principle as follows:

The possibilistic distribution of a given variable act as superior limit of the probabilistic distribution in such a way that an impossible event is also improbable, but an improbable event may not be impossible.

D.2 Definitions

An Fuzzy Set $\tilde{A}$ is characterized by a membership function $\mu(x)$ associating to each element x_1 its compatibility level with $\tilde{A}$. In this sense, the transition between the extreme situations of full membership and complete lack of membership of x_1 to the set $\tilde{A}$ is performed gradually in opposition to what happens in the theory of the classical sets associated with the Boolean logic. The fuzzy set $\tilde{A}$ can then be defined using ordered pairs in which each value x_1 is associated an membership value $\mu(x_1)$.

$$\tilde{A} = \left\{ (x_1, \mu_{\tilde{A}}(x_1)), x_1 \in X_1 \right\} \tag{D.1}$$

This means that a Fuzzy Set can be interpreted as an extension of the classical or rigid sets whose membership can be considered as an application of X_1 to the set $\{0,1\}$.

An α cut level of a Fuzzy Set $\tilde{A}$ is defined as a classical or rigid set A_α, whose elements have a membership not smaller than α (D.2).

$$A_\alpha = \left\{ x_1 \in X_1 : \mu_{\tilde{A}}(x_1) \geq \alpha \right\} \tag{D.2}$$

A Fuzzy Set $\tilde{A}$ can be represented by means of its cut levels using (D.3), in which $\mu_{A\alpha}(x_1)$ is given by (D.4)

$$\mu_{\tilde{A}}(x_1) = \sup_{\alpha \in [0.0,1.0]} \min(a, \mu_{A\alpha}(x_1)) \tag{D.3}$$

$$\mu_{A\alpha}(x_1) = \begin{cases} 1.0 \;\; if \;\; and \;\; only \;\; if \; x_1 \in A_\alpha \\ 0.0 \;\; if \;\; and \;\; only \;\; if \; x_1 \notin A_\alpha \end{cases} \tag{D.4}$$

As an example, Figure D.1 presents a membership function $\mu_A(x)$ and three different cut levels. In this context, it is possible to see that the 0.0 cut-level comprises the interval $[2.0,8.0]$, the 0.5 cut-level the interval $[3.0,7.0]$ and, finally, the 1.0 cut level the interval $[4.0,6.0]$.

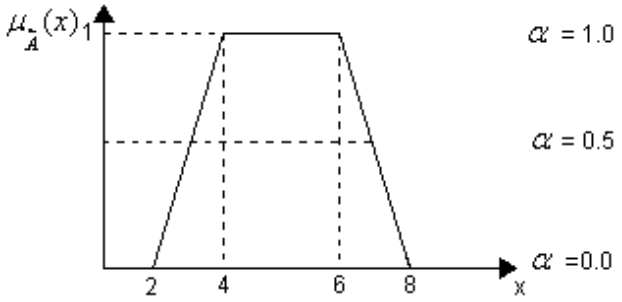

Figure D.1: Different *a* cut levels.

In order to present other definitions and concepts, let us now consider Figure D.2.

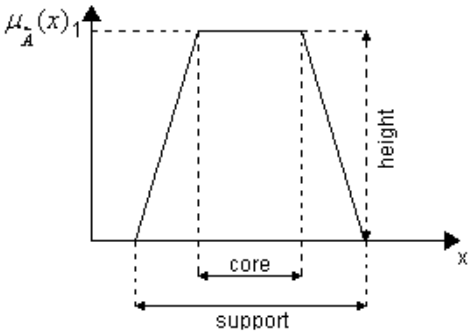

Figure D.2: Height, core and support of a fuzzy set (Soure: Monteiro, 2002).

The support set of a Fuzzy Set $\tilde{A}$ is defined as a set of values of x_1 having membership values not null with respect to $\tilde{A}$, as defined by (D.5).

$$S(\tilde{A}) = \left\{ x_1 \in X_1 : \mu_{\tilde{A}}(x_1) \geq 0.0 \right\} \tag{D.5}$$

The height of a given Fuzzy Set, $\tilde{A}$, $hgt(\tilde{A})$, is defined by (D.6).

$$hgt(\tilde{A}) = \sup_{x \in X} \mu_A(x) \tag{D.6}$$

Fuzzy Sets with height equal to 1.0 are called *normal*. Oppositely, they will be called *subnormal* if their height is smaller than 1.0.

The core of a Fuzzy Set is a crisp subset of X, such that it is defined by (D.7):

$$core(\tilde{A}) = \{x \in X \mid \mu_A(x) = 1\} \tag{D.7}$$

Finally, the width of a Fuzzy Set $\tilde{A}$ is defined as the difference between the supremum and the infimum of the support as defined by expression (D.8).

$$width(\tilde{A}) = \sup(S(\tilde{A})) - \inf(S(\tilde{A})) \tag{D.8}$$

D.3 Relations and operations using Fuzzy Sets

The membership function is a fundamental component of a Fuzzy Set and so the operations performed with these sets are usually defined by means of relations between these functions. In this context, and considering two Fuzzy Sets, $\tilde{A}$ and $\tilde{B}$, and their corresponding membership functions, $\mu_A(x)$ and $\mu_B(x)$, respectively, it could be defined the reunion ($\tilde{A} \cup \tilde{B}$), the intersection ($\tilde{A} \cap \tilde{B}$), the complementary ($C\tilde{A}$), the equality ($\tilde{A} = \tilde{B}$) and the inclusion ($\tilde{A} \supseteq \tilde{B}$) of these two Fuzzy Sets are defined by means of expressions (D.9), (D.10), (D.11), (D.12) and (D.13), respectively, (Zadeh, 1965):

$$\tilde{A} \cup \tilde{B} = \max_{x \in X} \left\{ \mu_{\tilde{A}}(x), \mu_{\tilde{B}}(x) \right\} \tag{D.9}$$

$$\tilde{A} \cap \tilde{B} = \min_{x \in X} \left\{ \mu_{\tilde{A}}(x), \mu_{\tilde{B}}(x) \right\} \tag{D.10}$$

$$C\,\tilde{A} = 1.0 - \mu_{\tilde{A}}(x), x \in X \tag{D.11}$$

$$\tilde{A} = \tilde{B} \quad if \quad and \quad only \quad if \quad \mu_{\tilde{A}}(x) = \mu_{\tilde{B}}(x) \tag{D.12}$$

$$\tilde{A} \supseteq \tilde{B} \quad if \quad and \quad only \quad if \quad \mu_{\tilde{A}}(x) \geq \mu_{\tilde{B}}(x) \tag{D.13}$$

D.4 Fuzzy numbers

A Fuzzy number is defined as a Fuzzy Set convex and normalized defined in the real line such that its membership function is continuous at least by intervals. A fuzzy number $\tilde{A}$ is positive, negative, non negative or non positive if it verifies the conditions (D.14), (D.15), (D.16) or (D.17), respectively.

$$\forall x \leq 0.0 \quad \mu_{\tilde{A}}(x) = 0.0 \tag{D.14}$$

$$\forall x \geq 0.0 \quad \mu_{\tilde{A}}(x) = 0.0 \tag{D.15}$$

$$\forall x < 0.0 \quad \mu_{\tilde{A}}(x) = 0.0 \tag{D.16}$$

$$\forall x > 0.0 \quad \mu_{\tilde{A}}(x) = 0.0 \tag{D.17}$$

A fuzzy number is normalized when there is at least a real element, x, such that the membership value in that point is 1.0, this is, the maximum value of the membership function that characterizes the Fuzzy Set in R is 1.0.

The convexity of a Fuzzy Set is verified if, given two cut levels α and α', in which $A_\alpha = [a_1(\alpha), a_3(\alpha)]$ and $A_{\alpha'} = [a_1(\alpha'), a_3(\alpha')]$, condition (D.18) is satisfied.

$$\alpha' < \alpha \Rightarrow [a_1(\alpha') \leq a_1(\alpha), a_3(\alpha') \leq a_3(\alpha)] \tag{D.18}$$

As an example, Figure D.3 presents a convex and normalized Fuzzy Set $\tilde{A}$ (at left) and a Fuzzy Set normalized but not convex (at right). In these conditions, the Fuzzy Set represented in the left side of Figure D.3 is a fuzzy number.

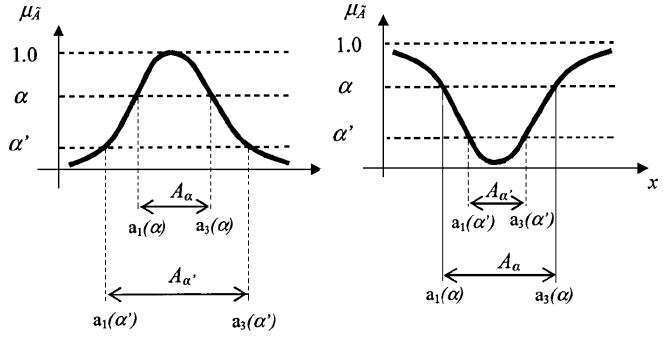

Figure D.3: Convex (at left) and non convex (at right) Fuzzy Sets (source: Braga, 2005).

Among several different types of fuzzy numbers, in the following paragraphs we will present the triangular and trapezoidal fuzzy numbers. In this context, a fuzzy number that verifies (D.19) is termed as triangular fuzzy number and its corresponding representation is presented on the left side of Figure D.4. This kind of representation can be used to model the uncertainty knowledge of a given numeric value a_2 admitting that the values within the interval $]a_1, a_2[\cup]a_3, a_4[$ are still possible representations of the variable having, however, compatibility degrees smaller than the one of a_2.

$$A_\alpha = [a_1 + \alpha.(a_2 - a_1); a_4 + \alpha.(a_3 - a_4)] \wedge a_2 = a_3 \tag{D.19}$$

Similarly, a fuzzy number that verifies (D.20) is termed as trapezoidal fuzzy number and its corresponding representation is presented on the right side of Figure D.4.

$$A_\alpha = [a_1 + \alpha.(a_2 - a_1); a_4 + \alpha.(a_3 - a_4)] \tag{D.20}$$

This kind of representation can be used to model the uncertainty associated with the knowledge of the interval of values assumed by a given variable. In this sense, the values in the interval $[a_2, a_3]$ have a 1.0 membership value meaning that they are possible values of that variable. Similarly to what was described for the triangular fuzzy number case, the values in the interval $]a_1, a_2[\cup]a_3, a_4[$ are also possible values of the variable, however associated with smaller credibility degrees.

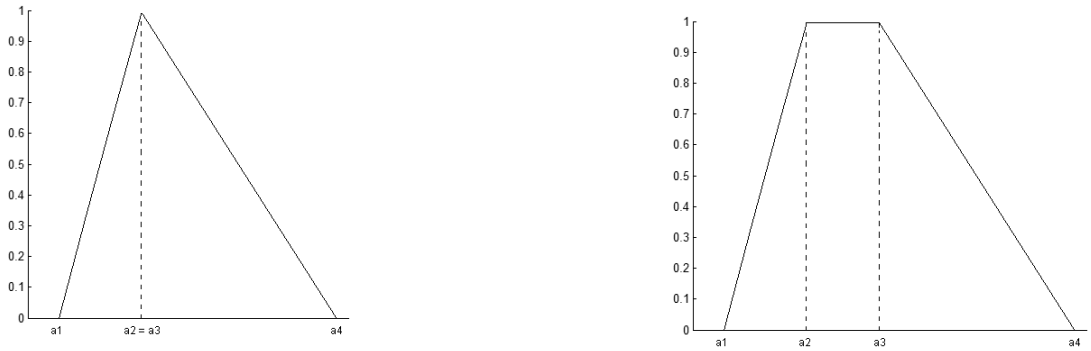

Figure D.4: Triangular fuzzy number (at left) and trapezoidal fuzzy number (at right).

D.5 Extension principle

The extension principle is one of the most important principles of the Fuzzy Set theory, since it allows generalizing to Fuzzy Sets the mathematical operations and functions defined in deterministic terms. It is defined as follows:

Let X be the Cartesian product of the universes X_1, X_2, …, X_n and let $\tilde{A}_1, \tilde{A}_2, ..., \tilde{A}_n$ be *n* Fuzzy Sets defined, respectively, in X_1, X_2, …, X_n. A Fuzzy Set $\tilde{B}$ in Y is defined by (D.21) and its membership function is given by (D.22).

$$\tilde{B} = \left\{ (y, \mu_{\tilde{B}}(y) : y = f(x_1, x_2, ..., x_n), (x_1, x_2, ..., x_n) \in X \right\} \quad \text{(D.21)}$$

$$\mu_{\tilde{B}}(y) = \sup_{\substack{y = f(x_1, x_2, ..., x_n) \\ 0 \ if \ f^{-1}(y) = \varnothing}} \min \left\{ \mu_{\tilde{A}1}(x_1), \mu_{\tilde{A}2}(x_2), ..., \mu_{\tilde{A}n}(x_n) \right\} \quad \text{(D.22)}$$

According to this principle, the membership of a given value y_1 given by (D.23) to the Fuzzy Set $\tilde{B}$ is, at least, given by (D.24). Existing several combinations of values of $x_1, x_2, ..., x_r$ that give originate, through f, the same value of y, the membership of y_1 will correspond to the supreme of the set integrating the membership values of all these combinations.

$$y_1 = f(x_{11}, x_{21}, ..., x_{n1}), \ x_{11} \in X_1, x_{21} \in X_2, ..., x_{n1} \in X_n \quad \text{(D.23)}$$

$$\mu_{\tilde{O}}(y_1) = \min \left\{ \mu_{\tilde{A}1}(x_{11}), \mu_{\tilde{A}2}(x_{21}), ..., \mu_{\tilde{A}n}(x_{n1}) \right\} \quad \text{(D.24)}$$

If n = 1, the Extension Principle will reduce to (D.25) and (D.26).

$$\tilde{B} = \left\{ (y, \mu_{\tilde{B}}(y) : y = f(x_1), x_1 \in X \right\} \quad \text{(D.25)}$$

$$\mu_{\tilde{O}}(y_1) = \sup_{y = f(x_1)} \mu_{\tilde{A}1}(x_{11}) \quad \text{(D.26)}$$

D.6 Definitions, theorems and properties of a binary operation using Fuzzy numbers

Let φ be a binary operation defined from R^2 to R. This operation is considered ascending or descending if and only if it verifies, respectively, the conditions (D.27) or (D.28) for all ordered pairs (x_1, x_2) and (y_1, y_2) in R^2.

$$(x_1 > x_2) \wedge (y_1 > y_2) \Rightarrow \varphi(x_1, x_2) > \varphi(y_1, y_2) \quad \text{(D.27)}$$

$$(x_1 < x_2) \wedge (y_1 < y_2) \Rightarrow \varphi(x_1, x_2) < \varphi(y_1, y_2) \quad \text{(D.28)}$$

The extension of the operation φ, ascending or descending, to the fuzzy numbers is performed using the Extension Principle, which results in the theorem presented by (Dubois *et al.*, 1980).

Let $\tilde{A}_1$ and $\tilde{A}_2$ be two fuzzy numbers whose membership functions are sobrejective and defined in $[0.0,1.0]$. Let φ be a binary function continuous and ascending or descending.

In this context, the extension $\varphi(\tilde{A}_1, \tilde{A}_2)$ *is still a fuzzy number whose membership function is sobrejective and defined of* R *in* $[0.0,1.0]$.

The membership function of the fuzzy number $\varphi(\tilde{A}_1, \tilde{A}_2)$ can be obtained using (D.29) that results from the application of the Extension Principle.

$$\mu_{\varphi(\tilde{A}_1,\tilde{A}_2)}(z) = \begin{cases} \sup\limits_{z=\varphi(x,y)} \min\left\{\mu_{\tilde{A}_1}(x), \mu_{\tilde{A}_2}(x)\right\} \\ 0.0 \quad if \quad \varphi^{-1}(z) = \varnothing \end{cases} \tag{D.29}$$

The binary operation, φ, has the following properties:

- Commutative;
- Associative;
- Distributive with respect to the reunion of the fuzzy sets:

$$\varphi(\tilde{A}_1, \tilde{A}_2 \cup \tilde{A}_3) = \varphi(\tilde{A}_1, \tilde{A}_2) \cup \varphi(\tilde{A}_1, \tilde{A}_3) \tag{D.30}$$

In this context, in the next paragraphs we will present the extension of unary arithmetic operations to the fuzzy numbers, namely, the product of a scalar by a fuzzy number, the division between 1.0 and a fuzzy number and the absolute value of a fuzzy number. We will also present the binary arithmetic operations, such as, the addition, the subtraction, the product and the division of two fuzzy numbers.

D.6.1 Unary operations

Taking the Extension Principle defined in D.5, namely for the case where $n = 1$, expressions (D.31), (D.32) and (D.33) define the product of a scalar by a fuzzy number, the division between 1.0 and a fuzzy number and the absolute value of a fuzzy number.

$$\mu_{\alpha.\tilde{A}(x)} = \mu_{\tilde{A}}(x/\alpha), \qquad \forall \alpha \in R \setminus \{0\} \tag{D.31}$$

$$\mu_{1.0/\tilde{A}(x)} = \mu_{\tilde{A}}(1.0/x), \qquad \forall \alpha \in R \setminus \{0\} \tag{D.32}$$

$$\mu_{\left|\tilde{A}(x)\right|} = \begin{matrix} \max(\mu_{\tilde{A}}(x), \mu_{\tilde{A}}(-x) & if \quad x \geq 0.0 \\ 0.0 & if \quad x < 0.0 \end{matrix}, \tag{D.33}$$

Following these definitions, it can be stated that:

- The product of a fuzzy number by a scalar preserves the distributive property with respect to the addition of two fuzzy numbers. Nevertheless, this property is not verified in the case of the product of a fuzzy number by a scalar ;
- If the fuzzy number $\tilde{A}$ is not non positive or non negative, then the division between 1.0 and $\tilde{A}$ is not convex and, consequently, the result is not a fuzzy number;
- The fuzzy number associated to the absolute value $\tilde{A}$ is non negative.

D.6.2 Binary operations

The extension of the binary operations to Fuzzy Sets is performed using the Extension Principle formulated to $n = 2$. In this context, in next paragraphs we will define the addition, the subtraction, the product and the division of two fuzzy numbers.

D.6.2.1 Addition

The binary operation addition is an ascending operation and, consequently, $f(\tilde{A}_1, \tilde{A}_2) = \tilde{A}_1 \oplus \tilde{A}_2$ is a fuzzy number whose membership function is given by (D.34).

$$\mu(\tilde{A}_1 \oplus \tilde{A}_2) = \sup_{z=x+y} \min(\mu_{\tilde{A}_1(x)}, \mu_{\tilde{A}_2(y)}) \tag{D.34}$$

D.6.2.2 Subtraction

The binary operation subtraction is neither an ascending nor a descending operation. In this context, this operation can be performed applying successively the Extension Principle as detailed in (D.35) to (D.38).

$$\tilde{A}_1 \Theta \tilde{A}_2 = \tilde{A}_1 \oplus (\Theta \tilde{A}_2) \tag{D.35}$$

$$\mu(\tilde{A}_1 \Theta \tilde{A}_2) = \sup_{z=x-y} \min(\mu_{\tilde{A}_1(x)}, \mu_{\tilde{A}_2(y)}) \tag{D.36}$$

$$\mu(\tilde{A}_1 \Theta \tilde{A}_2) = \sup_{z=x+y} \min(\mu_{\tilde{A}_1(x)}, \mu_{\tilde{A}_2(-y)}) \tag{D.37}$$

$$\mu(\tilde{A}_1 \Theta \tilde{A}_2) = \sup_{z=x+y} \min(\mu_{\tilde{A}_1(x)}, \mu_{-\tilde{A}_2(y)}) \tag{D.38}$$

D.6.2.3 Product

The product of two non negative numbers is an ascending binary operation being descending if the two numbers are non positives. In both of these situations, $\tilde{A}_1 \otimes \tilde{A}_2$ is a fuzzy number whose membership, in accordance with the Extension Principle, is given by (D.39). Following this definition, the product of two fuzzy numbers both positives or both negatives is a positive number.

$$\mu(\tilde{A}_1 \otimes \tilde{A}_2) = \sup_{z=x.y} \min(\mu_{\tilde{A}_1(x)}, \mu_{\tilde{A}_2(y)}) \tag{D.39}$$

The product of two numbers one of them being non positive and the other non negative is not an ascending nor a descending operation, and so, similarly to the subtraction case, the product of two fuzzy numbers is these conditions should be redefined by means of (D.40).

$$\tilde{A}_1 \otimes \tilde{A}_2 = -((-\tilde{A}_1) \otimes (\tilde{A}_2) \tag{D.40}$$

D.6.2.4 Division

The binary operation division is neither an ascending nor a descending operation. In this context, being $\tilde{A}_1$ and $\tilde{A}_2$ numbers non negative and positive, respectively, this operation can be redefined by means of (D.41). Applying the Extension Principle we will then obtain, successively, (D.42) to (D.44).

$$\tilde{A}_1 \, \mathrm{O} \, \tilde{A}_2 = \tilde{A}_1 \otimes (\tilde{A}_2)^{-1} \tag{D.41}$$

$$\mu(\tilde{A}_1 \, \mathrm{O} \, \tilde{A}_2) = \sup_{z=x/y} \min(\mu_{\tilde{A}_1(x)}, \mu_{\tilde{A}_2(y)}) \tag{D.42}$$

$$\mu(\tilde{A}_1 \, \mathrm{O} \, \tilde{A}_2) = \sup_{z=x.y} \min(\mu_{\tilde{A}_1(x)}, \mu_{\tilde{A}_2(1/y)}) \tag{D.43}$$

$$\mu(\tilde{A}_1 \, \mathrm{O} \, \tilde{A}_2) = \sup_{z=x/y} \min(\mu_{\tilde{A}_1(x)}, \mu_{\tilde{A}_2^{-1}(y)}) \tag{D.44}$$

D.7 Arithmetic operations extended to trapezoidal fuzzy numbers

The extension of the arithmetic operations to the case of trapezoidal fuzzy numbers is of particular interest given that this kind of representation is simply and efficiently used in computational applications. Additionally, the relations established for this kind of representation can also be used for the case of triangular fuzzy numbers, since that triangular numbers are simply a particular case of trapezoidal ones.

In this context, it should be mentioned that the membership function resulting from the inverse of a trapezoidal number, from the product of two trapezoidal number and from the division between two trapezoidal numbers presents non linear terms and, consequently, the resulting fuzzy number is not a trapezoidal fuzzy number. In fact, taking the product of two trapezoidal fuzzy numbers operation as an example, it can be demonstrated that the resulting membership function will present a concavity in its left branch and a convexity in its right branch as sketched in Figure D.5.

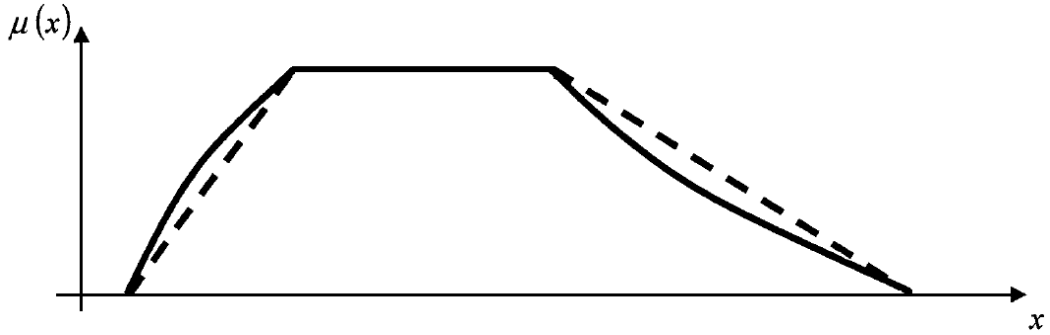

Figure D.5: Membership function resulting from the product of two trapezoidal fuzzy numbers (continuous line) and its corresponding trapezoidal membership function approximation (dashed line).

To establish these relations let us consider two trapezoidal fuzzy numbers, $\tilde{A}$ and $\tilde{B}$ defined by expressions (D.45) and (D.46).

$$\tilde{A} = [a_1, a_2, a_3, a_4] \tag{D.45}$$

$$\tilde{B} = [b_1, b_2, b_3, b_4] \tag{D.46}$$

In this context, Table D.1, presents the expressions to adopt in order to perform these arithmetic operations using trapezoidal fuzzy numbers.

Table D.1: Arithmetic operations extended to trapezoidal fuzzy numbers.

Product by a scalar $\sigma \in R$	- if σ is a non negative scalar $\sigma.\tilde{A} = [\sigma.a_1, \sigma.a_2, \sigma.a_3, \sigma.a_4]$ (D.47) - if σ is a non positive scalar $\sigma.\tilde{A} = [\sigma.a_4, \sigma.a_3, \sigma.a_2, \sigma.a_1]$ (D.48)
Inverse	$\tilde{A}^{-1} = [\frac{1}{a_4}, \frac{1}{a_3}, \frac{1}{a_2}, \frac{1}{a_1}]$, $\tilde{A}$ could be positive or negative (D.49)
Addition	$\tilde{A} \oplus \tilde{B} = [a_1 + b_1, a_2 + b_2, a_3 + b_3, a_4 + b_4]$ (D.50)
Subtraction	$\tilde{A} \Theta \tilde{B} = [a_1 - b_4, a_2 - b_3, a_3 - b_2, a_4 - b_1]$ (D.51)
Product	- Between two non negative fuzzy numbers $\tilde{A} \otimes \tilde{B} = [a_1.b_1, a_2.b_2, a_3.b_3, a_4.b_4]$ (D.52) - Between two non positive fuzzy numbers $\tilde{A} \otimes \tilde{B} = [a_4.b_4, a_3.b_3, a_2.b_2, a_1.b_1]$ (D.53) - Between two fuzzy numbers: $\tilde{A}$ non positive and $\tilde{B}$ non negative (D.54) $\tilde{A} \otimes \tilde{B} = [a_1.b_4, a_2.b_3, a_3.b_2, a_4.b_1]$ (D.55)
Division	- Between two fuzzy numbers: $\tilde{A}$ non positive and $\tilde{B}$ positive $\tilde{A} \Phi \tilde{B} = [\frac{a_1}{b_4}, \frac{a_2}{b_3}, \frac{a_3}{b_2}, \frac{a_4}{b_1}]$ (D.56) - Between two fuzzy numbers: $\tilde{A}$ non negative and $\tilde{B}$ negative $\tilde{A} \Phi \tilde{B} = [\frac{a_4}{b_4}, \frac{a_3}{b_3}, \frac{a_2}{b_2}, \frac{a_1}{b_1}]$ (D.57) - Between two fuzzy numbers: $\tilde{A}$ non positive and $\tilde{B}$ positive $\tilde{A} \Phi \tilde{B} = [\frac{a_1}{b_1}, \frac{a_2}{b_2}, \frac{a_3}{b_3}, \frac{a_4}{b_4}]$ (D.58) - Between two fuzzy numbers: $\tilde{A}$ non positive and $\tilde{B}$ negative $\tilde{A} \Phi \tilde{B} = [\frac{a_4}{b_1}, \frac{a_3}{b_2}, \frac{a_2}{b_3}, \frac{a_1}{b_4}]$ (D.59)

D.8 Defuzzification

The defuzzification relies in converting a fuzzy number into a real number. Such a procedure could be performed in several ways, being one of them the *Removal*, the *Central Value*, the *Amplitude* and the *Center of Mass*.

Following Kaufman *et al.* (1988), the comparison of fuzzy numbers should be performed using, successively, three criterions: the *Removal*, the *Central Value* and the *Amplitude* of fuzzy numbers, since, in general, when used individually they are not sufficient to distinguish fuzzy numbers.

D.8.1 Removal

In order to present the computation methodology of the *Removal* of a fuzzy number, let us now first consider the fuzzy number presented in Figure D.6.

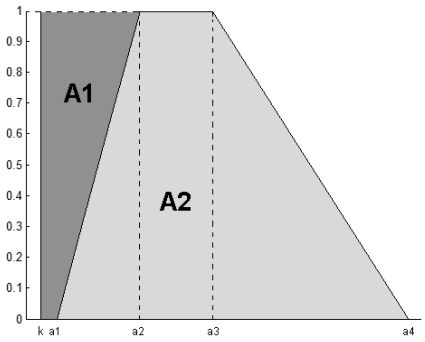

Figure D.6: Trapezoidal fuzzy number and the corresponding areas for the *Removal* computation.

The *Removal* of a fuzzy number is determined by the average of the areas determined by the left and by the right branches of the membership functions and it is determined by (D.60), in which A1 and A2 correspond to the areas represented in Figure (D.4).

$$\mathrm{Re}\,m(k) = \frac{A1 + (A1 + A2)}{2} \tag{D.60}$$

As it can be seen from Figure D.6, the area A1 is delimited, at left, by a vertical line passing through the value *k* and, at right, by the linear line defining the minimum value of the trapezoidal fuzzy number. It is also delimited by the horizontal lines corresponding to the 0.0 and 1.0 membership degree. The area A2 corresponds to the area under the membership function of the trapezoidal fuzzy number.

Considering this definition, for a given trapezoidal fuzzy number, the *Removal* could also be computed by expression (D.61).

$$\mathrm{Re}\,m(k) = -k + \frac{a_1 + a_2 + a_3 + a_4}{4} \tag{D.61}$$

D.8.2 Central value

The *Central Value* of a fuzzy number is defined as the mean value of the 1.0 cut level. In this context, its value is given by expression (D.62) considering the number in Figure D.6.

$$Central \quad Value = \frac{a_2 + a_3}{2} \tag{D.62}$$

D.8.3 Amplitude

The amplitude of a Fuzzy number corresponds to the difference between the maximum and the minimum value of its "1" cut. Regarding the trapezoidal Fuzzy number in Figure D.6, it is given by (D.63).

$$Amp = a_3 - a_2 \tag{D.63}$$

D.8.4 Center of Mass

The *Center of Mass* of a given fuzzy number, $\tilde{A}$, defined as a set of ordered pairs comprising, each of them, a element x of the universe under analysis and its corresponding membership value, is given by (D.64). If the membership function is continuous by segments, the *Center of Mass* is defined by (D.65).

$$CM(\tilde{A}) = \frac{\sum x.\mu_{\tilde{A}}(x)}{\sum \mu_{\tilde{A}}(x)} \tag{D.64}$$

$$CM(\tilde{A}) = \frac{\int x.\mu_{\tilde{A}}(x).dx}{\int \mu_{\tilde{A}}(x).dx} \tag{D.65}$$

APPENDIX E Publications in Conferences and Journals

Calculation of Nodal Marginal Prices Considering Load and Generation Price Uncertainties, Power Tech 2007, Lausanne, Switzerland, 1 to 5 July 2007

Calculation of Nodal Marginal Prices Considering Load and Generation Price Uncertainties

Bruno André Gomes João Tomé Saraiva, *member IEEE*

Abstract— **This paper presents the mathematical models and the solution algorithms of DC optimal power flow problems considering uncertainties represented by fuzzy numbers affecting loads as well as the elements of the cost function. The main purpose of this work corresponds to transfer the uncertainties affecting both the loads and the cost vector to the results that one usually obtain with such a DC optimal power flow model, that is, to characterize the uncertainties that affect the generations, the voltage phases, the branch flows. Apart from that, this paper also describes the algorithm to be used to calculate the uncertainties affecting the nodal marginal prices, since these prices are related with the dual variables of several constraints in the optimization problem. The developed algorithms are based in the solution of multiparametric problems in which one considers parameters both in the right hand side vector of the constraints (in order to represent load uncertainties) and in the cost function (to consider uncertainties in fuel costs, for instance). Finally, the paper includes a results of a Case Study designed to illustrate the application of the developed algorithms as well as results obtained for the IEEE 24 bus test system.**

***Index Terms*—uncertainties, fuzzy models, DC optimal power flow, nodal marginal prices.**

I. INTRODUCTION

The access to the transmission network is a crucial issue to be guaranteed in order to create and develop market mechanisms in the electric industry. The access to the transmission network shall be regulated by clear and transparent rules and must be accompanied by fair and well-balanced tariff mechanisms. The literature on this area already describes several tariff methods to allocate transmission costs to network users. These methods include average cost approaches, incremental methods and marginal approaches. For instance, reference [1] describes algorithms to compute short-term nodal marginal prices using the dual variables related with the optimal solution of a dispatch problem. However, marginal approaches have some drawbacks as follows:

- in the first place, short-term local marginal prices give an incomplete picture of the global transmission costs since they don't include investment costs. This means that the marginal based remuneration or congestion rent is typically reduced when compared to the real costs of transmission companies. This would originate an unbalance between revenues and costs that is termed as Revenue Reconciliation Problem. In countries where marginal based tariff terms exist, this unbalance is usually solved using more terms in transmission tariffs in order to guarantee that all costs are recovered;
- secondly, short term nodal marginal prices are very volatile since they are very dependent on a number of issues as the load level, generation costs and the availability of system components.

The treatment of uncertainties in power systems has long been addressed, namely when adopting probabilistic based models to represent reliability issues. Probabilistic models have then been used to model the uncertainty in the demand leading to probabilistic power flow models as the pioneering contributions in references [2-3] and later on several other references as [4-5]. The algorithms described in these papers typically use linearized expressions to build the probabilistic functions of the usual power flow results. In more recent years, they were developed models and solutions algorithms considering that uncertainties are represented in a more flexible way by fuzzy concepts rather by probabilistic models. References [6-7] detail some of these contributions when addressing power flow problems. These algorithms also adopt linearization techniques and correspond to very efficient algorithms in translating the fuzzy uncertainty in data to the membership functions of the results. In a recent advance, reference [8] allows one to integrate correlations between nodal data in an attempt to increase the realism of the models.

After modelling power flow problems considering fuzzy data, it was recognized that power flow operation was driven by economic criteria. This originated the development of a Fuzzy Optimal Power Flow model [9] that allows one to reflect load uncertainties in the results of OPF studies, namely in generation and in branch flows. In this case, we represented load uncertainties using fuzzy models, in particular, trapezoidal fuzzy numbers. Afterwards, using this Fuzzy OPF, we described in reference [10] how load uncertainties could be reflected in fuzzy distributions for nodal marginal prices. This means that with a single run in a very efficient way we can evaluate the impact of load uncertainties in the values that nodal marginal prices can assume and therefore characterize in a very accurate way their volatility given the possible variations of loads.

In this paper, we are enlarging this approach in order to consider not only load uncertainties but also uncertainties in generation or fuel prices. Once again, we model generation costs using trapezoidal fuzzy numbers and we aim at combining variations on the load vector and on the objective function coefficients to get insight on generation

Bruno André Gomes is with Escola Superior de Tecnologia e Gestão from Instituto Politécnico de Leiria, Morro do Lena, Alto Vieiro, Apartado 4163, 2401-951 Leiria, Portugal, bagomes@estg.ipleiria.pt

João Tomé Saraiva, FEUP/DEEC – Faculdade de Engenharia da Univ. do Porto and INESC Porto – Instituto de Engenharia de Sistemas e Computadores do Porto, Campus da FEUP, Rua Dr. Roberto Frias, 4200-465 Porto Portugal, jsaraiva@fe.up.pt

strategies, on possible branch flow values and also on the possible behaviour of nodal marginal prices.

Apart from this Introductory Section, Section II describes in a brief way the Fuzzy DC OPF model originally presented in [9] and Section III presents the mathematical formulation of the DC OPF problem considering uncertainties both in the loads and in the cost vector as well as the algorithm developed to solve the corresponding multiparametric optimization problem. Section IV describes how load uncertainties can be reflected on the membership functions of nodal marginal prices. Section V presents a Case Study designed to illustrate the developed approach as well as results obtained for the IEEE 24 bus text system and Section VI draws the most relevant conclusions.

II. BASIC FUZZY DC OPF MODEL

According to the model developed in [9], a Fuzzy Optimal Power Flow - FOPF - is an optimization study aiming at identifying the best generation strategy according to a generation cost function if at least one load is modelled by a fuzzy number. The FOPF approach adopts the DC model to represent the operation conditions of the network. The first step of the algorithm described in [9] corresponds to run a deterministic DC-OPF (1 to 5) study for a crisp version of the fuzzy load vector obtained by substituting each fuzzy load by its central value, Pl_k^{ctr}. For this crisp load vector the following crisp DC-OPF can be formulated:

$$\min f = \sum c_k.Pg_k + G.\sum PNS_k \quad (1)$$

$$\text{subj.} \quad \sum Pg_k + \sum PNS_k = \sum Pl_k^{ctr} \quad (2)$$

$$Pg_k^{min} \le Pg_k \le Pg_k^{max} \quad (3)$$

$$PNS_k \le Pl_k^{ctr} \quad (4)$$

$$P_b^{min} \le \sum a_{bk}.(Pg_k + PNS_k - Pl_k^{ctr}) \le P_b^{max} \quad (5)$$

In this model we are minimizing the generation cost given that Pg_k is the generation in node k, c_k is the corresponding cost and PNS_k is the power not supplied in node k. Pg_k^{min}, Pg_k^{max}, P_b^{min} and P_b^{max} are the minimum and maximum generation and branch flow limits and a_{bk} is the DC sensibility coefficient of the flow in branch b regarding the injected power in node k.

After performing this study and having identified a feasible and optimal solution for it, the next step corresponds to deal with load uncertainties. They can be represented by fuzzy numbers regarding the respective central values (6). At a given uncertainty level, for instance, at the 0-cut the uncertainty specified for load k can be modelled by a parameter Δ_k in $[\Delta_{k1}, \Delta_{k4}]$.

$$\tilde{Pl}_k = Pl_k^{ctr} + (\Delta_{k1}; \Delta_{k2}; \Delta_{k3}; \Delta_{k4}) \quad (6)$$

This representation can be extended to all loads affected by uncertainties. Their parameters can be integrated in the optimization problem (1-5) wherever loads appear on it. This means that new terms will be added to constraints (2) and (5). This process leads to the multiparametric formulation (7) to (9) where b and b' are vectors integrating the right hand side terms of the constraints considering that some of them are independent and some others depend on Δ_k. Using the inverse of the base matrix of the crisp DC-OPF problem one can integrate terms depending on Δ_k on the initial feasible and crisp solution (10).

$$\min f = c^t.X \quad (7)$$

$$\text{subj.} \quad A.X = b + b'(\Delta_k) \quad (8)$$

$$\Delta_{k1} \le \Delta_k \le \Delta_{k4} \quad (9)$$

$$X^{opt} = B^{-1}.(b + b'(\Delta)) \quad (10)$$

These parameters can turn the crisp solution not feasible in some zones of the hypervolume defined by (9). This is true for combinations of values of the parameters leading to a negative value of one variable. If that is the case, the algorithm proceeds by identifying vertices of that hypervolume according to some rules detailed in [9]. Once these vertices are identified, a set of parametric analysis fully described in [9] are run each of them leading to partial membership functions of generations, branch flows or PNS. The final results are obtained applying the Fuzzy Union Operator on those partial results.

This algorithm has to be enhanced namely to integrate an estimate of active losses because they are one of the causes leading to a geographic differentiation of nodal marginal prices. Therefore, if adopting a DC based algorithm it is crucial to integrate an estimate of these losses. Active losses in branch b from node i to node j are approximately calculated by (11) considering that voltage magnitudes are 1.0 pu. In this expression θ_i, θ_j and g_{ij} are the phase angles in nodes i and j and the conductance in branch ij.

$$Loss_{ij} \approx 2.g_{ij}.(1 - \cos\theta_{ij}) \quad (11)$$

Apart from other more involving processes, one simple way of computing an estimate of branch losses consists of running a set of DC-OPF crisp studies in an iterative scheme. At the end of each DC-OPF run, the phase angles and branch losses are computed and half of the losses in each branch is added to the load in each extreme bus. This change on loads leads to a change in generation and thus in phase angles. The process converges when, in two successive iterations, the differences between phase angles, in each node, are inferior than a specified level.

When running the DC-OPF parametric studies, loads are changed leading to changes in phase angles and in branch losses. In order to accommodate these changes, one can estimate, for each identified vertex, how active losses in each system branch are altered regarding the estimate obtained for the initial dispatch. If Δ_{kp} represents for vertex p the deviation of load in node k, the changes in branch ij active losses are approximately given by (12). The derivative in this expression is given by (13) where Z_{mn} represents the element of line m/column n of the inverse of the DC model admittance matrix. Finally, half of $\Delta Loss_{ij}$ is added to the load deviation in bus i. The other half is added to the deviation in bus j.

$$\Delta Loss_{ij} = \sum_{nodek} \frac{\partial Loss_{ij}}{\partial Pl_k}.\Delta_{kp} \quad (12)$$

$$\frac{\partial Loss_{ij}}{\partial Pl_k} = 2.g_{ij}.\sin\theta_{ij}.(-Z_{ik} + Z_{jk}) \quad (13)$$

III. COMBINING LOAD AND GENERATION COST UNCERTAINTIES

A. General Mathematical Models

In a condensed way, the problem described in Section II can be written as (17 – 18). In this formulation, the cost vector c represents generation costs considered as not affected by uncertainties, variables $\tilde{X}$ represent generations, branch flows and voltage phases and vector $\tilde{b}$ is the vector of independent terms in which we admit there is at least one trapezoidal fuzzy number. As described in Section II, the developed solution algorithm transforms this problem into a multiparametric problem by considering a parameter for each load variation and then converts it into a set of more manageable parametric optimization problems.

$$\min f = c^t.\tilde{X} \quad (17)$$

$$\text{subj.} \quad A.\tilde{X} \le \tilde{b} \quad (18)$$

If we now think about uncertainties in generation costs, we can consider a condensed formulation given by (19 – 20). In this case we are assuming that loads have no uncertainty and that vector c includes at least one generation cost represented by a trapezoidal fuzzy number.

$$\min f = \tilde{c}^t.\tilde{X} \quad (19)$$

$$\text{subj.} \quad A.\tilde{X} \le b \quad (20)$$

Finally, if we want to consider generation costs and load uncertainties simultaneously we get a problem as (21 – 22).

$$\min f = \tilde{c}^t.\tilde{X} \quad (21)$$

$$\text{subj.} \quad A.\tilde{X} \le \tilde{b} \quad (22)$$

B. Solution Algorithm for Problem (17-18)

The solution algorithm described in Section II for the general problem (17-18) does not perform an exhaustive search on the hypervolume containing all possible load combinations. In fact, it identifies a number of vertices of that hypervolume and it runs for each of them a parametric DC OPF study varying the load from the combination used to solve the initial deterministic problem (1-5) till each of these vertices. This approach may eventually lead to narrower membership functions of the results in case these parametric studies do not lead to the extreme possible behaviour of the resulting variables. This fact motivated the development of a more robust solution algorithm that will be described in the next paragraphs as follows:

- in the first place, it is identified a feasible and optimal solution for the initial deterministic DC-OPF problem (1-5) obtained by substituting each fuzzy load by the corresponding central value, Pl_k^{ctr};
- secondly, load uncertainties represented by parameters Δ_k are integrated in the initial optimization problem leading to the multiparametric formulation (17-18);
- in the third place, they are identified all critical regions. This means regions in the solution space where a base B of the multiparametric problem (17-18) remains feasible and optimal. This identification process is conducted using the algorithm proposed in [11]. Each critical region is defined by a number of linear inequalities function of the parameters Δ_k;
- in the fourth place, and for each critical region we compute the maximum and minimum values of the generator and branch flow expressions, function of Δ_k. For each variable regarding which we want to build its fuzzy membership function, this process implies solving a set of linear minimization and maximization problems related with several cuts between the 0 and 1 membership values;
- once all the critical regions are analysed, the membership function of the final results (generation, branch flows and voltage phases) can be obtained applying the fuzzy union operator to all the partial membership function obtained for each critical region identified in the previous step.

C. Solution Algorithm for Problem (19-20)

Let us now consider the problem (19-20), admitting uncertainties only affecting the cost vector. The solution algorithm is now structured as follows:

- in the first place, it is obtained a feasible and optimal solution for the deterministic DC-OPF problem (1-5) considering that the fuzzy coefficients of the cost vector are substituted by their central value, c_k^{ctr};
- secondly, we represent the uncertainties in generation or fuel prices by parameters Φ_k and we integrate them in the initial optimization problem leading to the multiparametric formulation (19-20);
- in the third place, we identify all critical regions in the solution space once again considering that such a region exists if there is a base B of the multiparametric problem (19-20) that is feasible and optimal. This identification is performed using the algorithm proposed in [11] and at the end of it each region is defined by a set of linear inequalities function of Φ_k;
- in the fourth place, for each variable of the problem, (generation, branch flows and voltage phases) we determine their extreme values for a number of cuts in the interval $[0,1]$. This corresponds to solve a number of optimization problems in which we minimize and maximize each variable subjected to the inequalities defining that critical region. As a result, for each variable and for each critical region we get a partial membership function representing the possible behavior of that variable in that region;
- finally, the partial membership functions obtained for each variable in the analysed critical regions are aggregated using the fuzzy union operator. This operator is adopted in order to obtain the widest possible behaviour of each variable.

D. Solution Algorithm for Problem (21-22)

At a final step, let us consider that there are uncertainties affecting both elements of the cost vector and elements of the right hand side of the constraints. In this case, the solution algorithm evolves as follows:

- in the first place, it is identified a feasible and optimal solution for the initial deterministic DC-OPF problem (1-5). This study is done substituting each fuzzy load and cost coefficient by the corresponding central value, Pl_k^{ctr} and c_k^{ctr} respectively;
- secondly, we represent load and cost coefficient uncertainties by parameters Δ_k and Φ_k and we integrate them in the initial optimization problem leading to the multiparametric formulation (21-22);
- in the third place, we identify all critical regions in a similar way to what was referred in sections III. B and C. The main difference is due to the fact that in this case, each critical region is related both with a feasibility criterium (due to the presence of parameters affecting the right hand side vector) and with an optimality criterium (due to the uncertainties affecting cost coefficients). In any case, a critical region is still defined as a subset of the solution space where there exists a feasible and optimal base B of the multiparametric problem (21-22). This identification is once again done using the algorithm described in [11]. At the end of this process, each critical region is defined by the conjunction of a set of linear inequalities;
- now, the algorithm evolves in a similar way to what was described in Sections III.B and III.C. This means that for each region, for each variable and for a number of cuts in the interval $[0,1]$ we solve minimization and maximization problems to identify the widest possible behavior of that variable in that region. The partial membership functions built for each variable in each region are aggregated using the fuzzy union operator.

IV. BUILDING THE MEMBERSHIP FUNCTIONS OF NODAL MARGINAL PRICES

Considering the problem addressed in Section II, nodal marginal prices can be obtained using the values of dual variables of the related optimization problem. For problem (1 to 5) expression (23) should be used to obtain a set of crisp nodal marginal prices related to the crisp load scenario integrating the central values of fuzzy loads. In this expression γ represents the dual variable of constraint (2) while the second term measures how much the cost function varies due to a change in branch losses caused by an increased of 1 unit of the load in bus k.

$$\rho_k = \gamma + \gamma.\frac{\partial Loss}{\partial Pl_k} - \sum \eta.\frac{\partial P_{ij}}{\partial Pl_k} + \sigma_k \qquad (23)$$

$$\frac{\partial f}{\partial Pl_k}(losses) = \frac{\partial f}{\partial Loss}.\frac{\partial Loss}{\partial Pl_k} \qquad (24)$$

The second term can be obtained using (24) considering that, once losses are estimated, they are treated as loads. Therefore, the first derivative in (24) corresponds to γ and the second derivative is given by (25) where the derivative of the losses in a branch ij is given by (13).

$$\frac{\partial Loss}{\partial Pl_k} = \sum_{\text{all branches}} \frac{\partial Loss_{ij}}{\partial Pl_k} \qquad (25)$$

The third term in (23) measures the variation of the cost function if a branch flow constraint is active. In this case, the dual variable of constraint (5), η, is non zero. It should be noted that, differently from constraint (2), an increase of 1 unit in the load in node k is not directly reflected on a change on the right term of branch flow constraints. In fact, the load in node k is multiplied by the symmetric of the sensitivity of the flow in branch ij regarding the load in node k. In (23) the derivative of P_{ij} regarding P_{lk} corresponds to the symmetric of this sensibility coefficient. Finally, the fourth term corresponds to the dual variables of constraint (4). These dual variables will only be non-zero if a new load unit in node k directly increases PNS.

The values given by (23) for the crisp load scenario have a membership degree 1.0. When running the parametric DC-OPF studies referred in Section II, nodal marginal prices are altered since load changes can turn the initial optimal basis infeasible. In this case, a Dual Simplex algorithm is used to recover feasibility. This process leads to changes in the basic variables and thus in the nodal marginal prices. Whenever this occurs, expression (23) is used to compute nodal marginal prices that can then be associated with their membership degree as indicated in [10]. At the end of this process, we have for each node a fuzzy membership function including several pairs (marginal price, membership degree) that reflect the changes on the basis of the optimisation problem and ultimately load uncertainties.

When addressing the problems described in Section III.A, building the membership function of nodal marginal prices follows a similar reasoning summarized as follows:

- in the first place, they are computed the nodal marginal prices related with the optimal solution of the initial DC OPF study. These values are obtained using (23) and are assigned 1.0 membership degree;
- then, along the solution algorithms described in Sections III.B, III.C and III.D, it is typically necessary to perform new iterations of the Primal or the Dual form of the Simplex Method. When that is done, there is a change on the basis of the problem as well as on the values of the dual variables. Whenever this change occurs, it is computed a new set of nodal prices using expression (23) and these prices are assigned a membership value reflecting the membership degree of the load combination at which that change occurred;
- at the end of this process, and for each node one has a number of nodal prices together with the corresponding membership degree. These values can be seen as a set of ordered pairs in which the first element is a price and the second is the membership value. The membership function of the nodal price at node k is obtained applying the fuzzy union operator to all these pairs.

V. CASE STUDY

A. *Results Obtained for a Small Illustrative Example*

A.1 Data

To illustrate the application of the algorithms described in Section III we used the small system presented in Figure 1. We considered 6 MW for the capacity of generators 1 and 2, 2 MW for the capacity of branch 1 and 5 MW for branches 2 and 3. All branches have the same impedance of 0.05+j1.0 pu, (base of 10 MVA, 10 kV).

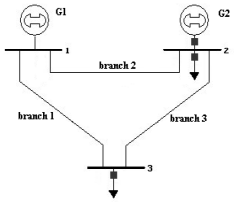

Fig. 1. Three bus/three branch power system.

A.2 Results Only Considering Load Uncertainties

In this case we used the trapezoidal fuzzy numbers (26 – 27) to describe loads in nodes 2 and 3 and the cost of generator 2 is the double of the cost of generator 1.

$$P_{c2} = (0.0;1.5;2.5;4.0)\ \text{MW} \quad (26)$$

$$P_{c3} = (2.0;3.0;4.0;5.0)\ \text{MW} \quad (27)$$

According to the algorithm in Section III.B, we solve a deterministic DC OPF study for the load values of 2.0 MW in node 2 and 3.5 MW in node 3, that is for the central values of the fuzzy numbers (26) and (27). Then, we integrated parameters Δ_2 and Δ_3 in order to build the corresponding multiparametric problem. As a result, Figure 2 represents in the plane Δ_2/Δ_3 the 0.0 and 1.0 cuts associated with the possible variations of these parameters.

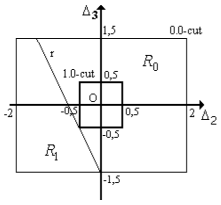

Fig. 2. 0.0 and 1.0 cuts representing the possible variation of the two parameters and identification of the critical regions in the solution space.

This figure also indicates that the optimal and feasible basis obtained for the initial deterministic run (point O) remains feasible in what is termed as region R_0. To the left hand side of line r, the value of one basic variable gets negative indicating that basis is no longer feasible. This means that we have to use the Dual Simplex to recover feasibility, thus defining a new critical region, R_1.

Then, for each of these two regions, we minimized and maximized the values of the output variables (generations, for instance) in the 0.0 and the 1.0 cuts subjected to the inequalities defining those regions. The partial results obtained for these two generations were aggregated leading to the fuzzy membership functions represented in Figure 3.

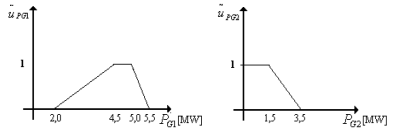

Fig. 3. Membership functions of P_{G1} and P_{G2}.

A.3 Results Considering Generation Cost Uncertainties

In this case we admitted that the generation costs are described by the trapezoidal fuzzy numbers (28 – 29). We also considered that all branches have a capacity of 5 MW and that loads in nodes 2 and 3 are 2.0 and 3.5 MW.

$$cP_1 = (0.5;1.5;2.5;3.5)\ €/\text{MW.h} \quad (28)$$

$$cP_2 = (1.5;2.5;3.5;4.5)\ €/\text{MW.h} \quad (29)$$

Applying the algorithm in Section III.C considering a parameter for each generation cost variation we obtain the results in Figures 4 and 5. Figure 4 represents the 0.0 and the 1.0 cuts related with the possible variations of the cost parameters. Once again, the algorithm starts by solving a deterministic DC-OPF using 2.0 and 3.0 €/MW.h for generation costs. This point is related to point O in Figure 4 and the corresponding basis remains optimal and feasible in region R_0. To the right hand side of line r, this basis is no longer optimal leading to the identification of the critical region R_1. Finally, the two generations were minimized and maximized in R_0 and R_1 leading to the membership functions in Figure 5. According to Figure 5, when the cost of generator 1 is smaller than the cost of generator 2 all the demand is supplied by generator 1, and vice-versa.

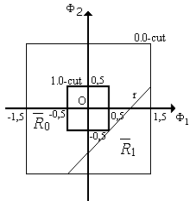

Fig. 4. 0.0 and 1.0 cuts representing the possible variations of the cost parameters and identification of the critical regions.

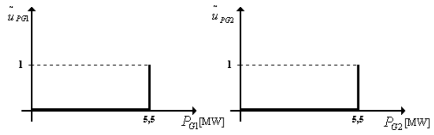

Fig. 5. Membership functions of P_{G1} and P_{G2}.

A.3 Results Considering Load and Cost Uncertainties

In this case we considered that the cost of generator 1 and load 2 are described by the trapezoidal fuzzy numbers (30) and (31). The cost of generator 2 is 3.0 €/MW.h, the load in node 3 is 3.5 MW and the capacity of branch 1 is 2 MW.

$$cP_1 = (0.5;1.5;2.5;3.5)\ €/\text{MW.h} \quad (30)$$

$$P_{c2} = (0.0;1.5;2.5;4.0)\ \text{MW} \quad (31)$$

Applying the algorithm in Section III.D considering two parameters (one in the cost function and another in the constraint right hand side vector) we started running a DC-OPF problem using a cost of 2.0 €/MW.h for generator 1 and a value of 2.0 MW for load 2. Then the two parameters are integrated in the problem and Figure 6 represents the 0.0 and 1.0 cuts of their possible variation. The basis of the initial problem (point O in Figure 6) remains feasible in region R_0. In this case, out of this region one loses feasibility or optimality leading to the identification of three other critical regions. For each of these four regions one minimizes and maximizes the generation variables submitted to the inequalities defining those regions and leading to the final membership functions in Figure 7.

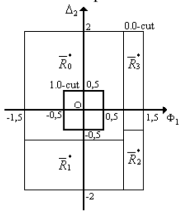

Fig. 6. 0.0 and 1.0 cuts representing the possible variation of the two parameters and identification of the critical regions.

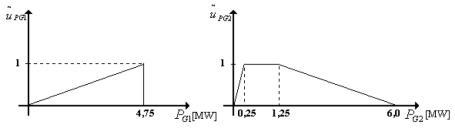

Fig. 7. Membership functions of P_{G1} and P_{G2}.

B. Results for the IEEE 24 Bus Test System

In this case we used the data in [10] to compute the membership functions of nodal marginal prices, due to load uncertainties. The computation of these membership functions was performed using the algorithm described in Section IV. Regarding the central values specified for the loads we admitted they were affected by uncertainties. At level 0.0 this uncertainty corresponded to 0.9 and 1.1 and at level 1.0 it corresponded to 0.95 and 1.05 multiplied by the central value. As an example, (32) to (38) represent the fuzzy membership functions obtained for some nodal prices. The values in bold correspond to the ones obtained for the deterministic DC-OPF study using expression (23) so that one can appreciate the impact on nodal prices from admitting uncertainties in load values.

$$\tilde{\rho}_1 = \{(7.00;1.0),(7.75;1.0),(\mathbf{8.12};1.0)\} \quad (32)$$

$$\tilde{\rho}_3 = \{(7.00;1.0),(7.72;1.0),(\mathbf{8.08};1.0)\} \quad (33)$$

$$\tilde{\rho}_6 = \{(7.00;1.0),(7.76;1.0),(\mathbf{8.13};1.0)\} \quad (34)$$

$$\tilde{\rho}_7 = \{(\mathbf{5.00};1.0)\} \quad (35)$$

$$\tilde{\rho}_{11} = \{(7.00;1.0),(8.00;0.46),(8.59;1.0),(\mathbf{9.13};1.0)\} \quad (36)$$

$$\tilde{\rho}_{17} = \{(7.00;1.0),(7.65;1.0),(7.99;1.0),(\mathbf{8.00};1.00)\} \quad (37)$$

$$\tilde{\rho}_{20} = \{(7.00;1.0),(7.13;1.0),(\mathbf{7.37};1.0),(8.00;0.46)\} \quad (38)$$

VI. CONCLUSIONS

In this paper, we formalized the DC-OPF dispatch problem considering three situations: the presence of uncertainties in the right hand side vector, in the cost vector and simultaneously in these two vectors. For each of these problems we described the developed solution algorithms based on linear multiparametric programming techniques. The use of these techniques leads to the identification of a number of critical regions in which the problem variables are minimized and maximized in order to build the final membership functions. This means that all possible combinations of loads and costs are exhaustively analysed since the referred critical regions cover all the uncertainty space. This has an important consequence since it leads to accurate membership functions actually representing the widest possible behaviour of each variable. In an era in which volatility prevails, we think that these models will be very useful in several domains and for different agents acting in the electricity sector.

REFERENCES

[1] M. Rivier, I. Perez Arriaga, G. Luengo, "JUANAC: A model for Computation of Spot Prices in Interconnected Power System", *Proceedings of PSCC' 90*, Graz, August 1990.

[2] B. Borkowska, "Probabilistic Load Flow", *IEEE Transaction on PAS, vol. PAS-93*, no. 12, pp. 752- 759, December 1974.

[3] R. N. Allan, M. R. G. Al-Sharkarchi, "Probabilistic Techniques in AC Load-Flow Analysis", *Proceedings of the IEE*, vol. 124, no. 2, pp. 154- 160, February 1977.

[4] R. N. Allan, A. M. Leite da Silva, "Probabilistic Load Flow Using Multilinearisations", *Proceedings of the IEE*, vol. 128, no. 5, pp. 280- 287, September 1981.

[5] T. S. Karakatsanis, N. D. Hatziargyriou, "Probabilistic Constrained Load Flow Based on Sensitivity Analysis", *IEEE Transactions on Power Systems*, vol. 9, no. 4, pp. 1853-1860, November 1994.

[6] V. Miranda, M. A. Matos and J. T. Saraiva, "Fuzzy Load Flow - New Algorithms Incorporating Uncertain Generation and Load Representation", *Proceedings of the 10th PSCC*, Butterworths, London, 1990.

[7] J. T. Saraiva and V. Miranda, "Identification of Hedging Policies in Generation/Transmission Systems", *Proceedings of PSCC 96*, Dresden, August 1996, pp. 779-785.

[8]J. T. Saraiva, N. Fonseca, M. A. Matos, "Fuzzy Power Flow – An AC Model Addressing Correlated Data", *Proceedings of the 8th International Conference on Probability Methods Applied to Power Systems*, PMAPS, Ames, Iowa, USA, September 2004.

[9] J. T. Saraiva, V. Miranda, L. M. V. G. Pinto, "Impact On Some Planning Decisions From a Fuzzy Modelling Of Power Systems", *IEEE Transactions on Power Systems*, vol. 9, no. 2, pp. 819-825, May 1994.

[10]J. T. Saraiva, "Evaluation of the Impact of Load Uncertainties in Spot Prices Using Fuzzy Set Models", *Proceedings of the 13th Power Systems Computation Conference*, Trondheim, Norway, June-July 1999, pp. 265-271.

[11] T. Gal, *Postoptimal Analysis, Parametric Programming and Related Topics*, McGraw Hill International Book Company, 1979.

Bruno André Gomes was born in Ovar, Portugal, in 1977. In 2001 he got his BSc in the Faculdade de Ciências e Tecnologia da Universidade de Coimbra and in 2005 he got the MSc degree from Faculdade de Engenharia da Universidade do Porto, FEUP. Currently, he is with the Escola Superior de Tecnologia e Gestão of the Instituto Politécnico de Leiria, Portugal, where he is lecturer and he is PhD student at FEUP.

João Tomé Saraiva was born in Porto, Portugal in 1962. In 1987, 1993 and 2002 he got his MSc, PhD, and Agregado degrees in Electrical and Computer Engineering from the Faculdade de Engenharia da Universidade do Porto, FEUP, where he is currently Professor. In 1985 he joined INESC Porto – a private research institute – where he was head researcher or collaborated in several projects namely in the scope of consultancy contracts wit the Portuguese Electricity Regulatory Agency.

Modeling Costs and Load Uncertainties in Optimal Power Flow Studies, European Electricity Markets 2008, EEM08, Lisbon, Portugal, 28 to 30 June 2008

Modeling Costs and Load Uncertainties in Optimal Power Flow Studies

Bruno André Gomes[1], João Tomé Saraiva[2], Luís Neves[3]
INESC Porto and FEUP/DEEC,
Rua Roberto Frias 378, 4200 465 Porto, Portugal, phone +351.22.5081880 fax: +351.222094150
E-mail: bgomes@ineseporto.pt, jsaraiva@fe.up.pt
Instituto Politécnico de Leiria, ESTG, Morro do Lena, Alto Vieiro, Apartado 4163, 2401-951 Leiria, Portugal
E-mail: lneves@estg.ipleiria.pt

Keywords **– Uncertainties, fuzzy models, DC optimal power flow, multiparametric programming.**

Abstract **– Modeling uncertainties in power systems has long interested researchers. Nowadays, as in 70's, the volatility associated with generation or fuel prices, for one side, and the uncertainties related with load forecasting and generation capacity, for another, places a new emphasis on this kind of problems. As a result of this renewed interest, in this paper we are enlarging the original Fuzzy Optimal Power Flow, FOPF, model in order to consider not only load uncertainties, but also uncertainties in generation or fuel prices, specified using trapezoidal fuzzy numbers. This new approach is based on multiparametric linear programming techniques that lead to the identification of a number of critical regions covering all the uncertainty space. This contributes to build more accurate membership functions of all variables, namely generations, branch flows and power not supplied.**

I. Introduction

THE development of electricity markets all over the world brings to the scientific community, to the players and to the regulatory authorities a new set of challenges. Among them, uncertainty became a structural element in this new environment that all kind of agents have to be able to deal with in order to guarantee the appropriate power system planning and operation as well as its own economical liquidity. When speaking about uncertainty modelling, the initial formulations adopted probabilistic models to represent reliability issues and also to model load uncertainties leading to probabilistic power flow models as the pioneering contributions in [1]-[2] and latter on several others papers as [3]-[4]. The algorithms in these papers typically use linearized expressions to build the probabilistic functions of the usual power flow outputs. However, given that load uncertainties are due to several factors, many of which of qualitative nature and dependent on hardly predictable events, such as economic growth, environmental constraints, political developments, and others, neither these probabilistic models, nor deterministic ones are adjusted to deal with this kind of uncertainties.

From the mid 80th onwards, we witnessed the development of a new class of approaches to model uncertainty. These new approaches adopted fuzzy models to represent the uncertain behaviour affecting several variables and parameters. These models strongly differ from probabilistic ones namely from a pure conceptual point of view. In fact, fuzzy models do not rely on the observation of a large number of events from which probabilistic distributions can then be derived. Differently, they are based on the experience of the users and on its own subjectivity. Accordingly, fuzzy models can be used in a profitable way to represent a different kind of uncertainty inherent, for instance, to a large number of expressions of our language. In this scope, reference [5] presented the first DC and AC fuzzy power flow models and references [6]-[7] describe approaches to translate the uncertainty affecting the demand in the results of DC Optimal Power Flow problems. Reference [8] details the integration of the Fuzzy DC OPF model in a Monte Carlo Simulation as a way to estimate the expected value of several results, as the Power Not Supplied. Finally, reference [9] describes an approach to identify the most adequate expansion plan so that the risk of not meeting the demand gets reduced while accommodating the inherent uncertainty.

Apart from this introduction, Section II describes the original Fuzzy Optimal Power Flow, FOPF, problem and Section III describes the new developed formulation, and solution algorithm to integrate load and costs uncertainties. Sections IV and V present Case Studies to illustrate the developed algorithms and highlight some important features. They are based on a six bus/eight branches system and on the IEEE 24 bus/38 branches test system. Finally, Section VI presents the most relevant conclusions.

II. Fuzzy Optimal Power Flow

A FOPF study, as it was originally conceived, corresponds to an optimization problem aiming at identifying the best generation strategy according to a generation cost function admitting that, at least, one load is represented by a fuzzy number. The FOPF adopts the DC approach to model the operation conditions of the network and includes power flow and generation limit constraints. Figure 1 presents the general FOPF algorithm.

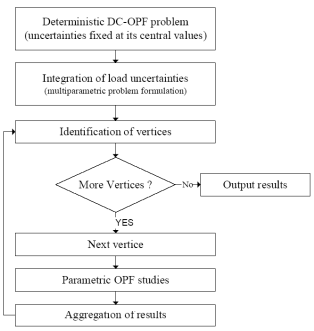

Fig. 1. Fuzzy DC Optimal Power Flow algorithm.

978-1-4244-1744-5/08/$25.00 ©2008 IEEE

As it can be seen in Figure 1, in the first step the FOPF runs the deterministic DC-OPF study (1-5) for the central values of the fuzzy numbers that represent loads.

$$\min f = \sum c_k.Pg_k + G.\sum PNS_k \quad (1)$$

$$\text{subj.} \quad \sum Pg_k + \sum PNS_k = \sum Pl_k^{ctr} \quad (2)$$

$$Pg_k^{min} \le Pg_k \le Pg_k^{max} \quad (3)$$

$$PNS_k \le Pl_k^{ctr} \quad (4)$$

$$P_b^{min} \le \sum a_{bk}.(Pg_k + PNS_k - Pl_k^{ctr}) \le P_b^{max} \quad (5)$$

In this model Pg_k is the generation in bus k with cost c_k and PNS_k is the power not supplied in bus k, Pg_k^{min}, Pg_k^{max}, P_b^{min} and P_b^{max} are the generation and branch flow limits and a_{bk} is the DC sensitivity coefficient of the flow in branch b regarding the injected power in bus k. If loads are represented by trapezoidal fuzzy numbers as in Figure 2, the central value Pl_k^{ctr} is defined as the average value of the 1.0-cut, that is, of the interval having 1.0 membership degree. In Figure 2, the 1.0-cut is given by $[Pl_{k,2};Pl_{k,3}]$ and Pl_k^{ctr} is given by (6). It is also important to refer that this kind of fuzzy representation was selected because it corresponds to the most generalized form of a fuzzy number. In fact, the rectangular or triangular fuzzy numbers, for instance, are simply particular cases of this one.

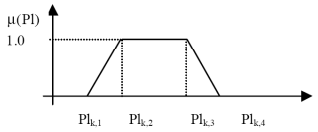

Fig. 2. Membership function of a trapezoidal fuzzy number.

$$Pl_k^{ctr} = (Pl_{k,2} + Pl_{k,3})/2 \quad (6)$$

After running the initial deterministic study (1-5) and having identified a feasible and optimal solution for it, the uncertainty parameters, Δ_k, are integrated in the problem leading to the multiparametric problem defined by (7-9).

$$\min f = c^t.X \quad (7)$$

$$\text{subj.} \quad A.X = b + b'(\Delta_k) \quad (8)$$

$$\Delta_{k1} \le \Delta_k \le \Delta_{k4} \quad (9)$$

Since the optimal solution of the crisp problem may not be feasible for all load combinations associated with (9), once the multiparametric linear programming problem is defined the algorithm proceeds by the identification of vertices of the hypervolume (9). As a general rule, these vertices correspond to feasible solutions leading to max or min values of each basic variable of the initial solution or, in the opposite side, to vertices corresponding to unfeasible solutions. In the end of this process all vertices surrounding the initial central value that lead to individual extreme values of the basic variables or, instead, to non-feasible solutions are identified. Afterwards, the algorithm proceeds by doing a set of two consecutive parametric DC-OPF studies for each identified vertex. As an example, let us consider that Figure 3 represents the rectangles enclosing all load combinations for the 0.0 and 1.0-cuts for a system with the trapezoidal fuzzy loads defined by (10) and (11).

$$P_{l1} = P_{l1}^{ctr} + (\Delta_{11};\Delta_{12};\Delta_{13};\Delta_{14}) \text{ MW} \quad (10)$$

$$P_{l2} = P_{l2}^{ctr} + (\Delta_{21};\Delta_{22};\Delta_{23};\Delta_{24}) \text{ MW} \quad (11)$$

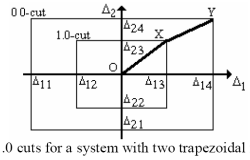

Fig. 3. 0.0 and 1.0 cuts for a system with two trapezoidal fuzzy loads.

Taking Figure 3 as reference and the vertex Y as an illustration, the first parametric study analyses load combinations on the segment OX considering that points O and X correspond, respectively, to $\alpha = 1.0$ and $\alpha = 0.0$ in the linear parametric optimization problem (12-14).

$$\min f = c^t.X \quad (12)$$

$$\text{subj.} \quad A.X = b + b'(1.0 - \alpha) \quad (13)$$

$$0.0 \le \alpha \le 1.0 \quad (14)$$

When point X is reached, the optimal and feasible solution is given by (15).

$$X_{opt} = B^{-1}.(b + b'(1.0 - \alpha)) \quad (15)$$

In the second parametric study, points X and Y correspond to $\alpha = 1.0$ and $\alpha = 0.0$, respectively. Performing another parametric DC-OPF study, it is possible to obtain the solution for Y, where the optimal and feasible basis is given by (16).

$$X_{opt} = B^{-1}.(b + b' + b''(1.0 - \alpha)) \quad (16)$$

These parametric studies are formulated in such a way that it is possible to guarantee that the values obtained in the first one are assigned to 1.0 membership degree while the values related with the second one have a membership degree that corresponds to the value of α, and so, it decreases from 1.0 to 0.0 membership degree (points X and Y, respectively). The final membership functions of branch flows, generation and Power Not Supplied can then be obtained by aggregating the partial membership functions of each variable obtained in each set of parametric studies, using the fuzzy union operator.

III. New Fuzzy Optimal Power Flow Model

A. Overview

Recognizing that the development of electricity markets and the volatility affecting fuel prices place a new emphasis on power system planning and operation as well in the economic liquidity of market agents, the New Fuzzy Optimal Power Flow, NFOPF, approach aims at, in first place, extending the original concept by translating to the results not only load uncertainties, but also generation costs uncertainties. Secondly, since computational resources are nowadays more powerful than in past, the NFOPF also enables obtaining a more accurate representation of this type of problems, since it adopts linear multiparametric

optimization techniques. In fact, these techniques lead to the identification of a number of critical regions covering all the uncertainty space meaning that they are effectively covered all the combinations of values of the parameters affected by uncertainties. This has an important consequence given that we can now obtain more accurate membership functions in the sense they actually represent the widest possible behavior of each variable. The original FOPF model in Section II only runs a number of parametric studies eventually leading to narrower membership functions when compared with the real ones.

The algorithms used to solve the multiparametric linear problems were originally proposed by Gal [10]. Starting at the initial optimal and feasible solution of the deterministic optimization problem as stated by (1-5), these algorithms perform a critical region identification process. This means that they search all the combination of values of the parameters affected by uncertainties for which exists an optimal and feasible basis. When doing this, we are extending the optimality and feasibility conditions ((17) and (18), respectively) so they become function of Φ_k (parameters modeling cost uncertainties) or Δ_k (parameters modeling load uncertainties). Then starting with the optimal and feasible solution of the initial deterministic optimization problem and considering each of these conditions, we find the set of other optimal and feasible solutions provided they are valid in some region of the uncertainty space. These regions are called critical regions and this process is conducted by pivoting over the initial basis as well as over all the new ones identified during the search process.

In this sense, let B be an optimal and feasible basis, ρ the index for the corresponding set of basic variables, A the columns of the non-basic variables in the Simplex tableau, C_0 the cost vector of the basic variables and C^T the cost vector of the non-basic variables. The optimality and feasibility conditions for a minimization linear problem can then be defined in terms of Φ_k and Δ_k by (17) and (18).

$$C^T(\Phi_k) - C_0^T.B_\rho^{-1}.A = (c + c'(\Phi_k)) - C_0^T.B_\rho^{-1}A \geq 0 \quad (17)$$

$$B_\rho^{-1}.b(\Delta_k) = B_\rho^{-1}(b + b'(\Delta_k)) \geq 0 \quad (18)$$

Since the dual solution does not depend on Δ_k for right hand side parametrization, a critical region, i.e., a region in the uncertainty space where B remains optimal and feasible, can be uniquely defined by the conditions in (18). By analogy, since the primal solution does not depend on Φ_k for cost parametrization, a critical region can be defined by the conditions given by (17). Apart from these conceptual aspects, two optimal and feasible basis, B_1 and B_2, are considered neighbor ones if and only if one can pass from B_1 to B_2 performing one dual pivot step in case of right hand side parametrization or one primal pivot step in case of cost vector parametrization.

As a final comment, the ultimate objective to attain when solving a multiparametric optimization problem is to find all possible optimal solutions, their corresponding optimal values and critical regions, which can be defined as a closed nonempty polyhedron, that is, a set of linear inequalities in Δ or Φ. Mathematically, this set of constraints can be expressed as the equivalent set of non-redundant constraints, which in turn can be identified through a non-redundant test for linear inequalities, like the one proposed by Gal [10].

B. Consideration of Load Uncertainties

Figure 4 presents the algorithm of the NFOPF. Similarly to the algorithm described in Section II, in this new approach it is also performed an initial deterministic DC-OPF problem (1-5) to identify a feasible an optimal solution associated to the central values of the fuzzy load representations. In second place, the parameters modelling load uncertainties are included in the original optimization problem leading to the problem (19-23).

$$\min f = \sum c_k.Pg_k + G.\sum PNS_k \quad (19)$$

$$\text{subj.} \quad \sum Pg_k + \sum PNS_k = \sum Pl_k^{ctr} + \sum \Delta_k \quad (20)$$

$$Pg_k^{min} \leq Pg_k \leq Pg_k^{max} \quad (21)$$

$$PNS_k \leq Pl_k^{ctr} + \Delta_k \quad (22)$$

$$P_b^{min} \leq \sum a_{bk}.(Pg_k + PNS_k - (Pl_k^{ctr} + \Delta_k)) \leq P_b^{max} \quad (23)$$

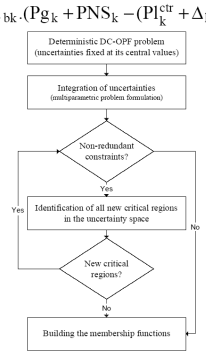

Fig. 4. New Fuzzy DC Optimal Power Flow algorithm.

Considering the inequalities associated to the feasibility condition (18), the algorithm identifies a set of non-redundant constraints defining new critical regions. If there are no non-redundant constraints, the algorithm stops. Otherwise, it performs a dual pivoting over the initial optimal and feasible solution to identify new critical regions. This process is repeated until no non-redundant constraints exist or until all identified critical regions correspond to already known ones. When this is over, all the uncertainty space was covered and we identified all critical regions in which a base B of the problem (19-23) remains feasible and optimal.

For a better understanding of this procedure, Figure 5 depicts the rectangles enclosing all load combinations between the 0.0 and 1.0-cuts for a system integrating two trapezoidal fuzzy loads. In this Figure, lines "a" and "b" represent constraints, for instance, related with branch flow or generator capacity limits, point O is the optimal and feasible solution of the initial deterministic DC-OPF problem and the dashed lines define the range of values of the uncertainties at the i^{th} level of the data membership functions.

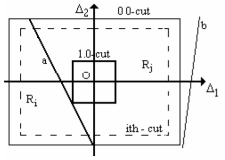

Fig. 5. Critical regions in the uncertainty space.

From Figure 5 it becomes clear that a set of non-redundant constraints, such as line "a", can define any critical region such as R_i and R_j. This is in fact very relevant given that it reduces the computational effort of the algorithm by defining a more precise and efficient search procedure of neighbour critical regions. This identification process is implemented using the feasible condition (18) described by the parameters of load vector uncertainties. Once this process is finished the critical regions are obtained by doing a dual pivoting over each of the optimal and feasible basis identified.

In order to build the membership functions of the output variables (generations, branch flows and Power Not Supplied) we must recall that, being a linear model, each variable in each critical region is represented by a linear expression. In this sense, if we are interested in capturing the widest possible behavior of a function $v(\Delta_1,\Delta_2)$ expressed in terms of the parameters Δ_1 and Δ_2 we will then have to solve the problem (24-27).

$$\min/\max f = v(\Delta_1,\Delta_2) \quad (24)$$

$$\text{subj.} \quad k_{1i}.\Delta_1 + k_{2i}.\Delta_2 \le b_i \quad (25)$$

$$\Delta_1^{\min\ i^{th}-cut} \le \Delta_1 \le \Delta_1^{máx\ i^{th}-cut} \quad (26)$$

$$\Delta_2^{\min\ i^{th}-cut} \le \Delta_2 \le \Delta_2^{máx\ i^{th}-cut} \quad (27)$$

In this problem we are minimizing and maximizing a function $v(\Delta_1,\Delta_2)$ subjected to the constraints modeling the non-redundant conditions (25) together with the possible ranges of the input uncertainties regarding the i^{th} cut under analysis (26-27). After solving this type of problems for several cuts, it is possible to build the membership function of v in this critical region. Once all critical regions are analyzed, the final membership function of v is obtained applying the Fuzzy Union Operator to the partial membership functions obtained for that variable in order to guarantee that the final result displays the widest possible behavior given the specified uncertainties.

C. Consideration of Cost Uncertainties

If we now want to consider cost uncertainties instead of load uncertainties we will obtain the condensed multiparametric linear problem (28) to (30), where loads are given by crisp values and $c(\Phi_k)$ includes at least on cost represented by a trapezoidal fuzzy number.

$$\min \quad f = c(\Phi_k)^t.\tilde{X} \quad (28)$$

$$\text{subj.} \quad A.\tilde{X} \le b \quad (29)$$

$$\Phi_{k1} \le \Phi_k \le \Phi_{k4} \quad (30)$$

In this case the solution algorithm presented in Figure 4 remains valid provided that some adaptations are made. In this sense, the algorithm starts by solving an initial deterministic DC-OPF problem (1-5) for the crisp values of the fuzzy cost representations to identify a feasible an optimal solution. Following the same strategy, the optimization problem (31-35) is obtained integrating the parameters representing cost uncertainties in the original problem.

$$\min f = \sum c_k(\Phi).Pg_k + G.\sum PNS_k \quad (31)$$

$$\text{subj.} \quad \sum Pg_k + \sum PNS_k = \sum Pl_k^{ctr} \quad (32)$$

$$Pg_k^{\min} \le Pg_k \le Pg_k^{\max} \quad (33)$$

$$PNS_k \le Pl_k^{ctr} \quad (34)$$

$$P_b^{\min} \le \sum a_{bk}.(Pg_k + PNS_k - Pl_k^{ctr}) \le P_b^{\max} \quad (35)$$

The identification of non-redundant constraints is implemented using the inequalities given by the optimality condition (17) described by the parameters of the cost vector uncertainties. In this case, the search procedure for critical regions is implemented performing a primal pivoting over the initial optimal and feasible basis as well as over all the new optimal and feasible basis identified along the search procedure.

When building the membership function of each variable we must recall that in this case each variable is constant inside each critical region, which means that changes will only happen if there is a basis change. In this sense, to build the partial membership functions the algorithm just has to consider each critical region and its corresponding non-redundant inequalities and determine its maximum membership degree. For doing this, the algorithm checks if any of the extreme points of a given cut level (vertices of the hypervolume defined by (30) in each cut level) belongs to the critical region under analysis. Once all partial membership function are obtained, we use the Fuzzy Union Operator to obtain the widest possible behaviour of each variable in the uncertainty space.

IV. CASE STUDY USING A SMALL EXAMPLE

A. Data

In the first case study, we tested the developed algorithms using the 6 bus/8 branch system of Figure 6.

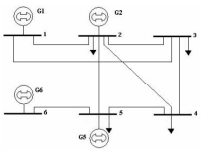

Fig. 6. Six bus/eight branch power system.

Table 1 presents the load central values, the per unit reactance of branches in a 100 MVA base, the capacity limits of generators and the central values of their generation costs. Finally, it should be referred that the branches capacities were set at 5 MW.

TABLE I
System data.

Bus	Load [MW]	Branch	Reactance [pu]	Bus	P_G^{max}/P_G^{min} [MW]	Cost [€/MW.h]
1	0.0	1-2	0.06	1	10/0	1.0
2	4.0	1-3	0.24	2	15/0	2.0
3	6.0	2-3	0.18	5	7/3	1.0
4	4.0	2-4	0.18	6	5/0	2.0
5	4.0	2-5	0.12	--	--	--
6	0.0	3-4	0.03	--	--	--
--	--	4-5	0.24	--	--	--
--	--	5-6	0.03	--	--	--

B. Results Considering Load Uncertainties

In the first place, we used the trapezoidal fuzzy numbers (36) to (38) to represent loads in buses 2, 4 and 5.

$$P_{c2} = (1.0;2.0;6.0;7.0)\ \text{MW} \quad (36)$$

$$P_{c4} = (1.5;3.0;5.0;6.5)\ \text{MW} \quad (37)$$

$$P_{c5} = (2.0;3.5;4.5;6.0)\ \text{MW} \quad (38)$$

According the algorithm described in Section III.B, it was firstly solved a deterministic DC-OPF problem for the central values of the loads. Once obtained its solution, it was formulated the multiparametric linear optimization problem integrating the parameters that represent load uncertainties. Solving this problem, the algorithm identified four different critical regions covering all the uncertainty space. Finally, they were built the membership functions of the generators at buses 1, 2, 5 and 6 sketched in Figure 7. From Figure 7 we can see that for 0.0-cut the generation varies from 3.5 to 8.71 for generator 1, from 0.0 to 9.79 MW for generator 2, from 3.0 to 7.0 for generator 5 while generator 6 remains at 0.0 MW. At the 1.0-cut these variations are 7.5 to 8.3, 0.0 to 6.19 and from 6.64 to 7.0 for generators 1, 2 and 5, respectively. Finally, PNS is zero for all uncertainty levels.

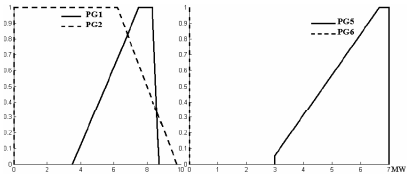

Fig.7. Membership functions of PG1, PG2, PG5 and PG6 admitting degenerate solutions.

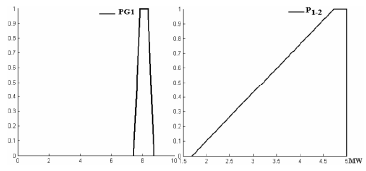

Fig. 8. Membership functions of PG1 (not considering degenerate solutions) and power flow in branch 1-2.

It must be also emphasized here that if we don't consider primal and dual degenerate solutions we obtain the membership function of PG1 presented in Figure 8. This function is narrower than the one in Figure 7 because it doesn't consider all possible combination of loads for each cut-level. On the right side of Figure 8 we can also see the membership function of the flow in branch 1-2. This flow can reach its limit as indicated in the Figure.

C. Results Considering Generation Cost Uncertainties

In this case we used the trapezoidal fuzzy numbers (39) and (40) to model the cost of the generators in buses 2 and 5. According to the algorithm described in Section III.C, once we obtain the solution of the deterministic DC-OPF problem for the central values of (39-40), we integrate cost uncertainties in order to build the problem (31-35). In this case, the algorithm found five different critical regions covering all the uncertainty space. According to Figure 9, PG1 can assume values 0.0, 7.85, 8.06 and 8.34 MW, PG2 0.0, 2.93, 6.66, 11.0 and 15.0 MW, PG5 3.0 and 7.0 MW and finally PG6 0.0 and 3.14 MW.

$$CP_{G2} = (0.5;1.5;2.5;3.5)\ €/\text{MW.h} \quad (39)$$

$$CP_{G5} = (0.25;0.75;1.25;1.75)\ €/\text{MW.h} \quad (40)$$

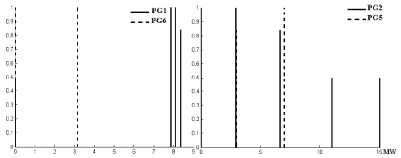

Fig. 9. Membership functions of PG1, PG6, PG2 and PG5.

Figure 10 displays the membership function of the power flow in branch 1-2. This Figure is very interesting since it indicates that for some combinations of the generation costs the direction of this flow can be reverted reaching its thermal limit (5 MW).

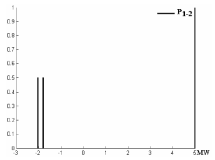

Fig. 10. Membership function of the power flow in branch 1-2.

V. CASE STUDY USING THE IEEE 24 BUS TEST SYSTEM

A. Data

The developed algorithms were also tested using the IEEE 24 bus/38 branch test system. Regarding the original data in [11], the load was increased to 5079.29 MW (Table II) and the total installed capacity is 5910 MW (Table III).

TABLE II
Load central values.

Bus	Load (MW)	Bus	Load (MW)	Bus	Load (MW)
1	192.46	7	222.75	15	564.89
2	172.85	8	304.72	16	178.20
3	320.76	9	311.85	18	593.41
4	132.46	10	347.49	19	322.54
5	126.52	13	472.23	21	228.10
6	242.35	14	345.71	--	---

Branch data can be obtained from [11] considering that the transformers have a capacity of 400 MW, the capacity of the branches 1 to 6 and 8 to 13 was set at 175 MW and of the remaining ones at 500 MW.

TABLE III
System installed capacity.

Bus/ Gen	Capacity (MW)	Cost (€/MW.h)	Bus/ gen	Capacity (MW)	Cost (€/MW.h)
1/1	40.0	3.0	15/3	24.0	2.0
1/2	40.0	3.0	15/4	24.0	2.0
1/3	152.0	4.0	15/5	24.0	2.0
1/4	152.0	4.0	15/6	310.0	6.0
2/1	40.0	3.0	16/1	310.0	5.5
2/2	40.0	3.0	18/1	800.0	9.0
2/3	152.0	4.0	21/1	800.0	8.0
2/4	152.0	4.0	22/1	100.0	2.0
7/1	200.0	5.0	22/2	100.0	2.0
7/2	200.0	5.0	22/3	100.0	2.0
13/1	394.0	6.0	22/4	100.0	2.0
13/2	394.0	6.0	22/5	100.0	2.0
13/3	394.0	6.0	22/6	100.0	2.0
15/1	24.0	2.0	23/1	310.0	5.0
15/2	24.0	2.0	23/2	310.0	5.0

B. Results Considering Load Uncertainties

In this case the load trapezoidal fuzzy numbers were built considering that at level 0.0 the uncertainty ranges from +/-10 per cent and at the 1.0 level it ranges from +/- 5 per cent of its central values. Figures 11 and 12 present the results obtained for the generators 7/2, 16/1, 18/1, 21/1 and for the Power Not Supplied at bus 14. PNS is not always zero due to transmission congestions on branches 14-16 and 16-17.

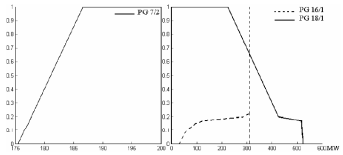

Fig. 11. Membership functions of generators 7/2, 16/1 and 18/1.

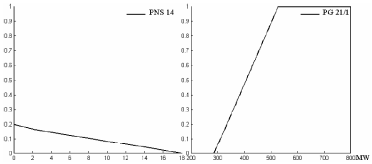

Fig. 12. Membership functions of Power Not Supplied at bus 14 and of the generator 21/1.

These results indicate that load variations are accommodated by generators 18/1 and 21/1 since they are the last ones to be dispatched because of their cost, on generator 16/1 because branches 14-16 and 16-17 reach their limits for some load combinations and also to a small extent by generator 7/2 because branch 7-8 also reaches its limit for some load combinations.

C. Results Considering Generation Cost Uncertainties

In this case we considered that the cost of generators 13/1, 13/2, 15/6, 16/1, 18/1 and 21/1 are described by the trapezoidal fuzzy numbers (41-46). Figure 13 presents the results obtained for these generators. As expected all generators exhibit a membership degree of 1.0 for the values corresponding to the results of the initial DC-OPF, which means 394, 310, 771.54, 310 and 0.0 MW for generators 13/1/2, 16/1, 21/1, 15/6 and 18/1, respectively. We can also see different generation strategies as a consequence of cost uncertainties of those generators.

$$CP_{G13/1} = (2.0;5.0;7.0;10.0)\ €/MW.h \quad (41)$$

$$CP_{G13/2} = (2.0;5.0;7.0;10.0)\ €/MW.h \quad (42)$$

$$CP_{G15/6} = (4.0;5.0;7.0;8.0)\ €/MW.h \quad (43)$$

$$CP_{G16/1} = (4.0;5.0;6.0;7.0)\ €/MW.h \quad (44)$$

$$CP_{G18/1} = (6.0;8.0;10.0;12.0)\ €/MW.h \quad (45)$$

$$CP_{G21/1} = (5.5;7.0;9.0;10.5)\ €/MW.h \quad (46)$$

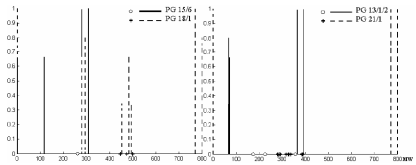

Fig. 13. Membership functions of generators 15/6, 18/1, 13/1/2 and 21/1.

VI. Conclusions

In this paper we presented a new Fuzzy Optimal Power Flow approach and highlight the main differences between this new approach and the original one. As it was shown this new approach can model not only load uncertainties but also cost uncertainties specified by trapezoidal Fuzzy numbers. Since this new approach is based on linear multiparametric programming techniques it can present more accurate results. This kind of models can play an important role in analysing the possible operation of power systems given the increasing volatility and unpredictably that is inherent to competitive markets.

VII. References

[1] B. Borkowska, "Probabilistic Load Flow", *IEEE Trans. PAS*, vol. PAS-93, no. 12, pp. 752- 759, December 1974.

[2] R. Allan, M. Al-Sharkarchi, "Probabilistic Techniques in AC Load-Flow Analysis", *Proc. of IEE*, vol. 124, pp. 154-160, Feb. 1977.

[3] R. N. Allan, A. M. Leite da Silva, "Probabilistic Load Flow Using Multilinearisations", *Proc. of IEE*, vol. 128, pp. 280-287, Sept. 1981.

[4] T. Karakatsanis, N. Hatziargyriou, "Probabilistic Constrained Load Flow Based on Sensitivity Analysis", *IEEE Trans. Power Systems*, vol. 9, pp. 1853-1860, Nov. 1994.

[5] V. Miranda, M. A. Matos, J. T. Saraiva, "Fuzzy Load Flow – New Algorithms Incorporating Uncertain Generation and Load Representation", *Proc. of 10th PSCC*, Butterworths, London, 1990.

[6] V. Miranda, J. Saraiva, "Fuzzy Modeling of Power System Optimal Load Flow, *IEEE Trans. Power Systems*, vol. 7, pp 843-849, May 1992.

[7] J. Saraiva, V. Miranda, L.Pinto, "Impact on Some Planning Decisions From a Fuzzy Modeling of Power Systems", *IEEE Trans. Power Systems*, vol. 9, pp. 819-825, May 1994.

[8] J. Saraiva, V. Miranda, L. Pinto, "Generation/ Transmission Power System Reliability Evaluation by Monte-Carlo Simulation Assuming a Fuzzy Load Description", *IEEE Trans. Power Systems*, vol. 11, pp. 690-695, May 1996.

[9] J. Saraiva, V. Miranda, "Identification of Hedging Policies in Generation / Transmission Systems", *Proc. of 12th PSCC*, Dresden, Germany, August 1996.

[10] T. Gal, *Postoptimal Analysis, Parametric Programming and Related Topics*, McGraw Hill International Book Company, 1979.

[11] Task Force of Application Probabilistic Methods Subcommittee, "IEEE Reliability Test System", *IEEE Trans. PAS*, vol. PAS-98, no. 6, pp. 2047 – 2054, Nov/Dec 1979.

Acknowledgements – the first author thanks Fundação para a Ciência e Tecnologia, FCT, that funded this research through the PhD grant nº **SFRH/BD/34314/2006.**

Demand and Generation Cost Uncertainty Modeling in Power System Optimization Studies, International Journal on Electrical Power Systems Research, Elsevier, Vol. 79, nº. 6, pp. 959-972, June 2009

Demand and Generation Cost Uncertainty Modeling in Power System Optimization Studies

Bruno André Gomes

INESC Porto and Departamento de Engenharia Electrotécnica e Computadores

Faculdade de Engenharia da Universidade do Porto, FEUP

Campus da FEUP Rua Roberto Frias 378, 4200 465 Porto, Portugal, bgomes@inescporto.pt

João Tomé Saraiva

INESC Porto and Departamento de Engenharia Electrotécnica e Computadores

Faculdade de Engenharia da Universidade do Porto, FEUP

Campus da FEUP, Rua Dr. Roberto Frias 378, 4200 – 465 Porto, Portugal, jsaraiva@fe.up.pt

Corresponding Author:

João Tomé Saraiva

INESC Porto and Departamento de Engenharia Electrotécnica e Computadores

Faculdade de Engenharia da Universidade do Porto

Campus da FEUP, Rua Dr. Roberto Frias 378, 4200 – 465 Porto, Portugal, jsaraiva@fe.up.pt

Phone : + 351.22.2094230, Fax: +351.22.2094150

Abstract – This paper describes the formulations and the solution algorithms developed to include uncertainties in the generation cost function and in the demand of DC – OPF studies. The uncertainties are modelled by trapezoidal fuzzy numbers and the solution algorithms are based on multiparametric linear programming techniques. These models are a development of an initial formulation detailed in several publications co-authored by the second author of this paper. Now, we developed a more complete model and a more accurate solution algorithm in the sense that it is now possible to capture the widest possible range of values of the output variables reflecting both demand and generation cost uncertainties. On the other hand, when modelling simultaneously demand and generation cost uncertainties, we are representing in a more realistic way the volatility that is currently inherent to power systems. Finally, the paper includes a case study to illustrate the application of these models based on the IEEE 24 bus test system.

Keywords – Uncertainties, generation cost uncertainties, demand uncertainties, fuzzy models, multiparametric linear programming.

1. Introduction

The treatment of uncertainties has been a concern among the power systems community for a long time. This fact is clear with the development of several models integrating uncertainty for instance under the form of probabilistic models. This is the case of reliability models and also regarding power flow approaches. In recent years, power systems went through a restructuring process that determined the unbundling of the traditional vertically integrated companies in different agents and providers that can be grouped in several activities as generation, transmission, distribution and retailing as well as in several coordination activities including the market operator, the system operator and the regulatory boards. The extreme activities of this value chain, generation and retailing, are typically provided through competitive mechanisms, while wiring transmission and distribution activities are framed in terms of monopoly regulated basis.

One of the consequences of the unbundling of power systems and the introduction of competition in some areas is related with the more volatile environment that companies and consumers are now facing. Apart from that, the cost of fuels are more volatile than in the past and is affected by very subjective factors that can determine quick changes of the market prices. This increased volatility affecting a number of factors contributes to reduce the available history regarding the behaviour of those factors and parameters and so it turns it more important to formalize the knowledge provided by planners and experts using human language.

At this point, it is important to recall that within the probabilistic models framework we admit that a phenomenon is reproducible which means that the rules governing it remain the same along time. Given the randomness of this type of events, probabilistic models rely on the observation of a large number of events from which one can derive probabilistic distributions. In fact, in periods of large volatility affecting not only the numerical values of several parameters, but also the legislation and regulations determining power system operation as well the change of paradigm affecting the whole industry, it becomes important to develop new models able to integrate a different type of uncertainty. In this sense, fuzzy models were conceived to represent the uncertainty inherent, for instance, to a large number of expressions of our language. In fact, expressions as "large", "more or less" or "approximately" do not result from the repetitive simulation of the same phenomenon but express the past experience of the user and his subjective evaluation. The formalization of this type of knowledge and its integration in several power system models can therefore contribute to enlarge the insight of the users regarding the possible ways a power system will be operated reflecting the specified uncertainties.

During the 90's they were published a number of contributions referred in Section 2 aiming at including in several power system operation and planning models demand uncertainties represented by trapezoidal fuzzy numbers. In line with these concerns, we recently resumed this area of research in order to develop more complete and more accurate models. In this sense, we are now considering not only demand uncertainties but also generation cost uncertainties both represented by trapezoidal fuzzy numbers, defined in Section 3. This means we are now able to investigate what are the consequences for power system operation from having simultaneously fuzzy representations of some nodal demands and some generation costs. On the other hand, the original solution algorithm developed back in the 90's adopted a simplified approach to build the membership functions for generations, branch flows and power not supplied. As a consequence of this simplified approach, the range of possible values obtained at that time could, in some cases, not correspond to the widest possible

behaviour of the problem outputs. In this paper, we describe the use of linear multiparametric optimization techniques that ensure that the whole uncertainty space is covered so that we are accurately transferring data uncertainty onto the results of the optimization problems.

Following these ideas, this paper is structured as follows. After this Introduction, Section 2 briefly addresses the integration of uncertainties in several power system studies, both using probabilistic and fuzzy set models. Section 3 presents the fundamental concepts of Fuzzy Set Theory useful to fully understand the remaining sections. Section 4 details the original Fuzzy DC Optimal Power Flow problem as well as the new formulations we have developed. Section 5 describes the developed solution algorithms and Section 6 presents results obtained with a Case Study based on the IEEE 24 bus Test System. Finally, Section 7 draws the most relevant conclusions.

2. Dealing with Uncertainty in Power Flow and Optimal Power Flow Studies

Probabilistic models were the traditional approach to incorporate uncertainties in several power system studies. The treatment of uncertainties and their integration namely in power flow studies started back in the 70's with the publication of the models described in references [1] to [5]. These papers describe the main concepts related with this problem as well as the initially developed algorithms using convolution techniques, the DC model and different linearized versions of the AC power flow problem. In general, these approaches aimed at translating to the results of traditional power flows the uncertainties specified in data under the form of probabilistic distributions. Due to the linearizations adopted in several of these models, it was soon realized that the results were affected by errors that would eventually be larger in the tails of the output distributions. Concerned with this problem, reference [6] describes the use of the Monte Carlo simulation technique to evaluate the accuracy of the results and references [7] and [8] propose the use of several linearization points to build partial probability distributions that, at the end, would be aggregated to provide the final outputs. This approach was conceived as a way to reduce the errors in the tails of the output distributions.

These models constitute the basic approaches developed to incorporate probabilistic data in power flow problems. In this sense, in subsequent years they were published some other contributions to enrich the previous models or to give them an increased realism. References [9] and [10] are two examples of this kind of contributions when considering network outages and operation constraints used to constrain the power flow results. Finally, reference [11] describes a new approach to the probabilistic power flow problem directed to the construction of the branch flow distributions in order to get useful information to be used in transmission investment planning problems.

Apart from probabilistic power flow models, the literature also includes a few references addressing the integration of probabilistic data in Optimal Power Flow models. In this scope, reference [12] admits that the demand has a normal distribution probability function and describes the computation of expected values of the output variables. Reference [13] considers that the demand is represented by a vector of random correlated variables so that nodal dependencies can be modelled. This paper adopts the First Order Second Moment Method in order to get the statistical properties of the output variables reflecting data uncertainty. Finally, reference [14] describes the use of a cumulant-based approach to compute the output probability distributions

while comparing these results with the ones obtained by Monte Carlo simulations as a way to evaluate their accuracy.

Apart from probabilistic models, the difficulty in forecasting the future behaviour of several parameters and data has long been addressed using scenario analysis and sensitivity approaches. As an example, reference [15] describes an approach to investigate how the optimal operation point of a power system can be affected by changing input data. In this case, the authors consider changes in the active or reactive load at a specified bus or at the thermal limit of a branch and adopt a Lagrange based formulation to obtain these sensitivities.

Since the yearly 90's Fuzzy Set models started to be applied to several power systems problems, namely in operation planning models recognizing that in some cases the uncertainty we want to deal with has not a probabilistic nature or we simply don't have enough data to build reliable probabilistic distributions. In some situations, the uncertainty is inherently related with human language since judgments using expressions as "more or less", "larger than", "approximately" are not a consequence of the repetition of an experience under the same conditions but are, in fact, a result of the past experience of the planner that integrates information and produces a judgment that, in any case, reflects his subjectivity. The mathematical formalization of this knowledge became an important aspect in different scientific areas as a way to express the volatility increasingly present in our world. Regarding power flow problems, reference [16] details the first DC and AC models admitting that at least one generation and demand are modelled by fuzzy numbers. As a result, voltages and branch flows are now represented by fuzzy numbers expressing the possible behaviour of the system given the specified uncertainties.

A subsequent step was given with references [17] and [18] with the development of a Fuzzy DC OPF model admitting that at least a demand was represented by a fuzzy number. As a result, generations, branch flows and if necessary power not supplied, PNS, are obtained as fuzzy representations translating data uncertainty. Afterwards, this approach was integrated in a Monte Carlo simulation [19] as way to obtain estimates of the expected value of the output variables reflecting fuzzy loads and reliability equipment data modelled with the usual probability based approaches. In this sense, the model in [19] has a hybrid nature when aggregating fuzzy and probabilistic models. The referred Fuzzy DC OPF model was also integrated in a methodology to identify the most adequate expansion plan so that the risk of not being able to meet the demand gets reduced while accommodating the inherent uncertainty [20]. Finally, reference [21] presents the basic concepts related with the simultaneous modelization of generation cost and demand uncertainties. These concepts, the mathematical formulations and the developed solution algorithms will now be fully detailed in this paper.

3. Fuzzy Set Basics

A fuzzy set Ã is defined as a set of ordered pairs (1) in which the first element, x_1, corresponds to an element of the universe X under analysis and the second is the membership degree of that element to the fuzzy set, $\mu_{\tilde{A}}(x_1)$. In normalized fuzzy sets, the membership degree takes values in $[0.0;1.0]$ and reflects the degree of compatibility of the elements of X with the proposition defining the fuzzy set. These membership degrees can be interpreted as a membership function $\mu_{\tilde{A}}(x)$ that assigns a membership degree to each element x.

$$\tilde{A} = \{(x_1; \mu_{\tilde{A}}(x_1)), x_1 \in X\} \quad (1)$$

A particular class of fuzzy sets corresponds to fuzzy numbers. A fuzzy set $\widetilde{A}$ is classified as a fuzzy number if it is a convex fuzzy set defined on the real line R such that its membership function is piecewise continuous. As an example, Figure 1 represents the membership function of a trapezoidal fuzzy number in which the membership degree is maximum in $[A_2; A_3]$ and decreases from 1.0 to 0.0 from A_2 to A_1 and from A_3 to A_4. Regarding this type of numbers and given the particular form of the membership function, they are uniquely defined if the values of A_1, A_2, A_3 and A_4 are known. This number is then usually written as $(A_1; A_2; A_3; A_4)$.

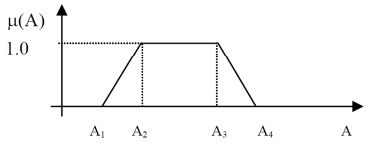

Figure 1 – Trapezoidal fuzzy number.

An α-level set or an α-cut of a fuzzy set $\widetilde{A}$ is defined in X as the hard set A_α obtained from Ã for each $\alpha \in [0.0;1.0]$ according to (2). As a result of this definition, the 0.0-cut of the fuzzy number in Figure 1 is the interval $[A_1; A_4]$ while the 1.0-cut is given by the interval $[A_2; A_3]$.

$$A_\alpha = \{x_1 \in X : \mu_{\widetilde{A}}(x_1) \geq \alpha\} \tag{2}$$

Finally, the Central Value of a fuzzy number corresponds to the mean value of the 1.0-cut. Regarding the trapezoidal fuzzy number in Figure 1, the Central Value of $\widetilde{A}$, A^{ctr}, is given by (3).

$$A^{ctr} = \frac{A_2 + A_3}{2} \tag{3}$$

4. Problem Formulation

4.1 Fuzzy Optimal Power Flow Model

References [17] and [18] describe the original Fuzzy DC OPF model in which we admitted that uncertainties only affected the demand vector. This formulation used the DC model to represent the operation of the transmission system and the solution algorithm is presented in Figure 2.

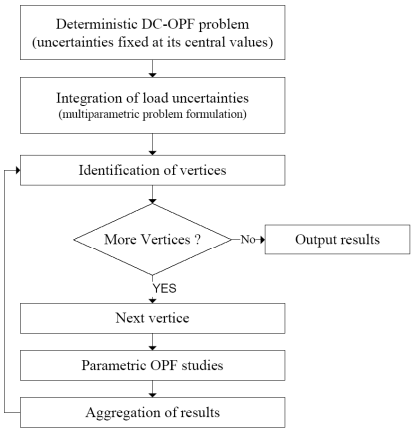

Figure 2 – Algorithm of the original Fuzzy DC Optimal Power Flow Model.

This algorithm starts by solving a deterministic DC OPF in which we substituted the fuzzy demands by the corresponding central values. This leads to the linear optimization problem (4 – 8).

$$min\ f\ -\sum c_k.Pg_k + G.\sum PNS_k \tag{4}$$

s.t. $$\sum Pg_k + \sum PNS_k = \sum Pl_k^{ctr} \tag{5}$$

$$Pg_k^{min} \le Pg_k \le Pg_k^{max} \tag{6}$$

$$PNS_k \le Pl_k^{ctr} \tag{7}$$

$$P_b^{min} \le \sum a_{bk}.(Pg_k + PNS_k - Pl_k^{ctr}) \le P_b^{max} \tag{8}$$

This problem minimizes the generation cost given that Pg_k is the generation in bus k having cost c_k, PNS_k is the power not supplied in bus k and the coefficient G penalizes power not supplied. In this formulation, Pg_k^{min}, Pg_k^{max}, P_b^{min} and P_b^{max} are the minimum and maximum generation and branch limits, a_{bk} is the DC sensitivity coefficient of the flow in branch b regarding the injected power in bus k and Pl_k^{ctr} is the central value of the load in node k.

After solving this initial deterministic problem, we get an initial optimal and feasible solution. However, the demand is affected by uncertainty and so this optimal and feasible basis can be no longer feasible for several combinations of the uncertainties. In order to take this into account, we introduce parameters Δ_k related with load uncertainties in the previous problem so that we formulate the multiparametric problem given by (9-11). In this problem, b and b' are vectors representing the right hand side terms of the constraints given that some of them are independent and some others depend on the parameters Δ_k used to model load uncertainties.

$$min\ f = c^t.X \tag{9}$$

$$\text{s.t.} \quad A.X = b + b'(\Delta_k) \tag{10}$$

$$\Delta_{k1} \le \Delta_k \le \Delta_{k4} \tag{11}$$

The solution algorithm described in [17] and [18] identifies vertices of the hypervolume defined by (11) and then solves a set of parametric linear programming problems in order to vary the load from the set of central values to the values associated with each of these vertices. While solving these parametric problems, one builds partial membership function for the generations, branch flows and PNS. The final membership function of each of these variables is obtained applying the Fuzzy Union Operator on those partial results.

Accordingly, this algorithm transforms the multiparametric problem (9-11) into a set of parametric problems and this represents a simplification that may lead to inaccuracies when obtaining the final results. This means that in several problems we could obtain membership functions that would not capture the widest possible behaviour of each variable. In this paper, we deal with the multiparametric problem by itself and we enlarge the Fuzzy Optimal Power Flow problem considering not only demand uncertainties but also generation cost uncertainties.

4.2 Condensed Formulations

In a condensed way, the DC-OPF problem admitting that at least one load is represented by a trapezoidal fuzzy number as the one sketched in Figure 1 can be formulated by (12-13). In this case, the vector of the right hand side terms of the constraints has at least one element represented by a trapezoidal fuzzy number representing a demand. As a result, the output variables of this problem (generations, branch flows and PNS) will also be represented by fuzzy numbers reflecting data uncertainty.

$$min\ f = c^t.\tilde{X} \tag{12}$$

$$\text{s.t.} \quad A.\tilde{X} \le \tilde{b} \tag{13}$$

A second problem corresponds to the integration of generation cost uncertainties modelled by trapezoidal fuzzy numbers. This problem can be formulated by (14-15). In this case, the generation costs are affected by uncertainties leading to uncertainties in the output variables.

$$min\ f = \tilde{c}^t.\tilde{X} \tag{14}$$

$$\text{s.t.} \quad A.\tilde{X} \le b \tag{15}$$

Finally, if we now consider both generator cost and load uncertainties modelled by trapezoidal fuzzy numbers then we get the condensed formulation (16-17). In the next section, we will detail the solution algorithms that were developed to solve these three problems.

$$min\ f = \tilde{c}^t.\tilde{X} \tag{16}$$

$$\text{s.t.} \quad A.\tilde{X} \le \tilde{b} \tag{17}$$

5. Solution Algorithms

5.1 General Aspects

The development of electricity markets and the volatility of fuel prices place a new emphasis on power system planning and operation as well as in the economic liquidity of the markets. Recognizing these concerns, the New Fuzzy Optimal Power Flow, NFOPF, approach aims at, in first place, extending the original concept by translating to the results not only load uncertainties, but also generation costs uncertainties. Secondly, since computational resources are nowadays more powerful than in past, the NFOPF also enables obtaining a more accurate solution for this type of problems, since it adopts linear multiparametric optimization techniques. The application of these techniques lead to the identification of a number of critical regions covering all the uncertainty space meaning that we are effectively covering all the combinations of values of the parameters affected by uncertainties. This has an important consequence given that we can now obtain more accurate membership functions in the sense they represent the widest possible behaviour of each variable. The original FOPF model described in Section 4 only runs a number of linear parametric studies, eventually leading to narrower membership functions when compared with the real ones.

The algorithms used to solve these linear multiparametric problems were originally proposed by Gal [22]. Starting at the initial optimal and feasible solution of the deterministic optimization problem as stated by (4-8), these algorithms identify the critical regions in the uncertain space. This means that they search all the combinations of values of the parameters affected by uncertainties for which there is an optimal and feasible basis. When running this process, we are extending the optimality and feasibility conditions ((18) and (19), respectively) so that they become function of Φ_k (parameters modelling cost uncertainties) or Δ_k (parameters modelling load uncertainties). Then, starting at the optimal and feasible solution of the initial deterministic DC OPF problem and considering each of these conditions, we find the set of other optimal and feasible solutions provided they are valid in some region of the uncertainty space. These regions are called critical regions and this process is conducted by pivoting over the initial basis as well as over all the new ones identified during the search process.

From a mathematical point of view, let B be an optimal and feasible basis, ρ the index for the corresponding set of basic variables, A the columns of the non-basic variables in the Simplex tableau, C_0 the cost vector of the basic variables and C^T the cost vector of the non-basic variables. The optimality and feasibility conditions for a minimization linear problem can then be defined in terms of Φ_k and Δ_k by (18) and (19).

$$C^T(\Phi_k) - C_0^T.B_\rho^{-1}.A = (c + c'(\Phi_k)) - C_0^T.B_\rho^{-1}A \geq 0 \quad (18)$$

$$B_\rho^{-1}.b(\Delta_k) = B_\rho^{-1}(b + b'(\Delta_k)) \geq 0 \quad (19)$$

Since the dual solution does not depend on Δ_k for right hand side parametrization, a critical region, i.e., a region in the uncertainty space where B remains optimal and feasible, can be uniquely defined by the conditions in (19). In a similar way, since the primal solution does not depend on Φ_k for cost parametrization, a critical region can be defined by the conditions given by (18). Apart from these conceptual aspects, two optimal and feasible basis,

B_1 and B_2, are considered neighbour ones if and only if one can pass from B_1 to B_2 performing one dual pivot step in case of right hand side parametrization or one primal pivot step in case of cost vector parametrization.

As a final comment, the ultimate objective to attain when solving a multiparametric optimization problem is to find all possible optimal solutions, their corresponding optimal values and critical regions, which can be defined as a closed nonempty polyhedron, that is, a set of linear inequalities established in terms of Δ, Φ, or both. Mathematically, this set of constraints can be expressed as the equivalent set of non-redundant constraints, which in turn can be identified through a non-redundant test for linear inequalities, like the one proposed by Gal [22].

5.2 Integration of Load Uncertainties

Figure 3 presents the algorithm of the NFOPF. Similarly to the algorithm described in Section 4, in this new approach it is also performed an initial deterministic DC-OPF problem (4-8) to identify a feasible an optimal solution associated to the central values of the fuzzy load representations. In the second place, the parameters modelling load uncertainties are included in the original optimization problem leading to the problem (20-24).

$$min\ f = \sum c_k . Pg_k + G.\sum PNS_k \tag{20}$$

$$\text{s.t.} \quad \sum Pg_k + \sum PNS_k = \sum Pl_k^{ctr} + \sum \Delta_k \tag{21}$$

$$Pg_k^{min} \le Pg_k \le Pg_k^{max} \tag{22}$$

$$PNS_k \le Pl_k^{ctr} + \Delta_k \tag{23}$$

$$P_b^{min} \le \sum a_{bk} . (Pg_k + PNS_k - (Pl_k^{ctr} + \Delta_k)) \le P_b^{max} \tag{24}$$

Following the algorithm in Figure 3, we will now identify a set of non-redundant constraints defining new critical regions considering the inequalities associated with the feasibility condition (19). If there are no non-redundant constraints, the algorithm stops indicating that the current basis is feasible in the whole uncertainty space. Otherwise, it performs a dual pivoting over the initial optimal and feasible solution to identify new critical regions. This process is repeated until no non-redundant constraints exist or until all identified critical regions correspond to already known ones. When this is over, all the uncertainty space was covered and we identified all critical regions in which a base B of the problem (20-24) remains feasible and optimal.

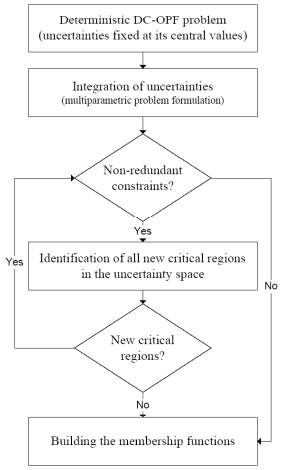

Figure 3. New Fuzzy DC Optimal Power Flow algorithm.

For a better understanding of this procedure, Figure 4 depicts the rectangles enclosing all load combinations between the "0.0" and "1.0-cuts" for a system supplying two trapezoidal fuzzy loads. In this Figure, lines "a" and "b" represent constraints, for instance, related with branch flow or generator capacity limits, point O corresponds to the optimal and feasible solution of the initial deterministic DC-OPF problem and the dashed lines define the range of values of the uncertainties at the i^{th} level of the data membership functions. From Figure 4 it becomes clear that non-redundant constraints, such as line "a", can define any critical region such as R_i and R_j indicated in this Figure. The process to identify these regions is implemented using the feasibility condition (19) described by the parameters of load vector uncertainties. In a systematic way, all critical regions are obtained by doing a dual pivoting over each of the optimal and feasible basis already identified.

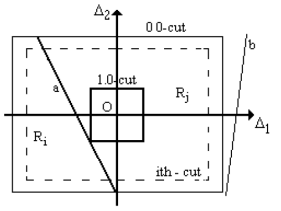

Figure 4. Critical regions in the uncertainty space.

In order to build the membership functions of the output variables (generations, branch flows and PNS) we must recall that, being a linear model, each variable in each critical region is represented by a linear expression. In this sense, if we are interested in capturing the widest possible behaviour of a linear function $v(\Delta_1, \Delta_2)$ expressed in terms of the parameters Δ_1 and Δ_2, we will then have to solve the problem (25-28).

$$min/\ max \quad f = v(\Delta_1, \Delta_2) \tag{25}$$

s.t. $k_{1i}.\Delta_1 + k_{2i}.\Delta_2 \le b_i$ (26)

$\Delta_1^{min\ i^{th}-cut} \le \Delta_1 \le \Delta_1^{máx\ i^{th}-cut}$ (27)

$\Delta_2^{min\ i^{th}-cut} \le \Delta_2 \le \Delta_2^{máx\ i^{th}-cut}$ (28)

In this problem we are minimizing and maximizing a function $v(\Delta_1, \Delta_2)$ subjected to the constraints modelling the non-redundant conditions (26) together with the possible ranges of the input uncertainties regarding the ith cut under analysis (27-28). After solving this problem for several cuts, it is possible to build the membership function of v in this critical region. Once all critical regions are analyzed, the final membership function of v is obtained applying the Fuzzy Union Operator to the partial membership functions obtained for that variable in order to guarantee that the final result displays the widest possible behaviour given the specified uncertainties.

5.3 Integration of Generation Cost Uncertainties

Let us now consider that at least one generation cost in vector c is modeled by a trapezoidal fuzzy number. Using a similar reasoning as the one adopted to consider demand uncertainties, we can formulate the multiparametric linear problem (29 – 31) in terms of the parameters Φ_k. In this formulation Φ_{k1} and Φ_{k2} represent the range of values of the cost c_k regarding the 0.0 cut of the corresponding trapezoidal fuzzy number.

$min \quad f = c(\Phi_k)^t.\widetilde{X}$ (29)

s.t. $A.\widetilde{X} \le b$ (30)

$\Phi_{k1} \le \Phi_k \le \Phi_{k2}$ (31)

The basic ideas behind the solution algorithm presented in Figure 3 can still be used provided that some adaptations are made. In the first place, the algorithm starts by solving an initial deterministic DC-OPF problem (4-8) for the crisp values of the fuzzy cost representations to identify a feasible an optimal solution. Following the same strategy, the linear multiparametric problem (32-36) is obtained including the parameters Φ_k used to model generation cost uncertainties.

$min \quad f = \sum c_k(\Phi).Pg_k + G.\sum PNS_k$ (32)

s.t. $\sum Pg_k + \sum PNS_k = \sum Pl_k^{ctr}$ (33)

$Pg_k^{min} \le Pg_k \le Pg_k^{max}$ (34)

$PNS_k \le Pl_k^{ctr}$ (35)

$P_b^{min} \le \sum a_{bk}.(Pg_k + PNS_k - Pl_k^{ctr}) \le P_b^{max}$ (36)

In order to identify non-redundant constraints leading to the definition of the critical regions in the uncertainty space, we will now use the optimality condition (18) written in terms of the parameters Φ_k. The identification of the critical regions is implemented performing a primal pivoting over the initial optimal and feasible basis as well as over all the new optimal and feasible basis identified along the search procedure.

When building the membership function of the output variables we must recall that cost vector parametrization implies that the uncertainty space is partitioned in several regions. In each of these regions there is an optimal

basis associated with an optimal solution. This means that for each critical region of the multiparametric problem the optimal basis is the same and so generations, branch flows and PNS remain the same inside that region. This also means that the values of these output variables will only change if there is a basis change, that is, if we move from one critical region to another one.

Accordingly, for each critical region, the partial membership function of any variable is built using the non-redundant inequalities defining that region together with the maximum membership degree of the output variables. This is simple done solving the system formed by the linear inequalities that define each critical region to determine the point in the critical region under analysis having the largest membership degree. Once all partial membership function are built, we use the Fuzzy Union Operator to aggregate all the results for the same variable to ensure that its final result displays the widest possible behaviour in the specified uncertainty space.

5.4 Simultaneous Integration of Demand and Generation Cost Uncertainties

Let us now consider that there are uncertainties affecting both elements of the cost and load vectors leading to the condensed problem (16-17). The solution algorithm presented in Figure 3 remains valid, provided once again that some adaptations are made. In the first place, the initial deterministic DC-OPF problem (4-8) is now run by substituting each fuzzy load and each fuzzy cost coefficient by their corresponding central values, Pl_k^{ctr} and c_k^{ctr} respectively. Once the optimal and feasible solution for this initial problem is obtained, it is built the linear multiparametric problem (37-41) integrating the load and the cost coefficient uncertainties in the initial optimization problem.

$$\min f = \sum c_k(\Phi).Pg_k + G.\sum PNS_k \tag{37}$$

$$\text{s.t.} \quad \sum Pg_k + \sum PNS_k = \sum Pl_k^{ctr} + \sum \Delta_k \tag{38}$$

$$Pg_k^{min} \le Pg_k \le Pg_k^{max} \tag{39}$$

$$PNS_k \le Pl_k^{ctr} + \Delta_k \tag{40}$$

$$P_b^{min} \le \sum a_{bk}.(Pg_k + PNS_k - (Pl_k^{ctr} + \Delta_k)) \le P_b^{max} \tag{41}$$

The process to identify non-redundant constraints is implemented using both the inequalities given by the optimality (18) and feasibility (19) conditions expressed as linear functions of the uncertainty parameters Φ_k and Δ_k, respectively. As a result of the increased number of parameters modelling data uncertainties, the search for all critical regions should be conducted in a more structured way. This leads to the adoption of a search tree as illustrated in Figure 5, where ρ_i defines the index for the set of basic variables in a given critical region i.

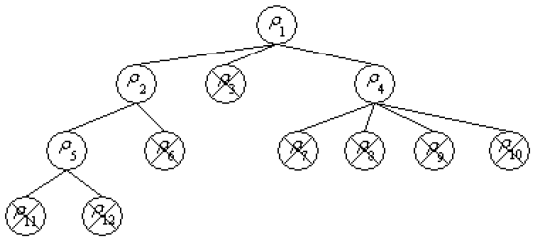

Figure 5: Search tree to illustrate the search procedure.

Departing from one node in the tree, one can find two kinds of neighbor basis. The first one is determined by the application of the feasibility condition (19) (in Figure 5 these bases correspond to nodes at the left of its departure node). The second type results from the optimality condition (18) (in Figure 5 these bases correspond to nodes on the right of its departure node). This process is repeated for each new node until no non-redundant constraints exist or all the identified critical regions correspond to already known ones. In Figure 5 and for illustration purposes, the crosses denote bases that are not new regarding previously identified ones. Similar to the algorithms described in Sections 5.2 and 5.3, each critical region is defined by a set of inequality conditions related, in this case, both with the feasibility and optimality conditions.

Once all critical regions are identified, the algorithm proceeds with the construction of the membership function of the final results. In order to do this, we once again recognize that in each region, the behavior of each variable is expressed by a linear expression and so, they are solved for each of them and for each critical region, optimization problems as (25-28) to identify the widest possible behavior of that variable in that region. In this case, however, the number of constraints is larger given that we are now considering all the non-redundant inequalities given by (18) and (19). Finally, the partial membership functions built for each variable in each region are aggregated using the Fuzzy Union Operator.

6. Case Study

6.1 System Data

The algorithms described in sections 5.2, 5.3 and 5.4 were used to build the membership functions of generations, branch flows and PNS considering a case study based on the IEEE 24 bus/38 branch test system. The original data for this system is given in [23]. Regarding data in this reference, the load was increased to 4456.83 MW and Table 1 presents the central values of the loads in the system. The total installed capacity is 5800 MW according to the data in Table 2.

TABLE 1 - Load central values.

Bus	Load (MW)	Bus	Load (MW)	Bus	Load (MW)
1	50.00	7	142.75	15	564.89
2	172.85	8	304.72	16	278.20
3	220.76	9	311.85	18	273.41
4	132.46	10	347.49	19	322.54
5	146.52	13	472.23	20	128.10
6	242.35	14	345.71	--	---

TABLE 2 - Installed capacity in the system.

Bus/Gen	Capacity (MW)	Cost (€/MWh)	Bus/Gen	Capacity (MW)	Cost (€/MWh)
1/1	40.0	3.0	15/3	24.0	2.0
1/2	40.0	3.2	15/4	24.0	2.0
1/3	152.0	4.0	15/5	24.0	2.0
1/4	152.0	4.3	15/6	310.0	6.7
2/1	40.0	3.7	16/1	310.0	5.5
2/2	40.0	3.7	18/1	800.0	9.0
2/3	152.0	4.1	21/1	800.0	8.0
2/4	152.0	4.2	22/1	100.0	1.5
7/1	200.0	4.4	22/2	100.0	1.7
7/2	200.0	4.5	22/3	100.0	1.9
13/1	394.0	6.1	22/4	100.0	2.0
13/2	394.0	6.2	22/5	100.0	2.1
13/3	394.0	6.7	22/6	100.0	2.2
15/1	24.0	2.0	23/1	200.0	5.0
15/2	24.0	2.0	23/2	310.0	4.8

Branch data can be obtained from [23] considering that the transformers have a capacity of 400 MW, the capacity of the branches 1 to 6 and 8 to 13 was set at 175 MW and the capacity of the remaining branches was set at 500 MW.

6.2 Results Considering Only Demand Uncertainties

In the first place, we considered that all loads were affected by uncertainty represented by trapezoidal fuzzy numbers as the one depicted in Figure 1. To build these numbers we considered an uncertainty range of +/-10 per cent at the 0.0 level and +/- 5 per cent at the 1.0 cut regarding the central values in Table 1. After running the algorithm described in Section 5.2 we obtained the membership functions sketched in Figures 6 and 7 for the generations at generators 1/4, 7/2, 15/6, 18/1 and 21/1. It should be mentioned that for the data referred above and for the load uncertainty ranges just specified, the branches 1-5 and 7-8 are at their capacity limit of 175 MW.

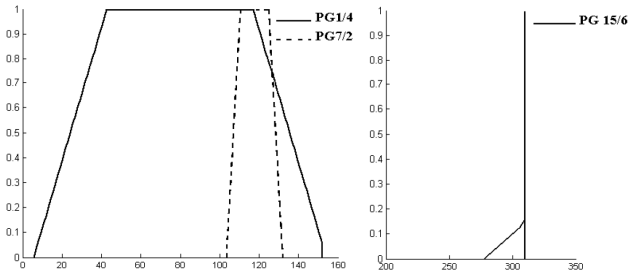

Figure 6. Membership functions of generators 1/4, 7/2 and 15/6 (generation values in MW).

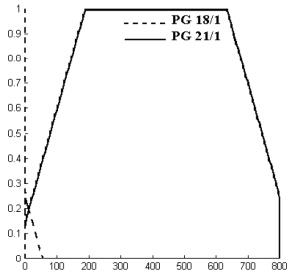

Figure 7. Membership functions of the generators 18/1 and 21/1 (generation values in MW).

These results indicate that load uncertainties are essentially accommodated by generator 21/1 since it is the last one to be dispatched because of its higher variable cost (see Table 2) and by the generators 1/4 and 7/2 given that branches 1-5 and 7-8 are at their capacity limits. As expected, from Figure 7 we can also see that when generator 21/1 is on limit, load variations are accommodated by generator 18/1 and so this one becomes the last one to be dispatched. The generation at the remaining generators is fixed, which means that despite load uncertainties there are a number of generators for which the generation values are not affected by those possible variations.

6.3 Results Considering Only Generation Cost Uncertainties

In the second place, we considered that the variable cost of some generators was modelled by trapezoidal fuzzy numbers. In this case, we considered that the cost of generators 1/1, 1/3, 13/1, 18/1, 21/1 and 23/1 are described by the trapezoidal fuzzy numbers (42-47). It should be noticed that the central values of these trapezoidal fuzzy numbers coincide with the costs indicated in Table 2 for these generators.

$$CP_{G1/1} = (2.50;2.85;3.15;3.50)\ €/\text{MWh} \quad (42)$$

$$CP_{G1/3} = (3.25;3.85;4.15;4.75)\ €/\text{MWh} \quad (43)$$

$$CP_{G13/1} = (5.60;6.00;6.20;6.60)\ €/\text{MWh} \quad (44)$$

$$CP_{G18/1} = (7.80;8.50;9.50;10.20)\ €/\text{MWh} \quad (45)$$

$CP_{G21/1} = (6.80;7.75;8.25;9.20)$ €/MWh (46)

$CP_{G23/1} = (4.60;4.75;5.25;5.40)$ €/MWh (47)

Figures 8 and 9 present the results obtained for these generators. These Figures indicate that the membership functions include the generation values obtained for the initial deterministic DC-OPF with 1.0 membership degree. This means that the values 152.0 MW for generators 1/3, 79.84 MW for generator 1/4, 0 MW for generator 18/1 and 411.24 MW for generator 21/1 belong to the membership functions of these generators, respectively. Then, due to different generation cost combinations determined by the specified cost uncertainties, there are different generation strategies leading to different values in each membership function. As an example, generator 1/3 can produce 79.84 or 81.56 MW with a credibility degree of 0.75 or 152.0 MW with a credibility degree of 1.0. Regarding this point, it must be emphasized that the membership function of generators 1/1, 13/1 and 23/1 are not here represented since for the specified generation cost uncertainties and load scenario their generation levels did not exhibit any variation.

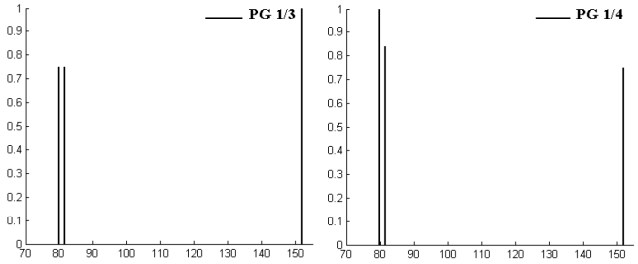

Figure 8. Membership functions of generators 1/3 and 1/4 (generation values in MW).

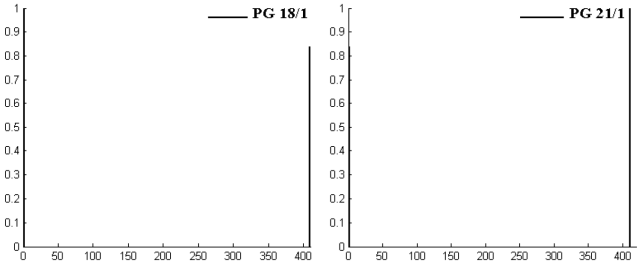

Figure 9. Membership functions of generators 18/1 and 21/1 (generation values in MW).

6.4 Results Considering Both Demand and Generation Cost Uncertainties

Similarly to what was described in Section 6.2, in this case we also considered that all specified loads are represented by trapezoidal fuzzy numbers whose uncertainty range are of +/-10 per cent at the 0.0 level and +/- 5 per cent at the 1.0 cut regarding the central values in Table 1. However, in this case we also considered the generation cost uncertainties given by (42 - 47). After running the algorithm described in Section 5.4, we obtained the membership functions sketched in Figures 10 and 11 for the generations at generators 1/3, 1/4, 7/2,

15/6, 18/1, 21/1 and 23/1. It should be mentioned that for the data referred above and for the specified uncertainty ranges, branches 1-5 and 7-8 are at their capacity limit of 175 MW.

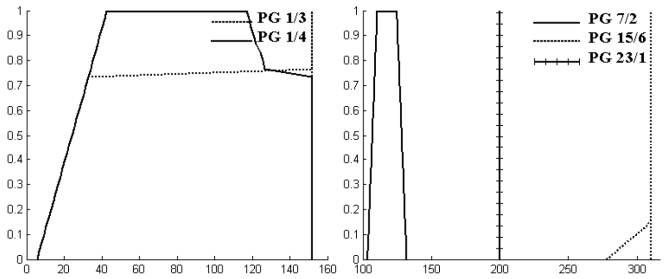

Figure 10. Membership functions of generators 1/3, 1/4, 7/2, 15/6 and 23/1 (generation values in MW).

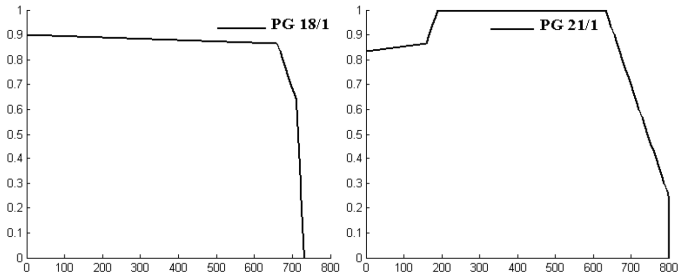

Figure 11. Membership functions of generators 18/1 and 21/1 (generation values in MW).

Comparing these results with the ones presented in Figures 6 and 7, we can see that some generators are affected by the specified cost uncertainties as, for instance, generators 1/3, 1/4, 18/1 and 21/1. Differently, some others as generators 7/2 and 15/6 are not affected by the specified cost uncertainties and so the membership functions obtained in Sections 6.2 and 6.4 are equal. In some other cases, as for instance generator 23/1 in Figure 10, the membership function is not affected neither by load uncertainties nor by cost uncertainties. This is a relevant and interesting result indicating that whatever are the combinations of load and generator cost values, the output of some variables is fixed and it does not vary regarding the value that was initially obtained when running the deterministic DC OPF study.

Apart from that, the capacity limit of branch 1-5 constrains the output level of the generators located at bus 1 leading to membership functions displaying large possible variations. Due to this branch limit constraint, the most expensive generator in bus 1 (generator 1/3 or generator 1/4) has to reduce its output so that the active flow constraint of branch 1-5 is enforced. From the specified generation cost uncertainties, it is also possible to conclude that there is a change regarding the system marginal generator, at least for some combination of the

specified costs. The membership functions of generators 18/1 and 21/1 presented in Figure 11 illustrate this fact, since for some combinations of the specified costs, the generator 18/1 becomes the system marginal generator while for other combinations the marginal one is the generator 21/1.

7. Conclusions

In this paper, we formalized a new Fuzzy DC Optimal Power Flow approach and highlighted the main differences between this new approach and the original one developed back in the 90's. As it was shown, this new approach accommodates not only load uncertainties represented by trapezoidal Fuzzy numbers but also generation cost uncertainties or both of them, in a simultaneously way. Additionally, since this new approach is based on linear multiparametric programming techniques it can present more accurate results than the algorithm originally conceived. These models and algorithms can be used by several entities and agents in the power sector namely to address expansion planning and operation planning problems in order to get more insight on the possible behavior of generations, branch flows and power not supplied reflecting data uncertainties modeled by fuzzy sets.

These features are especially interesting in the current very volatile and more unpredictable world in which this kind of tools will be very useful to map uncertainties on the results of optimization problems. Finally, it is also important to refer that this volatility and the more frequent change of patterns and assumptions reduces the history on system behavior. This ultimately means that the derivation and the use of probabilistic models will have to be done in a more cautious way. This problem can enlarge the possibility of incorporating the knowledge of experts in several models so that formulations and algorithms as the ones described in this paper can play a more significant role in the future.

Acknowledgement

The first author would like to thank Fundação para a Ciência e Tecnologia, FCT, that funded this research work through the PhD grant nº **SFRH/BD/34314/2006.**

References

[1] B. Borkowska, "Probabilistic Load Flow", *IEEE Transactions on PAS*, vol. PAS-93 (1974), 752-759.

[2] R. N. Allan, B. Borkowska, C. H. Grigg, "Probabilistic Analysis of Power Flows", *Proceedings of the IEE*, 121 (1974), 1551 – 1556.

[3] R. N. Allan, M. R. G. Al-Shakarchi, "Probabilistic a.c. Load Flow", *Proceedings of the IEE*, 123 (1976), 531 – 536.

[4] R. N. Allan, C. H. Grigg, D. A. Newey, R. F. Simmons, "Probabilistic Power-Flow Techniques Extended and Applied to Operation Decision Making", *Proceedings of the IEE*, 123 (1976), 1317 – 1324.

[5] R. N. Allan, M. R. G. Al-Shakarchi, "Probabilistic Techniques in a.c. Load Flow Analysis", *Proceedings of the IEE*, 124 (1977), 154 – 160.

[6] R. N. Allan, A. M. Leite da Silva, R. C. Burchett, "Evaluation Methods and Accuracy in Probabilistic Load Flow Solutions", *IEEE Transactions on PAS*, vol. PAS-100 (1981), 2539 – 2546.

[7] R. N. Allan, A. M. Leite da Silva, "Probabilistic Load Flow Using Multilinearisations", *IEE Proceedings*, 128, Pt. C (1981), 280 – 287.

[8] A. M. Leite da Silva, V. L. Arienti, "Probabilistic Load Flow by a Multilinear Simulation Algorithm", *IEE Proceedings*, vol. 137, Pt. C, (1990), 256 – 262.

[9] A. M. Leite da Silva, R. N. Allan, S. M. Soares, V. L. Arienti, "Probabilistic Load Flow Considering Network Outages", *IEE Proceedings*, 132, Pt. C (1985), 139 – 145.

[10] T. S. Karakatsanis, N. D. Hatziargyriou, "Probabilistic Constrained Load Flow Based on Sensitivity Analysis", *IEEE Transactions on Power Systems*, 9 (1994), 1853 – 1860.

[11] P. Zhang, S. T. Lee, "Probabilistic Load Flow Computation Using the Method of Combined Cumulants and Gram-Charlier Expansion", *IEEE Transactions on Power Systems*, 19 (2004), 676 – 682.

[12] M. E. El-Hawary, G. A. N. Mbamalu, "Stochastic Optimal Load Flow Using a Combined Quasi-Newton and Conjugated Gradient Technique", *Electric Power & Energy Systems*, 11 (1989), 85 – 93.

[13] M. Madrigal, K. Ponnambalam, V. H. Quintana, "Probabilistic Optimal Power Flow", *Proc. IEEE Canadian Conference on Electrical and Computer Enginnering, Waterloo, Canada, 1998*, pp. 385 – 388.

[14] A. Schellenberg, W. Rosehart, J. Aguado, "Cumulant-Based Probabilistic Optimal Power Flow (P-OPF) with Gaussian and Gamma Distributions", *IEEE Transactions on Power Systems*, 20 (2005), 773 – 781.

[15] P. R. Gribik, D. Shirmohammadi, S. Hao, C. L. Thomas, "Optimal Power Flow Sensitivity Analysis", *IEEE Transactions on Power Systems*, 5 (1990), 969 – 976.

[16] V. Miranda, M. A. Matos, J. T. Saraiva, "Fuzzy Load Flow – New Algorithms Incorporating Uncertain Generation and Load Representation", *Proceedings of the 10th PSCC, Butterworths, London, 1990*.

[17] V. Miranda, J. T. Saraiva, "Fuzzy Modelling of Power System Optimal Load Flow, *IEEE Transactions on Power Systems*, 7 (1992), 843 – 849.

[18] J. T. Saraiva, V. Miranda, L. M. V. G. Pinto, "Impact on Some Planning Decisions From a Fuzzy Modelling of Power Systems", *IEEE Trans. on Power Systems*, 9 (1994), 819 – 825.

[19] J. T. Saraiva, V. Miranda, L. M. V. G. Pinto, "Generation/Transmission Power System Reliability Evaluation by Monte-Carlo Simulation Assuming a Fuzzy Load Description", *IEEE Transaction on Power Systems*, 11 (1996), 690 – 695.

[20] J. T. Saraiva, V. Miranda, "Identification of Hedging Policies in Generation / Transmission Systems", *Proceedings of the 12th Power Systems Computation Conference, PSCC, Dresden, Germany, 1996*.

[21] B. A. Gomes, J. T. Saraiva, "Calculation of Nodal Marginal Prices Considering Load and Generation Price Uncertainties", *Proc. of the IEEE Lausanne Power Tech, Lausanne, Switzerland, 2007*.

[22] T. Gal, Postoptimal Analysis, Parametric Programming and Related Topics, McGraw Hill International Book Company, 1979.

[23] Task Force of Application of Probabilistic Methods Subcommittee, "IEEE Reliability Test System", *IEEE Transactions on PAS*, PAS-98 (1979) 2047 – 2054.

Biographies

Bruno André Gomes was born in Ovar, Portugal, in 1977. In 2001 he got his BSc from the Faculdade de Ciências e Tecnologia da Universidade de Coimbra and in 2005 he got his MSc from the Faculdade de Engenharia da Universidade do Porto, FEUP. Currently he has a grant from the Fundação para a Ciência e Tecnologia, FCT, and he is completing his PhD in FEUP.

João Tomé Saraiva was born in Porto, Portugal in 1962. In 1987, 1993 and 2002 he got his MSc, PhD, and Agregado degrees in Electrical and Computer Engineering from the Faculdade de Engenharia da Universidade do Porto where he is currently Professor. In 1985 he joined INESC Porto where he was head researcher or collaborated in several projects related with the development of DMS systems, quality in power systems, and tariffs for the use of transmission and distribution networks. Several of these projects were developed under consultancy contracts with the Portuguese Electricity Regulatory Agency.

Fuzzy Modeling of Load and Cost Uncertainties and Their Impact on Power Systems Operation, Mediterranean Conference and Exhibition on Power Generation, Transmission and Distribution 2008, MEDPOWER 2008, Thessaloniki, Greece, 2 to 5 November 2008

Fuzzy Modelling of Load and Cost Uncertainties and their Impact on Power Systems Operation

Bruno André Gomes
bgomes@inescporto.pt
INESC Porto – Instituto de Engenharia de Sistemas e Computadores do Porto
Campus da FEUP, Rua Dr. Roberto Frias, 4200-465 Porto, Portugal

João Tomé Saraiva, *member IEEE*
jsaraiva@fe.up.pt
INESC Porto – Instituto de Engenharia de Sistemas e Computadores do Porto
Faculdade de Engenharia da Univ. do Porto
Campus da FEUP, Rua Dr. Roberto Frias, 4200-465 Porto, Portugal

Luís M. Neves
lneves@estg.ipleiria.pt
Instituto Politécnico de Leiria – ESTG, Morro do Lena, Alto do Vieiro, 2411-901 Leiria, Portugal

ABSTRACT: Power systems are nowadays, more than ever, affected by uncertainties of multiple origins, such as physical, technical, economic, regulatory, political and environmental. Together, they create huge volatility associated with generation electricity prices, demand and generation capacity. As a result, modeling uncertainties in power systems is once again on the top of the agenda of researchers that aim at giving positive answers to the new requirements of the systems. In this sense, in this paper we are enlarging the original Fuzzy Optimal Power Flow, FOPF, model in order to consider not only load uncertainties, but also uncertainties in generation costs, specified using trapezoidal fuzzy numbers. This new approach is based on multiparametric linear programming techniques that lead to the identification of a number of critical regions covering all the uncertainty space contributing to build more accurate membership functions of all variables, namely generations, branch flows and power not supplied. The paper includes results of a case study based on the IEEE 24 bus test system to illustrate the application of the developed approach.

Keywords: Uncertainties, Fuzzy Models, DC Optimal Power Flow, Multiparametric Linear Programming.

I. INTRODUCTION

Power systems are nowadays, more than ever, affected by uncertainties. They are related with different variables, such as physical, technical, economic, regulatory, political, and environmental. As an attempt to deal with this new kind of concerns, in 2005 the European Union (EU) launched the European Union Emissions Trading System (EU ETS) which is a market based instrument that allows the participants to trade CO_2 allowances aiming at creating incentives to reduce CO_2 emissions in the EU. Since Renewable Energy Resources (RER) are carbon free, it is also being implemented in some European Countries a green certificate market as a way to create incentives to investors in this type of technologies. More recently and since energy efficiency is also an essential element of the EU energy policy, some member states also launched the White Certificates market (WhC) as a way to promote energy efficiency [1].

In case these market instruments work properly, it is expected a net electricity demand reduction, essentially driven by the WhC market and the investments financed by the revenues of the EU ETS [1] [2].

It is also expected that EU ETS alters the merit order of generators quite substantially decreasing the share of some predominant fuel sources more carbon intense like, for instance, coal and gas. This decrease can be larger if the green certificate system works properly in the promotion of RER investments. Simultaneously, it is expected a reduction of the new generation capacity investments given the expected demand reduction. It is also important to refer that the implementation of more ambitious quota for RER together with the green certificate system will reduce the price of the allowances within the EU ETS. Therefore market participants will face a net combined effect. In fact, they have to face uncertainties in fuel prices, cost of purchasing EU ETS allowances if the CO_2 emissions exceed the limited amount of allowances allocated in a administrative way, opportunity costs of selling allowances in case they are not fully used and, finally, uncertainties on demand and on RER generation levels [3] [4].

As a conclusion one can state that the idea of internalising the environmental damages due to energy generation and consumption into prices brings to the power sector a more conscious and sustainable way of planning and operating the system. On the other hand, it also brings to the sector a huge number of new uncertainties and challenges that will contribute to rise the cost of capital and alter investment decisions. Accordingly, market participants should be able to use models and adopt methods to address all these uncertainties and integrate them into the investment decision making processes. In fact, risk has to be adequately addressed if one wants to ensure that profits are large enough to compensate the cost of capital [5].

In line with these concerns, this paper details a model to address demand and generation cost uncertainties in power system operation planning admitting that these parameters are modeled using Fuzzy Set concepts. The developed model corresponds to a DC Optimal Power Flow problem that is solved using multiparametric techniques.

Apart from this Introduction Section, this paper is structured as follows. Section II details some general aspects related with uncertainty modeling. Sections III and IV present the mathematical models derived for the Fuzzy Optimal Power Flow (FOPF) problems and the

corresponding solution algorithm. Sections V and VI present two case studies. One of them uses a small three-bus network to illustrate and interpret the obtained results, while the second one is based on the IEEE 24 bus test system. Finally, Section VII draws the most relevant conclusions.

II.UNCERTAINTY MODELING

Uncertainty was traditionally modeled by probabilistic approaches or by scenario analysis. Probability models are adequate if the phenomenon under analysis has a repetitive nature and the possible outcomes of the experience are completely defined. This is for instance the case of throwing a die. In this case, it is possible to repeat the experience in the same conditions as many times as we want and the uncertainty derives from the complexity of the phenomenon that prevents us from forecasting the next outcome.

Apart from this theoretical framework, there are situations in which the uncertainty is related with the incomplete characterization of the phenomenon under analysis or derives from the lack of information required to build probability distributions, as it happens in very low frequency phenomena [6]. In other cases, uncertainty is related with vagueness in the sense that human language has an intrinsic subjective nature that turns each user a different user of language. In this sense, expressions as "larger than", "close to", "more or less" or "approximately" are inherently vague and their use do not reflect an historic average of past values but it rather corresponds to the subjective evaluation of each user. In these cases, probability theory is not fully adequate to model this type of uncertainty. Since the 60th of the last century, Fuzzy Set Models are under development and application to power systems aiming at providing a new framework to model the vague or the ill-defined nature of some phenomena.

One of the possible ways of modeling the uncertainty affecting active power corresponds to the use of trapezoidal fuzzy numbers as the one sketched in Figure 1. A trapezoidal fuzzy number is a particular case of a fuzzy number in which the membership function is piecewise linear and it can be used to express the uncertainty around the interval $[Pl_{k,2}; Pl_{k,3}]$. The values in this interval are considered as the most likely ones to occur and so they are assigned to the largest membership degree, 1.0. However, values from $Pl_{k,2}$ to $Pl_{k,1}$ and from $Pl_{k,3}$ to $Pl_{k,4}$ are not entirely discarded and so they are assigned decreasing membership grades from 1.0 to 0.0.

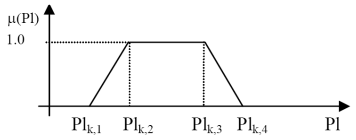

Figure 1. Membership function of a trapezoidal fuzzy number.

Regarding this number, the Central Value Pl_k^{ctr} is defined as the average value of the 1.0 cut, that is, of the interval having 1.0 membership degree. In Figure 1, the 1-cut of this fuzzy number is given by $[Pl_{k,2}; Pl_{k,3}]$ and so the central value of the load in node k, Pl_k^{ctr}, is given by (1).

$$Pl_k^{ctr} = (Pl_{k,2} + Pl_{k,3})/2 \quad (1)$$

III. FUZZY OPTIMAL POWER FLOW

According to [7, 8], a FOPF study was originally defined as an optimization problem aiming at identifying the best generation strategy driven by a generation cost function if at least one load is represented by a fuzzy number. The FOPF approach adopts the DC model to represent the operation conditions of the network.

Using the set of load central values extracted from the respective trapezoidal fuzzy numbers, it is possible to perform a deterministic DC-OPF study to identify an initial feasible and optimal solution. This initial problem is formulated as (2-6).

$$\min f = \sum c_k.Pg_k + G.\sum PNS_k \quad (2)$$

$$\text{subj.} \quad \sum Pg_k + \sum PNS_k = \sum Pl_k^{ctr} \quad (3)$$

$$Pg_k^{min} \le Pg_k \le Pg_k^{max} \quad (4)$$

$$PNS_k \le Pl_k^{ctr} \quad (5)$$

$$P_b^{min} \le \sum a_{bk}.(Pg_k + PNS_k - Pl_k^{ctr}) \le P_b^{max} \quad (6)$$

In this model we are minimizing the generation cost given that Pg_k is the generation in bus k having cost c_k and PNS_k is the power not supplied in bus k, Pg_k^{min}, Pg_k^{max}, P_b^{min} and P_b^{max} are the minimum and maximum generation and branch limits and a_{bk} is the DC sensitivity coefficient of the flow in branch b regarding the power in bus k.

Once this initial problem is solved, load uncertainties are integrated in the problem using parameters so that we formulate a multiparametric problem as (7-9). In this formulation b and b' are vectors integrating the right hand side terms of the constraints considering that some of them are independent and some others depend on the parameters Δ_k used to model load uncertainties.

$$\min f = c^t.X \quad (7)$$

$$\text{subj.} \quad A.X = b + b'(\Delta_k) \quad (8)$$

$$\Delta_{k1} \le \Delta_k \le \Delta_{k4} \quad (9)$$

These parameters can turn the solution of the initial problem not feasible in some areas of the hyper-volume defined by (9). If that is the case, the algorithm described in reference [7] proceeds identifying vertices of that hyper-volume according to some rules. Once these vertices are identified, it is run a parametric analysis for each of them leading to partial membership functions for generations, branch flows, phases and PNS. The final results are obtained applying the Fuzzy Union Operator on those partial results.

IV. NEW FUZZY OPTIMAL POWER FLOW

A. General Description

Recognizing that the development of electricity markets and the volatility affecting electricity generation costs place a new emphasis on power system planning and operation as well as in the economic liquidity of market agents, the New

Fuzzy Optimal Power Flow, NFOPF, approach aims at, in the first place, extending the original concept by translating to the results not only load uncertainties, but also generation cost uncertainties. Secondly, since computational resources are nowadays more powerful than in past, the NFOPF also enables obtaining a more accurate representation of this type of problems, since it adopts linear multiparametric optimization techniques. In fact, these techniques lead to the identification of a number of critical regions covering all the uncertainty space meaning that they are effectively covered all the combinations of values of the parameters affected by uncertainties. The adoption of these new techniques means that we can now obtain more accurate membership functions in the sense they actually represent the widest possible behaviour of each variable. The main reason for this improvement relies on the fact that the original FOPF model described in Section III only runs a number of parametric studies eventually leading to narrower membership functions when compared with the real ones.

The algorithms used to solve the multiparametric linear problems were originally proposed by Gal [9]. Starting at the initial optimal and feasible solution of the deterministic optimization problem as stated by (2-6), these algorithms perform a critical region identification process. This means that they search all the combinations of values of the parameters affected by uncertainties for which there is an optimal and feasible basis. When doing this, we are extending the optimality and feasibility conditions ((10) and (11), respectively) so they become function of Φ_k (parameters modelling generation cost uncertainties) or Δ_k (parameters modelling load uncertainties). Then, starting with the optimal and feasible solution of the initial deterministic optimization problem and considering each of these conditions, we find the set of other optimal and feasible solutions provided they are valid in some region of the uncertainty space. These regions are called critical regions and this process is conducted by pivoting over the initial basis as well as over all the new basis identified during the search process.

In this sense, let B be an optimal and feasible basis, ρ the index for the corresponding set of basic variables, A the columns of the non-basic variables in the Simplex tableau, C_b the cost vector of the basic variables and C_{nb} the cost vector of the non-basic variables. The optimality and feasibility conditions for a minimization linear problem can then be defined in terms of Φ_k and Δ_k by (10) and (11).

$$C_{nb}^T(\Phi_k) - C_b^T.B_\rho^{-1}.A = (C + C'(\Phi_k)) - C_b^T.B_\rho^{-1}A \geq 0 \quad (10)$$

$$B_\rho^{-1}.b(\Delta_k) = B_\rho^{-1}(b + b'(\Delta_k)) \geq 0 \quad (11)$$

Since the dual solution does not depend on Δ_k for right hand side parametrization, a critical region, i.e., a region in the uncertainty space where B remains optimal and feasible, can be uniquely defined by the conditions in (11). By analogy, since the primal solution does not depend on Φ_k for cost parametrization, a critical region can be defined by the conditions given by (10). Apart from these conceptual aspects, two optimal and feasible basis, B_1 and B_2, are classified as neighbor ones if and only if one can pass from B_1 to B_2 performing one dual pivot step in case of right hand side parametrization or one primal pivot step in case of cost vector parametrization.

As a final comment, the ultimate objective to attain when solving a multiparametric optimization problem corresponds to find all possible optimal solutions, their corresponding optimal values and critical regions, which can be defined as a closed nonempty polyhedron, that is, a set of linear inequalities in Δ or Φ. Mathematically, this set of constraints can be expressed as the equivalent set of non-redundant constraints, which in turn can be identified through a non-redundant test for linear inequalities, like the one proposed by Gal [9].

B. Consideration of Load Uncertainties

Figure 2 presents the algorithm of the NFOPF. In this new approach it is also performed an initial deterministic DC-OPF problem (2-6) to identify a feasible an optimal solution associated to the central values of the fuzzy load representations. In the second step, the parameters modeling load uncertainties are included in the original optimization problem leading to the problem (12-16).

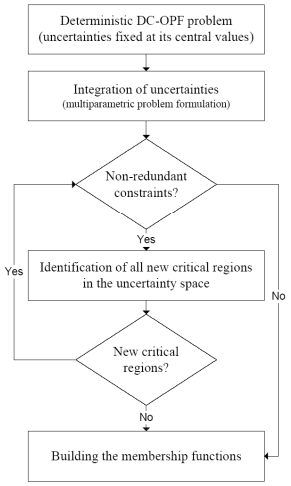

Figure 2. New Fuzzy DC Optimal Power Flow algorithm.

$$\min f = \sum c_k.Pg_k + G.\sum PNS_k \quad (12)$$

$$\text{subj.} \sum Pg_k + \sum PNS_k = \sum Pl_k^{ctr} + \sum \Delta_k \quad (13)$$

$$Pg_k^{min} \leq Pg_k \leq Pg_k^{max} \quad (14)$$

$$PNS_k \leq Pl_k^{ctr} + \Delta_k \quad (15)$$

$$P_b^{min} \leq \sum a_{bk}.(Pg_k + PNS_k - (Pl_k^{ctr} + \Delta_k)) \leq P_b^{max} \quad (16)$$

Considering the inequalities associated to the feasibility condition (11), the algorithm identifies a set of non-redundant constraints defining new critical regions. If there are no non-redundant constraints, the algorithm stops. Otherwise, it performs a dual pivoting over the initial optimal and feasible solution to identify new critical regions. This process is repeated until no non-redundant constraints exist or until all identified critical regions correspond to already known ones. When this is over, all

the uncertainty space was covered and we identified all critical regions in which a base B of the problem (12-16) remains feasible and optimal.

For a better understanding of this procedure, Figure 3 depicts the rectangles enclosing all possible load combinations between the 0.0 and 1.0-cuts for a system integrating two trapezoidal fuzzy loads. In this figure, lines "a" and "b" represent constraints, for instance, related with branch flow or generator capacity limits, point O represents the optimal and feasible solution of the initial deterministic DC-OPF problem and the dashed lines define the range of values of the uncertainties at the i^{th} level of the data membership functions.

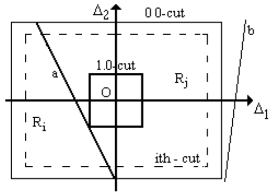

Figure 3. Critical regions in the uncertainty space.

From Figure 3 it becomes clear that a set of non-redundant constraints, such as line "a", together with the range of values of the uncertainties for a given cut level can define any critical region such as R_i and R_j.

This is in fact very relevant given that it reduces the computational effort of the algorithm by defining a more precise and efficient search procedure of neighbour critical regions. This identification process is implemented using the feasible condition (11) described by the parameters of load vector uncertainties. Once this process is finished, the critical regions are obtained by doing a dual pivoting over each of the optimal and feasible basis identified.

In order to build the membership functions of the output variables (generations, branch flows and Power Not Supplied) we must recall that, being a linear model, each variable in each critical region is represented by a linear expression. In this sense, if we are interested in capturing the widest possible behaviour of a function $v(\Delta_1,\Delta_2)$ expressed in terms of the parameters Δ_1 and Δ_2 we will then have to solve the problem (17-20).

$$\min/\max\ f = v(\Delta_1,\Delta_2) \tag{17}$$

$$\text{subj.}\quad k_{1i}.\Delta_1 + k_{2i}.\Delta_2 \le b_i \tag{18}$$

$$\Delta_1^{\min\ i^{th}-cut} \le \Delta_1 \le \Delta_1^{máx\ i^{th}-cut} \tag{19}$$

$$\Delta_2^{\min\ i^{th}-cut} \le \Delta_2 \le \Delta_2^{máx\ i^{th}-cut} \tag{20}$$

In this problem we are minimizing and maximizing a function $v(\Delta_1,\Delta_2)$ subjected to the constraints modelling the non-redundant conditions (18) together with the possible ranges of the input uncertainties regarding the i^{th} cut under analysis (19-20). After solving this type of problems for several cuts, it is possible to build the membership function of "v" in this critical region. Once all critical regions are analyzed, the final membership function of "v" is obtained applying the Fuzzy Union Operator to the partial membership functions obtained for that variable in order to guarantee that the final result displays the widest possible behaviour given the specified uncertainties.

C. Consideration of Generation Cost Uncertainties

If we now want to consider generation cost uncertainties we will obtain the condensed multiparametric linear problem (21) to (23), where loads are given by crisp values and $c(\Phi_k)$ includes at least one generation cost represented by a trapezoidal fuzzy number.

$$\min\quad f = c(\Phi_k)^t.\tilde{X} \tag{21}$$

$$\text{subj.}\quad A.\tilde{X} \le b \tag{22}$$

$$\Phi_{k1} \le \Phi_k \le \Phi_{k4} \tag{23}$$

In this case, the solution algorithm presented in Figure 2 can still be used considering the following adaptations. In this sense, the algorithm starts by solving an initial deterministic DC-OPF problem (2-6) for the crisp values of the fuzzy generation cost representations to identify a feasible an optimal solution. Following the same strategy, the optimization problem (24-28) is obtained integrating the parameters representing generation cost uncertainties in the original problem.

$$\min f = \sum c_k(\Phi).Pg_k + G.\sum PNS_k \tag{24}$$

$$\text{subj.}\quad \sum Pg_k + \sum PNS_k = \sum Pl_k^{etr} \tag{25}$$

$$Pg_k^{\min} \le Pg_k \le Pg_k^{\max} \tag{26}$$

$$PNS_k \le Pl_k^{etr} \tag{27}$$

$$P_b^{\min} \le \sum a_{bk}.(Pg_k + PNS_k - Pl_k^{etr}) \le P_b^{\max} \tag{28}$$

The identification of non-redundant constraints is implemented using the inequalities given by the optimality condition (10) described by the parameters of the cost vector uncertainties. In this case, the search procedure for critical regions is implemented performing a primal pivoting over the initial optimal and feasible basis as well as over all the new optimal and feasible basis identified along the search procedure.

When building the membership function of each variable we must recall that in this case each variable is constant inside each critical region, which means that changes will only occur if there is a basis change. In this sense, to build the partial membership functions, the algorithm just has to consider each critical region and its corresponding non-redundant inequalities and determine its maximum membership degree. This is simple done solving the system formed by the linear inequalities that define each critical region to determine the point having the largest membership degree that belongs to the critical region under analysis. Once all partial membership function are built, we use the Fuzzy Union Operator to aggregate all the results for the same variable to ensure that its final result displays the widest possible behaviour in the specified uncertainty space.

V. SMALL ILLUSTRATIVE EXAMPLE

A. Data

In this Section, we will present results obtained with the

algorithms described in Section 4 using the three bus power system of Figure 4. In this case, we want to illustrate the concepts associated with the addressed problems as well as discussing and analyzing the results. In this small illustrative network, generators in nodes 1 and 2 have a capacity of 3 MW. The branches have a capacity of 5 MW and a reactance of j1.0 pu (base 10 MVA, 10 kV).

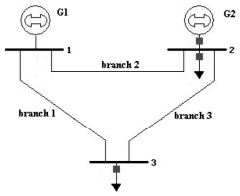

Figure 4. Three bus/three branch power system.

B. Results Considering Load Uncertainties

In this case loads in nodes 2 and 3 are described by the trapezoidal fuzzy numbers (29-30). Generation costs of generators 1 and 2 were set at 1.0 and 2.0 €/MW.h, respectively. After running the algorithm described in Section 4 we obtained the results presented in Figure 5 for generators 1, 2 and for the PNS at bus 2.

$$P_{c2} = (0.0;1.5;2.5;4.0)\ \text{MW} \quad (29)$$

$$P_{c3} = (2.0;3.0;4.0;5.0)\ \text{MW} \quad (30)$$

Starting at the solution associated with the central values of (29) and (30), that is, P_{c2} = 2.0 MW and P_{c3} = 3.5 MW, the algorithm identified four distinct critical regions covering all the uncertainty space. As expected, Figure 5 shows that the PNS is not always zero, since the maximum load of the system exceeds the total installed capacity.

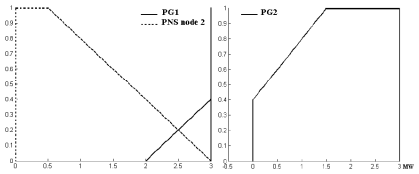

Figure 5. Membership function of PG1, PG2 and PNS.

B. Results Considering Generation Cost Uncertainties

In this case generation costs are represented by the trapezoidal fuzzy numbers (31-32) and loads in nodes 2 and 3 were set to the central values of (29-30). Figure 6 presents the membership functions built for the generators 1 and 2.

$$CP_{G1} = (0.5;0.75;1.25;1.5)\ €/\text{MW.h} \quad (31)$$

$$CP_{G2} = (0.25;1.5;2.5;3.75)\ €/\text{MW.h} \quad (32)$$

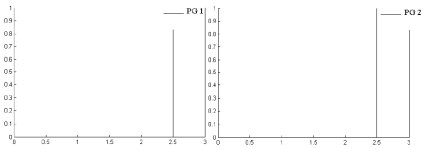

Figure 6: Membership function of PG1 and PG2.

As expected, for the central values of the generation costs (CP_1 = 1 €/MW.h and CP_2 = 2 €/MW.h, that generator 1 is less expensive than generator 2), generator 1will be at its capacity limit (3 MW) while generator 2 will generate the remaining load, this is, 2.5 MW. From Figure 6 it can also be seen that for membership degrees smaller than 0.83 it could also be possible that generator 2 produces 3.0 MW and generator 1 2.5 MW. At this respect, it must be emphasized that the 0.83 degree corresponds to the largest membership degree for which it is possible obtain such a combination of costs that turns generator 2 less expensive than generator 1.

VI. CASE STUDY USING THE IEEE 24 BUS SYSTEM

A. Data

The developed algorithms were also tested using the IEEE 24 bus/38 branch test system. Regarding the original data in [10], the load was increased to 5079.29 MW (Table I) and the total installed capacity is 5910 MW (Table II). Branch data can be obtained from [10] considering that the transformers have a capacity of 400 MW, the capacity of the branches 1 to 6 and 8 to 13 was set at 175 MW and of the remaining ones at 500 MW.

TABLE I – Load central values.

Bus	Load (MW)	Bus	Load (MW)	Bus	Load (MW)
1	192.46	7	222.75	15	564.89
2	172.85	8	304.72	16	178.20
3	320.76	9	311.85	18	593.41
4	132.46	10	347.49	19	322.54
5	126.52	13	472.23	21	228.10
6	242.35	14	345.71	--	---

TABLE II – Generation installed capacity.

Bus/ Gen	Capacity (MW)	Cost (€/MW.h)	Bus/ gen	Capacity (MW)	Cost (€/MW.h)
1/1	40.0	3.0	15/3	24.0	2.0
1/2	40.0	3.0	15/4	24.0	2.0
1/3	152.0	4.0	15/5	24.0	2.0
1/4	152.0	4.0	15/6	310.0	6.0
2/1	40.0	3.0	16/1	310.0	5.5
2/2	40.0	3.0	18/1	800.0	9.0
2/3	152.0	4.0	21/1	800.0	8.0
2/4	152.0	4.0	22/1	100.0	2.0
7/1	200.0	5.0	22/2	100.0	2.0
7/2	200.0	5.0	22/3	100.0	2.0
13/1	394.0	6.0	22/4	100.0	2.0
13/2	394.0	6.0	22/5	100.0	2.0
13/3	394.0	6.0	22/6	100.0	2.0
15/1	24.0	2.0	23/1	310.0	5.0
15/2	24.0	2.0	23/2	310.0	5.0

B. Results Considering Load Uncertainties

In this case, load trapezoidal fuzzy numbers were built considering that at level 0.0 the uncertainty ranges from +/- 10 per cent and at the 1.0 level it ranges from +/- 5 per cent of its central values.

Figures 7 and 8 present the results obtained for the generators 7/2, 16/1, 18/1, 21/1 and for the Power Not Supplied at bus 14. PNS is not always zero due to transmission congestion on branches 14-16 and 16-17.

These results indicate that load variations are accommodated by generators 18/1 and 21/1 since they are the last ones to be dispatched because of their costs, on

generator 16/1 because branches 14-16 and 16-17 reach their capacity limits for some load combinations and also to a small extent by generator 7/2 because branch 7-8 also reaches its capacity limit for some load combinations.

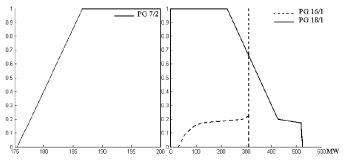

Figure 7. Membership functions of generators 7/2, 16/1 and 18/1.

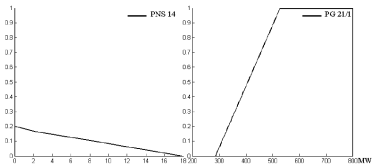

Figure 8. Membership functions of PNS at bus 14 and of the generator 21/1.

B. Results Considering Generation Cost Uncertainties

In this case we considered that the cost of generators 13/1, 13/2, 15/6, 16/1, 18/1 and 21/1 are described by the trapezoidal fuzzy numbers (33-38). Figure 9 presents the results obtained for these generators. As expected all generators display a membership degree of 1.0 for the values corresponding to the results of the initial DC-OPF, which means 394, 310, 771.54, 310 and 0.0 MW for generators 13/1/2, 16/1, 21/1, 15/6 and 18/1, respectively. We can also see different generation strategies as a consequence of the generation cost uncertainties specified for those generators.

$$CP_{G13/1} = (2.0;5.0;7.0;10.0)\ €/MW.h \quad (33)$$

$$CP_{G13/2} = (2.0;5.0;7.0;10.0)\ €/MW.h \quad (34)$$

$$CP_{G15/6} = (4.0;5.0;7.0;8.0)\ €/MW.h \quad (35)$$

$$CP_{G16/1} = (4.0;5.0;6.0;7.0)\ €/MW.h \quad (36)$$

$$CP_{G18/1} = (6.0;8.0;10.0;12.0)\ €/MW.h \quad (37)$$

$$CP_{G21/1} = (5.5;7.0;9.0;10.5)\ €/MW.h \quad (38)$$

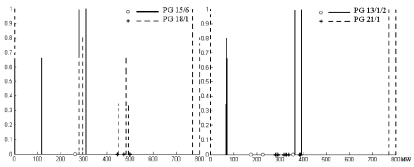

Figure 9. Membership functions of generators 15/6, 18/1, 13/1/2 and 21/1.

VII. CONCLUSIONS

In this paper we analysed the source of uncertainties affecting power operation planning problems and described from a conceptual point of view the probabilistic and the fuzzy set frameworks. Then, we described a new algorithm to solve the Fuzzy Optimal Power Problem admitting uncertainties affecting the load vector as well as the generation cost vector. This new approach can be used to model not only load but also generation cost uncertainties specified by trapezoidal Fuzzy numbers. Since this new approach is based on linear multiparametric programming techniques it can present more accurate results. This kind of models can play an important role in analysing the possible operation of power systems given the increasing volatility and unpredictably that is inherent to competitive markets.

VIII. ACKNOWLEDGMENT

The first author would like to thank Fundação para a Ciência e Tecnologia, FCT, that partially funded this research work through the PhD grant nº SFRH/BD/34314/2006.

IX. REFERENCES

[1] "White and Green: Comparison of Market-Based Instruments to Promote Energy Efficiency", U. Farinelli, T. B. Johansson, K. McCormick L. Mudanca, V. Oikonomou, M. Ortenvik, M. Patel, F. Santi, *Journal of Cleaner Production*, vol. 13, pp 1015-1026, August/September 2005.

[2] "Economic and Energy Impacts From Participation in the Regional Greenhouse Gas Initiative: A Case Study of the State of Maryland", M. Ruth, S.A. Gabriel, K.L. Palmer, D. Burtraw, A. Paul, Y. Chen, B. F. Hobbs, D. Irani, J. Michael, K. M. Ross, R. Conklin, J. Miller, *Energy Policy*, vol. 36, pp 2279-2289, April 2008.

[3] "Do Support Systems for RES-E Reduce EU-ETS-Driven Electricity Prices?", M. Rathmann, *Energy Policy*, vol. 35, pp 342-349, January 2007.

[4] "The Political Economy of International Green Certificates Market", P. Soderholm, *Energy Policy*, vol. 36, pp 2051-2062, June 2008.

[5] "Investment risks under uncertain climate change policy", W. Blyth, R. Bradley, D. Bunn, C. Clarke, T. Wilson, M. Yang, *Energy Policy*, vol. 35, pp 5766-5773, November 2007.

[6] "Fuzzy probabilistic model for medium-term power generation planning with environmental criteria", E. Muela, G. Schweickadrdt, F. Garcés, *Energy Policy*, vol. 35, pp 5643-5655, August 2007.

[7] "Fuzzy Modeling of Power System Optimal Load Flow", V. Miranda, J. Saraiva, , *IEEE Trans. Power Systems*, vol. 7, pp 843-849, May 1992.

[8] "Impact on Some Planning Decisions From a Fuzzy Modeling of Power Systems", J. Saraiva, V. Miranda, L.Pinto, *IEEE Trans. Power Systems*, vol. 9, pp. 819-825, May 1994.

[9] T. Gal, Postoptimal Analysis, Parametric Programming and Related Topics, McGraw Hill International Book Company, 1979.

[10] "IEEE Reliability Test System", Task Force of Application Probabilistic Methods Subcommittee, *IEEE Trans. PAS*, vol. PAS-98, no. 6, pp. 2047 – 2054, Nov/Dec 1979.

Bruno André Gomes was born in Ovar, Portugal, in 1977. In 2001 he got his BSc from the Faculdade de Ciências e Tecnologia da Universidade de Coimbra and in 2005 he got his MSc from the Faculdade de Engenharia da Universidade do Porto, FEUP. Currently he has a grant from the Fundação para a Ciência e Tecnologia, FCT, and he is completing his PhD in FEUP.

João Tomé Saraiva was born in Porto, Portugal in 1962. In 1987, 1993 and 2002 he got his MSc, PhD, and Agregado degrees in Electrical and Computer Engineering from the Faculdade de Engenharia da Universidade do Porto, FEUP, where he is currently Professor. In 1985 he joined INESC Porto – a private research institute – where he was head researcher or collaborated in several projects related with the development of DMS systems, quality in power systems, and tariffs due for the use of transmission and distribution networks. Several of these projects were developed under consultancy contracts with the Portuguese Electricity Regulatory Agency.

Luís Miguel Neves was born in Lisbon, Portugal, in 1968. In 1992, 1998 and 2005 he got his BSc, MSc and PhD in Faculdade de Ciências e Tecnologia da Universidade de Coimbra. Currently he is Professor Adjunto in the Instituto Politécnico de Leiria and Researcher in INESC Coimbra, Portugal.

Computation of Nodal Marginal Prices in the Presence of Load and Generation Cost Uncertainties, European Energy Markets 2009, EEM09, Leuven, Belgium, May 2009

Computation of Nodal Marginal Prices in the Presence of Load and Generation Cost Uncertainties

Bruno André Gomes[1], João Tomé Saraiva[2], Luís Neves[3]
INESC Porto and FEUP/DEEC,
Rua Roberto Frias 378, 4200 465 Porto, Portugal, phone +351.22.5081880 fax: +351.222094150
E-mail: bgomes@inescporto.pt, jsaraiva@fe.up.pt
Instituto Politécnico de Leiria, ESTG, Morro do Lena, Alto Vieiro, Apartado 4163, 2401-951 Leiria, Portugal
E-mail: lneves@estg.ipleiria.pt

***Keywords*— Uncertainties, fuzzy models, multiparametric programming, nodal marginal prices.**

***Abstract*— Marginal prices have been recognized as the core approach to the economic evaluation of generation and transmission services in an electricity market environment. In this context, this paper presents the New Fuzzy Optimal Power Flow algorithm as a model to addresses the impact of load and generation cost uncertainties in nodal marginal prices. Since loads and generation costs are represented by fuzzy numbers, nodal marginal prices will no longer be represented by deterministic values, but rather by fuzzy membership functions reflecting the specified uncertainties. The paper also presents the algorithm used for the integration of the transmission losses effect on the results. Since the proposed algorithm uses multiparametric programming techniques, it contributes to characterize in a better way the system behavior. Finally, it includes results based on the IEEE 24 bus/38 branch test system to illustrate the proposed approach.**

I. Introduction

THE development of market mechanisms in the electricity industry aims at developing procedures to turn electricity closer to a commodity to be traded in open markets. In this context, the access to the transmission network corresponds to a crucial issue since the access must be guaranteed in order to create conditions for the proper development of market mechanisms. In this scope, the literature on the area already describes several tariff methods to allocate transmission costs to network users [1]-[4], namely, based on average, incremental and marginal approaches.

Marginal pricing is broadly recognized as the core approach to the economic evaluation of generation and transmission services. However, marginal price approaches have several drawbacks. In the first place, pure marginal price tariff schemes may lead to perverse effects since, for example, more frequent transmission congestion would increase the nodal marginal price dispersion, and so increase the marginal remuneration or congestion rent. Secondly, pure short term marginal prices do not take into account transmission investment costs, and so it would not be possible to recover these costs. This under recovery problem is well known in the literature and it is termed as the Revenue Reconciliation problem [1]. Thirdly, since marginal prices depend on several factors, they are typically very volatile. Therefore, their computation should also be able to integrate uncertainties on loads and generation cost, especially in market environment, since they lead to changes in the dispatch policy and thus in marginal prices. Additionally, they should also integrate reliability data regarding system components since they also affect nodal marginal price values.

The nodal marginal price volatility makes it difficult to predict the marginal remuneration that could be obtained by a wiring company by its transmission activity. In this sense, and given that an adequate system coordination can only be achieved if the economical price signals include information related with uncertainties, several works [1]-[6] were developed in order to integrate uncertainties in the nodal marginal price computation. In general, these methods treat load uncertainties using probabilistic [2], [3] or fuzzy [1], [4], [5], [6] models.

Apart from this introduction, Section II describes the New Fuzzy Optimal Power Flow model. Sections III and IV present Case Studies based on a six bus/eight branches system and on the IEEE 24 bus/38 branches test system to illustrate the developed algorithms and also to highlight some important features. Finally, Section V presents the most relevant conclusions.

II. New Fuzzy Optimal Power Flow

Starting from the original concept of the Fuzzy Optimal Power Flow developed by the second author of this paper [4], the New Fuzzy Optimal Power Flow (NFOPF) model [7] is an optimization problem aiming at identifying the most adequate generation strategy, driven by an economic criterion, admitting that, at least, one load or generation cost is represented by a fuzzy number. Similarly to its original model, the NFOPF model also uses the DC approach to model the operation conditions of the network. However instead of

running a number of parametric studies, the new developed model uses multiparametric linear programming techniques. This in fact represents an important improvement, since it allows obtaining more accurate membership functions in the sense they actually represent the widest possible behavior of each variable.

A. Integration of Load Uncertainties

Figure 1 presents the algorithm of the NFOPF when it is only modeled load uncertainties.

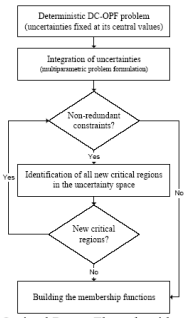

Fig. 1. New Fuzzy DC Optimal Power Flow algorithm [7]

As it can be seen from Figure 1, when considering load uncertainties, the algorithm starts by solving the deterministic DC-OPF problem (1-5) for the central values of the fuzzy numbers that represent loads.

$$\min f = \sum c_k . Pg_k + G . \sum PNS_k \quad (1)$$

$$\text{subj.} \quad \sum Pg_k + \sum PNS_k = \sum Pl_k^{ctr} \quad (2)$$

$$Pg_k^{min} \le Pg_k \le Pg_k^{max} \quad (3)$$

$$PNS_k \le Pl_k^{ctr} \quad (4)$$

$$P_b^{min} \le \sum a_{bk} . (Pg_k + PNS_k - Pl_k^{ctr}) \le P_b^{max} \quad (5)$$

In this model Pg_k is the generation in bus k with cost c_k and PNS_k is the power not supplied in bus k, Pg_k^{min}, Pg_k^{max}, P_b^{min} and P_b^{max} are the generation and branch flow limits and a_{bk} is the DC sensitivity coefficient of the flow in branch b regarding the injected power in bus k.

Once a feasible and optimal solution of this problem is identified, we integrate uncertainty parameters, λ_k, associated to each fuzzy load in the problem leading to the multiparametric optimization problem (6-10).

$$\min f = \sum c_k . Pg_k + G . \sum PNS_k \quad (6)$$

$$\text{subj.} \quad \sum Pg_k + \sum PNS_k = \sum Pl_k^{ctr} + \sum \lambda_k \quad (7)$$

$$Pg_k^{min} \le Pg_k \le Pg_k^{max} \quad (8)$$

$$PNS_k \le Pl_k^{ctr} + \lambda_k \quad (9)$$

$$P_b^{min} \le \sum a_{bk} . (Pg_k + PNS_k - (Pl_k^{ctr} + \lambda_k)) \le P_b^{max} \quad (10)$$

At this stage the algorithm proceeds by identifying all critical regions in the uncertainty space corresponding to the hypervolume defined by the parameters that model load uncertainties. This process is performed using the algorithms proposed in [8].

From a mathematical point of view, let B be an optimal and feasible basis and ρ the index of the corresponding set of basic variables. While analysing load uncertainties, the solution obtained for the initial deterministic problem can lose its feasibility, that is, the set of constraints (11) expressing the feasibility condition can be violated.

$$B_\rho^{-1} b(\lambda_k) = B_\rho^{-1} (b + b'(\lambda_k)) > 0 \quad (11)$$

Using these conditions and starting from the optimal and feasible solution of the initial deterministic DC-OPF problem, the algorithm proceeds by finding the set of other optimal and feasible solutions provided they are valid in some region of the uncertainty space. These regions are called critical regions and this process is conducted by pivoting over the initial basis as well as over all the new ones identified during the search process.

Since the dual solution does not depend on λ_k for right hand side parameterization a critical region, i.e., a region in the uncertainty space where B remains optimal and feasible, can be uniquely defined by the conditions in (11). This means that we can pass from one optimal and feasible basis to another performing a dual pivot step.

When the multiparametric optimization problem is completed, the algorithm proceeds by building the membership functions of the output variables. At this stage we must recall that being a linear model, each variable is represented by a linear expression. As a result, if we want to capture the widest possible behaviour of a variable represented by a linear function of the uncertainty parameters λ_1 and λ_2, say $v(\lambda_1, \lambda_2)$, we will then have to solve the problem (12-15).

$$min/max \quad f = v(\lambda_1, \lambda_2) \quad (12)$$

$$\text{s.t.} \quad k_{1i} . \lambda_1 + k_{2i} . \lambda_2 \le b_i \quad (13)$$

$$\lambda_1^{min\ i^{th}-cut} \le \lambda_1 \le \lambda_1^{máx\ i^{th}-cut} \quad (14)$$

$$\lambda_2^{min\ i^{th}-cut} \le \lambda_2 \le \lambda_2^{máx\ i^{th}-cut} \quad (15)$$

This problem is formulated for some α-cuts of the specified load uncertainties, meaning that, in some way, each fuzzy load is discretized in a number of intervals, each one associated with a α-cut. Once this discretization is completed, we reflect the uncertainties now represented by α-cuts, in the output variables of the problem. This corresponds to minimize and to maximize the linear expressions of each of these variables, subjected to the constraints modelling the non-redundant conditions (13), where k_{1i} and k_{2i} are real numbers, together with the possible ranges of the input uncertainties regarding the i^{th} cut under analysis (14) and (15). After solving this problem for the selected cuts, it is possible to build the membership function of v in the critical region under analysis. Once all regions are analyzed, the final membership function of v is obtained

applying the fuzzy union operator to the partial membership functions obtained for that variable.

B. Integration of Generation Cost Uncertainties

When the objective is to model generation cost uncertainties, the algorithm presented in Figure 1 is still valid provided that some adaptations are made. In this context, after identifying an optimal and feasible basis of the problem (1-5) formulated for the central values of the fuzzy numbers that represent generation costs, they are integrated the parameters that represent generation cost uncertainties leading to the multiparametric optimization problem (16-20).

$$\min f = \sum c_k(\Phi).Pg_k + G.\sum PNS_k \quad (16)$$

$$\text{subj.} \sum Pg_k + \sum PNS_k = \sum Pl_k^{ctr} \quad (17)$$

$$Pg_k^{min} \le Pg_k \le Pg_k^{max} \quad (18)$$

$$PNS_k \le Pl_k^{ctr} \quad (19)$$

$$P_b^{min} \le \sum a_{bk}.(Pg_k + PNS_k - Pl_k^{ctr}) \le P_b^{max} \quad (20)$$

Similarly to what was described in section II.A, at this stage the algorithm proceeds by identifying all critical regions in the uncertainty space defined by the hypervolume represented by the parameters that model the generation cost uncertainties. In this case, however, it must be observed that since the primal solution does not depend on Φ_k for cost parametrization, a critical region can be defined by the optimality condition (21). In this expression A is the matrix with the columns of the non-basic variables in the Simplex tableau, C_0 the cost vector of the basic variables and C^r the cost vector of the non-basic variables.

$$C^T(\Phi_k) - C_0^T.B_p^{-1}.A = (c + c'(\Phi_k)) - C_0^T.B_p^{-1}A \ge 0 \quad (21)$$

As a consequence, in this case we can pass from one optimal and feasible basis to another performing a primal pivot step.

Once again, when the multiparametric optimization problem is completed, the algorithm proceeds by building the membership functions of the output variables. To do this, we must recall that in this case each variable is constant inside each critical region, and so, the membership functions building process can be performed by simply solving the linear system formed by the inequalities that define each critical region to check if at least one point of a given cut level belongs to the critical region under analysis. Once all partial membership functions are obtained, they are aggregated using the fuzzy union operator to obtain the final membership function of the output variable under analysis.

C. Integration of Active Losses

Active losses in branch b are given by expression (22). As it can be seen, it depends on the magnitude and voltage phases on the extreme branch nodes i and j and also on the conductance g_{ij}. If we consider that voltage magnitudes are 1.0 pu, we can then obtain the simplified expression (23).

$$Loss_{ij} = g_{ij}.(V_i^2 + V_j^2 - 2.V_i.V_j.\cos\theta_{ij}) \quad (22)$$

$$Loss_{ij} = 2.g_{ij}.(1 - \cos\theta_{ij}) \quad (23)$$

Among several other available techniques described in literature, this algorithm adopts the approach described in [4] to consider an estimate of active losses. The corresponding iterative process evolves as follows:

1. Perform the deterministic DC OPF study (1-5);
2. Compute the nodal voltage phases according to the DC model;
3. Compute an estimate of the active power losses in each branch of the system;
4. Add half of the active power losses estimated for each branch to the load connected to the corresponding extreme buses;
5. Perform a new deterministic DC OPF study to update the generation strategy;
6. Compute the nodal voltage phases according with the DC model;
7. Finish if the difference between every voltage phases in two successive iterations is smaller than a specified value. Otherwise return to step 3.

In case we are trying to integrate the effect of the active losses on the results of the algorithms detailed in sections II.A and II.B then, for each extreme point in each identified critical region we must run the algorithm just detailed. As we will show in Sections III and IV, in general, this procedure introduces small deviations regarding the initial results.

D. Computation of Nodal Marginal Prices

The nodal marginal price in node k can be defined as the impact on the cost function of a short term operation problem regarding to a variation of the load in node k. According to [4] and for the problem (1–5), the nodal marginal price in a node k can be computed by expression (24).

$$\rho_k = \gamma + \sigma_k - \sum_{all\ branches} \eta_b.\frac{\partial P_b}{\partial P_{Lk}} + \gamma.\frac{\partial Losses}{\partial P_{Lk}} \quad (24)$$

In this expression:

- γ represents the dual variable of the generation/load balance equation (2);
- the second term represents the contribution from constrains (4) that are eventually on their limits. σ_k is the dual variable of the constraint in node k;
- the third term represents the contribution to the cost function from each branch flow constraint that is on its limit. In this expression, η_b represents the dual variable of the corresponding constraint and the derivative of the branch flow in branch b, P_b, regarding the load in bus k, P_{Lk}, is the symmetric of the corresponding sensibility coefficient;
- the fourth term represents the impact on the cost function from varying branch losses in the whole network due a variation of the load in bus k.

The algorithm developed to compute the nodal marginal prices membership functions comprises three distinct stages.

In the first place, the algorithm determines the maximum and minimum possible values of all variables in each cut level. Once this initial stage is completed, the algorithm can evolve to include the impact of the active transmission losses for each identified operating point in each cut level or, this impact can be neglected. Finally, the algorithm determines the nodal marginal prices using (24). When all partial membership functions are known, the final membership function is obtained applying the fuzzy union operator to all of them.

Following [7], when we only consider load uncertainties, generations, branch flows and PNS are described by linear membership functions. In opposition, when it is only modeled generation cost uncertainties the variable membership functions are described by pairs of power/membership values. In this context and since nodal marginal prices are described by the dual variables of the original problems, we could immediately expect that their membership functions would be described by ordered pairs of price/membership values, in case of load uncertainties modeling, and by linear segments in case of generation cost uncertainty modeling.

III. CASE STUDY USING A SMALL EXAMPLE

A. Data

In the first case study, we tested the developed algorithms using the 6 bus/8 branch system of Figure 2.

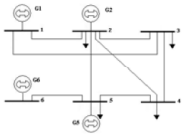

Fig. 2. Six bus/eight branch system

Table I presents the system data. It should be referred that the branches capacities were set at 8 MW and that the per unit reactance of branches are in a 100 MVA base.

B. Considering Load Uncertainties

In an attempt to model load uncertainties, loads in buses 2, 3, 4 and 5 where defined by the trapezoidal fuzzy numbers (25-28).

$$P_{L2} = (2.0;3.0;5.0;6.0)\ \text{MW} \quad (25)$$

$$P_{L3} = (1.0;1.5;2.5;3.0)\ \text{MW} \quad (26)$$

$$P_{L4} = (2.0;3.0;5.0;6.0)\ \text{MW} \quad (27)$$

$$P_{L5} = (1.0;2.5;3.5;5.0)\ \text{MW} \quad (28)$$

Figures 3 and 4 present the membership functions of generators at buses 1, 2 and 5 when we consider and do not take into account the effect of transmission losses. As it can be seen from these Figures, the effect of the transmission losses is almost negligible given the small system dimension. It is, however, clear from Figure 4 (at right) that the introduction of the losses effect implies an increase on the nodal marginal price on bus 3.

TABLE I
System data

Bus	Load [MW]	Branch	Reactance [pu]	Bus	P_G^{max}/P_G^{min} [MW]	Cost [€/MW.h]
1	0.0	1-2	0.06	1	10.0/3.0	15.0
2	4.0	1-3	0.24	2	15.0/0.0	20.0
3	2.0	2-3	0.18	5	7.0/2.0	12.0
4	4.0	2-4	0.18	6	5.0/0.0	21.0
5	3.0	2-5	0.12	--	--	--
6	0.0	3-4	0.03	--	--	--
--	--	4-5	0.24	--	--	--
--	--	5-6	0.03	--	--	--

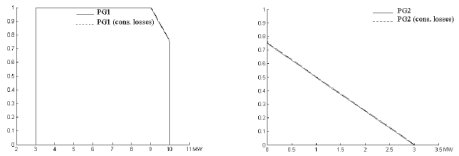

Fig. 3. Membership functions of generators at buses 1 and 2

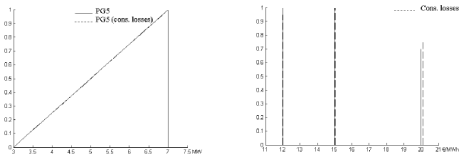

Fig. 4. Membership functions of generator at bus 5 (at left) and of the nodal marginal price on bus 3 (at right)

C. Considering Generation Cost Uncertainties

In this case, the generation cost of generators in buses 2 and 5 were defined by the trapezoidal numbers (29) and (30).

$$C_{PG2} = (9.0;16.0;24.0;31.0)\ €/\text{MWh} \quad (29)$$

$$C_{PG5} = (5.0;10.0;14.0;19.0)\ €/\text{MWh} \quad (30)$$

Figures 5 and 6 present the membership functions of generators at buses 1, 2 and 5 considering and not considering the effect of transmission losses. Once again we can see that the effect of the transmission losses is not significant. From Figure 6 (at right) we can also see that for membership values larger than 0.85 the marginal generator is the one in bus 1, and so, the nodal marginal price is 15 €/MWh. For membership values between 0.8 and 0.85 the marginal generator is the one in bus 2 and for membership values smaller than 0.8 the marginal generator is the one in bus 5. As a consequence, these marginal generators determine the system nodal marginal price in these uncertainty intervals.

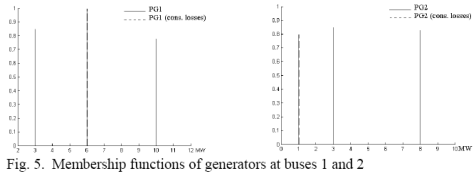

Fig. 5. Membership functions of generators at buses 1 and 2

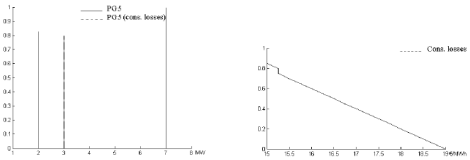

Fig. 6. Membership functions of generator at bus 5 (at left) and of the nodal marginal price at bus 3 (at right)

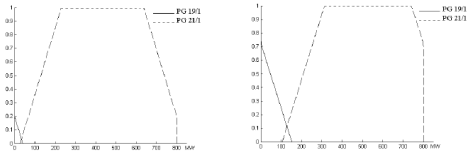

Fig. 7. Membership functions of generators 19/1 and 21/1 not considering the effect of the transmission losses (at left) and considering this effect (at right)

IV. CASE STUDY USING THE IEEE 24/38 BRANCH TEST SYSTEM

A. Data

The algorithms described in Section II were used to build the generation and marginal price membership functions considering a case study based on the IEEE 24 bus/38 branch test system. The original data for this system is given in [9]. Regarding the data in this reference, the load was increased to 4060.05 MW. Table II presents the central values of the loads and Table III the installed system capacity and the central values of the corresponding generation costs. The total installed capacity is 5226 MW according to the data in Table III. Branch data can be obtained from [9] considering that the transformers have a capacity of 400 MW, the capacity of the branches 1 to 6 and 8 to 13 was set at 175 MW and the capacity of the remaining branches was set at 500 MW.

TABLE II
Load central values

Bus	Load (MW)	Bus	Load (MW)	Bus	Load (MW)
1	220.48	9	385.82	17	0.00
2	270.80	10	216.49	18	226.76
3	3.94	11	40.00	19	265.53
4	32.67	12	10.00	20	103.92
5	105.94	13	162.45	21	50.00
6	187.65	14	262.88	22	10.00
7	218.77	15	650.36	23	0.00
8	398.09	16	225.50	24	12.00

TABLE III
Installed system capacity

Bus/ Gen	Capacity (MW)	Cost (€/MW.h)	Bus/ gen	Capacity (MW)	Cost (€/MW.h)
1/1	40.0	30.0	16/1	310.0	55.0
1/2	40.0	32.0	19/1	800.0	87.0
1/3	152.0	40.0	21/1	800.0	80.0
1/4	152.0	43.0	22/1	100.0	15.0
2/1	40.0	36.0	22/2	100.0	17.0
2/2	40.0	38.0	22/3	100.0	19.0
2/3	152.0	41.0	22/4	100.0	15.0
2/4	152.0	42.0	22/5	100.0	17.0
7/1	150.0	45.0	22/6	100.0	25.0
7/2	200.0	43.0	23/1	200.0	50.0
13/1	250.0	61.0	23/2	50.0	49.0
13/2	394.0	62.0	23/3	310.0	47.0
13/3	394.0	67.0	--	--	--

B. Results Considering only Load Uncertainties

In this case we considered trapezoidal fuzzy numbers to model loads. These numbers have at the 0.0 level the uncertainty ranges from +/-10 per cent and at the 1.0 level from +/- 5 per cent of its central value. Figure 7 presents the membership functions of generators 19/1 and 21/1 considering and not considering the effect of transmission losses.

As expected, load variations determine changes on the generation of generator 21/1 since it is the marginal one. When this generator gets its maximum capacity, generator 19/1 becomes the marginal one. Another important point illustrated by this Figure is related with the active losses impact. In this case, these generators have larger generation values for the same level of uncertainty due to the compensation of losses.

Figure 8 presents the nodal marginal prices at node 1 for the two situations previously presented. As referred in Section II, since nodal marginal prices are related with the dual variables of the original problem their membership functions are described by pairs of price/membership values. From Figure 8 it is possible to see that in the absence of the transmission losses, branch congestions or PNS effect, the marginal price in node 1 equals the generation cost of the marginal generator.

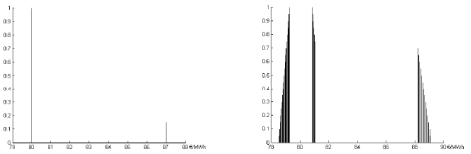

Fig. 8. Membership functions of the nodal marginal price in node 1 not considering the effect of transmission losses (at left) and considering this effect (at right)

When the effect of active losses is considered, the nodal marginal prices increase or decrease depending on the impact of load variations in active losses. For instance, when generator 19/1 is the marginal one, an increase of the load in node 1 implies an increase of active losses and so the marginal price in node 1 increases.

In order to check the effect of congested branches, the flow limit of branches 15-21 was reduced to 350 MW. As a consequence, for some combination of loads these branches get congested. Figure 9 presents the membership functions of generators 19/1 and 21/1 and of the marginal price in node 15 that were obtained in this case.

The analysis of these results indicates that the congestion on branches 15-21 implies a change of the marginal prices in most of the nodes, but more in particular in the ones that are closer to the congested branches. In case of node 15 in Figure 9, the marginal price increase means that a generation increase or a load reduction in this node contributes positively to alleviate the congestion. The membership function of generator 21/1 also reveals an interesting situation, since this generator does not reach its maximum limit of 800 MW,

differently from what was indicated in Figure 7. This is due to the congestion of branches 15-21.

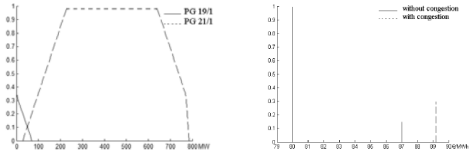

Fig. 9. Membership functions of generators 19/1 and 21/1 (at left) and of the nodal marginal price in node 15 (at right)

C. Results Considering only Cost Uncertainties

In this simulation, the trapezoidal fuzzy numbers (31-36) were used to model the cost of generators 1/1, 2/1, 7/1, 19/1, 22/2 and 23/2. Figure 10 presents the membership functions of generators 19/1 and 21/1.

$$CP_{G1/1} = (26.0,27.5,32.5,34.0) \quad (31)$$

$$CP_{G2/1} = (33.0,34.5,37.5,39.0) \quad (32)$$

$$CP_{G7/1} = (42.0,43.5,46.5,48.0) \quad (33)$$

$$CP_{G19/1} = (74.0,82.0,92.0,100.0) \quad (34)$$

$$CP_{G22/2} = (14.0,15.5,18.5,20.0) \quad (35)$$

$$CP_{G23/2} = (46.0,47.5,50.5,52.0) \quad (36)$$

As it was mentioned in Section II.B, in this case the membership functions of generators are represented by pairs of power/membership values. The above functions are related with two different generation strategies according to the specified generation cost uncertainties. In fact, when the generation cost of generator 19/1 is smaller than 80 €/MWh (generation cost of generator 21/1) this generator will generate 434.05 MW. For larger costs this generator will be at 0 MW and generator 21/1 will generate 434.05 MW. Figure 10 also indicates that the integration of active losses corresponds, in general, to an increase of generation values that depends on the adopted generation strategy because they have different impacts on active losses.

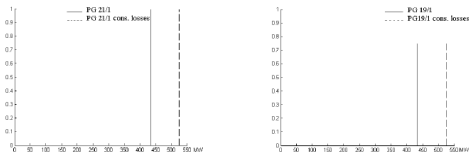

Fig. 10. Membership functions of generators 19/1 and 21/1 considering and not considering the effect of transmission losses

Figure 11 presents the nodal marginal price in node 1 in these two situations. In this case, the membership functions of the nodal marginal prices are linear, at least by segments. Considering the effect of active losses, leads to an increase of the nodal price in node 1. These results are in line with the ones in Figure 8 since we observed that a load increase in node 1 always implied an increase of active losses.

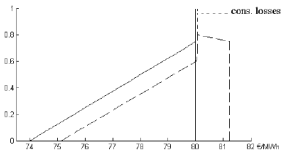

Fig. 11. Membership function of the nodal marginal price at node 1 considering and not considering the transmission losses effect

V. Conclusion

This paper describes a model to reflect load and generation cost uncertainties in power system operation studies, namely on generation values and on nodal marginal prices. This type of studies becomes more important in a market environment and also in a situation in which generation costs display a large volatility. This means that the developed models can be of interest for several agents in today power systems, namely to generation companies, to transmission companies, to retailers and to regulatory agencies as a way to get a better insight on the possible behavior of power systems taking into account the specified uncertainties. As a result, we consider there is a large potential application of these concepts which justifies the on going research effort in this area.

VI. References

[1] Leão, M. T. P., Saraiva, J. T., "Solving the Revenue Reconciliation Problem of Distribution Network Providers Using Long-Term marginal Prices", IEEE Transactions on Power Systems, Vol. 18, No. 1, February 2003.

[2] Rivier, M., Pérez-Arriaga, I. J., Luengo, G., "JUANAC: A Model for Computation of Spot Prices in Interconnected Power Systems", 10th PSCC Conference, Graz, Austria, August 1990.

[3] Baughman, Martin L., Lee, Walter W., "A Monte Carlo Model for Calculating Spot Market Prices of Electricity", IEEE Transactions on Power Systems, Vol. 7, No. 2, May 1992.

[4] Saraiva J. T., "Evaluation of the Impact of Load Uncertainties in Spot Prices Using Fuzzy Set Models", 13th Power Systems Computation Conference, 1999.

[5] Certo, Jorge, Saraiva, J. P., "Evaluation of Target Prices for Transmission Congestion Contracts Using a Monte Carlo Accelerated Approach", IEEE Porto Power Tech Conference, September 2001.

[6] Jesus, Paulo M., Leão, T., "Impact of Uncertainty and Elastic Response of Demand in Short Term Marginal Prices", 8th International Conference on Probabilistic Methods Applied to Power Systems, Ames, Iowa, September, 2004.

[7] Gomes, B.A, Saraiva, J.P., Neves, L., "Modelling Costs and Loads Uncertainties in Optimal Power Flow Studies", 5th European Electricity Energy Markets Conference, May, 2008.

[8] Gal, T., *Postoptimal Analysis, Parametric Programming and Related Topics*, McGraw Hill International Book Company, 1979.

[9] Task Force of Application of Probabilistic Methods Subcommittee (1979) IEEE Reliability Test System. IEEE Transactions on PAS PAS-98 2047-2054.

Acknowledgements – the first author thanks Fundação para a Ciência e Tecnologia, FCT, that funded this research through the PhD grant nº **SFRH/BD/34314/2006.**

Impact of Load and Generation Prices Uncertainties in Spot Prices, IEEE Power Tech, Bucharest, Romania, July 2009

Impact of Load and Generation Price Uncertainties in Spot Prices

Bruno A. Gomes, João T. Saraiva, *Member IEEE,* Luís M. Neves

***Abstract* — In this paper it is presented a formulation for the DC Optimal Power Flow problem considering load and generation cost uncertainties and the corresponding solution algorithms. The paper also details the algorithms implemented to allow the integration of losses on the results as well the algorithm developed to compute the nodal marginal price in the presence of such uncertainties. Since loads and generation costs are represented by fuzzy numbers, nodal marginal prices are no longer represented by deterministic values, but instead, by membership functions. To illustrate the application of the proposed algorithms, this paper also includes results based on a small 3 bus system and on the IEEE 24 bus/38 branch test system.**

Index Terms— Uncertainties, fuzzy models, DC optimal power flow, multiparametric programming, nodal marginal prices

I. Introduction

THE development of electricity markets and the consequent unbundling process of the vertically integrated companies becomes a current practice in a wide number of countries all over the world. In this context, several authors refer that one of the main goals of a tariff methodology is the identification or development of methods that promote the efficient use of the system and that at the same time guarantee the long-term system reliability. In this sense, several tariff methods were proposed, namely average, incremental, and marginal approaches [1, 2]. Essentially motivated by their intrinsic simplicity and easiness of implementation the average based methods have been the ones traditionally used in the computation of the transmission tariffs. Nevertheless, since this kind of methods can not provide adequate economic signals for the efficient system planning and operation, marginal methods are very attractive given their economic foundation. These methods, however, also display several drawbacks which are typically related with their inability to adequately remunerate the transmission activity, since their computation usually does not take into account long-term investment cost. This under recovery problem is in fact well known in the literature and it is termed as the Revenue Reconciliation problem [3]. Another drawback of this methodology approach is related with their temporal and spatially volatility, which suggests that their computation should integrate uncertainties on loads and generation cost, especially in a market environment, since they lead to changes in the dispatch policy and thus in marginal prices. Additionally, they should also integrate reliability data regarding system components since this issue also affects the value of nodal marginal prices.

The treatment of uncertainties in power systems has long been addressed. Probabilistic methods were the pioneering methodologies developed in this area. Papers [4] [5] describe the main concepts related with this problem as well as the initially developed algorithms using convolution techniques, the DC model and different linearized versions of the AC power flow problem. Apart from data having probabilistic nature, there are situations in which the uncertainty has not a random nature but it derives, for instance, from the incomplete characterization of the phenomenon under analysis or from insufficient frequency phenomena. In other cases, uncertainty is related with vagueness in the sense that the human language has an intrinsic subjective nature. In this context, since the 80's Fuzzy Set models are under development and application to power systems in order to provide a new framework to model the vague or ill defined nature of some phenomena. This application already occurred or is under way in areas as Fuzzy Power Flow, Fuzzy Optimal Power Flow, risk analysis and reinforcement strategies, generation planning, reliability models, fuzzy reactive power control, fuzzy dispatch and fuzzy clustering of load curves or even in transient or steady state stability analysis.

In this context, reference [6] describes a Fuzzy DC Optimal Power Flow model admitting that, at least, one load is represented by a fuzzy number. As a result, generations, branch flows and power not supplied, PNS, displays fuzzy representations translating data uncertainty. Afterwards, using this Fuzzy OPF, reference [6] also describes how load uncertainties can be reflected in fuzzy distributions for nodal marginal prices. In this paper we are now enlarging this approach in order to consider not only load uncertainties, but also generation cost uncertainties represented by fuzzy numbers. Additionally, the developed solution algorithms use multiparametric linear optimization techniques that allow obtaining more accurate descriptions of the possible behavior of the system under the form of membership functions.

After this Introduction Section, Section II describes the New Fuzzy Optimal Power Flow (NFOPF) model and the

This work was supported by the Fundação para a Ciência e Tecnologia through the PhD grant nº SFRH/BD/34314/2006.

Bruno A. Gomes is with FEUP/DEEC – Faculdade de Engenharia da Univ. do Porto and INESC Porto – Instituto de Engenharia de Sistemas e Computadores do Porto, Campus da FEUP, Rua Dr. Roberto Frias, 4200-465 Porto Portugal, bgomes@inescporto.pt

João T. Saraiva is with FEUP/DEEC – Faculdade de Engenharia da Univ. do Porto and INESC Porto – Instituto de Engenharia de Sistemas e Computadores do Porto, Campus da FEUP, Rua Dr. Roberto Frias, 4200-465 Porto Portugal, jsaraiva@fe.up.pt

Luís M. Neves is with Escola Superior de Tecnologia e Gestão from Instituto Politécnico de Leiria, Morro do Lena, Alto Vieiro, Apartado 4163, 2401-951 Leiria, Portugal, lneves@estg.ipleiria.pt

algorithm developed to integrate losses and Section III details the computation of nodal marginal prices in the presence of load and generation cost uncertainties. Section IV and V present results based on a three bus/three branch system and on the IEEE 24 bus/38 branch test system. Finally Section VI presents the most relevant conclusions.

II. NEW FUZZY OPTIMAL POWER FLOW ALGORITHM

A. General Aspects

Starting from the original concept of the Fuzzy Optimal Power Flow developed by the second author of this paper [6], the NFOPF model [7] is an optimization problem aiming at identifying the most adequate generation strategy, driven by an economic criterion, admitting that, at least, one load or generation cost is represented by a fuzzy number. Similarly to its original model, the NFOPF also uses the DC approach to model the operation conditions of the network. However, instead of running a number of parametric studies, the new developed model uses multiparametric linear programming techniques. This in fact represents an important improvement, since it allows obtaining more accurate membership functions in the sense they actually represent the widest possible behavior of each output variable. Figure 1 presents the corresponding flowchart of the algorithm.

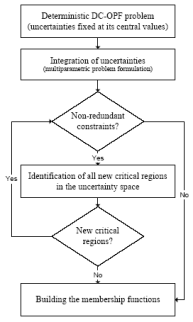

Fig. 1. New Fuzzy DC Optimal Power Flow algorithm [7]

B. Initial Deterministic Study

As it can be seen from Figure 1, the NFOPF algorithm starts with the execution of a deterministic OPF (1-5) considering the central values of the fuzzy numbers that represent loads and generation costs, P_{Lk}^{ctr} and c_k^{ctr}, respectively.

$$min\ f = \sum c_k^{ctr}.Pg_k + G.\sum PNS_k \quad (1)$$

$$\text{subj.}\ \sum Pg_k + \sum PNS_k = \sum P_{Lk}^{ctr} \quad (2)$$

$$\mathrm{Pg_k^{min}} \le \mathrm{Pg_k} \le \mathrm{Pg_k^{max}} \quad (3)$$

$$PNS_k \le P_{Lk}^{ctr} \quad (4)$$

$$P_b^{min} \le \sum a_{bk}.(Pg_k + PNS_k - P_{Lk}^{ctr}) \le P_b^{max} \quad (5)$$

In this model $\mathrm{Pg_k}$ is the generation in bus k having cost $\mathrm{c_k}$ and $\mathrm{PNS_k}$ is the power not supplied in bus k, $\mathrm{Pg_k^{min}}$, $\mathrm{Pg_k^{max}}$, $P_b^{\min}$ and $P_b^{\max}$ are the generation and branch flow limits and $\mathrm{a_{bk}}$ is the DC sensitivity coefficient of the flow in branch b regarding the injected power in bus k.

Once a feasible and optimal solution of this problem is identified, they are integrated parameters representing each fuzzy load or generation cost leading to a multiparametric optimization problem.

C. Integration of Uncertainties

Following the algorithm presented in Figure 1, after identifying a solution for the deterministic problem (1-5), the algorithm tries to find other optimal and feasible basis in regions of the uncertainty space based on the optimality (6) or feasibility (7) conditions. These regions are called critical regions and this process is conducted by pivoting over the initial basis as well as over all the new ones identified during the search process.

$$\mathrm{C^T}(\Phi_k) - \mathrm{C_0^T}.\mathrm{B_\rho^{-1}}.\mathrm{A} = (\mathrm{c} + \mathrm{c'}(\Phi_k)) - \mathrm{C_0^T}.\mathrm{B_\rho^{-1}}.\mathrm{A} \ge 0 \quad (6)$$

$$\mathrm{B_\rho^{-1}}.\mathrm{b}(\Delta_k) = \mathrm{B_\rho^{-1}}(\mathrm{b} + \mathrm{b'}(\Delta_k)) \ge 0 \quad (7)$$

In these expressions, B be is an optimal and feasible basis, ρ the index for the corresponding set of basic variables, A represents the columns of the non-basic variables in the Simplex tableau, C_0 is the cost vector of the basic variables, C^T is the cost vector of the non-basic variables, Φ_k is the vector of the parameters that model generation cost uncertainties and Δ_k is the vector of the parameters modeling load uncertainties.

As a final comment, the ultimate objective to attain when solving a multiparametric optimization problem is to find all possible optimal solutions, their corresponding optimal values and critical regions. These regions can be defined as a closed nonempty polyhedron and mathematically represented by a set of linear inequalities in Δ or Φ. Mathematically, this set of constraints can be expressed as the equivalent set of non-redundant constraints, which in turn can be identified through a non-redundant test for linear inequalities, like the one proposed by Gal [8].

D. Consideration of Load Uncertainties

The integration of the parameters that model load uncertainties in the optimal and feasible solution of the deterministic problem (1-5) leads to the multiparametric optimization problem (8-12).

$$min\ f = \sum c_k^{ctr}.Pg_k + G.\sum PNS_k \quad (8)$$

$$\text{subj.}\ \sum Pg_k + \sum PNS_k = \sum P_{Lk}^{ctr} + \sum \Delta_k \quad (9)$$

$$\mathrm{Pg_k^{min}} \le \mathrm{Pg_k} \le \mathrm{Pg_k^{max}} \quad (10)$$

$$PNS_k \le P_{Lk}^{ctr} + \Delta_k \quad (11)$$

$$P_b^{min} \le \sum a_{bk}.(Pg_k + PNS_k - (P_{Lk}^{ctr} + \Delta_k)) \le P_b^{max} \quad (12)$$

Considering the inequalities associated to the feasibility condition (7), the algorithm identifies a set of non-redundant constraints defining new critical regions. If there are no non-redundant constraints, the algorithm stops. Otherwise, it performs a dual pivoting over the initial optimal and feasible solution to identify new critical regions. This process is repeated until no non-redundant constraints exist or until all identified critical regions correspond to the already known ones. When this is over, all the uncertainty space was covered and we identified all critical regions in which a base B of the problem (8-12) remains feasible and optimal.

At this stage the algorithm proceeds by building the membership functions of the output variables (generations, branch flows and PNS). Given that the problem is linear, each variable in each critical region is represented by a linear expression. In this sense, in order to capture the widest possible behaviour of each variable the algorithm solves several minimizing and maximizing linear optimization problems for several different cut levels and for each function that represent the behaviour of each variable subjected to the non-redundant conditions together with the possible ranges of the input uncertainties regarding the i^{th} cut under analysis. For illustration purposes, if we consider a system having two loads affected by uncertainty, this problem can be formulated by (13-16).

$$\min/\max \; f = v(\Delta_1, \Delta_2) \tag{13}$$

$$\text{subj.} \quad k_{1i}.\Delta_1 + k_{2i}.\Delta_2 \le b_i \tag{14}$$

$$\Delta_1^{\min\ i^{th}-cut} \le \Delta_1 \le \Delta_1^{máx\ i^{th}-cut} \tag{15}$$

$$\Delta_2^{\min\ i^{th}-cut} \le \Delta_2 \le \Delta_2^{máx\ i^{th}-cut} \tag{16}$$

In this model $v(\Delta_1,\Delta_2)$ is the linear expression that represents the behaviour of the variable v in terms of the load uncertainty parameters Δ_1 and Δ_2 in the critical region under analysis, k_{1i} and k_{2i} are real numbers, and $\Delta_1^{\min\ i^{th}-cut}$, $\Delta_1^{\max\ i^{th}-cut}$, $\Delta_2^{\min\ i^{th}-cut}$ and $\Delta_2^{\max\ i^{th}-cut}$ are the minimum and maximum values of the load uncertainties in the i^{th} - cut under analysis.

Once all critical regions are analyzed, the final membership function of an output variable is obtained applying the fuzzy union operator to the partial membership functions obtained for that variable. This guarantees that the final result displays the widest possible behavior given the specified uncertainties.

E. Consideration of Generation Cost Uncertainties

The integration of the parameters that model generation cost uncertainties in the optimal and feasible solution of the deterministic problem (1-5) leads to the multiparametric optimization problem (17-21).

$$\min f = \sum c_k(\Phi).Pg_k + G.\sum PNS_k \tag{17}$$

$$\text{subj.} \sum Pg_k + \sum PNS_k = \sum P_{Lk}^{ctr} \tag{18}$$

$$Pg_k^{\min} \le Pg_k \le Pg_k^{\max} \tag{19}$$

$$PNS_k \le P_{Lk}^{ctr} \tag{20}$$

$$P_b^{min} \le \sum a_{bk}.(Pg_k + PNS_k - P_{Lk}^{ctr}) \le P_b^{max} \tag{21}$$

Similarly to what was described in Section II.D, considering the inequalities associated to the optimality condition (6) the algorithm tries to identify new optimal and feasible basis in the uncertainty space and the corresponding critical regions defined by the parameters that model generation cost uncertainties. Once again, if there are no more critical regions the algorithm stops. Otherwise, it performs a primal pivoting over the initial identified optimal and feasible basis. This process is repeated until non-redundant constraint exists or until all identified basis correspond to the already known ones.

When this process is completed the algorithm builds the membership functions of the output variables. This process is conducted taking into account that in this case each variable is constant inside each critical region. As a consequence, to build the membership functions the algorithm just has to solve the linear inequality system defined by the parameters that model generation cost uncertainties in each critical region to check if, at least, one point of a given cut level belongs to the region under analysis. For a given variable, once all partial membership functions are obtained, they are aggregated using the fuzzy union operator to obtain the final membership function of the output variable under analysis.

F. Integration of Active Losses

Active losses in branch b are given by (22). As it can be seen, it depends on the voltage magnitude and phase on the extreme branch nodes i and j and also on the conductance g_{ij}. If we consider that voltage magnitudes are 1.0 pu, we can then obtain the simplified expression (23).

$$Loss_{ij} = g_{ij}.(V_i^2 + V_j^2 - 2.V_i.V_j.\cos\theta_{ij}) \tag{22}$$

$$Loss_{ij} = 2.g_{ij}.(1 - \cos\theta_{ij}) \tag{23}$$

Among several other available techniques described in literature, this algorithm adopts the approach described in [6] to consider an estimate of active losses. The corresponding iterative process evolves as follows:

1. Perform the deterministic DC OPF study (1-5);
2. Compute the voltage phases according to the DC model;
3. Compute an estimate of the active power losses in each branch of the system;
4. Add half of the estimated active power losses for each branch to the loads in the corresponding extreme buses;
5. Perform a new deterministic DC OPF study to update the generation strategy;
6. Compute the nodal voltage phases according with the DC model;
7. Finish if the difference between every voltage phases in two successive iterations is smaller than a specified value. Otherwise return to step 3.

In case we are trying to integrate the effect of the active losses on the results of the algorithms detailed in sections II.D and II.E then, for each extreme point in each identified critical region we must run the algorithm just detailed. As we will

show in Sections IV and V, in general, this procedure introduces small deviations regarding the initial results.

III. MARGINAL PRICE COMPUTATION

A. Deterministic Evaluation

The short term nodal marginal price in node k is defined as the impact on the cost function of a short term operation problem regarding to a variation of the load in node k. Given this definition in deterministic terms and for the problem (1-5), short term marginal prices can be computed using (24).

$$\rho_k = \gamma + \sigma_k - \sum_{all\ branches} \eta_b \cdot \frac{\partial P_b}{\partial P_{Lk}} + \gamma \cdot \frac{\partial Losses}{\partial P_{Lk}} \quad (24)$$

In this expression:

- γ represents the dual variable of the generation/load balance equation (2);
- the second term represents the contribution from constrains (4) that are eventually on their limits. σ_k is the dual variable of the constraint in node k;
- the third term represents the contribution from each branch flow constraint that is on its limit. In this expression, η_b represents the dual variable of the corresponding constraint (5) and the derivative of the flow in branch b, P_b, regarding the load in bus k, P_{Lk}, is the symmetric of the corresponding sensibility coefficient;
- the fourth term represents the impact on the cost function from varying branch losses in the whole network due a variation of the load in bus k.

B. Nodal Marginal Prices Membership Functions

The algorithm presented in Section II could also be used to compute the nodal marginal price membership functions when they are modelled load or generation cost uncertainties. In this context, the computation of the nodal marginal price membership functions comprises three distinct stages. In the first place, the algorithm determines the maximum and minimum possible values of all variables in each cut level. Once this initial stage is completed, the algorithm can evolve to include the impact of the active losses for each identified operating point in each cut level or, this impact can be neglected. Finally, the algorithm determines the nodal marginal prices using (24). When all partial membership functions are known for a given node, the final membership function is obtained applying the fuzzy union operator.

Since nodal marginal prices are described by the dual variables of the original problems their membership functions will be described by ordered pairs of price/membership values, in case of load uncertainties modeling, and by linear segments in case of generation cost uncertainty modeling.

IV. CASE STUDY USING A THREE BUS/THREE BRANCH SYSTEM

A. Data

To illustrate the application of the algorithms described in Section II and III we used the small system presented in Figure 2. In this example, we considered that generator 1 has a capacity of 3 MW and that generator 2 as a capacity of 7 MW. The capacity of branches was set at 5 MW. All branches have the same impedance of 0.05+j1.0 pu, (base of 10 MVA, 10 kV). The generation cost of generator 1 is 10 €/MWh and of generator 2 is 20 €/MWh. The central value of the load on bus 2 is 2.0 MW and on bus 3 is 3.5 MW.

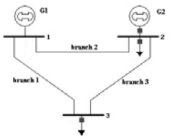

Fig. 2. Three bus/three branch system

B. Considering Load Uncertainties

In order to model load uncertainties, load in nodes 2 and 3 were defined by the trapezoidal fuzzy numbers (25) and (26).

$$P_{L2} = (0.0;1.5;2.5;4.0)\ \text{MW} \quad (25)$$

$$P_{L3} = (2.0;3.0;4.0;5.0)\ \text{MW} \quad (26)$$

Figure 3 presents the membership functions of the generators at buses 1 and 2 and of the marginal price in bus 3 considering and not considering the effect of active losses.

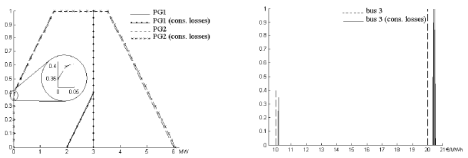

Fig. 3. Membership functions of generator 1 and 2 (at the left) and of the nodal marginal prices at bus 3 (at the right), both considering and not considering the effect of transmission losses

As we can see from Figure 3 (at left), when the system load is at its minimum (2 MW) only generator 1 is in service since it is the less expensive one. When this generator achieves its maximum capacity of 3 MW generator 2 starts to produce. As expected, in this system the effect of transmission losses is neglectable given the system dimension. Without surprise the membership function of nodal marginal price in bus 3 when they are not considered the transmission losses presents a value of 10 €/MWh with a membership value of 0.4 and a value of 20 €/MWh with a membership value of 1.0. In this context it is also important to mention that all buses present the same nodal marginal price membership functions since they are not considered losses and there are no branch congestions or PNS. As expected, this Figure also indicates that a load increase in bus 3 implies an increase of losses and, as a consequence, nodal marginal price in this bus also increases. It is also interesting the fact that the membership degree of the 10.17 €/MWh is now smaller then the one identified for the 10 €/MWh when the losses effect was neglected. This situation results from the fact that when active

losses are considered and for uncertainties larger than 0,35, the marginal generator becomes generator 2.

C. Considering Generation Cost Uncertainties

In order to model generation cost uncertainties, the generation costs of generators at buses 1 and 2 were defined by the trapezoidal fuzzy numbers (27) and (28).

$$C_{PG1} = (5.0;7.5;12.5;15.0)\ €/MWh \quad (27)$$

$$C_{PG2} = (7.5;15.0;25.0;32.5)\ €/MWh \quad (28)$$

Figure 4 presents the membership functions of generators 1 and 2 and of the nodal marginal price on bus 3.

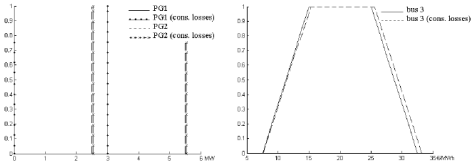

Fig. 4. Membership functions of generators 1 and 2 (at the left) and of the nodal marginal price on bus 3 (at the right), both considering and not considering the effect of active losses

As it can be seen from Figure 4 (at the left), given the specified generation cost uncertainties they were identified two possible generation strategies. In the first one, the two generations are in service and, in the second one generator 2 is at 5.5 MW supplying the entire load, that is 2 MW at bus 2 and 3,5 MW at bus 3. Since generator 2 is always the marginal generator, it defines the system marginal price as it can be seen from the membership function at the right side of Figure 4. This Figure also indicates that the nodal marginal price on bus 3 increases when considering active losses. This in fact shows that a load increase on this node implies an increase of the system active losses.

V. CASE STUDY USING A 24 BUS/38 BRANCH SYSTEM

A. Data

The algorithms described in Section II and III were used to build the generation and marginal price membership functions considering a case study based on the IEEE 24 bus/38 branch test system. The original data for this system is given in [9]. Regarding the data in this reference, the load was increased to 4308.05 MW. Table II presents the central values of the loads and Table III the installed system capacity and the central values of the corresponding generation costs.

TABLE II
Load central values

Bus	Load (MW)	Bus	Load (MW)	Bus	Load (MW)
1	220.48	9	385.82	17	0.00
2	270.80	10	216.49	18	226.76
3	3.94	11	40.00	19	265.53
4	32.67	12	10.00	20	103.92
5	105.94	13	162.45	21	100.00
6	187.65	14	262.88	22	100.00
7	218.77	15	650.36	23	0.00
8	398.09	16	225.50	24	120.00

The total installed capacity is 5536 MW according to the data in Table III. Branch data can be obtained from [9] considering that the transformers have a capacity of 400 MW, the capacity of the branches 1 to 6 and 8 to 13 was set at 175 MW and the capacity of the remaining branches was set at 500 MW.

TABLE III
Installed system capacity

Bus/ Gen	Capacity (MW)	Cost (€/MW.h)	Bus/ gen	Capacity (MW)	Cost (€/MW.h)
1/1	40.0	30.0	18/1	310.0	38.0
1/2	40.0	32.0	19/1	800.0	87.0
1/3	152.0	40.0	21/1	700.0	80.0
1/4	152.0	43.0	22/1	100.0	15.0
2/1	40.0	36.0	22/2	100.0	17.0
2/2	40.0	38.0	22/3	100.0	19.0
2/3	152.0	41.0	22/4	100.0	15.0
2/4	152.0	42.0	22/5	100.0	17.0
7/1	150.0	45.0	22/6	100.0	25.0
7/2	200.0	43.0	23/1	200.0	50.0
13/1	250.0	61.0	23/2	50.0	49.0
13/2	394.0	62.0	23/3	310.0	47.0
13/3	394.0	67.0	--	--	--
16/1	310.0	55.0	--	--	--

B. Considering Load Uncertainties

In this case we considered trapezoidal fuzzy numbers to model loads. These numbers have at the 0.0 level the uncertainty ranges from +/-10 per cent and at the 1.0 level from +/- 5 per cent of its central value. Figure 5 presents the membership functions of generators 13/3, 19/1 and 21/1 considering and not considering the effect of active losses.

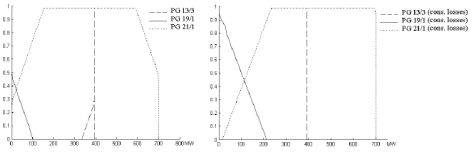

Fig. 5. Membership functions of generators 13/3, 19/1 and 21/1 not considering the transmission losses effect (at the left) and considering this effect (at the right)

As it can be seen from Figure 5 in presence of active losses, generators exhibit greater generation values for the some level of load uncertainty, which in fact corresponds to the losses compensation. An important consequence of this is the fact that when transmission losses are considered generator 13/3 is never the marginal generator. This situation justifies the absence of the 67 €/MWh value in the membership function of the nodal marginal price in bus 10 when they are considered the active losses effect as it can be seen in Figure 6.

When the effect of active losses is considered, the nodal marginal prices increase or decrease depending on the impact of load variations in the active losses. For instance, when generator 21/1 is the marginal one, an increase of the load in node 10 implies an increase of active losses and so the marginal price in node 10 increases.

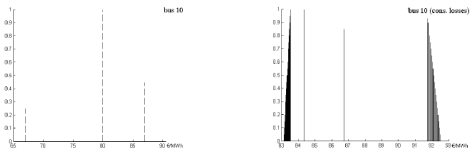

Fig. 6. Membership functions of the nodal marginal price at bus 10 not considering the effect of transmission losses (at the left) and considering this effect (at the right).

C. *Considering Generation Cost Uncertainties*

In this case we considered that the generation costs of the generators 1/1, 2/1, 2/4, 13/3, 19/1, 21/1 and 23/2 are represented by the trapezoidal fuzzy numbers (29-35). As a consequence, Figures 7 and 8 present the membership functions of generators 13/3, 19/1 and 21/1 and of the nodal marginal price on bus 10 considering the generation cost uncertainties just mentioned.

$$C_{PG1/1} = (26.0;27.5;32.5;34.0)\ €/\text{MWh} \quad (29)$$

$$C_{PG2/1} = (33.0;34.5;37.5;39.0)\ €/\text{MWh} \quad (30)$$

$$C_{PG2/4} = (37.0;39.5;44.5;47.0)\ €/\text{MWh} \quad (31)$$

$$C_{PG13/3} = (58.0;61.0;73.0;76.0)\ €/\text{MWh} \quad (32)$$

$$C_{PG19/1} = (74.0;82.0;92.0;100.0)\ €/\text{MWh} \quad (33)$$

$$C_{PG21/1} = (71.0;74.0;86.0;89.0)\ €/\text{MWh} \quad (34)$$

$$C_{PG23/2} = (77.0;78.5;81.5;83.0)\ €/\text{MWh} \quad (35)$$

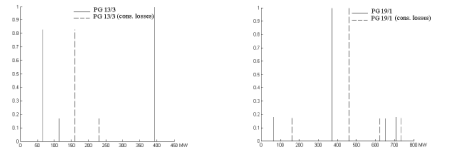

Fig. 7. Membership functions of the generators 13/3 and 19/1 when they are considered the transmission losses effect and when they are not considered

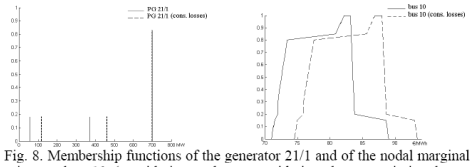

Fig. 8. Membership functions of the generator 21/1 and of the nodal marginal price on bus 10 (considering and not considering the transmission losses effect)

From Figures 7 and 8 we can recognize once again that for some levels of uncertainty generators exhibit larger generation values as a consequence of the compensation of losses. In Figure 8 it is once again visible that a load increase in bus 10 has an increasing impact on the global system active losses thus determining an increase of the nodal marginal price in that bus.

VI. Conclusion

In this paper we present the NFOPF model as an algorithm to evaluate the impact of load and generation cost uncertainties on the nodal marginal prices computation. It was also described the algorithms developed to integrate an estimate of the active transmission losses on the results. Since this algorithm uses multiparametric programming techniques it allows attaining more accurate representation of the variable membership functions. Given the current volatility and unpredictability of several input parameters, this model could play an important role in analyzing the possible system behavior and its corresponding impact at the agent's making decision process level.

References

[1] Shirmohammadi, D., Gorenstin, X. V., Pereira, M. V. P., "Some Fundamental Technical Concepts about Cost Based Transmission Pricing", IEEE Transactions on Power Systems, Vol. 11, No. 2, May 1996.

[2] Lima, J.W. Marangon, "Allocation of Transmission Fixed Charges: An Overview", IEEE Transactions on Power Systems, Vol. 11, No. 3, August 1996.

[3] Leão, M. T. P., Saraiva, J. T., "Solving the Revenue Reconciliation Problem of Distribution Network Providers Using Long-Term marginal Prices", IEEE Transactions on Power Systems, Vol. 18, No. 1, February 2003.

[4] Allan R. N., Al-Shakarchi M. R. G, "Probabilistic a.c. Load Flow", Proceedings of the IEE Vol. 123 No. 12, 531-536, 1976.

[5] Borkowska B., "Probabilistic Load Flow", IEEE Transactions PAS PAS-93 Vol. 12 752-759, 1974.

[6] Saraiva, J. T., "Evaluation of the Impact of Load Uncertainties in Spot Prices Using Fuzzy Set Models", 13 th PSCC in Trondheim, July 1999.

[7] Gomes, B. A., Saraiva, J. T., Neves, L., "Modelling Costs and Load Uncertainties in Optimal Power Flow Studies", 5th International Conference on the European Electricity Markets, Portugal, May 2008.

[8] Gal, T., *Postoptimal Analysis, Parametric Programming and Related Topics*, McGraw Hill International Book Company, 1979.

[9] Task Force of Application of Probabilistic Methods Subcommittee (1979) IEEE Reliability Test System. IEEE Transactions on PAS PAS-98 2047-2054.

Bruno André Gomes was born in Ovar, Portugal, in 1977. In 2001 he got his BSc from the Faculdade de Ciências e Tecnologia da Universidade de Coimbra and in 2005 he got his MSc from the Faculdade de Engenharia da Universidade do Porto, FEUP. Currently he has a grant from the Fundação para a Ciência e Tecnologia, FCT, and he is completing his PhD in FEUP.

João Tomé Saraiva was born in Porto, Portugal in 1962. In 1987, 1993 and 2002 he got his MSc, PhD, and Agregado degrees in Electrical and Computer Engineering from the Faculdade de Engenharia da Universidade do Porto, FEUP, where he is currently Professor. In 1985 he joined INESC Porto – a private research institute – where he was head researcher or collaborated in several projects related with the development of DMS systems, quality in power systems, and tariffs due for the use of transmission and distribution networks. Several of these projects were developed under consultancy contracts with the Portuguese Electricity Regulatory Agency.

Luís Miguel Neves was born in Lisbon, Portugal, in 1968. In 1992, 1998 and 2005 he got his BSc, MSc and PhD in Faculdade de Ciências e Tecnologia da Universidade de Coimbra. Currently he is Professor Adjunto in the Instituto Politécnico de Leiria and Researcher in INESC Coimbra, Portugal.

Dealing with Load and Generation Cost Uncertainties in Power System Operation Studies – A Fuzzy Approach, Handbook of Power Systems, Springer, Series on Energy Systems, Rebennack, P. M. Pardalos, M. V. F. Pereira, N. A. Illadis (Eds), to be published in March 2010

Dealing With Load and Generation Cost Uncertainties in Power System Operation Studies – A Fuzzy Approach

Bruno A. Gomes and João Tomé Saraiva

Abstract Power Systems are currently facing a change of the paradigm that determined their operation and planning while being surrounded by multiple uncertainties sources. As a consequence, dealing with uncertainties is becoming a crucial issue in the sense that all agents should be able to internalize them in their models in order to guarantee that activities are profitable and that operation and investment strategies are selected according to an adequate level of risk. Taking into account the introduction of market mechanisms and the volatility of fuel prices, this paper presents the models and the algorithms developed to address load and generation cost uncertainties. These models correspond to an enhanced approach regarding the original Fuzzy Optimal Power Flow, FOPF, model developed by the end of the 90ies that only considered load uncertainties. The paper also describes the algorithms developed to integrate an estimate of active transmission losses and to compute nodal marginal prices reflecting such uncertainties. The developed algorithms use multiparametric optimization techniques and are illustrated using a Case Study based on the IEEE 24 bus test system.

1. Introduction

Power systems were always affected by uncertainties. They were traditionally related with load growth, consumer response to demand-side options, longevity and performance of life-extended or converted plants, potential supply of renewable resources, measurement errors or forecast inaccuracy, unscheduled outages, technological developments, fuel prices or even regulatory requirements. In fact, these uncertainties are related with variables of different nature, such as physical, technical, economic, regulatory and political.

Bruno André Gomes
INESC Porto, Departamento de Engenharia Electrotécnica e Computadores
Faculdade de Engenharia da Universidade do Porto
Campus da FEUP, Rua Dr. Roberto Frias 378, 4200 465 Porto, Portugal, bgomes@inescporto.pt
João Tomé Saraiva
INESC Porto, Departamento de Engenharia Electrotécnica e Computadores
Faculdade de Engenharia da Universidade do Porto
Campus da FEUP, Rua Dr. Roberto Frias 378, 4200 – 465 Porto, Portugal, jsaraiva@fe.up.pt

Nowadays, power systems are also facing new challenges since uncertainties are also due to the introduction of market mechanisms in the sector and with the growing consciousness about environmental concerns. Apart from these new concerns, some others clearly increased their relevance, namely the volatility of fuel prices, the difficulty in predicting the availability of several primary resources highly used in Renewable Energy Resources (RER) as well as the difficulty in predicting demand evolution, for instance as a consequence of economic problems in wider geographical areas.

On the other hand, the climate change is also putting a new pressure in the sector. As an attempt to tackle this problem, in 2005 the European Union (EU) launched the Emissions Trading System (ETS) to trade CO_2 allowances to create incentives to reduce emissions. Since RER are carbon free, it was also implemented in some European Countries a Green Certificate market to induce investments in these technologies. More recently and since energy efficiency is also an essential element of the EU energy policy, some member states also launched White Certificates markets (WhC) to promote energy efficiency.

In case these market instruments work properly, it is expected a net electricity demand reduction and consequently a decrease in new generation capacity investment and on the share of some generators more carbon intense. It is also important to refer that the implementation of a more ambitious quota for RER together with the Green Certificate system will contribute to reduce the price of the allowances within the EU ETS. As a result, market participants will face a net combined effect. In fact, they have to face uncertainties in fuel prices, in the cost of purchasing ETS allowances if the CO_2 emissions exceed the administratively fixed limit, opportunity costs for selling allowances in case they are not fully used and, finally, uncertainties on demand and on RER generation levels [31].

As a conclusion, internalizing the environmental damages due to energy generation and consumption into prices is bringing to the power sector a more conscious and sustainable way to plan and operate the system. On the other hand, it also brings a huge number of uncertainties and challenges that can contribute to raise the cost of capital and change investment decisions. Accordingly, market participants should use models and adopt methods that are able to address all these uncertainties and integrate them into decision-making processes. This means that risk has to be adequately addressed if one wants to have a complete and consistent picture of what can be the future power system operation while ensuring that profits are large enough to compensate the cost of capital.

Following these ideas, this paper is structured as follows. After this Introduction, Section 2 briefly addresses methodologies available in the literature to integrate uncertainties in several power system studies. Section 3 presents the fundamental concepts of Fuzzy Set theory useful to fully understand the remaining sections. Section 4 details the original Fuzzy Optimal Power Flow problem and Section 5 describes the New Fuzzy DC Optimal Power Flow (NFOPF) problem and the developed solution algorithms. Finally, Section 6 presents results obtained with a Case Study based on the IEEE 24 bus Test System and Section 7 draws the most relevant conclusions.

2. Uncertainty Modelling in Power System Studies

When planning and operating a power system it is necessary to perform power flow studies in order to assess and monitor the steady state security of the system. These studies are one of the most frequently performed network calculations and there are several well developed techniques to make these studies very quickly and accurately. Traditionally, these methods had a deterministic nature in the sense they admit that all values and parameters were completely and fully known. However, since system parameters like nodal loads and generation levels can not be considered perfectly constant, they were soon developed models to address the presence of uncertainties affecting these values. In this context, in the literature there are models admitting different types of data, namely Probabilistic, Fuzzy, Boundary and Interval Arithmetic ones.

Probabilistic methods were the pioneering methodologies developed in this area. Given their subsequent development, they can be organized in classes, such as simulation, analytical or a combination of both [20]. Papers [1, 2, 3 4, 8] describe the main concepts related with this problem as well as the initially developed algorithms using convolution techniques, the DC model and different linearized versions of the AC power flow problem. In general, these approaches translate to the results of traditional power flows the uncertainties specified in data under the form of probabilistic distributions. In view of the linearizations adopted in several of them, it was soon realized that the results were affected by errors that would eventually be larger in the tails of the output distributions. Addressing this issue, reference [6] uses a Monte Carlo simulation based technique to evaluate the accuracy of the results and [5] and [18] propose the use of several linearization points to build partial probability distributions that, at the end, are aggregated to provide the final outputs. This approach was conceived to reduce the errors in the tails of the output distributions.

In subsequent years they were published other contributions that enhanced these models or contributed to give them an increased realism. References [16] and [19] are just two examples of these enhancements when considering network outages and operation constraints used to constrain the power flow results. Finally, reference [36] describes a new approach to the probabilistic power flow problem in order to build branch flow distributions to be used in transmission investment planning problems.

Apart from Probabilistic Power Flow models, the literature also includes a few references addressing the integration of probabilistic data in Optimal Power Flow (OPF) models, as it is the case of references [12, 21, 33].

Departing from the idea in [5] in terms of using multiple points to linearize the power flow equations, in [11] it was presented, for the first time, the Boundary Load Flow algorithm as a methodology to integrate load uncertainties in Power Flow studies. However, following [11] the method is computationally intensive and could occasionally fail in getting the correct solution if the function exhibits extreme changes during the solution.

Apart from data having probabilistic character, there are situations in which the uncertainty has not a random nature but it derives, for instance, from the incomplete characterization of the phenomenon under analysis or from insufficient information required to build probability distributions, as it happens in very low frequency phenomena. In other cases, uncertainty is related with vagueness in the sense that human language has an intrinsic subjective nature. In this sense, expressions as "larger than", "close to", "more or less" or "approximately" are inherently vague and their use does not reflect an historic average of past values but it reflects a subjective evaluation of each user.

Probability theory is not fully adequate to model this type of uncertainty. Since the 80ies Fuzzy Set models have been developed and applied to power systems in order to provide a new framework to model the vague or the ill-defined nature of some phenomena namely in Fuzzy Power Flows, Fuzzy Optimal Power Flows, risk analysis and reinforcement strategies [27], generation planning [24], reliability models, fuzzy reactive power control, fuzzy dispatch, fuzzy clustering of load curves and in transient or steady state stability evaluation.

Regarding power flow problems, the first DC and AC models admitting that at least one generation and demand are modelled by fuzzy numbers are described in [22]. As a result, voltages and branch flows are now modelled by fuzzy numbers displaying their possible behaviour under the specified uncertainties.

References [23] and [29] give a step forward in this area because they describe a Fuzzy DC OPF model admitting that, at least, one load is represented by a fuzzy number. As a result, generations, branch flows and power not supplied, PNS, (representing the power that the system cannot attend) display fuzzy representations translating data uncertainty. Afterwards, this approach was integrated in a Monte Carlo simulation [30] to obtain estimates of the expected value of PNS reflecting fuzzy loads and the reliability life cycle of equipments modelled by probability based approaches. In this sense, the model in [30] has a hybrid nature when aggregating fuzzy and probabilistic models. This Fuzzy DC OPF model was also used to identify the most adequate expansion plan so that the risk of not being able to meet the demand gets reduced while accommodating the inherent uncertainty [28]. Finally, reference [14] presents the basic concepts related with the simultaneous modelling of generation cost and demand uncertainties in Optimal Power Flow studies.

As we previously mentioned, the Interval Arithmetic model [34] represents another class of models within this field. In this contribution loads are represented by arithmetic intervals and the power flow problem is solved using linearized expressions. Since uncertainties are represented by intervals, it is not possible to consider qualitative information on the phenomenon under analysis or even knowledge related with some kind of repetitive events. To overcome this conceptual problem, reference [10] presents a distribution power flow model that uses a multi-point linearized procedure to find bounded intervals of loads that vary according to a probability distribution.

3. Fuzzy Set Basics

This section details some basic concepts of Fuzzy Set Theory that are essential to fully understand the next sections. In the first place, a fuzzy set $\tilde{A}$ is a set of ordered pairs (3.1) in which the first element, x_1, is an element of the universe X under analysis and the second is the membership degree of that element to the fuzzy set, $\mu_{\tilde{A}}(x_1)$. These values measure the degree of compatibility of the elements of X with the proposition defining the fuzzy set meaning that $\mu_{\tilde{A}}(x)$ corresponds to a membership function that assigns a membership degree in $[0.0;1.0]$ to each element x.

$$\tilde{A} = \{(x_1; \mu_{\tilde{A}}(x_1)), x_1 \in X\} \tag{3.1}$$

Among all possible classes of fuzzy sets, a fuzzy number $\tilde{A}$ is a fuzzy set that is convex and it is defined on the real line R such that its membership function is piecewise continuous. As an example, Figure 3.1 reproduces the membership function of a trapezoidal fuzzy number. Its membership degree is maximum in $[A_2; A_3]$ and decreases from 1.0 to 0.0 from A_2 to A_1 and from A_3 to A_4. Once one knows that a fuzzy set belongs to this particular class, the shape of the membership function is known and so such a number is uniquely defined by the values A_1, A_2, A_3 and A_4. Therefore, a trapezoidal fuzzy number is usually denoted as $(A_1; A_2; A_3; A_4)$.

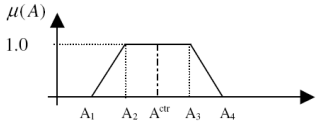

Fig. 3.1 Trapezoidal fuzzy number.

An α - level set or an α - cut of a fuzzy set $\tilde{A}$ is defined as the hard set A_α obtained from $\tilde{A}$ for each $\alpha \in [0.0;1.0]$ according to (3.2). Taking the number in Figure 3.1 as an example, the 0.0-cut is the interval $[A_1; A_4]$ and the 1.0-cut is given by the interval $[A_2; A_3]$. The Central Value of a fuzzy number is defined as the mean value of its 1.0-cut. Regarding the trapezoidal fuzzy number in Figure 3.1, the Central Value of $\tilde{A}$, A^{ctr}, is given by (3.3).

$$A_\alpha = \{x_1 \in X : \mu_{\tilde{A}}(x_1) \geq \alpha\} \tag{3.2}$$

$$A^{ctr} = (A_2 + A_3)/2 \tag{3.3}$$

Finally, let us consider two fuzzy sets $\tilde{A}$ and $\tilde{B}$ represented by their membership functions $\mu_{\tilde{A}}(x)$ and $\mu_{\tilde{B}}(x)$. The literature describes several operators to perform the union of $\tilde{A}$ and $\tilde{B}$. The original contribution of Lotfi Zadeh [35] defines the fuzzy union operator using (3.4). The membership grade of an element x in $\tilde{C} = \tilde{A} \cup \tilde{B}$ corresponds to the maximum of the membership grades of x in $\tilde{A}$ and in $\tilde{B}$. This ensures that the fuzzy set $\tilde{C}$ has the largest membership degrees when comparing them to the grades in $\tilde{A}$ and in $\tilde{B}$.

$$\mu_{\tilde{C}}(x) = max\left(\mu_{\tilde{A}}(x), \mu_{\tilde{B}}(x)\right) \tag{3.4}$$

4. Fuzzy Optimal Power Flow

A FOPF study can be defined as an optimization problem aiming at identifying the most adequate generation strategy driven by a generation cost function, and admitting that, at least, one load is represented by a fuzzy number. The original model described in [29, 30] uses the DC approach to represent the operation conditions of the network and includes power flow and generation limit constraints. In the first step, the algorithm developed to reflect load uncertainties in the results of this optimisation exercise solves the deterministic DC-OPF problem (4.1-4.5). This problem is run considering that the fuzzy load in node k is represented by its central value, Pl_k^{ctr}, as defined in Section 3.

$$\min Z = \sum c_k . Pg_k + G . \sum PNS_k \tag{4.1}$$

$$\text{s.t.} \quad \sum Pg_k + \sum PNS_k = \sum Pl_k^{ctr} \tag{4.2}$$

$$Pg_k^{min} \le Pg_k \le Pg_k^{max} \tag{4.3}$$

$$PNS_k \le Pl_k^{ctr} \tag{4.4}$$

$$P_b^{min} \le \sum a_{bk} . (Pg_k + PNS_k - Pl_k^{ctr}) \le P_b^{max} \tag{4.5}$$

In this model Pg_k is the generation in bus *k*, c_k is the corresponding variable cost, PNS_k is the power not supplied in bus *k* and G is the penalization specified for the power not supplied. On the other hand, $Pg_k^{\min}$, $Pg_k^{\max}$, $P_b^{\min}$ and $P_b^{\max}$ are the generation and branch flow limits, a_{bk} is the DC sensitivity coefficient of the flow in branch *b* regarding the injected power in bus *k*.

Once a feasible and optimal solution to this problem is identified, we integrate uncertainty parameters, λ_k, associated to each fuzzy load in the problem leading to the condensed multiparametric problem (4.6-4.8).

$$\min Z = c^t.X \tag{4.6}$$

$$\text{s.t. } A.X = b + b'(\lambda_k) \tag{4.7}$$

$$\lambda_{k1} \le \lambda_k \le \lambda_{k4} \tag{4.8}$$

In this model, A is the coefficient matrix, X is the vector of the decision variables, namely generations, b is the right hand side vector, $b'(\lambda_k)$ is a vector of linear expressions on λ_k and λ_{k1}, λ_{k4} are the minimum and maximum values of the load uncertainty on bus k. This means that they correspond to the extreme values of the 0.0-cut of the load membership function in bus k.

Constraints (4.8) define a hypervolume determined by the load uncertainty ranges, and in fact it encloses an infinite number of load combinations. Since the optimal solution of the crisp problem may not be feasible for all load combinations in this hypervolume, the algorithm proceeds identifying some vertices of this hypervolume. As a general rule, these vertices correspond to feasible solutions leading to maximum or minimum values of each basic variable in the initial solution or, alternatively, to vertices associated with unfeasible solutions. When this identification process is over, we have identified all vertices around the initial central value leading to individual extreme values of the basic variables or, instead, to non-feasible solutions. Afterwards, the algorithm proceeds by running a set of two consecutive parametric DC-OPF studies for each identified vertex. In order to clarify this procedure, let us admit a two fuzzy load system defined by (4.9) and (4.10) using the central values and a fuzzy deviation. For this case, Figure 4.1 represents the rectangles enclosing all possible load combinations for the 0.0 and 1.0-cuts.

$$P_{l1} = P_{l1}^{ctr} + (\Delta_{l1}; \Delta_{l2}; \Delta_{l3}; \Delta_{l4}) \text{ MW} \tag{4.9}$$

$$P_{l2} = P_{l2}^{ctr} + (\Delta_{21}; \Delta_{22}; \Delta_{23}; \Delta_{24}) \text{ MW} \tag{4.10}$$

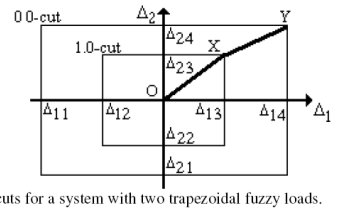

Fig. 4.1. 0.0 and 1.0 cuts for a system with two trapezoidal fuzzy loads.

Taking Figure 4.1 as reference and the vertex Y as an illustration, the first parametric study analyses load combinations along the segment OX considering that points O and X correspond, respectively, to $\alpha = 1.0$ and $\alpha = 0.0$ in the linear parametric optimization problem (4.11-4.13).

$$\min Z = c^t.X \quad (4.11)$$

$$\text{s.t. } A.X=b+b'(1.0-\alpha) \quad (4.12)$$

$$0.0 \le \alpha \le 1.0 \quad (4.13)$$

When point X is reached, the optimal and feasible solution is given by (4.15).

$$X_{opt} = B^{-1}.(b + b'(1.0 - \alpha)) \quad (4.15)$$

The second parametric study is used to analyse load combinations along the segment *XY* and its starting point corresponds to the solution obtained for point *X* in the first study. In this second study, points *X* and *Y* correspond to $\alpha = 1.0$ and $\alpha = 0.0$ respectively and it is possible to obtain the solution for *Y*, given by (4.16).

$$X_{opt} = B^{-1}.(b + b'+b''(1.0 - \alpha)) \quad (4.16)$$

These parametric studies are formulated in such a way that it is possible to guarantee that the values obtained in the first one are assigned to 1.0 membership degree while the values obtained with the second one have a membership degree that corresponds to the value of α, and so, it decreases from 1.0 to 0.0 membership degree (points *X* and *Y*, respectively). For each variable under analysis it is therefore possible to build a membership function. Each of these functions is a partial one in the sense that each of them results from the analysis of only some combinations of the fuzzy loads. This means that when running the parametric problems to move the solution from O to X and then from X to Y we are only analyzing the load combinations on the segments OX and XY. The final step corresponds to aggregate the partial membership functions obtained for each variable (branch flows, generation and PNS) for each analyzed vertex. This aggregation is performed using the fuzzy union operator so that it is possible to capture the widest possible behavior of each branch flow, generation or PNS, underlying the specified load uncertainties. Although the literature describes many other operators, the fuzzy union operator as defined in Section 3 ensures that the final results are the widest possible, thus representing the possible operation of the system, that is, what may happen given the specified uncertainties.

5. New Fuzzy Optimal Power Flow Model

5.1 General Aspects

The original FOPF model described in Section 4 simplified the multiparametric problem (4.6) to (4.8) that described in an exact way the impact of load uncertainties in a number of parametric problems. This simplification, although convenient from the point of view of computational efficiency, would mean not to analyse in a systematic way all load combinations in the hypervolume described by (4.8), but only the ones lying on the segments departing from the central load combination (point *O* in Figure 4.1) to the identified vertices (as point *Y* in Figure 4.1). As a consequence, the final results for generations, branch flows or PNS could be narrower than what they should be, that is, we were eventually not capturing the widest possible behaviour of the system when reflecting load uncertainties. Apart from the above problem, we considered that it would be important to extend the original concept by translating to the results not only load uncertainties, but also generation cost uncertainties, namely in view of the current volatility of fuel prices and also considering the development of market mechanisms in the sector.

As a result, the NFOPF enables obtaining more accurate solutions, since it adopts linear multiparametric optimization techniques and it allows addressing in a simultaneous way load and generation cost uncertainties. Considering load uncertainties as an example, the application of multiparametric techniques lead to the identification of a number of critical regions that effectively cover the uncertainty space corresponding to the hypervolume defined by (4.8). This ultimately means that this is a more realistic and accurate approach to address uncertainties in power system operation and planning.

The algorithms used to solve linear multiparametric problems were originally proposed in [13]. Starting at the initial optimal and feasible solution of the deterministic optimization problem stated by (4.1) to (4.5) these algorithms identify critical regions in the uncertainty space, considering that their union covers the entire uncertainty space. When running this identification step, we admit that the problem integrates uncertainty parameters in the right hand side vector, λ_k, to model load uncertainties and uncertainty parameters in the cost function, Δ_k, to model generation cost uncertainties.

From a mathematical point of view, let *B* be an optimal and feasible basis, ρ the index for the corresponding set of basic variables, *A* the columns of the non-basic variables in the Simplex tableau, C_0 the cost vector of the basic variables and C^T the cost vector of the non-basic variables. While analysing load uncertainties, the solution obtained for the initial deterministic problem can lose its feasibility, that is, the set of constraints (5.1) expressing the feasibility condition can be violated. Similarly, when analyzing generation cost uncertainties, the solution obtained for

the initial deterministic problem can lose its optimality, that is, the set of constraints (5.2) expressing the optimality condition can be violated.

$$B_\rho^{-1}.b(\lambda_k) = B_\rho^{-1}(b + b'(\lambda_k)) \geq 0 \quad (5.1)$$

$$C^T(\Delta_k) - C_0^T.B_\rho^{-1}.A = (c + c'(\Delta_k)) - C_0^T.B_\rho^{-1}A \geq 0 \quad (5.2)$$

Using these two conditions, the solution algorithm starts at the optimal and feasible solution of the initial deterministic DC-OPF problem and it proceeds to find the set of other optimal and feasible solutions provided they are valid in some region of the uncertainty space. These regions are called critical regions and each of them corresponds to a region in the uncertainty space where there is a basis B that is optimal and feasible. Their identification is conducted by pivoting over the initial basis as well as over all the new ones identified during the search process.

Since the dual solution does not depend on λ_k for right hand side parameterization, a critical region can be uniquely defined by the conditions in (5.1). Similarly, since the primal solution does not depend on Δ_k for cost parameterization, a critical region can be defined by the conditions given by (5.2). Apart from these conceptual aspects, two optimal and feasible basis, B_1 and B_2, are considered neighbour ones if and only if one can pass from B_1 to B_2 performing one dual pivot step in case of right hand side parameterization, one primal pivot step in case of cost vector parameterization or one step of each type if we are addressing the simultaneous parameterization of cost and load uncertainties.

As a final comment, the ultimate objective to attain when solving a linear multiparametric problem is to find all possible optimal solutions, their corresponding optimal values and critical regions, which can be defined as a closed nonempty polyhedron. These regions correspond to a set of linear inequalities in λ_k, Δ_k, or both. Mathematically, these constraints can be expressed as an equivalent set of non-redundant constraints, which in turn can be identified through a non-redundancy test for linear inequalities, as the one proposed by [13].

5.2 Integration of Load Uncertainties

The algorithm developed to solve the NFOPF problem is detailed in Figure 5.1. It starts with the solution of the deterministic Fuzzy DC-OPF problem (4.1-4.5) considering the central values of the load fuzzy numbers. It should be mentioned that this formulation is general in the sense that it admits that some loads are represented by fuzzy numbers while the value of some others is deterministic. In this case, each fuzzy load is associated with a parameter λ_k modeling its uncertainty while the value of deterministic loads is fixed. After obtaining an optimal and feasible solution for this deterministic problem, the algorithm

integrates in this initial problem the parameters used to model load uncertainties. This leads to the linear multiparametric optimization problem (5.3-5.7).

$$\min \quad Z = \sum c_k . Pg_k + G.\sum PNS_k \tag{5.3}$$

$$\text{s.t.} \quad \sum Pg_k + \sum PNS_k = \sum Pl_k^{ctr} + \sum \lambda_k \tag{5.4}$$

$$Pg_k^{min} \le Pg_k \le Pg_k^{max} \tag{5.5}$$

$$PNS_k \le Pl_k^{ctr} + \lambda_k \tag{5.6}$$

$$P_b^{\min} \le \sum a_{bk} . (Pg_k + PNS_k - (Pl_k^{ctr} + \lambda_k)) \le P_b^{\max} \tag{5.7}$$

When solving this problem, it is possible that the optimal and feasible basis identified for the initial deterministic DC-OPF problem is no longer feasible in some regions of the uncertainty space represented by the hypervolume defined by (4.8). This means that for some combinations of the parameters λ_k the optimal and feasible basis of the deterministic DC-OPF problem leads to negative values of some basic variables.

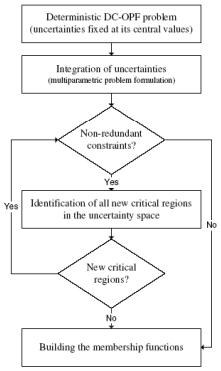

Fig. 5.1 Solution algorithm of the NFOPF integrating active load uncertainties.

Following the algorithm in Figure 5.1, we will now use the feasibility condition (5.1) to identify new critical regions. Each of these regions is represented by the maximum and minimum excursion of each load parameter together with the set of non-redundant constraints obtained from the inequalities associated with the feasibility condition (5.1). If there are no non-redundant constraints, the algorithm stops. Otherwise, it performs a dual pivoting over the initial optimal and feasible basis to identify new critical regions. This process is repeated until no non-redundant constraints exist or until all identified critical regions correspond to

already known ones. When this process is completed all the uncertainty space is covered and for all identified critical regions there is a feasible and optimal basis *B* of the problem (5.3-5.7).

In order to illustrate this procedure, let us consider Figure 5.2. It displays the rectangles related with the 0.0 and 1.0-cuts for a two trapezoidal fuzzy load system. Lines *a* and *b* represent constraints, for instance, related with branch flow or generator capacity limits, point *O* represents the optimal and feasible solution of the initial deterministic DC-OPF problem and the dashed lines define the rectangle representing the ith cut of the fuzzy load membership functions. In this case, the constraint represented by line *a* determines a basis change admitting that the process started in point *O*, that is, in region R_j. This means that the feasibility condition (5.1) including the load vector uncertainties is used to define the regions R_i and R_j. In a systematic way, all critical regions are obtained by performing a dual pivoting over each of the optimal and feasible already identified basis.

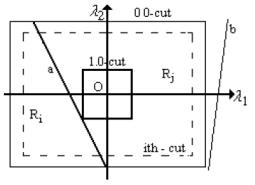

Fig. 5.2 Critical regions in the uncertainty space for a two fuzzy load system.

In order to build the membership functions of the output variables (generations, branch flows and PNS) it is important to identify their extreme possible behaviour reflecting data uncertainty. The adoption of a linear formulation for the OPF problem, a DC OPF approach, ensures that the behaviour of each output variable *v* is represented by a linear expression in function of the uncertain parameters. This means that the behaviour of *v* is described by a linear function of the uncertainty parameters λ_1 and λ_2, say $v(\lambda_1,\lambda_2)$ in each identified critical region. If we want to capture the possible behaviour of $v(\lambda_1,\lambda_2)$ in a critical region, we have to compute its minimum and maximum values in that region. This corresponds to solve the problem (5.8) to (5.11) once it terms of minimization and once as a maximization problem.

$$min/\,max \quad f = v(\lambda_1,\lambda_2) \tag{5.8}$$

$$\text{s.t.} \quad k_{1i}.\lambda_1 + k_{2i}.\lambda_2 \le b_i \tag{5.9}$$

$$\lambda_1^{\min\ i^{th}-cut} \le \lambda_1 \le \lambda_1^{máx\ i^{th}-cut} \tag{5.10}$$

$$\lambda_2^{\min\ i^{th}-cut} \le \lambda_2 \le \lambda_2^{máx\ i^{th}-cut} \tag{5.11}$$

This problem should be formulated for some α-cuts of the specified load uncertainties, meaning that each fuzzy load is discretized in a number of intervals, each one associated with a α-cut. Once this discretization is done, we reflect the uncertainties now represented by α-cuts, in the output variables of the problem. The computation of the minimum and maximum values of v corresponds to minimize and to maximize the linear expression describing v subjected to the constraints modelling the non-redundant conditions (5.9), where k_{1i} and k_{2i} are real numbers, together with the possible ranges of the input uncertainties regarding the i^{th} cut under analysis (5.10) and (5.11). Constraints (5.9) define the critical region under analysis and they result from the process of identification of these regions, that is, from the application of the feasibility condition (5.1). After minimizing and maximizing v for the selected cuts, it is possible to build the membership function of v in the critical region in analysis. Once all regions are analyzed, the final membership function of v is obtained applying the fuzzy union operator (as defined in Section 3) to the partial membership functions obtained for v.

5.3 Integration of Generation Cost Uncertainties

In this case, the linear multiparametric optimization problem (5.12-5.16) integrates in the cost vector C^T the parameters Δ_k to model generation cost uncertainties.

$$min \quad Z = \sum c_k(\Delta_k).Pg_k + G.\sum PNS_k \tag{5.12}$$

$$\text{s.t.} \quad \sum Pg_k + \sum PNS_k = \sum Pl_k^{ctr} \tag{5.13}$$

$$Pg_k^{min} \le Pg_k \le Pg_k^{max} \tag{5.14}$$

$$PNS_k \le Pl_k^{ctr} \tag{5.15}$$

$$P_b^{min} \le \sum a_{bk}.(Pg_k + PNS_k - Pl_k^{ctr}) \le P_b^{max} \tag{5.16}$$

In order to identify non-redundant constraints leading to the definition of the critical regions in the uncertainty space, we will now use the optimality condition (5.2) in terms of the parameters Δ_k. In this case, the critical regions are identified performing a primal pivoting over the initial optimal and feasible basis as well as over all new optimal and feasible basis identified along the search procedure.

When solving problems as (5.12-5.16), we should recall that each variable (generations, branch flows and PNS) is constant for all generation cost combinations inside each identified critical region. Therefore, the values of these output variables will only change if there is a basis change, which means moving from one critical region to another one.

Accordingly, for each critical region, the partial membership function of any variable is built considering the non-redundant inequalities defining that region and the maximum membership degree of that output variable. This is simply done solving the linear system formed by the inequalities that define each critical region

to check if at least one point of a given cut level belongs to the critical region under analysis. Once all these pairs are obtained, they are aggregated using the fuzzy union operator to obtain the final membership function of the output variable under analysis. Therefore, when addressing generation cost uncertainties, the possible behaviour of the output variables is represented by pairs each of them including the value of the output variable and corresponding membership degree. This result corresponds, in some way, to the dual of the type of results obtained for load uncertainties. This should not be an entire surprise since when addressing load uncertainties we are multiparameterizing the right hand side vector, while for generation cost uncertainties we are running a cost function multiparameterization study. From a conceptual point of view, this means that these two problems correspond to a primal and dual version of the same problem.

5.4 Simultaneous Integration of Cost and Load Uncertainties

The linear multiparametric optimization problem (5.17-5.21) includes parameters to model generation cost uncertainties, Δ_k, and parameters related with load uncertainties, λ_k, so that we can address, simultaneously, the impact of these uncertainties in the output variables.

$$min\ Z = \sum c_k(\Delta_k).Pg_k + G.\sum PNS_k \tag{5.17}$$

$$\text{s.t.}\quad \sum Pg_k + \sum PNS_k = \sum Pl_k^{ctr} + \sum \lambda_k \tag{5.18}$$

$$Pg_k^{min} \le Pg_k \le Pg_k^{max} \tag{5.19}$$

$$PNS_k \le Pl_k^{ctr} + \lambda_k \tag{5.20}$$

$$P_b^{\min} \le \sum a_{bk}.(Pg_k + PNS_k - (Pl_k^{ctr} + \lambda_k)) \le P_b^{\max} \tag{5.21}$$

The presence of the parameters Δ_k and λ_k will eventually turn the optimal and feasible basis identified for the initial DC-OPF problem as unfeasible or not optimal in some regions of the uncertainty space. Thus a basis change means that we identify critical regions defined by sets of non-redundant constraints related both with the feasibility (5.1) and optimality (5.2) conditions. These constraints are linear functions of the uncertainty parameters λ_k and Δ_k.

Once all critical regions are identified, the algorithm proceeds with the construction of the membership functions of the final results. In order to do this, we once again recognize that in each critical region, the behaviour of each variable is expressed by a linear expression and so, for each of them and for each critical region, we solve optimization problems as (5.8-5.11) to get the widest possible behaviour of that variable in that region. In this case, however, the number of constraints is larger because we are now considering the non-redundant inequalities coming both from the application of (5.1) and (5.2).

5.5 Integration of Active Losses

Active losses in branch b from node i to node j are calculated in an exact way by expression (5.22), which depends on voltage phases and magnitudes (θ_i, θ_j, V_i and V_j) and on the branch conductance g_{ij}. Considering that voltage magnitudes are approximated to 1.0 pu in the DC model, we obtain the approximated expression (5.23) [26].

$$Loss_{ij} = g_{ij}.(V_i^2 + V_j^2 - 2.V_i.V_j.\cos\theta_{ij}) \quad (5.22)$$

$$Loss_{ij} = 2.g_{ij}.(1 - \cos\theta_{ij}) \quad (5.23)$$

A simple way of integrating this estimate of active losses in the crisp formulation (4.1-4.5) is detailed in the following iterative process.

1. Perform the deterministic DC OPF study formulated by (4.1-4.5);
2. Compute the nodal voltage phases, according to the DC model;
3. Compute an estimate of the active losses in each branch of the system;
4. Add half of the active losses estimated for each branch to the load connected to the corresponding extreme buses;
5. Perform a new deterministic DC OPF study to update the generation strategy;
6. Compute the nodal voltage phases according with the DC model;
7. Finish if the difference between every voltage phase in two successive iterations is smaller than a specified value. Otherwise return to step 3.

To take into account the effect of the active losses on the results of the algorithms presented in Sections 5.2, 5.3 and 5.4, for each extreme point of the identified critical regions we must run the algorithm just detailed. As it will be shown in Section 6, in general the impact of active losses is reduced and so this procedure typically originates small deviations regarding the initial results.

5.6 Computation of Nodal Marginal Prices

Marginal pricing is broadly recognized as the core approach to the economic evaluation of generation and transmission services. However, marginal pricing has several drawbacks. In the first place, tariff schemes based on short-term marginal prices may lead to perverse effects since, for example, more frequent transmission congestion could enlarge the nodal marginal price dispersion and so increase the marginal remuneration, or congestion rent. Secondly, pure short-term nodal prices do not take into account transmission investment costs and so, it would not be possible to recover these costs. This under recovery problem is well known in the literature and it is termed as the Revenue Reconciliation problem [17]. Thirdly, since marginal prices depend on several factors, they are typically very volatile.

Therefore, following [26], their computation should internalize several aspects as follows:

- uncertainties clearly affect load values especially in market environment. Therefore, load uncertainties and their consequences on nodal marginal prices are certainly a major issue that should be investigated;
- uncertainties also affect generation costs. Changes on generation costs will originate changes in the dispatch policy and thus in nodal marginal prices;
- nodal marginal prices depend on the system components that are available in instant t. Therefore, the consequence of the non ideal nature of the system components, that is, their reliability on nodal marginal prices should be investigated.

The nodal marginal price volatility makes it difficult to predict the marginal remuneration that could be recovered by the transmission provider. In this sense, several works were developed to integrate uncertainties in the nodal marginal price computation. In general, these methods treat load uncertainties using probabilistic models [7, 25] or fuzzy approaches [9, 15, 17, 26].

The short-term nodal marginal price in bus k can be defined as the impact on the cost function of a short-term operation planning problem regarding to a unit variation of the load in node k. Let us consider the crisp DC OPF model (4.1-4.5) including the branch loss estimate as described in Section 5.5. According to [26] the nodal marginal price in node k is given by (5.24):

$$\rho_k = \gamma + \gamma.\frac{\partial Losses}{\partial P_{Lk}} + \sigma_k - \sum_{all\ branches} \eta_b.\frac{\partial P_b}{\partial P_{Lk}} \tag{5.24}$$

In this expression:

- γ represents the dual variable of the generation/load balance equation (4.2);
- the second term represents the impact on the cost function, Z, from varying branch losses in the whole network due a variation of the load in bus k.
- the third term represents the contribution from constrains (4.4) that are eventually on their limits. σ_k is the dual variable of the constraint in node k;
- the fourth term represents the contribution to the cost function, Z, from each branch flow constraint that is on its limit. In this expression, η_b represents the dual variable of the corresponding constraint and the derivative of the branch flow in branch b, P_b, regarding the load in bus k, P_{Lk}, is the symmetric of the corresponding sensitivity coefficient.

The algorithm developed to compute the nodal marginal prices membership functions comprises three distinct stages. In the first stage, the algorithm determines the maximum and minimum possible values of all variables in each cut level. Once this initial stage is completed, the algorithm can evolve to include the impact of the active transmission losses for each identified operating point in each cut level or this impact can be neglected. At last, the algorithm determines the

nodal marginal prices using (5.24). In order to build the membership function of nodal marginal prices and similarly to what was described in Sections 5.2, 5.3 and 5.4, one also obtains partial membership functions of nodal marginal prices. When they are all known, the final membership function is obtained applying the fuzzy union operator to all of them.

5.7 Final Remarks

Regarding the expected results, it should be mentioned that three distinct situations can occur:

- when only modelling load uncertainties, each variable in each critical region is represented by a linear expression. Therefore, generations, branch flows and PNS are described by linear (at least by segments) membership functions. In a different way, since nodal marginal prices are related with the dual variables of this optimization problem, their membership functions are described by pairs of price/membership value;
- when only modelling generation cost uncertainties, each variable is constant inside each critical region. This means that their corresponding membership functions are described by pairs of power/membership value. Since the nodal marginal prices are related with the dual variables of the original problem, in this case the membership functions of the nodal marginal prices are described by linear, at least by segments, membership functions;
- finally, when considering both load and generation cost uncertainties, primal and dual variables of the original problem are represented by linear expressions of the parameters used to model uncertainties. As a result, generation, branch flows, PNS and nodal marginal prices are described by linear (at least by segments) membership functions.

6. Case Study

6.1 Data

The algorithms described so far were used to build the membership functions of generations, branch flows, PNS and nodal marginal prices considering a Case Study based on the IEEE 24 bus/38 branch test system. The original data for this system is given in [32]. Regarding the data in this reference, the load was increased to 4060.05 MW. Table 6.1 presents the installed capacities and the central values of the generation costs and Table 6.2 indicates the central values of the loads. The total installed capacity is 5226 MW according to the data in Table 6.1. Branch data can be obtained from [32] considering that the transformers have

a capacity of 400 MW, the capacity of the branches 1 to 6 and 8 to 13 was set at 175 MW and the capacity of the remaining branches was set at 500 MW.

Table 6.1 Installed system capacity.

Bus/Gen	Capacity [MW]	Cost [€/MWh]	Bus/Gen	Capacity [MW]	Cost [€/MWh]
1/1	40.0	30.0	16/1	310.0	55.0
1/2	40.0	32.0	19/1	800.0	87.0
1/3	152.0	40.0	21/1	800.0	80.0
1/4	152.0	43.0	22/1	100.0	15.0
2/1	40.0	36.0	22/2	100.0	17.0
2/2	40.0	38.0	22/3	100.0	19.0
2/3	152.0	41.0	22/4	100.0	15.0
2/4	152.0	42.0	22/5	100.0	17.0
7/1	150.0	45.0	22/6	100.0	25.0
7/2	200.0	43.0	23/1	200.0	50.0
13/1	250.0	61.0	23/2	50.0	49.0
13/2	394.0	62.0	23/3	310.0	47.0
13/3	394.0	67.0	-- -	- -	- -

Table 6.2 Load central values.

Bus	Load [MW]	Bus	Load [MW]	Bus	Load [MW]
1	220.48	9	385.82	17	0.00
2	270.80	10	216.49	18	226.76
3	3.94	11	40.00	19	265.53
4	32.67	12	10.00	20	103.92
5	105.94	13	162.45	21	50.00
6	187.65	14	262.88	22	10.00
7	218.77	15	650.36	23	0.00
8	398.09	16	225.50	24	12.00

6.2 Results Only Considering Load Uncertainties

In order to test the algorithm presented in Section 5.2, we considered trapezoidal fuzzy numbers to model loads. These numbers have at the 0.0 level the uncertainty range from +/-10 per cent and at the 1.0 level from +/- 5 per cent of its central value. Figure 6.1 presents the membership functions of generators 19/1 and 21/1 considering and not considering the effect of transmission losses.

As expected, the load variation determines changes on the generation of generator 21/1 since it is the marginal one. When this generator reaches its maximum capacity of 800 MW, generator 19/1 becomes the marginal one. Another important point illustrated by these functions is related with the impact of

active losses. In this case, these generators have larger generation values for the same level of uncertainty due to the compensation of losses.

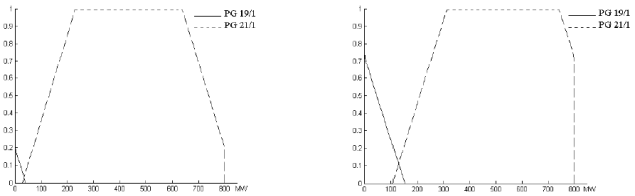

Fig. 6.1 Membership functions of generators 19/1 and 21/1 not considering the effect of the transmission losses (at the left) and considering this effect (at the right).

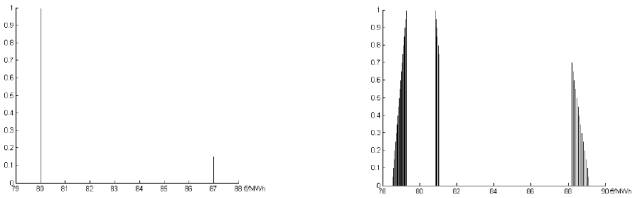

Fig. 6.2 Membership functions of the nodal marginal price in node 1 not considering the effect of transmission losses (at the left) and considering this effect (at the right).

Figure 6.2 presents the nodal marginal prices at node 1 for the two situations previously presented. As referred in Section 5.7, since nodal marginal prices are related with the dual variables of the original problem their membership functions are described by pairs of price/membership values. From Figure 6.2 it is possible to see that in the absence of the transmission losses, branch congestions or PNS effect, the marginal price in node 1 equals the generation cost of the marginal generator. When the effect of active losses is considered, the nodal marginal prices increase or decrease depending on the impact of load variations in active losses. For instance, when generator 19/1 is the marginal one, an increase of the load in node 1 increases active losses and so the marginal price in node 1 also increases.

In order to check the impact of congested branches, the flow limit of branches 15-21 was reduced to 350 MW. As a consequence, for some combination of loads these branches get congested. Figure 6.3 presents the membership functions of generators 19/1 and 21/1 and of the marginal price in node 15 in this case.

The analysis of these results indicates that the congestion on branches 15-21 implies a change of the marginal prices in most of the nodes, but more in particular in the ones that are closer to the congested branches. In case of node 15 in Figure 6.3, the marginal price increase means that a generation increase or a

load reduction in this node contributes to alleviate the congestion. The membership function of generator 21/1 in Figure 6.3 reveals that now this generator doesn't reach its maximum limit of 800 MW, differently from what was indicated in Figure 6.1. This is due to the congestion of branches 15-21.

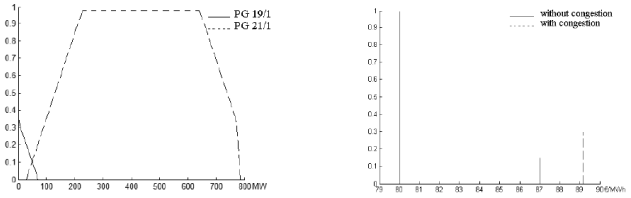

Fig. 6.3 Membership functions of generators 19/1 and 21/1 (at the left) and of the nodal marginal price in node 15 (at the right).

6.3 Results Only Considering Generation Cost Uncertainties

In this simulation, the trapezoidal fuzzy numbers (6.1-6.6) were used to model the cost of generators 1/1, 2/1, 7/1, 19/1, 22/2 and 23/2. In this case, Figure 6.4 presents the membership functions of generators 19/1 and 21/1.

$$CP_{G1/1} = (26.0,27.5,32.5,34.0) \quad (6.1)$$

$$CP_{G2/1} = (33.0,34.5,37.5,39.0) \quad (6.2)$$

$$CP_{G7/1} = (42.0,43.5,46.5,48.0) \quad (6.3)$$

$$CP_{G19/1} = (74.0,82.0,92.0,100.0) \quad (6.4)$$

$$CP_{G22/2} = (14.0,15.5,18.5,20.0) \quad (6.5)$$

$$CP_{G23/2} = (46.0,47.5,50.5,52.0) \quad (6.6)$$

As it was mentioned in Sections 5.3 and 5.7, in this case the membership functions of generators are represented by pairs of power/membership values. The functions in Figure 6.4 reflect two different generation strategies according to the specified cost uncertainties. In fact, when the cost of generator 19/1 is smaller than 80 €/MWh (which corresponds to the cost of generator 21/1) this generator will generate 434.05 MW. For larger costs this generator will be at 0 MW and generator 21/1 will generate 434.05 MW. Figure 6.4 also indicates that when active losses are included there is, in general, an increase of generation values. This increase depends on the adopted generation strategy because of their different impacts on active losses.

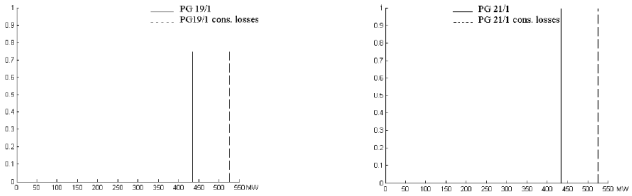

Fig. 6.4 Membership functions of generators 19/1 and 21/1 considering and not considering the effect of transmission losses.

Figure 6.5 presents the nodal marginal price of node 1 in these two situations. As mentioned in Section 7.3, the membership functions of the nodal prices are linear, at least by segments for cost uncertainties. Considering the effect of active losses, there is an increase of the nodal price in node 1. These results are in line with the ones in Figure 6.2 since we observed that a load increase in node 1 contributed to increase active losses.

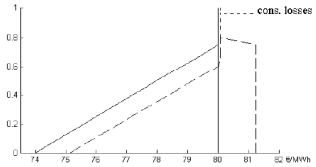

Fig. 6.5 Membership function of the nodal marginal price at node 1 considering and not considering the transmission losses effect.

6.4 Results Considering Load and Generation Cost Uncertainties

In this simulation we considered the load uncertainties used in Section 6.2 and the generation cost uncertainties specified in Section 6.3. Figure 6.6 presents the membership functions of generators 13/3, 19/1 and 21/1. Simultaneously modelling load and generation cost uncertainties turns the problem and the results more complex since they reflect characteristics of both cases analysed in Sections 6.2 and 6.3. In fact, the different generation strategies and generation values become function not only of load uncertainties but also of the generation cost uncertainties. As a result, for some combinations of the specified uncertainties there is congestion on the branches 8-9, 16-19 and 11-13. The congestion on branches 16-19 and 11-13 prevents generators 19/1 and 13/3 from having larger

outputs. If active losses are considered as in the right side of Figure 6.6, the generation values are larger for some uncertainty levels.

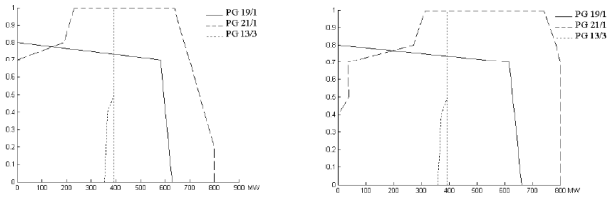

Fig. 6.6 Membership functions of generators 13/3, 19/1 and 21/1 when they are not considered the transmission losses effect (at the left) and when they are considered (at the right).

Figure 6.7 presents the membership functions of the nodal marginal prices in nodes 15 and 21. This Figure indicates that these two prices are very similar. This was expected since the nodal marginal prices incorporate the dual variable of the generation/load balance equation and the impact of increasing the load regarding congestion and active losses. For nodes 15 or 21 this impact is very similar, explaining that these two membership functions are similar.

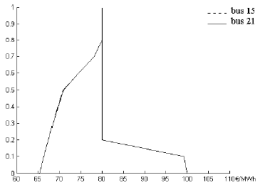

Fig. 6.7 Membership functions of nodal marginal prices on buses 15 and 21.

In line with what was mentioned in Section 6.2, Figure 6.8 presents the results obtained when the limits of branches 15-21 are reduced to 350 MW. Comparing these results with the ones in Figure 6.3 we can see that in this case the effect of the congestion on branches 15-21 is not so clear because the maximum generation of generator 19/1 is no longer determined by congested branches but, instead, by the specified generation cost uncertainties.

Finally, Figure 6.9 presents the membership functions of the nodal marginal prices on nodes 15 and 21 when the limits of branches 15-21 are set to 350 MW. As expected the membership functions of these prices are no longer similar, as they were on Figure 6.7. The congestion of branches 15-21 determine a maximum price of 80 €/MWh for node 21 and a value larger than 105 €/MWh for node 15. This situation is in line with what was mentioned in Section 6.2, because the nodal

marginal price increase in bus 15 means that a generation increase or a load reduction in this node contributes to alleviate congestion in branches 15-21.

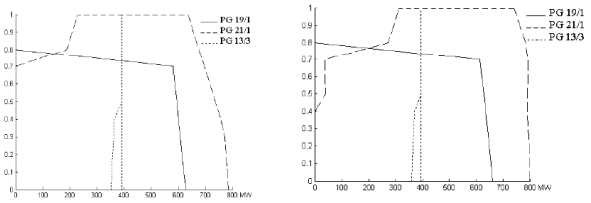

Fig. 6.8 Membership functions of generators 13/3, 19/1 and 21/1 when they are not considered the transmission losses effect (at left) and when they are considered (at right).

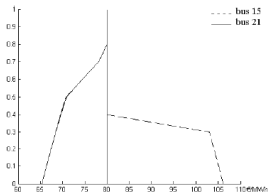

Fig. 6.9 Membership functions of nodal marginal prices on buses 15 and 21.

7. Conclusions

In this paper we presented the most relevant concepts of the original Fuzzy DC Optimal Power Flow developed back in 90ies and also the New Fuzzy DC Optimal Power Flow model. As it was shown, this new approach can be used to model not only load uncertainties, but also generation cost uncertainties or both, simultaneously. Since it uses linear multiparametric optimization techniques, it is possible to obtain more accurate results than with the original model. Additionally, it was described the algorithm developed to integrate an estimate of active transmission losses on the results and also the approach used to compute and build the nodal marginal price membership functions.

This model can be very useful for a variety of agents acting in the electricity sector given the current volatility of several inputs to this type of studies. Generation cost uncertainties, namely fuel costs, and the demand level uncertainties, related with the wide spread economic recession, are just two

elements that should be internalized. Apart from their volatility, it should be mentioned that for several of these changes there is no or little history meaning that the derivation of probabilistic functions to model these recent events can be questioned. As a result, fuzzy set based models can gain a new area of application. These models can also be used in a profitable way to get more insight on the possible system behaviour by generation companies, transmission providers or regulatory agencies to help them taking more sounded decisions at different levels, such as expansion planning, operation planning or regulatory and tariff aspects.

Acknowledgements: The first author would like to thank Fundação para a Ciência e Tecnologia, FCT, that funded this research work through the PhD grant nº **SFRH/BD/34314/2006.**

References

1. Allan R. N., Al-Shakarchi M. R. G. (1976) Probabilistic a.c. Load Flow. Proceedings of the IEE 123 531-536
2. Allan R. N., Al-Sharkarchi M. (1977) Probabilistic Techniques in a.c. Load-Flow Analysis. Proceedings of IEE Vol. 124 154-160
3. Allan R. N., Borkowska B., Grigg C. H. (1974) Probabilistic Analysis of Power Flows. Proceedings of the IEE, 121 1551-1556
4. Allan R. N., Grigg C. H., Newey D. A., Simmons R. F. (1976) Probabilistic Power-Flow Techniques Extended and Applied to Operation Decision Making. Proceedings of the IEE 123 1317-1324
5. Allan R. N., Leite da Silva A. M. (1981) Probabilistic Load Flow Using Multilinearisations. Proceedings of IEE Vol. 128 280-287
6. Allan R. N., Leite da Silva A. M., Burchett R. C. (1981) Evaluation Methods and Accuracy in Probabilistic Load Flow Solutions. IEEE Transactions on PAS Vol. PAS-100 2539-2546
7. Baughman Martin L., Lee Walter W. (1992) A Monte Carlo Model for Calculating Spot Market Prices of Electricity. IEEE Transactions on Power Systems Vol. 7 No. 2 584-590
8. Borkowska B. (1974) Probabilistic Load Flow. IEEE Transactions PAS PAS-93 Vol. 12 752-759
9. Certo J., Saraiva J. T. (2001) Evaluation of Target Prices for Transmission Congestion Contracts Using a Monte Carlo Accelerated Approach. IEEE Porto Power Tech Conference
10. Chaturvedi A., Prasad K., Ranjan R. (2006) Use of Interval Arithmetic to Incorporte the Uncertainty of Load Demand for Radial Distribution System Analysis. IEEE Transactions on Power Delivery Vol. 21 No. 2 1019-1021
11. Dimitrivski A., Tomsovic K. (2004) Boundary Load Flow Solutions. IEEE Transactions on Power Systems Vol. 19 No. 1 348-355

12. El-Hawary M. E., Mbamalu G. A. N. (1989) Stochastic Optimal Load Flow Using a Combined Quasi-Newton and Conjugated Gradient Technique. Electric Power & Energy Systems Vol. 11 No. 2 85-93
13. Gal T. (1979) Postoptimal Analysis, Parametric Programming and Related Topics. McGraw Hill International Book Company
14. Gomes B. A., Saraiva J. T. (2007) Calculation of Nodal Marginal Prices Considering Load and Generation Price Uncertainties. Proceedings of the IEEE Lausanne Power Tech 849-854
15. Jesus P. M., Leão T. P. (2004) Impact of Uncertainty and Elastic Response of Demand in Short Term Marginal Prices. 8th International Conference on Probabilistic Methods Applied to Power Systems 32-37
16. Karakatsanis T. S., Hatziargyriou N. D. (1994) Probabilistic Constrained Load Flow Based on Sensitivity Analysis. IEEE Transactions on Power Systems Vol. 9 1853-1860
17. Leão M. T., Saraiva J. T. (2003) Solving the Revenue Reconciliation Problem of Distribution Network Providers Using Long-Term Marginal Prices. IEEE Transactions on Power Systems Vol. 18 No. 1 339-345
18 Leite da Silva A. M., Arienti V. L. (1990) Probabilistic Load Flow by a Multilinear Simulation Algorithm. IEE Proceedings Vol. 137 Pt. C 256-262
19. Leite da Silva A. M., Allan R. N., Soares S. M., Arienti V. L. (1985) Probabilistic Load Flow Considering Network Outages. IEE Proceedings Vol. 132 Pt. C 139-145
20. Lien Chun (2005) Probabilistic Load Flow Computation Using Point Estimate Method. IEEE Transactions on Power Systems Vol. 20 No. 4 1843-1851
21 Madrigal M., Ponnambalam K., V. H. Quintana (1998) Probabilistic Optimal Power Flow. Proceedings IEEE Canadian Conference on Electrical and Computer Engineering 385-388
22. Miranda V., Matos M. A., Saraiva J. T. (1990) Fuzzy Load Flow – New Algorithms Incorporating Uncertain Generation and Load Representation. Proceedings of the 10th Power Systems Computation Conference 621-625
23. Miranda V., Saraiva J. T. (1992) Fuzzy Modelling of Power System Optimal Load Flow. IEEE Transactions on Power Systems 7 843-849
24. Muela E., Schweickardt G., Garcés F. (2007) Fuzzy Possibilistic Model for Medium-Term Power Generation Planning with Environmental Criteria. Energy Policy Vol. 35 5643-5655
25. Rivier M., Pérez-Arriaga I. J. (1993) Computation and Decomposition of Spot Prices for Transmission Pricing. 11th Power Systems Computation Conference
26. Saraiva J. T. (1999) Evaluation of the Impact of Load Uncertainties in Spot Prices Using Fuzzy Set Models. 13th Power Systems Computation Conference
27. Saraiva J. T., Miranda, V. (1993) Impacts in Power System Modelling From Including Fuzzy Concepts in Models. Proceedings of Athens Power Tech Vol. 1 417-422

28. Saraiva J. T., Miranda V. (1996) Identification of Hedging Policies in Generation / Transmission Systems. Proceedings of the 12th Power Systems Computation Conference Vol. 2 779-785
29. Saraiva J. T., Miranda V., Pinto L. M. V. G. (1994) Impact on Some Planning Decisions from a Fuzzy Modelling of Power Systems. IEEE Transactions on Power Systems 9 819-825
30. Saraiva J. T., Miranda V., Pinto L. M. V. G. (1996) Generation/Transmission Power System Reliability Evaluation by Monte-Carlo Simulation Assuming a Fuzzy Load Description. IEEE Transaction on Power Systems 11 690-695
31. Soderholm P. (2008) The Political Economy of International Green Certificates Market. Energy Policy Vol. 36 2051-2062
32. Task Force of Application of Probabilistic Methods Subcommittee (1979) IEEE Reliability Test System. IEEE Transactions on PAS PAS-98 2047-2054
33. Verbic G., Canizares C. A. (2006) Probabilistic Optimal Power Flow in Electricity Markets Based on a Two-Point Estimate Method. IEEE Transactions on Power Systems Vol. 21 No. 4 1883-1893
34. Wang Z., Alvarado, F. L. (1992) Interval Arithmetic in Power Flow Analysis. Transactions on Power Systems Vol. 7 No. 3 1341-1349
35. Zadeh, L. (1965) Fuzzy Sets. Information and Control Vol. 8 338 - 353
36. Zhang P., Lee S. T. (2004) Probabilistic Load Flow Computation Using the Method of Combined Cumulants and Gram-Charlier Expansion. IEEE Transactions on Power Systems Vol. 19 No. 1 676-682